

***COX-2 and the vascular system:
interactions with endothelial
pathways and the eNOS system.***

A thesis submitted to Imperial College of London for the
degree of Doctor of Philosophy

Malak Al-Yamani

July 2016

Imperial College London

Faculty of Medicine

National Heart and Lung Institute

Dept. of Cardiothoracic Pharmacology

Declaration

I declare that this thesis is my own work, except where work by others has been properly referenced and acknowledged.

Copyright Declaration

The copyright of this thesis rests with the author and is made available under a Creative Commons Attribution-Non Commercial-No Derivatives licence. Researchers are free to copy, distribute or transmit the thesis on the condition that they attribute it, that they do not use it for commercial purposes and that they do not alter, transform or build upon it. For any reuse or distribution, researchers must make clear to others the licence terms of this work.

Dedication

I dedicate this thesis firstly to my father, Abdullah Alyamani who I am sure would have been very proud of me. My mother, Sameerah, has been my rock in life and provided me with unconditional love and support at all times. I am very grateful and proud to be your daughter. Maisa, Mae and Malekah, my lovely sisters, who have been nothing but caring, supportive and my best friends in life – this is also dedicated to you.

Finally but most importantly, to my husband, Abdulrahman Alqublan, and my two beautiful daughters, Ameerah and Maryam; thank you for being patient and understanding for the last few years.

Without you all I would not be where I am and you all have a special place in my heart.

Acknowledgments

When I first found out that I was accepted for a PhD I did not imagine that it would be a rollercoaster of fantastic and exciting opportunities combined with stress and difficult times. Without Jane Mitchell, I would not be here submitting this thesis. Words cannot describe how influential, supportive and inspiring she has been first and foremost as a woman and also as a supervisor.

I am very grateful to my co-supervisor, Dr Martina Slingsby, with whom I began this PhD and helped me with the endothelial cell morphology work and all my work in my first year. Dr Nicholas Kirkby has been fantastic in particular in helping with all animal work, mass spectrometry measurements and general lab queries. I am thankful also to Dr Blerina Ahmetaj-Shala for assisting with myography work, methylarginine experiments and all my work in the second year of my PhD. She along with Ms Hime Gashaw, our general laboratory manager who has helped with everyday lab work, have been my great friends.

Dr Louis Harrington McKenzie and Dr William Wright trained me in myography and Dr Daniel Reed and Ms Nura Adam trained me in BOEC experiments. I thank these people for their training and guidance.

The methylarginine related experiments were carried out at the MRC Clinical Sciences Centre with Dr James Leiper's Group and I am very grateful for their help. Special thanks also to Prof Tim Warner's lab at Queen Marys University for the clinical study experiments. I was also lucky enough to use the confocal microscope at the FILM facility, Imperial College and the scanning electron microscope with the generous assistance of Mr Andrew Rogers at the Royal Brompton Hospital - I am grateful for all of your help.

Publication

Papers in peer reviewed journals

- Ahmetaj-Shala B, Kirkby NS, Knowles R, **Al-Yamani M**, Mazi S, Wang Z, Tucker AT, Mackenzie L, Warner TD, Leiper J, Mitchell JA. (2015). "The COX-2/ADMA axis: relevance to arthritis, anti-inflammatory and anti-thrombotic therapy". *Circulation*. 132(17):e213-4. doi: 10.1161/CIRCULATIONAHA.115.017260
- Kirkby NS, Zaiss AK, Urquhart P, Jia J, Austin PJ, **Al-Yamani M**, Lundberg MH, MacKenzie LS, Warner TD, Nicolaou A, Herschman HR, Mitchell JA. (2013). C MSMS confirms that COX 1 drives vascular prostacyclin whilst gene expression pattern reveals non vascular sites of COX 2 expression. *PLoS ONE*. 9;8(7):e69524. doi:
- Kirkby NS, Lundberg MH, Harrington LS, Leadbeater PDM, Milne GL, Potter CMF, **Al-Yamani M**, Adeyemi O, Warner TD, Mitchell JA. (2012). Cyclooxygenase-1, not cyclooxygenase-2, is responsible for physiological production of prostacyclin in the cardiovascular system. *PNAS*. Oct 8;109(43):17597-602. doi:

Published Abstracts

- **Al-Yamani M**, Kirkby NS, Lundberg MH, Paul-Clark M, Warner TD and Mitchell JA. (2014). Effect of genetic deletion of cyclo-oxygenase isoforms on endothelial cell morphology in the mouse aortic arch. British Pharmacological Society. PA2 online.
- Ahmetaj-Shala B, **Al-Yamani M**, Kirkby NS, Leiper J and Mitchell JA. (2014). "Increased sensitivity to eNOS inhibition in vessels from cyclo-oxygenase-(COX)-2 knock-out mice associates with elevated plasma levels of ADMA and L-NMMA". British Pharmacological Society. PA2 online.
- **Al-Yamani M**, Slingsby MH, Kirkby NS, Ahmetaj-Shala B, Warner TD and Mitchell JA. (2014). "Effect of genetic deletion of cyclo-oxygenase isoforms on endothelial cell morphology in the mouse aortic arch". British Pharmacological Society. PA2 online.
- Ahmetaj-Shala B, Kirkby NS, Knowles R, **Al-Yamani M**, Warner TD, Leiper J and Mitchell JA. (2013). "Evidence That Links Cyclo-oxygenase-2 Inhibition with Increased Asymmetric Dimethylarginine: Novel Explanation of Cardiovascular Side Effects

Associated With Anti-inflammatory Drugs". 128; 22. A11282. American Heart Association. Circulation.

- Ahmetaj-Shala B, Kirkby NS, **Al-Yamani M**, Wang Z, Leiper J and Mitchell JA. (2013). "Blood pressure effects of the COX-2 inhibitor parecoxib are associated with elevated levels of the endogenous eNOS inhibitor L-NG-monomethyl L-arginine (L-NMMA) and asymmetric dimethyl L-arginine (ADMA)". British Pharmacological Society. PA2 online.
- Reed DM, George PM, **Al-Yamani M**, Francis C, Feyereisen LB, Swain W, Iglarz M, Wan A, Garfield B, Wort JS, Mitchell JA. (2013). "A novel and translatable cell assay for the study of vascular signalling in pulmonary arterial hypertension". European Respiratory Society. ERS.
- **Al-Yamani M**, Kirkby NS, Harrington L, Lundberg MH, Paul-Clark M, Warner TD and Mitchell JA. (2012). Role of the endothelium and COX-1 in prostacyclin generation by whole vessels stimulated with different agonists. British Pharmacological Society. PA2 online.

Abstract

Endothelial cells release protective hormones such as prostacyclin and nitric oxide involving the enzyme pathways of cyclooxygenase and nitric oxide synthase (NOS). Both prostacyclin and nitric oxide act to oppose the effects of thromboxane A₂ released following the actions also of cyclooxygenase by platelets. Cyclooxygenase (cyclooxygenase-2) is also present in inflammation and is the therapeutic target for the nonsteroidal anti-inflammatory group of drugs (NSAIDs). NSAIDs are among the most popular in the world. But NSAIDs also have side effects in the gut, this is why selective cyclooxygenase-2 types of NSAID were introduced. However, now after their introduction, there is an important concern regarding the cardiovascular side effects caused by all NSAIDs that work by blocking cyclooxygenase-2.

My PhD thesis has used a number of techniques to show that the constitutive isoform (cyclooxygenase-1) drives prostacyclin in blood vessels and that in the kidney knocking out cyclooxygenase-2 results in changes in genes and proteins that regulate the methylarginines ADMA and LNMMA which are NOS inhibitors. I show that in cyclooxygenase-2 knock out mice ADMA and LNMMA are increased and that eNOS responses are reduced and that the effect is reversed by the substrate L-arginine. This work suggests that ADMA could explain why NSAIDs that work by blocking cyclooxygenase-2 affects endothelial responses in an indirect way. The data also suggests that ADMA could be a biomarker and that for some people L-arginine supplements might be protective.

By using a mathematical model that I devised myself I also showed that cyclooxygenase-2 knock out causes morphological changes in the endothelium that suggest that in that region the enzyme might be pro-inflammatory and that for this observation a relationship with eNOS does not seem to be involved.

Abbreviations

| | |
|---|-------------------------|
| 1. 12-O-tetradecanoylphorbol-13-acetate | TPA |
| 2. 4',6'-diamidino-2-phenylindole | DAPI |
| 3. 6-keto prostaglandin F _{1α} | 6-ketoPGF _{1α} |
| 4. acetylcholine | Ach |
| 5. acetylcholinesterase | AChE |
| 6. Adenomatous Polyp Prevention on Vioxx | APPROVe |
| 7. adenosine triphosphate | ATP |
| 8. alanine-glyoxylate aminotransferase 2 | AGXT |
| 9. analysis of variance | ANOVA |
| 10. antibiotic geneciting | G418 |
| 11. Antiplatelet Trialists' Collaboration | APTCC |
| 12. anti-viral drug ganciclovir | GANC |
| 13. asymmetric dimethylarginine | ADMA |
| 14. B-Cell Lymphoma 6 | BCL-6 |
| 15. blood outgrowth endothelia cell | BOEC |
| 16. bovine serum albumin | BSA |
| 17. calcium ionophore | Ca ²⁺ |
| 18. calcium-independent phospholipase A2 | iPLA2 |
| 19. Celecoxib Long term Arthritis Study | CLASS |
| 20. chemoattractant receptorhomologous molecule | CRHT2 |
| 21. chicken embryo fibroblasts | CEF |
| 22. complementary DNA | cDNA |
| 23. COX-1 knockout | COX-1KO |
| 24. COX-2 knockout | COX-2KO |
| 25. cyclic guanosine-3',5-monophosphate | cGMP |
| 26. cyclic guanylate monophosphate | cGMP |
| 27. Cyclooxygenase | COX |
| 28. cytosolic phospholipase A2 | cPLA2 |
| 29. Cytosolic prostaglandin E synthase | cPGES |

| | |
|--|-----------------|
| 30. diacylglycerol | DAG |
| 31. dimethylarginine dimethylaminohydrolase | DDAH |
| 32. Dulbecco's modified Eagle's medium | DMEM |
| 33. endothelial growth media-2 | EGM2 |
| 34. endothelial nitric oxide synthase | eNOS |
| 35. endothelium derived relaxing factor | EDRF |
| 36. endothelium derived relaxing factor | EDRF |
| 37. enzyme-linked immunoabsorbent assay | ELISA |
| 38. exchange protein activated by cAMP | EPAC |
| 39. Facility for by Light Microscopy | FILM |
| 40. foetal bovine serum | FBS |
| 41. gastro intestinal | GI |
| 42. G-protein coupled receptor | GPCRs |
| 43. guanylate cyclase | GC |
| 44. guanylate cyclase | GC |
| 45. High pressure liquid chromatography | HPLC |
| 46. human epidermal growth factor | hEGF |
| 47. human fibroblastic growth factor-B | hFGF-B |
| 48. inducible nitric oxide synthase | iNOS |
| 49. inositol trisphosphate | IP ₃ |
| 50. intracellular calcium | Ca _i |
| 51. Leica Application Suite Advanced Fluorescence Lite | LAS AF |
| 52. lipopolysaccharide | LPS |
| 53. Liquid chromatography-Mass Spectrometry | LC-MS/MS |
| 54. L-N ^G -nitroarginine methyl ester hydrochloride | L-NAME |
| 55. micromolar | μM |
| 56. microsomal prostaglandin E synthase-1 | mPGES-1 |
| 57. millimolar | mM |
| 58. mitogen-activated protein | MAP |
| 59. mixed lineage kinase | MLK |
| 60. multiple reactions monitoring | MRM |
| 61. N ^G monomethyl-L-arginine | L-NMMA |

| | |
|---|------------------|
| 62. nitric oxide synthase | NOS |
| 63. nitric oxide | NO |
| 64. non-steroidal anti-inflammatory drugs | NSAIDs |
| 65. nuclear transcription factor κ B | NF κ b |
| 66. omega-3 | ω -3 |
| 67. omega-6 | ω -6 |
| 68. para-formaldehyde | PFA |
| 69. peroxidise | POX |
| 70. peroxisome proliferator activated receptors | PPARs |
| 71. phosphate buffered saline | PBS |
| 72. phosphodiesterases | PDES |
| 73. phospholipase A ₂ | PLA ₂ |
| 74. phospholipase B | PLB |
| 75. phospholipase C | PLC |
| 76. phospholipase D | PLD |
| 77. physiological saline solution | PSS |
| 78. polymerase chain reaction | PCR |
| 79. potassium physiological saline solution | KPSS |
| 80. prostacyclin | PGI ₂ |
| 81. prostacyclin receptor | IP |
| 82. prostaglandin D | DP |
| 83. prostaglandin E | EP |
| 84. prostaglandin endoperoxide 2 | PGG ₂ |
| 85. prostaglandin F | FP |
| 86. prostaglandin H synthase | PGHS |
| 87. prostaglandin H ₂ | PGH ₂ |
| 88. prostaglandin synthetase | PTGS |
| 89. prostaglandin-endoperoxidase synthase 2 | Ptgs2 |
| 90. prostaglandin-endoperoxide synthase 1 | Ptgs1 |
| 91. prostaglandins | PG |
| 92. prostaglandin E synthase | PGES |
| 93. protein arginine methyl transferase | PRMT |

| | |
|---|------------------|
| 94. protein kinase | PK |
| 95. protein kinase A | PKA |
| 96. protein kinase C | PKC |
| 97. Protein Kinase G | PKG |
| 98. proton pump inhibitors | PPI |
| 99. relative centrifugal force | RCF |
| 100. Scanning Electron Microscope | SEM |
| 101. secretory phospholipase A2 | sPLA2 |
| 102. serine 530 | Ser-530 |
| 103. smooth muscle cells | SMCs |
| 104. sodium nitroprusside | SNP |
| 105. soluble guanylate cyclase | sGC |
| 106. symmetric dimethylarginine | SDMA |
| 107. thromboxane A ₂ | TXA ₂ |
| 108. thromboxane mimetic | U46619 |
| 109. thromboxane receptor | TP |
| 110. tumor necrosis factor alpha | TNF- α |
| 111. vascular endothelial growth factor | VEGF |
| 112. Vioxx Gastrointestinal Outcomes Research | VIGOR |
| 113. wild type | WT |
| 114. α -keto- δ -(<i>N,N</i> -dimethylguanidino)valeric acid | DMGV |

Table of contents

| | |
|---|----|
| <i>COX-2 and the vascular system: interactions with endothelial pathways and the eNOS system.</i> | 1 |
| Declaration..... | 2 |
| Copyright Declaration | 2 |
| Dedication | 3 |
| Acknowledgments..... | 4 |
| Publication | 5 |
| Papers in peer reviewed journals | 5 |
| Published Abstracts..... | 5 |
| Abstract..... | 7 |
| Abbreviations | 8 |
| Table of contents | 12 |
| List of figures | 17 |
| List of tables | 21 |
| Chapter 1: General Introduction..... | 23 |
| Discovery of COX-1 and COX-2 | 24 |
| COX-1 | 24 |
| COX-2 | 25 |
| Products of COX and associated synthetic pathways | 27 |
| Specific prostanoids production and biological actions of COX products..... | 28 |
| Prostacyclin and prostacyclin synthase | 28 |
| TX and TX synthase | 29 |
| PGE ₂ and PGE ₂ synthase enzymes | 30 |
| mPGES-1..... | 30 |
| cPGES | 31 |
| mPGES-2..... | 31 |
| Other prostanoid synthase pathways..... | 32 |
| Prostanoid receptors | 32 |
| Prostacyclin and IP receptors..... | 33 |
| Thromboxane and TP receptors | 35 |
| PGE ₂ and EP receptors | 36 |

| | |
|---|----|
| PGF _{2α} and FP receptors and PGD ₂ , DP receptors, CRTH2, and PPAR | 38 |
| Role of prostanoids in health and disease | 39 |
| Prostanoids in inflammation, pain and fever | 39 |
| Gastrointestinal tract | 41 |
| Renal and Cardiovascular function | 42 |
| Drugs that act on the COX pathways: NSAIDs | 45 |
| Side effect of NSAIDs | 46 |
| Hypersensitivity reactions..... | 47 |
| Gastrointestinal side effects | 47 |
| Cardiovascular and renal side effects and the introduction of COX-2 selective NSAIDs 49 | |
| Mechanisms that are thought to explain how COX-2 blockers cause cardiovascular events | 52 |
| The NO pathways..... | 53 |
| Methylarginines | 55 |
| Summary | 57 |
| Hypothesis..... | 58 |
| Aims..... | 58 |
| Chapter 2: General Methods | 60 |
| Experimental animals..... | 61 |
| Genotyping procedure for COX-1 and COX-2 | 61 |
| COX-1 gene deletion strategy | 62 |
| COX-2 gene deletion strategy | 64 |
| IP receptor deletion | 65 |
| Mouse tissues preparation for imaging using En face confocal microscopy..... | 66 |
| Mouse preparation for staining protocol | 66 |
| General staining protocol for mice aortic arches | 66 |
| Mounting of mouse aortic arches..... | 67 |
| En face confocal microscopy settings | 68 |
| Scanning Electron Microscope (SEM) | 68 |
| Quantification | 69 |
| Tissue collection, processing and prostanoid release bioassay | 70 |
| Vascular release assays..... | 70 |
| Plasma, serum and urine collection..... | 70 |
| Analysis and assays | 70 |
| PGI ₂ measurement by immunoassay | 70 |
| Prostanoid measurement using LC/MS-MS..... | 71 |

| | |
|---|----|
| Protein and gene extractions and assays | 72 |
| Protein extraction | 72 |
| Western blotting | 72 |
| RNA extraction | 73 |
| RT-qPCR..... | 73 |
| Measurement of amino acids and methyl arginine analogues using LC-MS/MS..... | 74 |
| Vascular contraction and relaxation bioassays | 76 |
| Tissues preparation and loading for Isometric wire myography..... | 76 |
| Protocol for myograph..... | 76 |
| Blood pressure measurement using radio-telemetry | 77 |
| Measuring methyl arginine analogues and creatinine levels in human healthy volunteer samples | 77 |
| Studies with human endothelial cells | 78 |
| Isolation and culture of blood outgrowth endothelial cells (BOECs) | 78 |
| Cell plating | 80 |
| General staining protocol for staining BOECs..... | 80 |
| Cellomics | 81 |
| Data analysis and statistics | 81 |
| Chapter 3: Location of COX-1 and COX-2 immunoreactivity in blood vessels and implications for prostacyclin release..... | 82 |
| Rational | 83 |
| Specific Aims | 84 |
| Methods..... | 84 |
| Results..... | 86 |
| Expression of COX-1 and COX-2 in key regions of the freshly isolated vessel..... | 86 |
| Role of COX-1 and COX-2 in prostacyclin release by freshly isolated blood vessels. | 86 |
| Effect of time postmortem on COX-1 and COX-2 expression and activity in mouse aorta. | 86 |
| 3.5.4 Expression of COX-1 and COX-2 in key regions of the vessel after stimulation in culture..... | 87 |
| Summary..... | 89 |
| Conclusions | 90 |
| Limitation | 90 |
| Chapter 4: The link between COX-2 and eNOS..... | 97 |
| Rational | 98 |
| Specific Aims | 99 |

| | |
|--|-----|
| Methods | 99 |
| Experimental animals and tissue collection | 99 |
| Western blotting | 100 |
| RT-qPCR..... | 100 |
| LC-MS/MS measurements | 100 |
| Data and statistical analysis | 101 |
| Results | 102 |
| COX-1 and COX-2 in the kidney and role on renal markers of dysfunction | 102 |
| Effects of COX-2 gene deletion of methylarginine and amino acid levels..... | 102 |
| Effect of COX-2 gene deletion on Ddah1 and related methylarginine pathways | 103 |
| Effects of inhibiting COX-2 pharmacologically in wild type mice and in healthy human volunteers on methylarginine and other amino acid levels | 104 |
| Summery | 106 |
| Conclusions | 107 |
| Limitation | 107 |
| Chapter 5: Effects of Global COX-2 gene deletion on eNOS response in isolated aorta..... | 124 |
| Rational | 125 |
| Specific Aims | 125 |
| Methods | 126 |
| Experimental animals and tissue collection | 126 |
| Protocols for myograph studies..... | 126 |
| Data and statistical analysis:..... | 127 |
| Results | 128 |
| Effects of COX-2 gene deletion on vasomotor responses of mouse aorta | 128 |
| Effect of COX-2 gene deletion on endothelial dependent and independent relaxation responses of aorta | 128 |
| Effect of COX-2 gene deletion on the potency and efficacy of the methylarginine eNOS inhibitors and, for comparison, with L-NAME | 128 |
| Effect of COX-2 gene deletion in COX-2 knockout mice on eNOS expression..... | 129 |
| Summary | 130 |
| Limitation | 130 |
| Chapter 6: Endothelial cell morphology and shear stress: design of an algorithm to quantify alignment | 140 |
| Introduction | 141 |
| Endothelial cell morphology | 142 |
| Shear stress and the endothelium..... | 143 |

| | |
|---|-----|
| Rational | 144 |
| Specific Aims | 145 |
| Methods | 146 |
| Mouse tissue and associated staining | 146 |
| Human endothelial cells | 146 |
| Imaging..... | 147 |
| Data and statistical analysis | 147 |
| Results | 148 |
| Morphology of endothelium in the aortic arch | 148 |
| Quantification of nuclear alignment..... | 148 |
| Effect of COX-1, COX-2 or eNOS knock out on endothelial cell morphology | 150 |
| Morphology of human endothelial cells in culture versus mouse aortic arch | 152 |
| BOEC and modelling of shear stress in vitro..... | 153 |
| Summary | 154 |
| Limitations..... | 155 |
| Chapter 7: General Discussion | 170 |
| COX-2 prostacyclin hypothesis versus my work | 175 |
| The link between the kidney, COX-2 and ADMA | 176 |
| Responses to eNOS in vessels from COX-2 knock out mice. | 179 |
| Morphology of endothelial cells, correlation with regions of directional shear and influence by loss of COX-2 and eNOS | 180 |
| Implications of my work, limitations and future experiments | 182 |
| References | 184 |

List of figures

| Chapter 1 figures | Page |
|---|-------------|
| <i>Figure 1.1: COX-1 and COX-2 characteristics</i> | 26 |
| <i>Figure 1.2: Pathways leading to the synthesis of prostanoids from arachidonic and receptor subtypes preferentially activated by selected prostanoids</i> | 32 |
| <i>Figure 1.3: Prostacyclin signalling pathways including those mediated by cell surface IP receptors and by cytosolic PPARβ signalling pathways</i> | 34 |
| <i>Figure 1.4: TXA₂ signalling pathways mediated by cell surface TP receptors</i> | 35 |
| <i>Figure 1.5: PGE₂ signalling via EP receptor subtypes</i> | 37 |
| <i>Figure 1.6: Schematic that shows prostaglandin (PG)D₂ and PGF_{2α} signalling pathways</i> | 39 |
| <i>Figure 1.7: localization and function of cyclo-oxygenase (COX) in kidney substructures</i> | 43 |
| <i>Figure 1.8: Pathways that cause gastric damage by NSAIDs</i> | 48 |
| <i>Figure 1.9: selected time line of events in the area of COX-2 drugs and cardiovascular events</i> | 51 |
| <i>Figure 1.10: structures of L-arginine and related molecules where there are substitutions on the guanidino arginine</i> | 55 |
| <i>Figure 1.11: Pathways for formation, release and breakdown of methyl arginines</i> | 57 |
| | |
| Chapter 2 figures | |
| <i>Figure 2.1 COX-1 gene deletion strategy</i> | 63 |
| <i>Figure 2.2: schematic that shows the breeding setup for generating COX-1 KO mice</i> | 64 |
| <i>Figure 2.3: Strategic generation of COX-2^{-/-} mice.</i> | 65 |
| <i>Figure 2.4: The deletion of IP gene in mice</i> | 66 |
| <i>Figure 2.5: Different ways of cutting the aortic arches open</i> | 68 |
| <i>Figure 2.6 Representative 6-Keto PGF_{1α} Standard curve</i> | 71 |
| <i>Figure 2.7: Schematic shows how the vessel was loaded on the mounting jaws</i> | 76 |
| | |
| Chapter 3 figures | |
| <i>Figure 3.1: Expression of COX-1 and COX-2 in key regions of the freshly isolated vessel</i> | 92 |

| | |
|---|----|
| <i>Figure 3.2: Role of the endothelium and COX-1 and COX-2 in prostacyclin release by freshly isolated blood vessels</i> | 93 |
| <i>Figure 3.3: Effect of time post-mortem on COX-1 and COX-2 expression and activity in the endothelium of mouse aorta</i> | 94 |
| <i>Figure 3.4: Effect of time post-mortem on COX-1 and COX-2 expression in different regions of the mouse aorta</i> | 95 |
| <i>Figure 3.5: Effect of genetic knock out of COX-1 and COX-2 compared to wild type (WT) on eicosanoid formation measured using LC-MS/MS by isolated mouse aorta in vitro</i> | 96 |

Chapter 4 figures

| | |
|--|-----|
| <i>Figure 4.1: Role of COX-1 and COX-2 on renal markers of dysfunction</i> | 108 |
| <i>Figure 4.2: Effects of COX-2 gene deletion on methylarginine levels in kidney</i> | 109 |
| <i>Figure 4.3: Effects of COX-2 gene deletion on methylarginine levels in plasma</i> | 110 |
| <i>Figure 4.4: Effects of COX-2 gene deletion on plasma L-arginine levels</i> | 111 |
| <i>Figure 4.5: Effect of COX-2 gene deletion on DDAH1 in different tissues</i> | 113 |
| <i>Figure 4.6: Effect of COX-2 gene deletion on mRNA expression of DDAH1 and DDAH2 in renal medulla</i> | 114 |
| <i>Figure 4.7: Effect of COX-2 gene deletion on related methylarginine pathways (Agxt2 and Arg2)</i> | 115 |
| <i>Figure 4.8: Effect of COX-2 gene deletion on related methylarginine pathways (Prmt1)</i> | 116 |
| <i>Figure 4.9: Effect of IP gene deletion on methylarginine levels in plasma</i> | 117 |
| <i>Figure 4.10: Effect of IP gene deletion on mRNA expression of DDAH1 and DDAH2 in renal medulla</i> | 118 |
| <i>Figure 4.11: Effect of IP gene deletion on related methylarginine pathways (Agxt2 and Arg2)</i> | 119 |
| <i>Figure 4.12: Effect of IP gene deletion on related methylarginine pathways (Prmt1)</i> | 120 |
| <i>Figure 4.13: Effects of inhibiting COX-2 pharmacologically on arterial pressure in mice</i> | 121 |
| <i>Figure 4.14: The effect of Paercoxib (COX-2 pharmacological inhibitor) on the levels of plasma L-arginine in mice treated with or without Paercoxib</i> | 122 |

Chapter 5 figures

| | |
|---|-----|
| <i>Figure 5.1: Effects of COX-2 gene deletion on vasomotor responses of mouse aorta</i> | 131 |
|---|-----|

| | |
|---|-----|
| <i>Figure 5.2: Effects of COX-2 gene deletion on relaxation responses with Ach of mouse aorta with and without L-arginine</i> | 133 |
| <i>Figure 5.3: Effects of COX-2 gene deletion on relaxation responses with SNP of mouse aorta with and without L-arginine</i> | 134 |
| <i>Figure 5.4: Effect of COX-2 gene deletion on the potency and efficacy of the methylarginine eNOS inhibitor (ADMA)</i> | 135 |
| <i>Figure 5.5: Effect of COX-2 gene deletion on the potency and efficacy of the methylarginine eNOS inhibitor (L-NMMA)</i> | 136 |
| <i>Figure 5.6: Effect of COX-2 gene deletion on the potency and efficacy of eNOS inhibitor (L-NAME)</i> | 137 |
| <i>Figure 5.7: Effect of COX-2 gene deletion on Nos3 expression</i> | 139 |

Chapter 6 figures

| | |
|---|-----|
| <i>Figure 6.1: the three different regions within the mouse aortic arch</i> | 157 |
| <i>Figure 6.2: Scanning electron microscopy images of the mouse aortic arch and thoracic aorta</i> | 158 |
| <i>Figure 6.3: The steps that have been used to measure the nuclear alignment, density and size</i> | 159 |
| <i>Figure 6.4: Calculation of nuclear angle of orientation in Image J software</i> | 160 |
| <i>Figure 6.5: An outline for how the nuclear alignment density and average size were quantified</i> | 161 |
| <i>Figure 6.6: Quantification of endothelial cells in mouse aortic arch</i> | 162 |
| <i>Figure 6.7: Quantification of EC and SMC layers at 5μm, 10μm and 15μm depth</i> | 163 |
| <i>Figure 6.8: Quantification of EC in WT, COX-1 and COX-2 KO mouse aortic arches</i> | 164 |
| <i>Figure 6.9: The effect of eNOS gene deletion on the relaxation responses of mice aorta</i> | 165 |
| <i>Figure 6.10: Quantification of EC in WT and eNOS KO mouse aortic arch</i> | 166 |
| <i>Figure 6.11: Isolating blood outgrowth endothelial Cells (BOECs)</i> | 167 |
| <i>Figure 6.12: Modeling shear stress on the orbital shaker using Blood out growth endothelial cells from human</i> | 168 |
| <i>Figure 6.13: Nuclear morphology profile for human cultured cells (Blood out growth endothelial cells)</i> | 169 |

Chapter 7 figures

| | |
|--|-----|
| <i>Figure 7.1: example of comments online</i> | 171 |
| <i>Figure 7.2: Share prices for Merck Co after withdrawing Vioxx</i> | 172 |
| <i>Figure 7.3: Share prices for Pfizer after withdrawing Valdecoxib</i> | 173 |
| <i>Figure 7.4: Stepped care approach to management of musculoskeletal symptoms</i> | 174 |
| <i>Figure 7.5: COX-2/NO pathway in the Kidney</i> | 178 |

List of tables

| Chapter 1 tables | Page |
|--|-------------|
| <i>Table 1.1. Isoforms of PGE₂ synthases</i> | 30 |
| <i>Table 1.2. Receptor pathways and functions associated with prostaglandin (PG)E₂ signalling</i> | 36 |
| | |
| Chapter 2 tables | |
| <i>Table 2.1 Details of the antibodies and the Reagents that have been used for staining mouse aortic arches</i> | 67 |
| <i>Table 2.2. Antibodies information that have been used for western blotting</i> | 72 |
| <i>Table 2.3 : list of Syber Green primers used in my thesis</i> | 74 |
| <i>Table 2.4: list of Taqman primers used in my thesis</i> | 74 |
| <i>Table 2.5: List of healthy volunteer donors with successful isolations of BOEC</i> | 80 |
| <i>Table 2.6: A list of the antibodies that used in staining the BOECs</i> | 81 |
| | |
| Chapter 4 tables | |
| <i>Table 4.1: Effects of COX deletion on kidney, plasma and urine methylarginine metabolites</i> | 112 |
| <i>Table 4.2: Plasma and urine methylarginines in healthy volunteers taking naproxen or celecoxib</i> | 123 |
| | |
| Chapter 5 tables | |
| <i>Table 5.1: The effect of the admission of L-arginine on contractile responses of U46619 on mice aorta</i> | 132 |
| <i>Table 5.2: Effect of COX-2 gene deletion on the potency and efficacy of the methylarginine eNOS inhibitors and, for comparison, with L-NAME</i> | 138 |

Chapter 6 tables

Table 6.1: Development of endothelial cell imaging

143

Chapter 1: General Introduction

Discovery of COX-1 and COX-2

Cyclo-oxygenase (COX), also referred to as prostaglandin synthetase (PTGS), prostaglandin H synthase (PGHS) or prostaglandin endoperoxide synthase, is a fundamentally important enzyme system that converts arachidonic acid to prostaglandins (PGs). PGs are potent biological mediators of a wide range of homeostatic processes as well as being central to the immune system and inflammatory processes. We now know that there are two isoforms of COX: COX-1 which is known as a house keeping gene and so is expressed constitutively in all cells and COX-2 which is induced in inflammation and proliferation. COX-2 is also present constitutively in certain specialized areas of the body where there is no inflammation. COX-1 and COX-2 are very important targets for human health and well-being. COX-1 in platelets is the target for low dose aspirin that is used by millions of people to prevent heart attacks and strokes whilst COX-2 is the target for the nonsteroidal anti-inflammatory drugs (NSAIDs) used by millions of people all over the world to treat pain, inflammation and fever and they can prevent cancer. But aspirin has side effects in the gastrointestinal tract where it causes ulcers and bleeding and NSAIDs that also have side effects in the gut, cause cardiovascular events, particularly heart attacks and strokes.

COX-1

What we now know as PGs were first discovered in the 1930s where experiments using seminal fluid identified substances that contracted vascular smooth muscle in simple bioassay experiments¹. These substances were purified and their structures found to be included in a family of fatty acid molecules that have in common with each other the fact that they have 20 carbon atoms¹. The first COX enzyme (what we now know as COX-1) was purified in 1977 from sheep vesicular glands and shown to be a heme containing protein of 70 KDa². This form of COX was then sequenced in 1988³ where the full-length cDNA corresponding to 2.8 kb mRNA was found to encode a protein of 600 amino acids that had not much similarity with any other protein in amino acid or nucleotide sequence libraries at the time. When they cloned this first COX the authors said *'the availability of a full-length cDNA clone coding for prostaglandin G/H synthase (COX) should facilitate studies of the regulation of expression of this enzyme and the structural features important for catalysis and for interaction with anti-inflammatory drugs'*³. They could not have known at the time

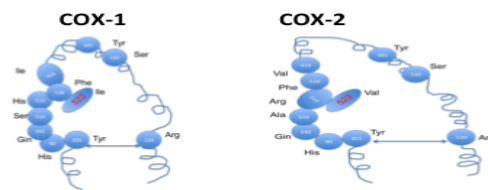
that only a year or so later their work could be used to show a completely new form of COX, what we now know as COX-2.

COX-2

In the years of 1989-1991 three groups all working on completely different projects found in their experiments what we now know is COX-2. The first study was by Rosen in 1989 who was working on airway epithelial cells and pathways that regulate their growth. In their experiments they stimulated sheep airway epithelial cells with serum and showed that the PGs they were releasing were increasing when the cells proliferated⁴. They showed that a 70 KDa COX protein and corresponding 2.8 kb mRNA (which we now know is COX-1) was expressed but that levels did change in the same way as the PG release did change. They used Northern blots probed at low stringency (which means their probe would not be so specific and might pick up related entities) to find what they called *'a new tissue-specific 4.0 kb mRNA species exhibiting increased expression during cell culture'* and that *'is derived from a distinct gene. Its relatedness to cyclooxygenase and its increase in parallel with enzymatic activity further suggest that the larger mRNA may encode for a cyclooxygenase'*⁴. Then in a separate group looking at completely different biology questions the scientists in the group found what we now know is COX-2 because they were looking at sequences of genes induced by the cancer-mitogen TPA⁵. This group directed by Professor Herschman was interested in cancer and had been working on all genes induced by TPA, they called these genes TIS genes which stands for 'TPA inducible sequence' genes⁶. They found that the TIS-10 gene that is induced in mouse fibroblasts by TPA encoded a protein with a predicted 604 amino acid and that *'a computer search identified striking similarities between the predicted TIS-10 protein product and the murine, sheep and human prostaglandin synthase/cyclooxygenase proteins'*⁵. In the same year (1991) a group lead by Professor Simmons used rous sarcoma virus to stimulate chicken embryo fibroblasts and found a new gene that they called CEF-147⁷. CEF-147 encoded the same ≈600-amino acid protein found by the other groups and went on to show that protein sequence of CEF-147 shared 59% amino acid identity with sheep prostaglandin G/H synthase (that was the gene they had already in the database and what we now know is COX-1). Fitting in with the other two studies and proliferating cells Professor Simmons stated that *'a distinguishing feature of src-*

*inducible prostaglandin synthase mRNA is its low abundance in nonproliferating chicken embryo fibroblasts and its relatively high abundance in src-transformed cells*⁷.

The first demonstration of human COX-2 was using activated human endothelial cell by Professor Hla's group in 1992⁸. This paper was also the first to show that the new form of COX found at the time could actually make PGs⁸. The previous studies^{5,7} showed sequence homology but not actual enzyme function. Thus, two isoforms of COX are encoded by different genes and on different chromosomes but have about 60% sequence identity with the greatest similarity at the catalytically important sites. The three-dimensional structures for COX-1 and COX-2 have many superimposable regions and both isoforms are homodimers of ≈600 amino acids. For both COX-1 and COX-2 cyclooxygenase and peroxidase active sites are located in the catalytic domain⁹. For COX-1, PTGS-1 is the gene that *codes for a 2.8 kb mRNA that is relatively stable. By contrast, PTGS-2 is the gene that codes the 4 kb COX-2 mRNA and contains an unstable sequence in the 3'-untranslated region*¹⁰. The main difference between the two isoforms is the location of the amino acid residue 523 on the active site. In COX-2, the valine-523 has a wider central channel compared to the isoleucine-523 in COX-1, which also gives an additional hydrophobic side pocket within the substrate-binding site. This larger active site has been used as a helpful difference for designing selective inhibitors of the COX-2 isoform because larger molecules can fit in it than in the smaller site of COX-1 (Figure 1.1).



| | COX-1 | COX-2 |
|----------------------------------|--|---------------------|
| Expression | constitutive | induced |
| mRNA size | 2.8kb on chromosome 9 | 4kb on chromosome 1 |
| Protein molecular weight | 70 kDa | 72/74 kDa |
| Similarities in structure | Both isoforms contain the three main domains; helical membrane binding domain, the catalytic domain, and the terminal epidermal growth factor (EGF) domain | |
| Differences in structure | The amino acid residue 523 on the active site for COX-2, (valine-523) has a wider central channel compared to the same residue (isoleucine-523) in COX-1, thus COX-2 has an additional hydrophobic side pocket within the substrate-binding site | |

Figure 1.1: COX-1 and COX-2 characteristics. Cyclo-oxygenase (COX)-1 and COX-2 share 60% homology with important differences at the gene, message and protein level. COX-2 has a

larger active site due to a polar hydrophilic side-pocket that forms due to substitution of Ile523, His513, and Ile434 in COX-1 by Val523, Arg513, and Val434 in COX-2.

Products of COX and associated synthetic pathways

There is sometimes confusion about the terms used to refer to 'COX products' and in what actually constitutes a direct product of the enzyme COX. Eicosanoids are biologically active molecules made by oxidation of 20-carbon fatty acids, either omega-3 (ω -3) or omega-6 (ω -6) fatty acids. Eicosanoids are grouped into sub categories including the PGs, thromboxanes (TX), leukotrienes, lipoxins and eoxins. Prostanoids are a subgroup of eicosanoids formed from arachidonic acid and is used as a term to collectively refer to the PGs, thromboxane and the prostacyclin. To be completely correct there is just one prostanoid product of COX which is PGH_2 . However because PGH_2 is the substrate for other prostanoids including prostacyclin and TXA_2 which are in fact formed by downstream synthase enzymes, all of the prostanoids are commonly referred to as 'COX products'.

Prostanoids are synthesized in the cells as a response to hormonal stimuli or physical disturbance. The first step in their synthesis begins after any stimulus that increases intracellular calcium. Consequently, phospholipase A_2 (PLA_2) is activated which cleaves arachidonic acid from membrane-bound lipids. COX then converts arachidonic acid to PGH_2 in a two-step action: the 'oxygenase' site incorporates two molecules of oxygen into the arachidonic acid to form PGG_2 and the peroxidase activity catalyzes a 2-electron reduction of PGG_2 to PGH_2 (Figure 1.2).

There are four classes of phospho-lipases: PLA (PLA_1 and PLA_2), PLB, PLC, and PLD, that are grouped according to the bond hydrolyzed on phospholipid substrates. PLA_2 is needed to be present to liberate free arachidonic acid and more than 30 isoforms have been identified including; cytosolic (cPLA_2), calcium-independent (iPLA_2) and secretory (sPLA_2). Both cPLA_2 and sPLA_2 are calcium dependent enzymes, however, they require different concentrations of calcium to be active, e.g. cPLA_2 needs micromolar (μM) concentrations of calcium for their activation and sPLA_2 needs millimolar (mM) concentrations of calcium for activation¹¹. Unlike cPLA_2 and sPLA_2 , iPLA_2 is not a calcium dependent enzyme¹².

PLA₂'s play an important role in regulating inflammation and smooth muscle contraction. It has been reported that during prostanoid synthesis, activation of cPLA₂ and sPLA₂ is the common route for liberating arachidonic acid. In 2011, Murakami et al. reported that iPLA₂ plays a role in phospholipid remodelling and not in the signalling¹¹.

Since PLA₂ was found to play a critical role in liberating arachidonic acid, researchers became more interested in studying PLA₂ especially considering that anti-inflammatory drugs exert their effects (inflammation and pain relief) through inhibiting arachidonic acid metabolism. A full description of PLA₂ biology is found in the review by Professor Dennis¹³

Specific prostanoids production and biological actions of COX products

The production of specific prostanoids not only depends on COX but more importantly depends on the presence of the isomerase/synthase enzymes and to add a layer of complexity, the biological effects depends on the distribution of the prostanoid receptors (7 trans-membrane G-protein coupled receptor (GPCRs)) and/or peroxisome proliferator activated receptors (PPARs) within surrounding cells. Once PGH₂ is formed by COX it is further metabolised to a range of prostanoids by the 'downstream synthases'¹⁴. For my thesis I have focused on prostacyclin, thromboxane and PGE₂.

Prostacyclin and prostacyclin synthase

Prostacyclin was first discovered in 1976 by the Nobel Prize winner Sir John Vane¹⁵. Since then there have been many studies carried out investigating the structure and the function of prostacyclin. Prostacyclin is a very important protective hormone made in the endothelium of all blood vessels. Its actions include vasodilation, inhibition of platelet activation and reduction in processes linked to atherosclerosis¹⁶. The signaling of prostacyclin and its relevance to cardiovascular disease is discussed later in the introduction. Prostacyclin is formed once PGH₂ has been made by COX due to the action of prostacyclin synthase. Because endothelial cells are enriched with both COX and prostacyclin synthase blood vessels are the main site in the body where prostacyclin is made¹⁷⁻¹⁹. Prostacyclin synthase is also known as prostaglandin-I synthase (EC 5.3.99.4) or CYP8A1 and it is encoded by *PTGIS* gene. The protein was first purified by Professor De Witt in 1983²⁰ where it was

found to be an iron containing protein of 52 KDa molecular weight²⁰. Prostacyclin synthase, as is the case with TX synthase (see below) is suicide inactivated²¹ which means that once it has fulfilled its biochemical activity it is inactivated and requires new protein to be made to maintain prostacyclin release. This helps to explain why prostacyclin is often released in bursts and why any basal release of prostacyclin is usually low. This might be important when thinking about the endothelium and how it makes protective hormones such as prostacyclin and NO (see below). Prostacyclin is released for a shorter time than NO when cells are stimulated with a particular agonist²² although this is not the whole story because endothelial cells can be made to release prostacyclin for longer times when they are given the substrate, arachidonic acid, directly²². Mutations and polymorphisms in the prostacyclin synthase gene have been reported and shown to be linked with essential hypertension, myocardial infarction, and cerebral infarction²³.

TX and TX synthase

TX found in platelets was discovered in 1975 by the group of the Noble Prize winner Professor Bengt Samuelsson²⁴. The two major TXs are TXA₂ and TXB₂. TXA₂ is the active form but is an unstable intermediate with a half-life of 30 seconds that is then broken down to the inactive TXB₂. TXA₂ is a powerful mediator that acts in direct opposition to prostacyclin. This means that it is a vasoconstrictor, activates platelets and stimulates many of the processes associated with atherosclerosis²⁵. Before its structure was known about TXA₂ was discovered and studied as a unknown biological factor known as rabbit aorta contracting substance (RCS)²⁶.

The production of TXA₂ depends on the conversion of PGH₂ from COX by the enzyme TXA synthase. TXA₂ synthase is also known as TBXAS1 (CYP5A1 gene) and, like prostacyclin synthase, is a cytochrome P450 type enzyme. In humans, is encoded by the TBXAS1 gene. The human TXA₂ synthase is also similar to prostacyclin synthase in that it is a 60 KDa protein with 533 amino acids and a heme prosthetic group. It is well know that the platelet is the major site that release TXA₂ is released and they are also the main site for TXA₂ synthase expression. Genetic polymorphisms in TXA₂ synthase have been found²⁷ and in some studies has been linked to stroke. The reason suggested was that the reduced function

of TXA₂ synthase would mean that the cardioprotective actions of aspirin could not be achieved in those patients²⁸.

PGE₂ and PGE₂ synthase enzymes

PGE₂ is a major mediator of inflammation in diseases such as rheumatoid arthritis and osteoarthritis. PGE₂ also has important roles in the cardiovascular system but because the effects of PGE₂ are more complex than those of prostacyclin or TXA₂ (because of opposing actions of its receptors; see below) it is generally considered as a mediator in terms of inflammation, fever and cancer.

The production of PGE₂ from PGH₂ formed by COX requires the action of prostaglandin E synthase (PGES)²⁹, of which there are three forms of the gene: mPGES-1, mPGES-2 and cytosolic (cPGES, PTGES3)²⁹. It was also thought that PGE₂ could be formed directly from PGH₂ in some conditions without the need for any downstream enzymes; this is why PGE₂ is commonly measured as a readout for COX activity¹⁴. Details of the three forms of PGES are given in Table 1.1 and discussed in a little more detail below.

| PGE ₂ isoforms | mRNA size | Protein molecular weight | Subcellular location | Transcriptional regulation | Tissue distribution |
|---------------------------|-----------|--------------------------|------------------------------|----------------------------|--|
| mPGES-1 | 14.8 kb | 15—16 kDa | Nuclear membrane | Inducible | Prostate, testis, placenta, mammary gland, bladder |
| cPGES | 1.9 kb | 26 kDa | Cytoplasm Y Nuclear membrane | Constitutive | Ubiquitous |
| mPGES-2 | 2 kb | 33 kD | Golgi Y Cytoplasm | Constitutive | Brain, heart, skeletal muscle, kidney, liver |

Table 1.1. Isoforms of PGE₂ synthases.

mPGES-1

Human mPGES-1 was first identified in 1999 by Professor Jakobsson³⁰. There are parallels between mPGES-1 and COX-2. For example, both COX-2 and mPGES-1 are inducible genes. The expression of mPGES-1 is induced in cells and tissues by inflammatory stimuli and so is thought to be an important target for drugs in the treatment inflammatory diseases such as arthritis and cancer^{31,32}. Studies where deletion of mPGES-1 encoding gene had been made gave rise to the link between mPGES-1 and the production of PGE₂ in inflammatory

conditions. mPGES-1, is an membrane bound protein and three units of mPGES-1 form the active enzyme. mPGES-1 needs glutathione for its catalytic activity. As mentioned above, in normal cells mPGES-1 is expressed at low levels but upon pro-inflammatory stimuli, endotoxins and growth factors, e.g. interleukin-1 β lipopolysaccharide (LPS) and epidermal growth factor³¹, the enzyme is induced. The interesting thing about mPGES-1 is that because it is induced by the same things that induces COX-2 it is thought to be directly linked to PGE₂ production by PGH₂ produced by COX-2 more than COX-1. This has led to the suggestions that mPGES-1, rather than other forms of PGES, could be a better target than COX-2 for drugs to treat inflammation, pain, fever and cancer³¹. This is because inhibiting PGES reduces PGE₂ but does not affect TXA₂ or prostacyclin.

cPGES

cPGES is expressed constitutively in a variety of tissues and cells and unlike mPGES-1 is not affected by pro-inflammatory stimuli. cPGES resides most often in the cytosol but moves to endoplasmic reticulum after calcium ionophore challenge. Because cPGES is constitutively expressed it is thought to be one of the isoforms that converts COX-1-derived PGH₂ to PGE₂²⁹, but not COX-2-derived PGH₂ to PGE₂ in cells, particularly during the immediate PGE₂- that is released as a response elicited by calcium-evoked stimuli. It co-localizes with COX-1 in the endoplasmic reticulum, rather than with nuclear COX-2, following cell activation. This may account, at least to some part, for its favourable coupling with COX-1, although there could be other regulatory mechanisms happen in this regard. Thus, in line with the roles of COX-1 in vivo, cPGES may contribute physiologically to the production of PGE₂ required for the maintenance of tissue homeostasis in the healthy body.

In a comprehensive study published in Nature in 2009 the role of PTGES gene polymorphism in susceptibility to severity of arthritis was studied in a Swedish population and found to have an association amongst women. Several PTGES SNPs were associated with disease and higher mPGES-1 expression was found in synovial tissue³³.

mPGES-2

mPGES-2 was first purified in 1999 from the microsomal fraction of bovine heart³⁴. Human and donkey cDNAs were subsequently after that identified in 2002³⁵. mPGES-2 is structurally

different to mPGES-1. At 41 kDa protein and 378-385 amino acids it is larger than mPGES-1, which is 16 kDa and 152-153 amino acids. In addition mPGES-2 does not really depend on glutathione for its catalytic activity. It is not clear under which conditions mPGES-2 regulates PGE₂ production this was not helped by the information from mice that are lacking mPGES-2 that showed no specific phenotype and no alteration in PGE₂ levels in several tissues including the liver, kidney, heart, and brain or in LPS-stimulated macrophages³⁶.

Other prostanoid synthase pathways

In addition to prostacyclin, TXA₂ and PGE₂ COX derived PGH₂ can be converted by specific downstream synthase enzymes to PGD₂ and PGF_{2α} by specific isomerase enzymes. Whilst these pathways are important, for example as mediators of allergy and labor, they have not featured in my thesis but are discussed in detail elsewhere^{37,38}.

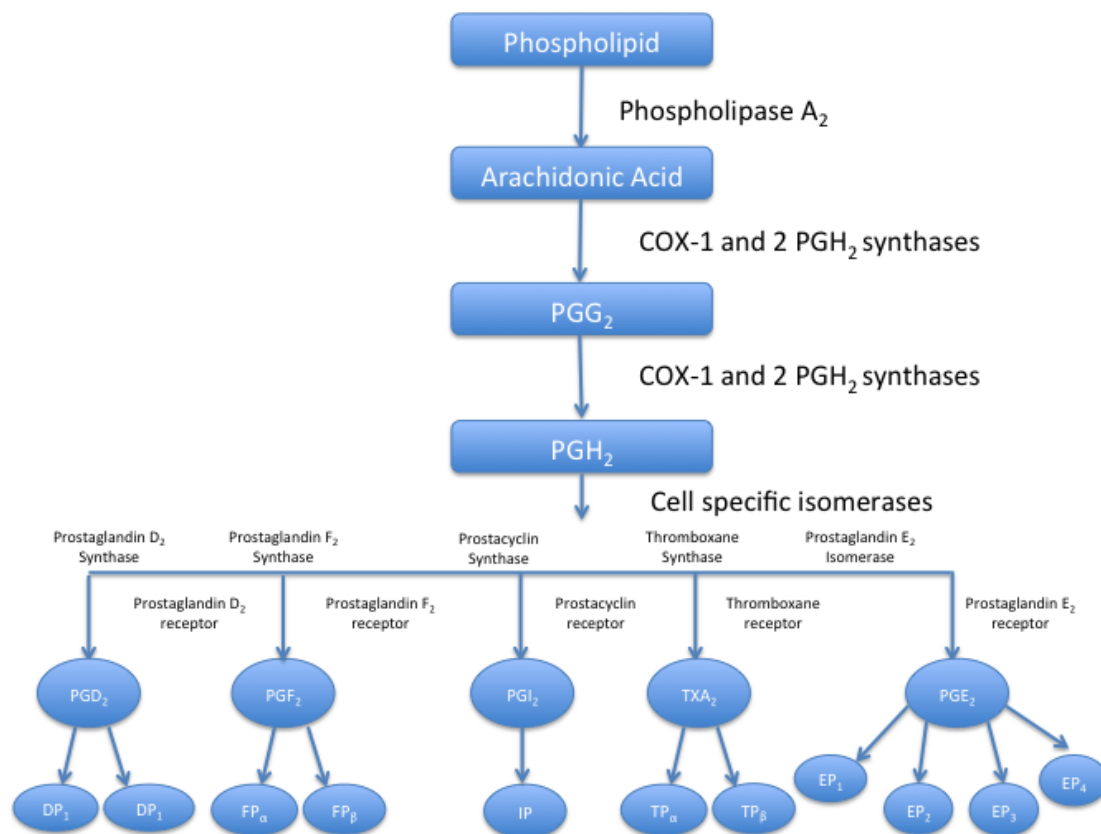


Figure 1.2: Pathways leading to the synthesis of prostanoids from arachidonic and receptor subtypes preferentially activated by selected prostanoids.

Prostanoid receptors

There are five well-defined prostanoid receptors named according to the first letter of their primary ligands: PGD₂ (DP), PGE₂ (EP), PGF_{2α} (FP), prostacyclin (IP) and TXA₂ (TP)³⁹ (Figure

1.2). The activation of each prostanoid receptor is associated with the activation of different signal transduction pathways that are leading to a wide range of biological effects including platelet activation/inhibition, cell proliferation/inhibition, sleep induction, fever induction and smooth muscle contraction/relaxation⁴⁰.

Prostacyclin and IP receptors

Prostacyclin acts on two main types of receptor. These are prostacyclin receptors on the surface of cells called IP receptors and prostacyclin can also activate the cytosolic nuclear receptor PPAR β ⁴¹. IP receptors are G protein-coupled receptors, which are a large family of 7- seven-transmembrane domain receptors. IP receptor activation causes activation of membrane bound adenylate cyclase which then causes the conversion of ATP to the intracellular signalling molecule cAMP. cAMP then phosphorylates protein kinase A leading to alterations in calcium within cells resulting in, for platelets inhibition of activation and for vessels vasodilation. cAMP also works through a second pathway defined by the actions of exchange protein directly activated by cAMP (EPAC). There are 2 EPAC isoforms, EPAC1 and EPAC2⁴². Both EPACs are guanine-nucleotide exchange factors for the Ras-like GTPases, Rap1 and Rap2. Rap1 and Rap2 operate separately to the originally defined cAMP pathway of protein kinase A. Once it has been made the intracellular concentration of cAMP is kept low in cells because of breakdown by cAMP phosphodiesterases (PDEs) such as PDE4. Prostacyclin can also activate the PPAR β ^{41,43} which is a cytosolic nuclear receptor. Less is known about the relative role of PPAR β in prostacyclin signalling but it has been shown to mediate some of the anti-platelet effects^{44,45} and remodelling in fibroblasts⁴⁵, kidney⁴⁶ and heart^{47,48} that is a result of either by endogenous prostacyclin being present^{41,46} or by exogenous prostacyclin drugs such as treprostinil⁴¹. Prostacyclin can also activate tumour cells via PPAR β ⁴⁹.

The signalling of PPAR β can happen via genomic and non-genomic pathways. Firstly activation of PPAR β can go through the classical PPAR-RXR signalling to regulate target gene induction. Secondly because PPAR β binds up BCL-6 when the PPAR β is activated by agonists this causes the PPAR β to release the BCL-6 that it had bound to it and that the BCL-6 is then free to do its anti-inflammatory signalling. Thirdly activated PPAR β binds and then represses PKC α causing a block on PKC α signalling^{41,44} (Figure 1.3).

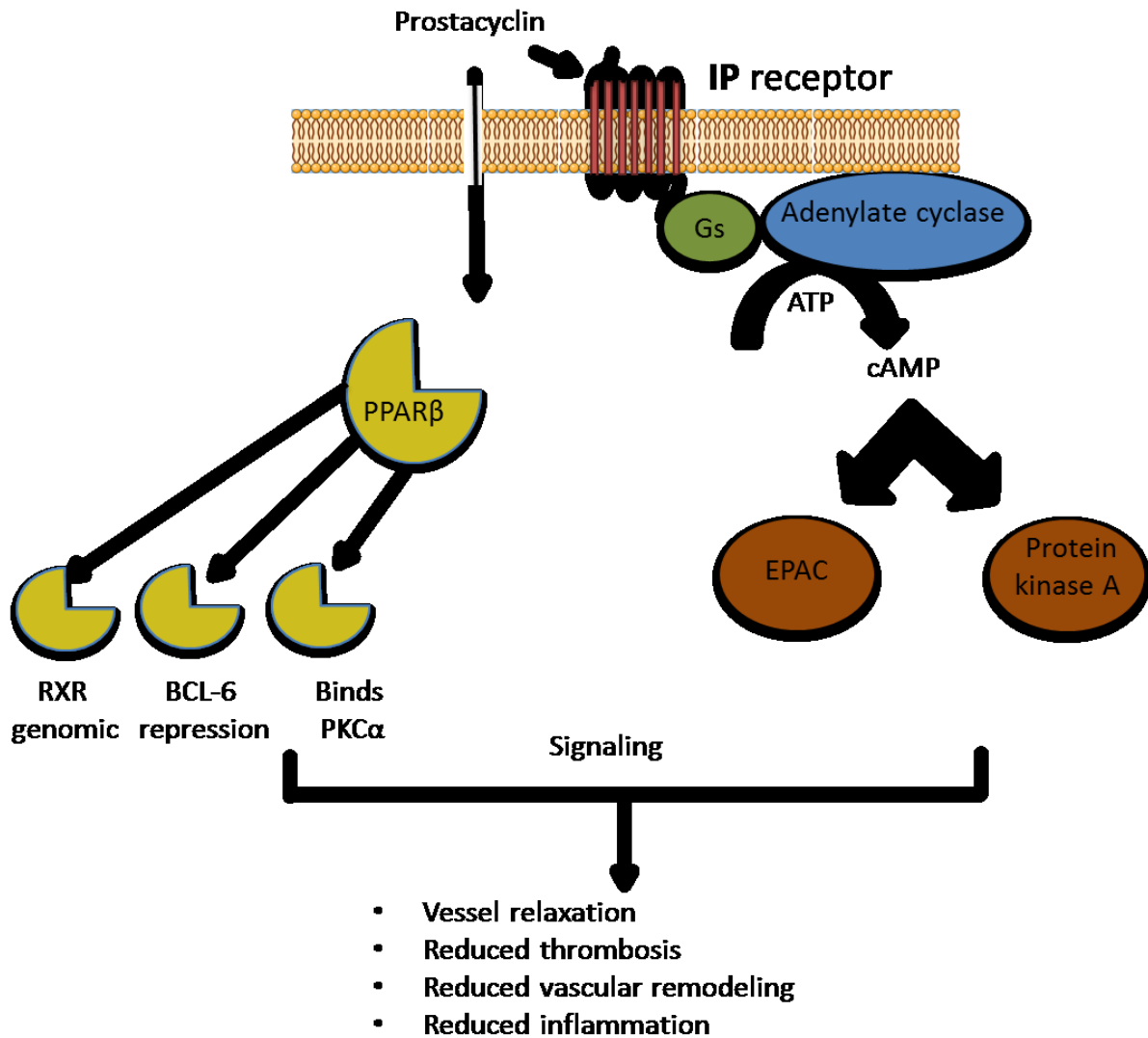


Figure 1.3: Prostacyclin signalling pathways including those mediated by cell surface IP receptors and by cytosolic PPARβ signalling pathways. Prostacyclin activates cell surface G protein-coupled IP receptor linked to the Gs alpha subunit that is linked to activation of adenylate cyclase that converts ATP to cAMP. cAMP then activates protein kinase A (PKA) or activates 'exchange proteins activated by cAMP' (EPAC). Prostacyclin also activates peroxisome proliferator-activated receptor (PPAR)β which then acts by (i) genomic pathways via retinoid X receptor (RX), (ii) release of bound and repressed 'B-Cell Lymphoma 6' (BCL-6) and/or (iii) binding and repressing protein kinase C (PKC)α. Figure is modified from Mitchell et al., 2014⁴¹ and Lezoualc 2016⁴².

Genetic variants in the human IP receptor such as V25, R212H⁵⁰ and V53V/S328S⁵¹ have been identified and shown to affect receptor function and susceptibility to deep vein thrombosis⁵¹.

Thromboxane and TP receptors

Thromboxane plays an important role in platelet aggregation and smooth muscle constriction which is mediated by action of the TXA₂ TP receptor. The TP receptor was cloned in 1991⁵² and like the IP receptor is a G protein–coupled receptor. From the same gene on chromosome 19p13.3 two separate TP isoforms are formed called TP α and TP β . TP α is expressed in many cells and tissues including platelets⁵³ but TP β is more rare but is present on endothelial cells. The most well-characterized TP signalling is through G α which TP agonists activate leading to activation of recruitment of the phosphoinositide second messenger system and formation of diacylglycerol (DAG) causing activation of protein kinase C and IP₃ and increased calcium⁵³ (Figure 1.4). TP α receptors are also shown to be linked to the heterotrimeric G proteins G₁₂ and G₁₃⁵⁴. TXA₂ mediated G₁₃ signalling through the Rho kinase pathway is thought to mediate platelet shape change and granule secretion 62 (Figure 1.4).

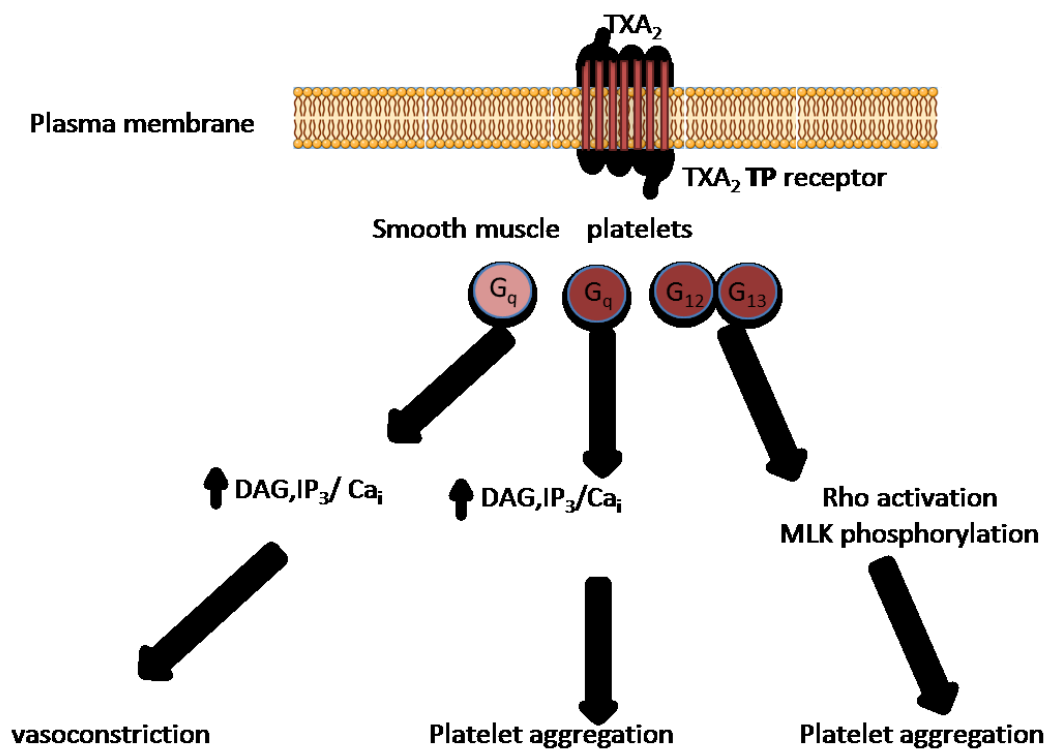


Figure 1.4: TXA₂ signalling pathways mediated by cell surface TP receptors. Thromboxane (TX)A₂ binds to its cell surface surface G protein–coupled receptor TP which in smooth muscle and platelets is linked to to G α subunit resulting in increase in diacylglycerol (DAG) and inositol trisphosphate (IP₃) to increase intracellular calcium (Ca_i). In platelets TP receptors are additionally linked to G₁₂ and G₁₃ which is linked to Rho activation and mixed lineage kinase (MLK). These signaling events result in contraction of smooth muscle and aggregation of platelets.

Identification of functional polymorphisms of the TP receptor gene have been identified⁵⁵ and in other studies TP receptor polymorphisms were associated with human disease of asthma⁵⁶, cerebral⁵⁷.

PGE₂ and EP receptors

PGE₂ is a major product of PGH₂ from COX where prostacyclin synthase and TX synthase are not expressed or are overwhelmed by substrate (PGH₂). The receptor signalling for PGE₂ is particularly complicated because it can bind to four different PGE₂ receptors, these are EP₁, EP₂, EP₃, and EP₄, each of which are encoded by distinct genes. The pathways are activated from their binding are listed below (Table 1.2).

| Prostanoid | Receptors | Signal Transduction | Main functions |
|------------------|-----------------|---|--|
| PGE ₂ | EP ₁ | G _q coupled Increase inositol phosphate3 and Ca ²⁺ | <ul style="list-style-type: none"> • Pain signaling • Bronchostriction |
| | EP ₂ | G _s coupled Activates adenylate signalling resulting in increase cAMP | <ul style="list-style-type: none"> • Deactivation of mast cell • Bronchodilation • Vasodilation |
| | EP ₃ | G _i coupled Inhibits adenylate cyclase resulting in decrease cAMP | <ul style="list-style-type: none"> • Fever • Vasoconstriction • bronchoconstriction |
| | EP ₄ | G _s coupled Activates adenylate signalling resulting in increase cAMP | <ul style="list-style-type: none"> • Deactivation of mast cell • Bronchodilation • Vasodilation |

Table 1.2. Receptor pathways and functions associated with prostaglandin (PG)E₂ signalling.

As with the other prostanoid cell surface receptors EP receptors are G protein–coupled receptors but there is now increasing evidence that they can be expressed on the nuclear membrane too. The EP₂ and EP₄ receptors are linked to stimulation of adenylate cyclase

and increased cAMP and PKA signalling. EP₄ can also activate PI3K whilst the EP₁ receptor leads to elevation of intracellular calcium (Figure 1.5). The EP₃ subtype exists in multiple isoforms which are generated through alternative splicing which signalling separately and cause different intracellular responses. The nuclear localization of EP receptors include EP₁, EP₂, EP₃ α , and EP₄. The effect of nuclear EP receptors is not yet clear.

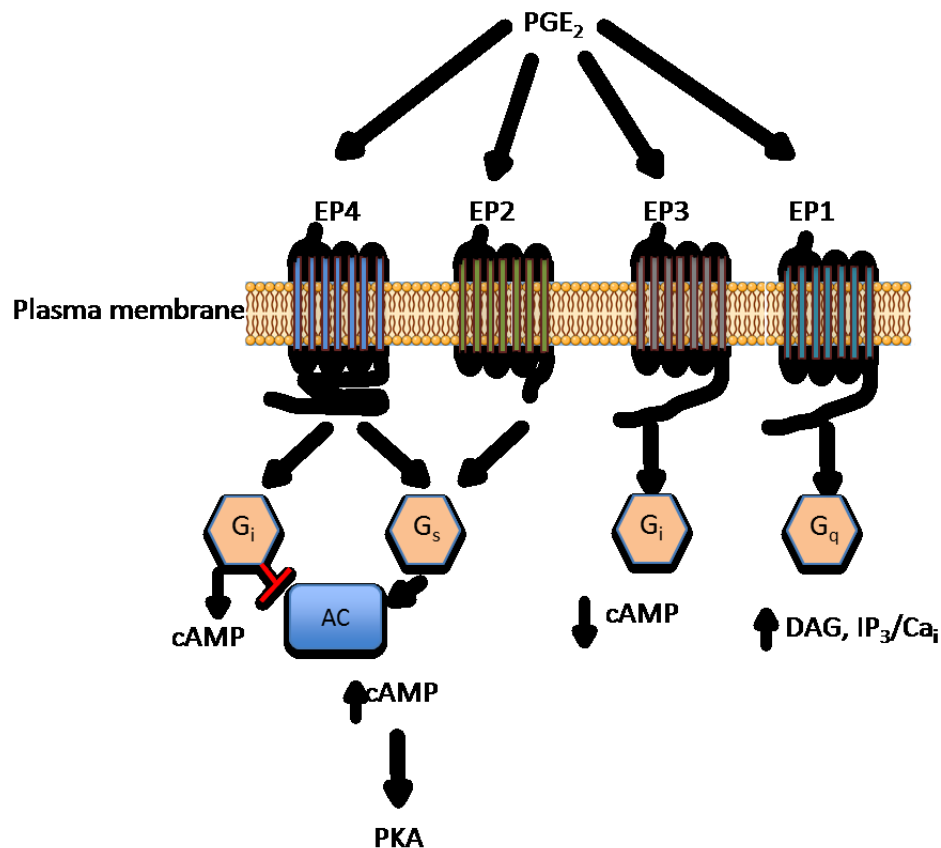


Figure 1.5: PGE₂ signalling via EP receptor subtypes. Prostaglandin (PG)_{E2} activates four receptors EP₁₋₄, each linked to different G protein mediated pathways. EP₂ and EP₄ receptors are linked to stimulation G_s and subsequent activation of adenylate cyclase (AC), increase in cAMP and activation of protein kinase A (PKA). EP₄ can also reduce AC activity via G_i. The EP₁ activates via G_q to increase diacylglycerol (DAG) and inositol trisphosphate (IP₃) to increase intracellular calcium (Ca_i). EP₃, like EP₄ acts via G_i to inhibit AC and. Modified from ⁵⁸.

Because the EP receptors can act with opposing function, such as with EP₂ causing vasodilation and EP₃ causing vasoconstriction the final effect of PGE₂ in a certain tissue at a certain time will depend upon which of the EP receptors are most highly expressed. This has provided scientists with a therapeutic opportunity. For example it has been suggested that selective EP₂ agonists as neuroprotective agents⁵⁹ and EP₄ agonists in the treatment of

cardiovascular disease including acute myocardial infarction⁶⁰. In cancer the role of specific EP receptors maybe dependent on the stage of malignancy and the type of cancer. In breast cancer EP2 and EP4 are therapeutic targets⁵⁸ whereas in colon cancer EP3 and EP1 have roles in the disease⁶¹.

PGF_{2α} and FP receptors and PGD₂, DP receptors, CRTH2, and PPAR

PGF_{2α} plays an important role in the physiological process such as hypertrophic cell growth, the induction of interleukin synthesis, luteolysis and uterine contraction and is used with PGE₂ to induce labour. PGF_{2α} binds to FP, EP1 and EP3 receptors. Two splice forms of FP (FPA and FPB) exist in humans⁶². Binding PGF_{2α} to its receptors through the activation of the heterotrimeric G-protein Gq (Figure 1.6) and with this property activates a subset of signalling cascades including PLC and subsequently calcium release and activation of protein PKC⁶². PKC activates the Mitogen-activated protein (MAP) kinase pathways via Raf (MAP kinase kinase kinase) and MEK (MAP kinase kinase). Moreover, other pathways can be activated when the activation of PGF_{2α} occurs via Gi, leading either direct activation of the Ras pathway, or indirection activation through Shc-GRB2-SOS complex formation. The activation of the MAP kinase pathway mediates cell growth, mitogenesis and uterine contraction.

PGD₂ is like PGI₂ in that it inhibits platelet aggregation and causes relaxation of both vascular and non-vascular smooth muscle cells. PGD₂ binds and activates two G-protein-coupled receptors; DP1 receptors expressed on a number of cell types and chemoattractant receptorhomologous molecule (CRHT2; DP2) expressed on T Helper type2 cells (Figure 1.6). These two receptors are important in allergy but their particular roles and how they function together or antagonistically is complex and still being worked out but antagonists of CRHT2 may show promise in allergic disease⁶³. Binding to the DP receptor mediates several physiological events such as cell survival, sleep induction and allergic responses¹⁸. PPAR_γ may also be a receptor for PGD₂ but how this receptor works with DP and CRHT2 in causing the effects of PGD₂ is not completely confirmed.

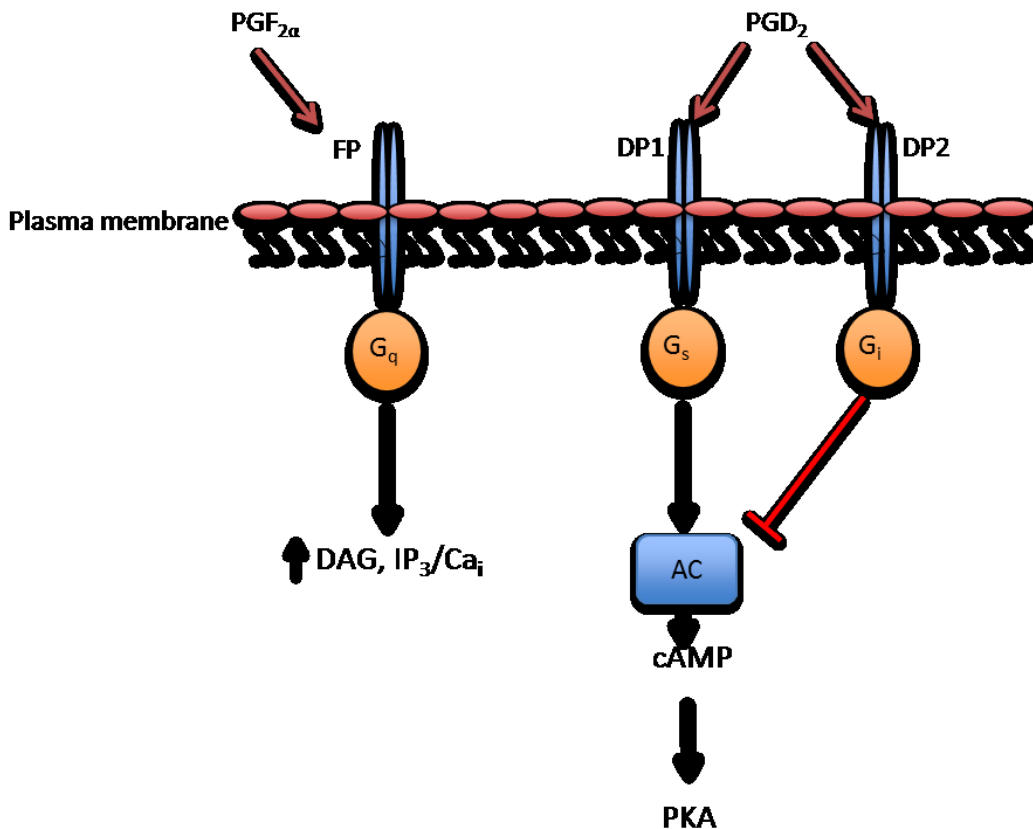


Figure 1.6: Schematic that shows prostaglandin (PG)D₂ and PGF_{2α} signalling pathways. PGD₂ and PGF_{2α} activate surface G-couple receptors (FP and DP) linked to G_q, G_s and G_i signalling pathways.

Role of prostanoids in health and disease

As mentioned above prostanoids are very important signaling molecules that are involved in all aspects of health and disease. In regard of the controlling of homeostatic processes my PhD has focused on the cardiovascular and renal systems but prostanoids also regulate aspects of immunity, endocrinology, neurology, reproduction and gastrointestinal and airway functions. In disease prostanoids mediate inflammation, infection, pain, fever and cancer. Because my work has concentrated on trying to work out how loss of COX-2 might be involved in the cardiovascular side effect caused by the NSAIDs I have restricted information here to the role of prostanoids in inflammation and in the cardiovascular system and where relevant linked them into what is known about NSAIDs in these systems.

Prostanoids in inflammation, pain and fever

The role that prostanoids have in inflammation, pain and fever are extremely well established. Prostanoids play an important role in generating inflammatory responses. The

biosynthesis of PGs increases in inflamed tissue resulting in the development of the cardinal signs of acute inflammation. In 1971 Vane demonstrated the mechanism of action for aspirin (acetylsalicylic acid) and other aspirin-like drugs and that was through inhibiting PG biosynthesis⁶⁴. This finding highlighted to the world the important role of PG biosynthesis as an inflammatory mediator⁶⁵. More specifically, as explained earlier and below it is now known that COX isoforms are targets of NSAIDs. COX-2 is weakly constitutively present in inflammatory cells but is rapidly induced during inflammatory responses and cellular differentiation. More importantly, COX-2 plays a clear role at inflammatory sites. Mice lacking COX-2 have a reduction in acute inflammation and in PGE₂ production in the air pouch model of inflammation⁶⁶. Now we know that in terms of inflammation prostanoids, working on the receptor pathways explained above, mediate leak of the endothelium, which breaks the barrier for plasma and causes swelling but it was in the early 1970s that Professor Timothy Williams first showed how prostanoids (PGE₂) caused leak by acting together with vasodilators in a synergistic way⁶⁷. Prostanoids also mediate the recruitment of inflammatory cells to the site of inflammation. Swelling and the presence of inflammatory cells will by itself be a painful thing but prostanoids will also act on pain nerves directly without the need for an actual inflammation situation happening. The main prostanoid for pain is thought to be PGE₂ which in peripheral nerves sensitizes primary afferent nerves via EP1 and EP4 and interactions with TRPV1 channels and bradykinin receptors. PGE₂ can also be a signal for pain in the central nervous system being released in the spinal cord and brain and where it can act both presynaptic and post-synaptically. EP2 is expressed in spinal cord neurons of the nociceptive system whilst EP1, EP3 and EP4 are expressed in primary pain afferent nerves⁶⁸.

Prostanoids mediate fever and this is why NSAIDs reduce our temperature when we are ill. In humans and in animal models it is COX-2 driven PGs that produce fever with work from my group showing that COX-2 knock out mice have a reduced temperature response to LPS⁶⁹. Also COX-2 selective NSAIDs reduce fever in people in the same way that non-selective drugs do. Acting on cell surface receptors described above, it is thought that PGE₂ and prostacyclin are the main prostanoids that mediate fever.

As mentioned, NSAIDs are used to treat arthritis but it is important to say that they do not modify the disease, they control the symptoms of pain. In fact it is increasingly known that prostanoids are involved in wound healing and resolution⁷⁰, which explains why NSAID can delay these processes in some conditions.

Inflammation is not only a bad thing to be blocked it is also very much an essential part of the immune response. Prostanoids are known to be very important in modulating immune responses with recent work highlighting, in addition to PGE₂, prostacyclin⁷¹. The delay in resolution known to happen with use of NSAIDs can in part be explained by the loss of proper function of immune cells that is mediated by prostanoids.

Gastrointestinal tract

The protective role of prostanoids in the stomach and the gut are very well known. Prostacyclin is a very important mediator in protection in the gut where it protects the gastric mucosa from gastric acid, keeps blood flow correct and reduces inflammation. In fact PGE₁ (which activates IP receptors) has been used as a treatment with NSAIDs (diclofenac) to protect the stomach in a formulation called Arthrotec. The gastrointestinal side effects of NSAIDs are an important problem and were the main reason that COX-2 selective drugs were brought to the clinic. These side effects show how important prostanoids are in protecting the gut. When COX-2 was first discovered it was thought that COX-1 was the main form of COX in the gut and so selective COX-2 NSAIDs would have fewer side effects. However we now know that both COX-1 and COX-2 prostanoids are formed in and protect the gut⁷². In 2000 Professor Wallace showed that blocking either only COX-1 or COX-2 did not damage the gut but that blocking both together, as happens with traditional non-selective NSAIDs caused damage⁷². This explains why selective COX-2 drugs are less damaging to the gastrointestinal tract than older style NSAIDs.

As well as the stomach prostanoids also are in other regions of the gut but it is important to mention that prostanoids, particularly PGE₂ is linked to cell turnover and cancer in the colon. Because of these facts NSAIDs, particularly aspirin⁷³ and COX-2 inhibitors can prevent colon cancer⁷⁴.

Renal and Cardiovascular function

COX and prostanoids have major regulation functions in the cardiovascular and renal biological systems because they work in the kidney, in blood vessels, on platelets and in the heart. Cardiovascular homeostasis is also regulated by pathways in other organs like the brain and is affected by the immune system, which also are highly influenced by COX and the prostanoids. Understanding the mechanisms of cardiovascular side effects caused by inhibition of COX-2 by NSAIDs (discussed below) has been a central question in my PhD thesis. At the moment these are not completely understood but it seems that protective effects in the kidney, blood vessels and on platelets may all play a role.

Prostanoids have complicated roles in the kidney where they act as controlling mediators to protect the kidney from stress by maintaining renal function, fluid and salt and blood pressure. As with all tissues and organs there are high levels of COX-1 in the kidney, but also in the kidney, very importantly, COX-2 expressed⁷⁵. COX-1 is highly expressed in the collecting duct, in the thick ascending limb and macula densa but low levels of COX-1 are found in the cortical and medullary interstitial cells where COX-2 is instead high. COX-1 and COX-2 are both present in the cortical thick ascending limb. The key site for COX-2 expression in the kidney is in the renal medullary interstitial fibroblasts where although COX-1 is present it seems that COX-2 is the main active isoform in these fibroblasts. These cells are sensors of osmotic pressure. In these cells changes in osmotic pressure, through the transcription factor NFAT, regulate COX-2 in a constitutive way, without inflammation⁷⁶. COX-2 is also expressed in some endothelial cells in the kidney and in the epithelium. From work using NSAIDs in people and laboratory animals including genetic models, COX-2 has been shown to be the controlling isoform in the kidney for renal function, especially during disease. COX-2 and mPGES1 are co-expressed in some renal structures including in the macula densa⁷⁵. Clinical studies found that selective COX-2 inhibitors reduces glomerular filtration rate and renal blood flow, which is even more pronounced during physiologically stress, such as salt depletion, or in patients with cardiovascular or renal disease⁷⁵.

Prostacyclin and PGE₂ are the main prostanoids of the kidney. Their effects, as is the same with all structures, are regulated by their receptor pathways that I have described above. In the kidney prostacyclin and PGE₂ maintain glomerular filtration rate by acting on afferent

arterioles and can act locally on the glomerulus to affect further COX-2 expressed in the macula densa in low salt diets⁷⁷. As well as this in addition to regulation of functions and blood flow in the kidney COX and prostanoids can also work in the regulation of renin release⁷⁸ which affects blood pressure and cardiovascular function via the renin-angiotensin pathway.

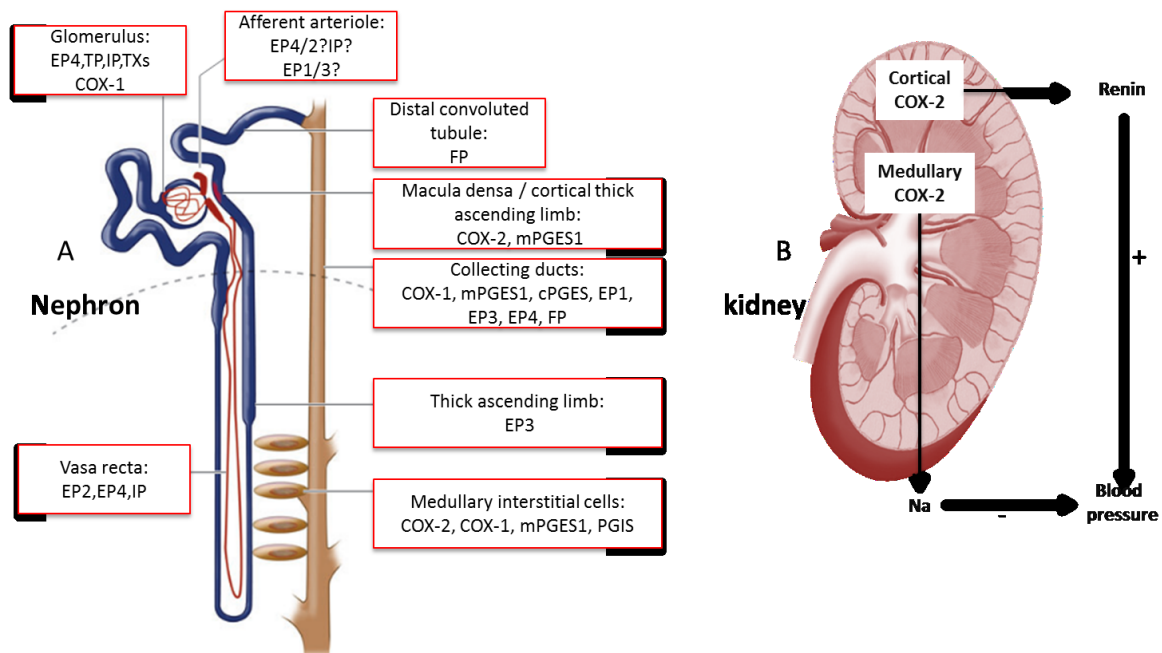


Figure 1.7: localization and function of cyclo-oxygenase (COX) in kidney substructures. A: the nephron, COX-1 is localized to all cells but particularly including the glomerulus, collecting ducts and intestinal cells of the medulla. COX-2 is more specially localized to the macula densa and renal intestinal cells (fibroblasts). EP receptors are expressed throughout the nephron. B: the kidney, on a gross level COX-2 is highly enriched in the inner region of the medulla with lower levels in the cortex. Under salt and other stress COX-2 expression is increased in the cortex. In the medulla COX-2 regulates sodium (Na) balance, in the cortex COX-2 regulates renin – together with other pathways this modulates blood pressure. Modified from Hao and Breyer, 2008⁷⁵.

COX and prostanoids are powerful regulators of platelet and vascular function and thrombosis. As described above, TXA₂ activates platelets and contracts vessels while prostacyclin inhibits platelet function and is a vasodilator. In the cardiovascular system prostacyclin and thromboxane are in a fine and very delicate balance. Blocking TXA₂ in platelets with low dose aspirin is the way in which aspirin protects people from heart attacks and strokes. Low dose aspirin works because it is a permanent blocker of COX-1 that drives TXA₂ in platelets and because platelets do not have a nucleus so they cannot make new COX enzyme. This means that as the effect of taking a little aspirin each day builds up

the platelet is more affected than the cells like endothelial cells that have a nucleus. Endothelial cells are the main sites of prostacyclin release but the isoform of COX that is expressed there is currently not agreed. Work from my group and contained in my thesis shows that this is COX-1⁷⁹ but other groups suggest that it is COX-2⁸⁰ (see below). Even though COX-1 is highly expressed in blood vessels it is agreed that COX-2 is induced in endothelial cells and in smooth muscle during inflammation such as that caused by atherosclerosis^{81,82} but even where blood vessels are very damaged by plaques in atherosclerosis the total amount of COX-2 is not enough to make a difference compared with COX-1 to prostacyclin release⁸². This only happens when a very big inflammatory stimulus is given with LPS causing a situation like septic shock⁸³.

Even though it is not agreed which isoform of COX is in vessels, the protective role that prostacyclin has in the cardiovascular system is agreed by everyone. The therapeutic possibilities of prostacyclin have been shown in pulmonary hypertension where drugs that work on IP and PPAR β receptors are used to treat this condition⁴¹.

COX and prostanoids are also expressed and have important functions within the heart. In the heart COX is important in cardiac myocytes, coronary endothelium, nerves and fibroblasts. As with other organs COX-1 is highly expressed in the heart where prostacyclin⁷⁹ and PGE₂⁸³ are main prostanoids that are being released there. In isolated heart muscle prostacyclin causes positive inotropic and chronotropic effects⁸⁴ which means it makes the heart contract more powerfully and more quickly. Prostacyclin is protective in the heart where as well as its effects on the heart muscle is a dilator of coronary vessels^{84,85}. Prostacyclin protects against ischemia reperfusion injury, which is the type of injury that happens after a heart attack and has the action to reduce remodelling (cardiac hypertrophy) by reducing cardiac fibroblast proliferation⁸⁵. TXA₂ acting on TP receptors causes contraction of coronary arteries and tachycardia, which is where the heart beats too fast⁸⁵. This is likely to be an action directly on the heart because similar results were seen in isolated atrium preparations. TXA₂ also caused arrhythmias in animal models again by actions directly on the heart itself⁸⁵. PGE₂ is also very important in the heart where, as with other organs, its effects are dependent on which receptors are present. Early work from Hohlfield et al. (1997)⁸⁶ showed that the protective effects in the heart of PGE₂ after ischemia and

reperfusion were mediated by the EP3 receptor. PGE₂, like PGI₂, has direct effects on heart contractility but conflicting results have been observed, probably because of the relative distribution of EP receptors in different experimental procedures. For example PGE₂ from COX-2 can contribute to ischemic injury by EP2 and EP4 or be protective by EP4⁸⁵. Using mPGES-1^{85,87} knock out mice it was found that PGE₂ protects against remodeling and fibrosis in the heart, something that was shown using EP4 knock out mice⁸⁷ and selective agonists⁸⁸ to be caused to some extent by EP4 receptors. As in other vessels PGF_{2α} in the heart can be a vasoconstrictor but is also shown to cause remodeling after injury by the FP receptor pathway⁸⁵.

Drugs that act on the COX pathways: NSAIDs

NSAIDs such as aspirin, ibuprofen, diclofenac and naproxen are medications that are widely used to treat a range of conditions such as headaches, fever and inflammation (pain, redness, swelling and heat). They are amongst the most widely taken over the counter medications in the world. They are a first line treatment for arthritis and can prevent cancer. As an example it is estimated that about 70% of people 65 years or older take NSAIDs at least once per week, with half of them taking at least 7 doses per week. In 2000, more than 111 million prescriptions were written for NSAIDs in the United States⁸⁹ and another approximately 30 billion NSAIDs are bought without prescription as over-the-counter drugs each year⁹⁰. NSAIDs do not treat the disease of arthritis but by blocking prostanoid production they reduce swelling and pain and in that way help to relieve the symptoms, this is why they are so popular. However, there is one very important disease where NSAIDs, maybe by working on more than one mechanism (eg blocking COX-1 in platelets and blocking COX-2 in cancer cells) act in a positive way to actually prevent the disease itself and that disease is cancer.

The evidence for NSAIDs preventing cancer began with results from the Nurses study which is a large population study where nurses in the US are involved with tracking their life style and disease. In this study it was found that nurses that took aspirin regularly had a great reduction in colon cancer⁹¹. More recently large placebo-controlled trials were carried out where aspirin was taken every other day⁹² ⁹³ and the people followed and their results collected together for 10 years. In these trials no effect on cancer prevention was found for

aspirin. Now with more trials recent analysis of all trials it has been found that looking at 51 trials (77,000 participants) randomly assigned to daily aspirin versus no aspirin or other anti-platelet agent aspirin does actually reduce the cancer including death from cancer. From this analysis colon cancer and cancer from the gastrointestinal tract are the most protected^{94,95}. Most recently in 2016 another analysis also proves the link between aspirin and preventing cancer⁹⁶. Because aspirin affects platelets particularly Professor Patrono in Italy has suggested that the anti-cancer effects of aspirin are on COX-1 in platelets specifically⁹⁷. This might be true for aspirin but COX-2 selective NSAIDs can also prevent colon cancer. The two main COX-2 selective drugs Vioxx (rofecoxib) and Celebrex (celecoxib) do not affect platelets at all and so there might be two ways that NSAIDs can prevent cancer these are by (i) blocking COX-1 in platelets and (ii) blocking COX-2 in tumor cells. There are a very large number of papers showing a role for COX-2 in cancer. A current pubmed search of 'COX-2' and 'cancer' brings up 8171 (30th June 2016). For the COX-2 side of NSAID in cancer it is thought that COX-2, through PGE₂, contributes to cancer cell proliferation because COX-2 is induced in tumors^{98,99} and COX-2 blockers kill cancer cells in vitro⁹⁹.

Even though there is the large body of papers showing how aspirin or COX-2 selective NSAIDs can prevent cancer they are not used clinically to do this. The COX-2 selective NSAID Celecoxib was licensed in Europe for use to prevent colon cancer but it was withdrawn in 2011 because of the concern about side effects (see below).

Side effect of NSAIDs

As mentioned before NSAIDs are very popular drugs because they work. However, NSAIDs have side effects and because so many doses of NSAIDs are taken around the world the side effects that they cause constitutes an important global health problem. For instance it has been pointed out that in the USA alone there are 30 billion NSAIDs doses taken as over the counter drugs every year. However, NSAIDs have side effects which because they are so commonly taken have a big impact on world health. The main side effects are (i) hypersensitivity which is like an allergy, (ii) in the gastrointestinal system, (iii) in the kidney, (iv) in the cardiovascular system.

Hypersensitivity reactions

NSAIDs are the most common cause of drug-induced hypersensitivity of all drugs taken. Hypersensitivity to a drug is a 'side effect' but of a special nature. Hypersensitivity is caused by the immune system reacting to a drug and in the case of NSAIDs this can take a number of forms and affect a number of organ systems including skin, mucosal membranes, gut or most notorious the airways where the condition known as 'aspirin sensitive asthma' is used to explain symptoms that happen from taking NSAIDs (not only aspirin) that are similar to asthma. NSAIDs are now in fact, the most common class of drugs involved in hypersensitivity drug reactions¹⁰⁰. The mechanism of NSAID hypersensitivity is not clear and because drug reactions can vary a lot it might be that there is more than one mechanism involved. For at least some forms of NSAID hypersensitivity (eg aspirin sensitive asthma) it is thought that blocking COX-1 causes an increase in leukotrienes which then cause asthma symptoms. This is because leukotrienes are increased in aspirin sensitive asthma and because COX-2 selective NSAIDs like Celebrex do not cause reactions in sensitive people¹⁰¹.

Gastrointestinal side effects

The gastrointestinal side effects caused by NSAIDs are commonly in the upper gastrointestinal part, most notably in the stomach. It is thought that over a year in the US the percentage of people getting gastrointestinal side effects from NSAIDs is 2.5% and 4.5%, and for the more serious side effects which are perforation, ulcers, bleeds and blockages is about 1% to 1.5% of people take the drugs regularly¹⁰². These are caused by more than one way (Figure 1.8). The stomach is very acidic and one of the ways that NSAIDs causes side effects is by blocking the pathways that protect the stomach from the acid. This is by reducing release of protective mediators there like mucin and by reducing the buffering by lowering bicarbonate (HCO_3), (Figure 1.8). On the other hand NSAIDs also cause gastric damage by acting on blood vessels in the stomach causing contraction, reducing blood flow and causing ischemia and inflammation (Figure 1.8).

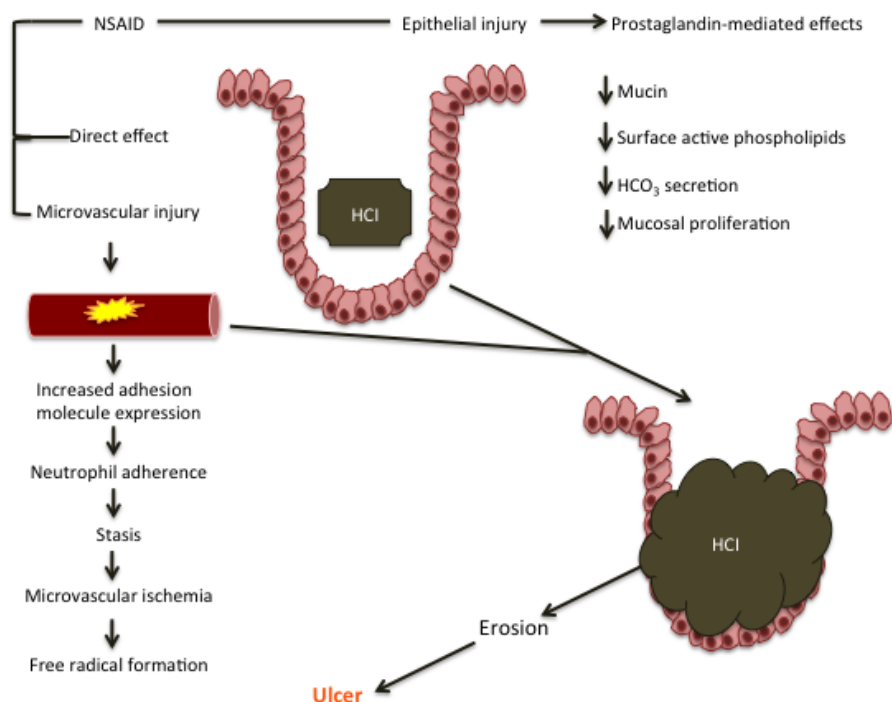


Figure 1.8: Pathways that cause gastric damage by NSAIDs. NSAIDs have a topical effect in the stomach by reducing protective effects that protect from the acid environment. They also work by entering the systemic circulation and then affecting blood flow in the stomach walls and within the gastric mucosa causing constriction of local vessels, inflammation and ischemia.

As mentioned above NSAIDs cause gastrointestinal side effects by blocking both COX-1 and COX-2 which is why selective inhibitors of COX-2 were developed to have less side effects in the gut. This does not mean that gastrointestinal side effects are no longer a problem because (i) even selective COX-2 inhibitors cause some gastrointestinal side effects and (ii) with the newer side effects in the cardiovascular system (see below) now older style NSAIDs (that block both isoforms) are being prescribed again. Since the recommendation from the American Heart Association for prescribing NSAIDs was introduced in 2007 that for anyone with a risk of cardiovascular disease should not take a COX-2 inhibitor the advice has been that COX-2 selective NSAIDs be prescribed with caution and instead patients with arthritis be given an older style drug like ibuprofen or naproxen¹⁰³. Naproxen has the least risk of cardiovascular side effects of any of the NSAID class¹⁰⁴. However, older style NSAIDs that block COX-1 as well as COX-2 are more toxic to the gut. This has meant that the recommendation is now that proton pump inhibitors (PPI) be given with NSAIDs to protect the stomach¹⁰⁵. This has come with its own problems though because PPI inhibitors might themselves cause cardiovascular side effect¹⁰⁶ (see below) and because PPI inhibitors with

naproxen might protect damage in the stomach but only to cause damage further down the gastro intestinal tract causing damage in the lower intestine¹⁰⁷.

Cardiovascular and renal side effects and the introduction of COX-2 selective NSAIDs

After the discovery of COX-2 and because of the gastrointestinal side effects caused by NSAIDs around in the early 1990s COX-2 selective drugs were introduced the clinic. The main ones were Vioxx (rofecoxib) from Merck & Co and Celebrex (celecoxib) from Pfizer. Both Vioxx and Celebrex had their first clinical trials in 2000 the Vioxx trial was called VIGOR¹⁰⁸ and the Celebrex trial was called CLASS¹⁰⁹. In both trials the COX-2 selective drugs were compared with traditional NSAIDs in the case of Vioxx it was naproxen and in the case of Celebrex it was diclofenac and ibuprofen. In both trials the COX-2 selective drug did better on gastrointestinal side effects than the traditional NSAID, although for Celebrex in the CLASS study this benefit was only significant when the data on gastrointestinal side effects caused by both ibuprofen and diclofenac groups were combined. This caused some controversy because the study was not in the beginning designed to analyze the data this way. Nevertheless both COX-2 inhibitors, Celebrex and Vioxx were brought into the clinic after these trials and became blockbuster drugs. But even in the beginning there were concerns about the fact that COX-2 inhibitors could be increasing the risk of cardiovascular side effects. In the VIGOR trial for Vioxx they were higher than for naproxen but at the time this was put down to the fact that naproxen has antiplatelet effects and that the higher numbers of cardiovascular events (mainly heart attacks) in people taking the Vioxx was not because it was an actual side effect but because they didn't have the protection that was assumed to be given by those people taking naproxen¹⁰⁸. As the COX-2 inhibitors continued to be used clinical data was being accumulated and as time in the clinic continued reports about cardiovascular side effects increased. The main reason at the time that there was no firm conclusion about cardiovascular side effects and the COX-2 inhibitors was that there were not placebo controlled trials in the patient group taking the drugs, ie those people with arthritis. This is because for those kinds of trials the group that was being compared to the COX-2 inhibitor needed to be on some kind of medication to control their pain. Now we know that all NSAIDs, because they block COX-2, have some level of risk of increasing cardiovascular events. Just before the VIGOR and CLASS trials a study was performed in healthy male volunteers given the COX-2 inhibitor Celebrex and then markers of

prostacyclin and TXA₂ in their urine were measured. This study was by Professor Garret Fitzgerald's group and showed that the COX-2 inhibitor Celebrex reduced urinary markers of prostacyclin without affecting levels of the marker for TXA₂¹¹⁰. Later the same results were found to be the case for Vioxx (in the paper called by its chemical number MK 966)¹¹⁰. These early data showing a trend to increased cardiovascular events in clinical trials and that COX-2 selective drugs reduce urinary markers of prostacyclin but not of TXA₂ led the field to be thinking that COX-2 inhibitors actually had cardiovascular side effects. Then in 2004 the first placebo controlled trial where a COX-2 inhibitor was in a large number of people compared to a control group with no other NSAID was published. This study was called APPROVE and was done as a cancer prevention study where people at risk of getting colon cancer were treated with Vioxx to see if the appearance of colon polyps, which are precancerous growths, could be reduced by blocking COX-2. The statement in the paper is *'The Adenomatous Polyp Prevention on Vioxx (APPROVe) Trial was designed to evaluate the hypothesis that three years of treatment with rofecoxib would reduce the risk of recurrent adenomatous polyps among patients with a history of colorectal adenomas. Potential thrombotic events were adjudicated by an independent committee, and all safety data were monitored by an external safety-monitoring committee¹¹¹. We report the cardiovascular findings from the study'*. The study was not designed to test for cardiovascular findings but because they were found to be higher the study group decided that they should publish these findings first. The study had 877 patients in the placebo group and 980 in the Vioxx group taking 25mg per day for 3 years. For cardiovascular reactions these were recorded through the 3 years and up to 14 days after the last dose of the study. In the paper the events measured were stated as *'Thrombotic events included fatal and nonfatal myocardial infarction, unstable angina, sudden death from cardiac causes, fatal and nonfatal ischemic stroke, transient ischemic attack, peripheral arterial thrombosis, peripheral venous thrombosis, and pulmonary embolism'*. The end point used in the Antiplatelet Trialists' Collaboration (APTC) study was also analyzed¹¹¹' APTC is commonly used and is defined as *'the combined incidence of death from cardiovascular, hemorrhagic, and unknown causes; nonfatal myocardial infarction; and nonfatal ischemic and hemorrhagic stroke¹¹¹*. The paper found the following results that there were 46 cardiac events in the Vioxx group compared to just 26 in the placebo group. The cardiac events were made up from mainly myocardial infarction (heart attack) and ischemic stroke¹¹¹.

The data in this paper proved devastating to the COX-2 field and after the data was released the manufactures of Vioxx (Merck Co) immediately withdrew the drug world wide¹¹². Now more than 10 years later the fact that blocking COX-2 with NSAIDs definitely causes cardiovascular side effects is totally agreed. More recent papers of the collection of trial data shows how this is true for all NSAIDs, not just for COX-2 selective inhibitors. In a paper published in the journal Lancet in 2013 it was estimated that selective COX-2 inhibitors (called coxibs in this paper) caused, in people at a higher risk of cardiovascular events, a theoretical increase of 9 extra cardiovascular events for every 1000 people taking drug for a year and for diclofenac and ibuprofen an increase of 10 and 12 respectively. The paper showed that for people in a low risk bracket there would be the same for coxib, diclofenac and ibuprofen groups; 2 extra events in 1000 per year¹⁰⁴.

The early work suggesting a link between COX-2 inhibitors and cardiovascular events and now with the newer papers confirming that this is true has caused a chain reaction that still continues today (Figure 1.9). This chain includes the withdrawal of Vioxx, warnings from the FDA, changing diclofenac from over the counter to prescription only and the removal of Celebrex as a cancer prevention treatment. Figure 1.9 shows some of the events that have marked the COX-2 story.

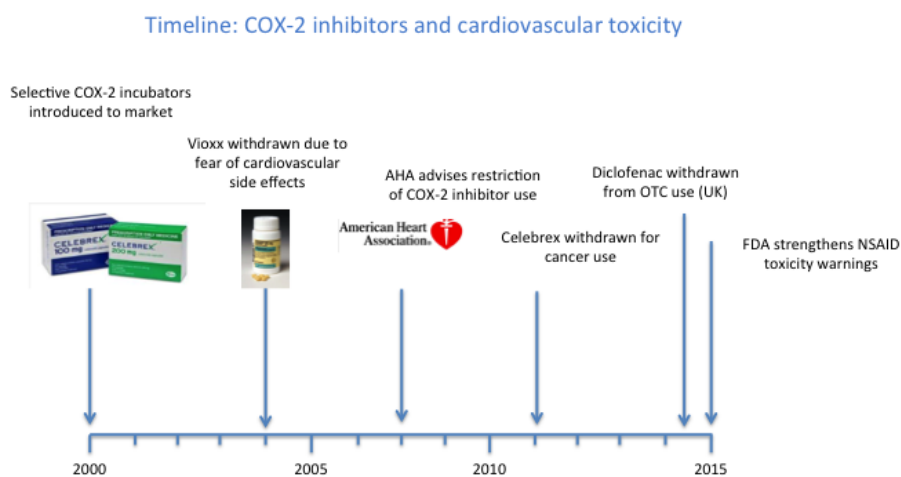


Figure 1.9: selected time line of events in the area of COX-2 drugs and cardiovascular events.

Mechanisms that are thought to explain how COX-2 blockers cause cardiovascular events

The mechanisms behind the cardiovascular side effects caused by NSAIDs are not known and understanding them was the reason behind my PhD research question. When I started my PhD the main explanation was that NSAIDs block COX-2 in blood vessels to reduce prostacyclin release without affecting platelet TXA₂¹¹³. This became what is known as the '*COX-2 – prostacyclin hypothesis*'. This is based on the facts that drugs that work by blocking COX-2 (all NSAIDs) (i) have an increased risk of causing cardiovascular side effects (individuals risk is increased by about 30%), (ii) COX-2 selective drugs (like Celebrex and Vioxx) reduce urinary prostacyclin without affecting TXA₂ and (iii) the cardiovascular phenotype seen in COX-2 knock mice is also seen in prostacyclin IP knock out mice. The COX-2 – prostacyclin hypothesis is based on the knowledge that if the prostacyclin TXA₂ balance is turned the other way – ie if TXA₂ is reduced without affecting prostacyclin, like happens with aspirin, then the cardiovascular system is protected. In this way the COX-2 prostacyclin hypothesis puts COX-2 inhibitors in a bracket that could be thought of as an 'anti-aspirin' effect.

Work conducted in my group before I started my thesis and work that I have continued during the course of my PhD studies does not agree with the COX-2 – prostacyclin hypothesis because neither we nor any other group has been able to show that COX-2 is actually present in blood vessels unless they are activated with a strong inflammation stimulus. Also what the COX-2 prostacyclin hypothesis completely does not seem to include is the fact that COX-1 is very strongly expressed in blood vessels and is directly linked to the prostacyclin release seen in every tissue⁷⁹.

An alternative explanation for how NSAIDs might cause cardiovascular side effects is to do with COX-2 in the kidney. Here everyone agrees that COX-2 is expressed (see above) and that blocking COX-2 in the kidney causes increased blood pressure especially in people with kidney dysfunctions or on high salt diets^{114,115}. It is known that where kidney function is reduced the pathway in the kidney that regulates methylarginine is altered. Methylarginines are methylated arginine molecules, some of which are biologically active where they compete with L-arginine as a substrate for nitric oxide (NO) formation in blood vessels and in other tissues. There is a long history of interactions between the NO and prostacyclin

pathways and between the enzymes that regulate them. Also, in a paper published in 2012 it was shown that when COX-2 is knocked out in mice endothelial NO synthase (eNOS) responses were reduced⁸⁰. In my PhD I have tested the idea that there could be a link between COX-2 in the kidney and methylarginine production and that this might have effects on the cardiovascular system and so in the section below I have introduced literature about the methylarginine and eNOS

The NO pathways

NO is a colorless gas, with a short biological half-life of 5-10 seconds and has a lipophilic non-polar structure. It is involved in a wide range of biological functions. In 1980 Professor Furchgott¹¹⁶ first showed that the endothelium released a hormone that caused vasodilatation and this mediator was initially named endothelium derived relaxing factor (EDRF), which was later on identified as NO¹¹⁷. In the first paper showing EDRF by Furchgott they performed simple experiments on rabbit aortic rings; they found that when endothelium was left on the vessel acetylcholine caused the blood vessel in an organ bath to relax. However, they could not find the same effect when the endothelium was absent from artery¹¹⁶. This paper started a whole new field of 'NO biology' and in 1998 Professor Furchgott was one of three scientists to get the Nobel Prize for 'NO in the cardiovascular system'. Following this study, more experiments were carried out to help in understanding the biological opportunities of NO and in 1992 NO was called 'molecule of the year by Science Magazine¹¹⁸.

Shortly after that EDRF was discovered Professor Moncada and colleagues showed that it was in fact NO produced from the endothelial cells, more specifically from the amino acid L-arginine^{117,119}. The enzyme that makes NO in the endothelium is called eNOS (or NOSIII) and it is a membrane bound enzyme that requires calcium¹²⁰. L-arginine is the amino acid that is used as the substrate for NO by the eNOS enzyme.

The release of NO from endothelial cells has many common effects to those seen with prostacyclin. NO relaxes blood vessels, inhibits platelet function, protects against atherosclerosis and is important in the immune system¹²¹. As well as this and in addition to the endothelial NOS (NOSIII or eNOS) there are two other isoforms. NOSI (or nNOS¹²²) is in

the brain and is calcium dependent, NOSII (or iNOS¹²³) is induced in cells by bacterial or inflammatory stimuli and NOSIII (or eNOS¹²⁰) is present in endothelial cells and is also dependent on calcium. nNOS is important in nerves for communicating with other nerves and for interacting with relaxation of smooth muscle in places like the airway. iNOS is important in killing bacteria and tumor cells while eNOS is really critical in the maintenance of a healthy cardiovascular system.

As stated above, for all NOS enzymes the reaction is that L-arginine is converted to L-hydroxyl arginine and then to NO with L-citrulline and molecular oxygen as bi products¹²¹. NO causes its effects by activating the enzyme soluble guanylate cyclase (sGC), sometimes it is said that sGC is the 'receptor' for NO. Along with Professor Furchgott, Professor Murad got the Nobel Prize in 1998 for his part in the story where he showed that sGC was the '*ubiquitous sensor of NO*'. NO binds to sGC hemo group and activates sGC leading to an increase in intracellular cyclic guanylate monophosphate (cGMP) concentrations from the conversion of GTP. cGMP results in the activation of Protein Kinase G (PKG). The activation of PKG leads to decrease the intracellular Ca²⁺ in smooth muscle. This activation results in dephosphorylating of myosin light chains that decreases vascular tone.

From the very early studies of NO biology it was found that molecules where another chemical group had been added onto the guanidine nitrogen of L-arginine could be competitive inhibitors with arginine for the active site of NOS (Figure 1.10). The first one described was monomethyl-L-arginine (L-NMMA) and then came nitro-L-arginine (NIO) and then nitro-L-arginine methylester (L-NAME). These molecules have been very useful in understanding NOS biology and showing how it is involved in regulating blood pressure and vascular functions. Then afterwards in 1992 the group of Patrick Vallance showed how a molecule made in the body called N^G,N^G-dimethylarginine (asymmetrical dimethylarginine, ADMA) was a natural modified L-arginine molecule that could inhibit eNOS functions in the body¹²⁴.

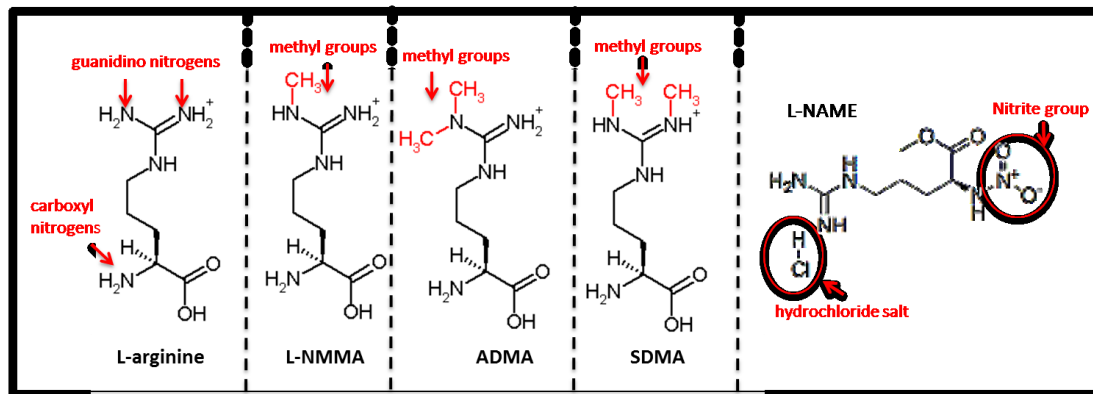


Figure 1.10: structures of L-arginine and related molecules where there are substitutions on the guanidino arginine. The guanidino arginine is the one that goes to make the 'N' of NO and can have substitutions on there. The ones important to NOS biology are with methyl groups or with nitrite groups resulting in L-N-methylarginine (LNMMA), symmetric dimethylarginine (SDMA), asymmetric dimethylarginine (ADMA) and L-N^G-nitroarginine methyl ester hydrochloride (L-NAME).

Now we know a lot more about ADMA and its synthetic pathways. ADMA is now a recognized and agreed biomarker of cardiovascular risk¹²⁵ and its levels in the plasma are linked to death¹²⁶.

Methylarginines

Methylarginines are released from proteins by proteolysis (break down of proteins) and are made by the methylation (addition of an extra methyl group) of L-arginine, an essential amino acid required for the NO formation process. Methylation of arginines is catalyzed by the enzymes protein arginine methyltransferases (PRMTs). There are nine known forms of PRMT grouped in to two types; type 1 PRMTs, which are non-myelin basic protein-specific and type 2, which are myelin basic protein-specific. Once formed after protein breakdown (proteolysis) free methylarginine residues are released into the cytosol and then into plasma where they circulate to different cells and tissues.

There are three known methylarginine residues produced in mammals: L-NMMA, ADMA and symmetric dimethylarginine SDMA (Figure 1.10). Only asymmetrically methylated forms (L-NMMA and ADMA), but not symmetrically methylated arginine (SDMA), inhibit NOS. Type 1 PRMT's are responsible for the formation of both L-NMMA and ADMA whereas type 2 PRMTs are responsible for the formation of both L-NMMA and SDMA.

ADMA is involved in various diseases such as diabetes, atherosclerosis and chronic kidney disease. In particular, there has been focus on cardiovascular conditions as high levels of ADMA in the plasma are associated with cardiovascular diseases (increased blood pressure, vascular resistance, heart failure, hypertension and coronary artery disease).

It was believed that the kidney cleared methylarginines after their release from the cells into the plasma without reincorporation into proteins or further catabolism. However, in 1976 McDermott et al.¹²⁷ suggested that there is a catabolic pathway for both ADMA and L-NMMA but not SDMA¹²⁷. Ogawa et al.¹²⁸ identified the enzyme that catalyzed ADMA to citrulline and either mono- or dimethylamines¹²⁸. This enzyme is now known as dimethylarginine dimethylaminohydrolase (DDAH) and it plays important role in regulating ADMA levels *in vivo* and because it blocks NOS it also plays a role in regulating the NO system too. Two DDAH isoforms exist; DDAH1 and DDAH2¹²⁹ (Figure 1.11). DDAH1 is expressed predominately and mainly in neuronal tissue (cerebellum and cerebrum) whereas DDAH2 is predominantly expressed in immune tissue (monocytes, macrophages, neutrophils as well as the thymus, spleen and lymph nodes). Both DDAH1 and DDAH2 are expressed in the kidney¹²⁹. DDAH inhibition causes the accumulation of methylarginines resulting in blocking NO synthesis and causing vasoconstriction^{130,131}.

There is less known about the other pathway that metabolizes ADMA called alanine-glyoxylate aminotransferase 2 (AGXT2) (Figure 1.11). AGXT2 is a class III pyridoxal-phosphate-dependent mitochondrial aminotransferase¹³² that causes transamination of ADMA to α -keto- δ -(*N,N*-dimethylguanidino)valeric acid (DMGV). AGXT2 but not AGXT1 can metabolize ADMA as well as NMMA and SDMA¹³². AGXT2 is expressed in mitochondria in the liver and kidney of various species¹³³.

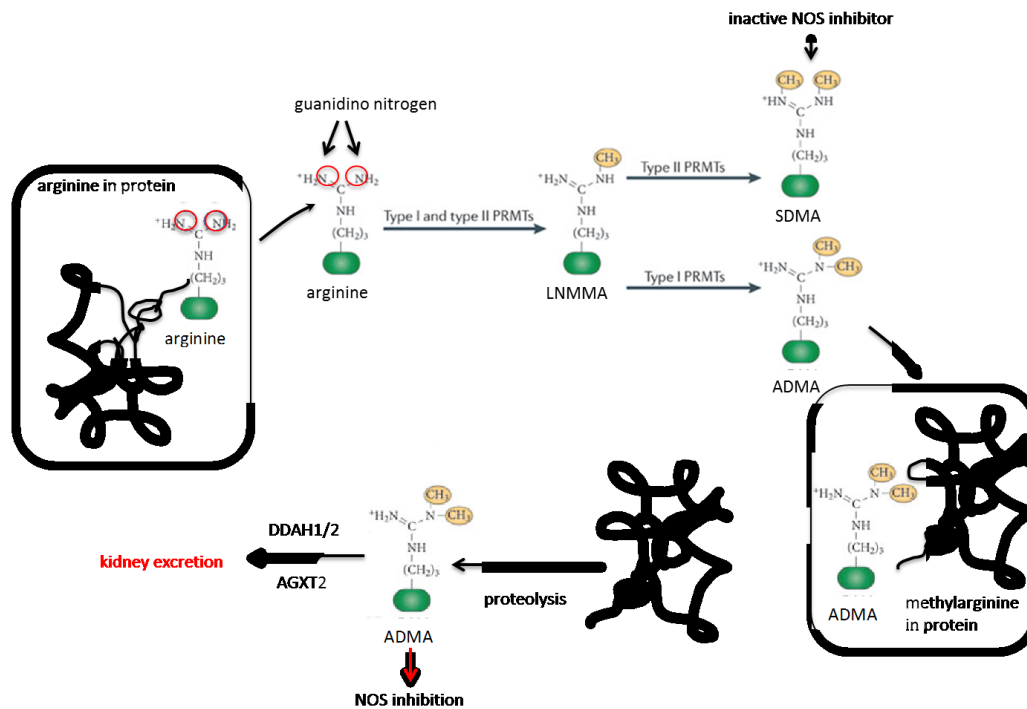


Figure 1.11: Pathways for formation, release and breakdown of methyl arginines. Arginine residues in proteins are methylated by protein arginine methyltransferases (PRMTs) to form L-N-methylarginine (LNMMA), symmetric dimethylarginine (SDMA), asymmetric dimethylarginine (ADMA). These are released after proteolysis and metabolized by dimethylaminohydrolase (DDAH) or alanine-glyoxylate gminotransferase 2 (AGXT2).

Summary

Prostanoids are extremely important biological mediators formed at a starting point from COX. There are two forms of COX, COX-1 that is constitutive in all cells and COX-2 that is induced in inflammation but also expressed constitutively in some places. COX-2 in inflammation causes pain and inflammation and can lead to cancer and so it is a target to be inhibited by drugs. In fact the most common type of drugs that we buy in the pharmacy for pain are drugs that work on this pathway, they are called NSAIDs and include the most famous faces of drugs in the world like aspirin and ibuprofen. NSAID have side effects in the gastro intestinal tract, most common are in the stomach. COX-2 selective drugs were introduced to avoid these side effects. But after they were introduced even though they became blockbuster drugs they had problems because of cardiovascular side effects. These are mainly heart attacks but also strokes. We do not understand how these side effects are caused but we think it is to do with a block of prostacyclin from blood vessels or in the kidney. NO is a sister pathway to prostacyclin in blood vessels and NO and the prostacyclin

pathway are very connected. There is a part of the NO pathway called methylarginine biology where endogenous forms of the substrate L-arginine are made that can compete with L-arginine and inhibit NOS. The methylarginine pathway is controlled in the kidney and is badly affected when kidney function is lowered. Because NSAIDs reduce kidney function and because there was a paper published during my PhD that showed COX-2 knockout mice had reduced eNOS responses there is a supposed link in theory that blocking COX-2 can be somehow influencing eNOS in blood vessels. My PhD has been to study how COX-1 and COX-2 operate in tissues and in blood vessels and to specifically investigate how COX-2 block might affect the methylarginine pathways. I have also performed a small-related piece of research looking at endothelial cells and blood vessels form and structure. While this was not so directly related to my starting question it came out of the technical study I was doing to image COX-2. This work forms a linked separate chapter at the end of my thesis and the background that is related to that work is in an introduction section in that chapter (Chapter 6). Thus, with the very important need to understand how COX-2 inhibitors cause side effects in the human body related to cardiovascular function the big hypothesis that my PhD has worked within is shown below. This is an important hypothesis that my work has contributed to in terms of the basic science but I have not addressed the whole large hypothesis because it will take time to see if my findings are really important to people.

Hypothesis

'COX-2 protects the cardiovascular system independently of actions in blood vessels and understanding how this can happen will allow us to find ways to protect people that will get side effects when taking NSAIDs'

Aims

1. Determine the role of COX-1 and COX-2 in prostacyclin release by blood vessels
2. Investigate the link between COX-2 and the methylarginine and other amino acid pathways
3. Investigate the function of COX-2 methylarginine relationships in vessels in vitro and in the whole system in vivo

4. Find a way of quantifying endothelial cell morphology in tissue and to use this to address how COX and NOS might affect vascular structure.

Chapter 2: General Methods

Experimental animals

In my thesis I have used genetically modified mice where cyclooxygenase (COX)-1, COX-2 or prostacyclin IP receptor genes were deleted. Animal studies were conducted in accordance with Animals (Scientific Procedures) Act 1986 (UK), and after local review by the Imperial College Ethical Review Panel.

The COX-1 and COX-2 colonies were on a C57BL/6J background (Harlan, UK). They were created in the USA at the University of North Carolina by Professor Oliver Smithies' group^{134,135}. For the COX-1 knock out colony both male and female were homozygous for COX-1, thus their offspring were 100% homozygous for COX-1 knock out. In contrast, the COX-2 knock out colony required crossing homozygous males with heterozygous females because homozygous females are infertile. This generated two possible genotypes: heterozygotes for COX-2 knock out and homozygote for COX-2 knock out (experimental animals). A wild-type line, originally bred from inter-crossing COX-1 knock out and COX-2 knock out animals, was used as controls for both knock out strains. For IP receptor knock out, mice were on C57BL/6N background. These were supplied by Professor Rolf M. Nüsing¹³⁶ but the line was originally developed by Professor Shuh Narumiyas group¹³⁷. Like for the COX-1 knock out colony IP knock out mice were generated by crossing male and female mice were homozygous for IP knock out, meaning their offspring were 100% homozygous for IP knock out. Wild-type C57BL/6N mice purchased from Harlan, UK, were used as controls from IP knock out studies. Throughout the breeding process all the colonies were genotyped for COX-1, COX-2 or IP knockout. In my thesis, genotyping for COX-1 and COX-2 (details below) were done with the help of my supervisor Dr Kirkby whereas IP knockout genotyping was performed by Dr Nüsing's laboratory.

Genotyping procedure for COX-1 and COX-2

DNAeasy Tissue Kit (Qiagen,69056) was used to extract the DNA from ear clips. To isolate the DNA, first the tissue was digested with Qiagen proteinase K followed by Qiagen lysis buffer and ethanol. The lysate was then added to DNA-binding mini-spin columns and washed using supplied wash buffer. The DNA was eluted from the columns using Qiagen elution buffer. Three-primer polymerase chain reaction (PCR) was performed to identify genotype. The extracted DNA was added to tubes (GE healthcare, 27-9559-01) that contain

Illustra PuReTaq Ready-To Go PCR beads with 3 primers (Invitrogen; see below). A Techgene PCR machine was set to: 5 minutes initial denaturing at 94°C, 32 cycles (COX-1 PCR) and 35 cycles (COX-2 PCR) of: 15 seconds denaturing at 94°C, 15 seconds annealing at 60°C (COX-1 PCR) or 55°C (COX-2 PCR) and 60 seconds extension at 72°C. After all cycles were complete, 5 minute final extension was performed at 72°C and samples stored at 4°C. DNA was then separated by electrophoresis on agarose gels (1%, Sigma, UK) containing a fluorescent DNA stain (GelRed, Cambridge Bioscience, UK) and bands measured by UV transillumination.

5' AGGAGATGGCTGCTGAGTTGG was the forward primer for the WT allele, which yielded a fragment of 601bp to represent COX-1^{+/+}. The COX-1 null allele (with the neomycin insert) was identified with a forward primer 5' GCAGCCTCTGTTCCACATACAC, which yielded a fragment of 646bp to represent COX-1 KO. The reverse primer for both COX-1 WT (COX-1^{+/+}) and mutant allele (COX-1 KO) was 3' AATCTGACTTTCTGAGTTGCC.

The COX-2 forward primer for the WT allele was 5' ACACACTCTATCACTGGCACC which yielded a fragment of 760bp to represent COX-2^{+/+}. The COX-2 null allele (with the neomycin insert) was identified with a forward primer 5' ACGCGTCACCTTAATATGCG which yielded a fragment of 905bp to represent COX-2 KO. The reverse primer for both COX-2 WT (COX-2^{+/+}) and mutant allele COX-2 KO was 3' ATCCCTTCACTAAATGCCCTC¹³⁸.

COX-1 gene deletion strategy

To create mice that lacking COX-1, also known as prostaglandin-endoperoxide synthase 1 (Ptgs1) the active catalytic site was targeted¹³⁴. Within the COX-1 gene the serine 530 (Ser-530) amino acid is located in the active site and required for activity. Moreover, this site is known to be the acetylating site of aspirin. Complementary DNA (cDNA) sequencing for mouse Ptgs1 showed that exon 11 contained the codon for Ser-530. 129 mouse strain embryonic stem (ES) cell DNA was used to synthesise a 357bp probe which was used then to screen E14TG2a mouse ES cells for the 5' end of exon 11 on the Ptgs1 gene¹³⁹. The 3' region of the Ptgs1, which contained exon 11, was then isolated and was approximately 15kb. The constructing targeting vector contained a 4.3kb NotI-XhoI fragment, a 2.3kb BamHI fragment and a herpes simplex virus thymidine kinase insert. The targeted vector was then linearized with NotI and then electroporated into trypsinised 129 derived E14TG2a ES cells.

The Neo gene insert confers resistant to antibiotic geneticin (G418), thus in order to be able to get the vector targeted colonies an antibiotic G418 was added. In addition, anti-viral drug ganciclovir (GANC) was also added to remove viral thymidine kinase-containing colonies and provide a 10-fold enrichment of the correctly targeted genes. DNA was then isolated from the remaining G418 and GANC resistant colonies and a Southern blot analysis was performed. C57BL/6 blastocysts were then injected with cells from two of the successfully vector targeted clones (Figure 2.1) ¹³⁴.

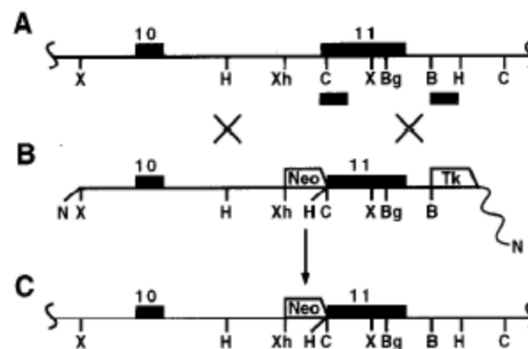


Figure 2.1 COX-1 gene deletion strategy

To disrupt COX-1 gene (*Ptgs1*) the 1 kb of intron 10 was targeted with the splice junction and first 44 bp of exon 11 to disrupt the Ser-530 amino acid. (A) The 3' end of the target gene. Black bars indicate the target sites for the probes. The restriction sites are designated X (*Xba*I), H (*Hind*III), Xh (*Xho*I), C (*Cl*aI), Bg (*Bgl*III), B (*Bam*HI). X represents homologous recombination. (B) The targeting construct. (C) Homologous recombination of the targeting construct into the COX-1 gene, resulting in a Neo positive and Tk negative gene. Figure adapted from ¹³⁴. N=NotI restriction site; Neo=neomycin; *Ptgs1*=prostaglandin synthase 1; Tk=thymidine kinase

COX-1 knock out mice were generated by injecting cells from two of the targeted clones into C57Bl/6 blastocysts resulting in the birth of four male chimeras. Chimeras were mated with C57Bl/6 females according to the breeding plan in Figure 2.2 below ¹³⁴.

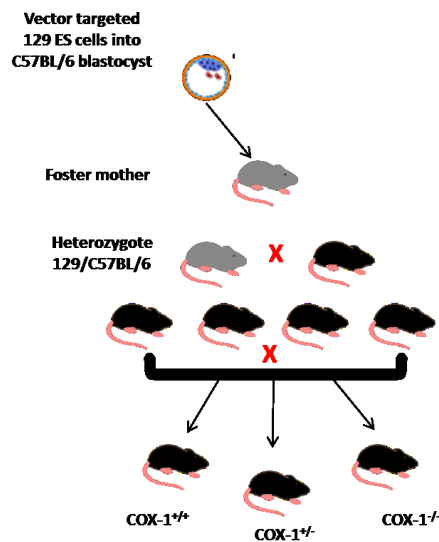


Figure 2.2: schematic that shows the breeding setup for generating COX-1 KO mice. (C57BL/6) blastocysts were injected with targeted vector clone using embryonic stem (ES) cells from the 129 strain). The blastocysts inserted into foster mother to generate male chimera. The chimera mice was breed with C57BL/6 to produce heterozygote siblings, those siblings were then inbred to create wild type (COX-1^{+/+}), heterozygote (COX-1^{+/-}) and homozygote COX-1 (COX-1^{-/-}) genotypes. Figure adapted from¹³⁴.

COX-2 gene deletion strategy

To create mice lacking functional COX-2, Tyr-371 and His-374 on exon 8 were targeted by insertion of a Neo gene and a 104bp deletion. Exon 10 was also truncated¹³⁵. As for COX-1, these mutations removed the active site of the enzyme. Mouse strain 129 derived ES cell line E14TG2a was used to isolate COX-2 gene (also known as prostaglandin-endoperoxidase synthase 2; *Ptgs2*). A 408 bp probe specific to exon 10 on the COX-2 gene, but not present in the corresponding region of COX-1 gene, was used to locate the COX-2 gene in a λ bacteriophage clone containing a 16kb fragment of BamHI digested genomic DNA. This probe was used as well as specific primers to exon 1, 4, 7, 8 and 10 in COX-2 gene to verify the λ clone and to distinguish between COX-1 and COX-2 cDNA^{140,141}. To disrupt the COX-2 gene in the ES cell line E14TG2s, the λ clone targeting construct was used. This construct consists a Neo gene inserted between EcoRI (E) and BstXI (Bx) in exon 8, a 104 bp deletion in exon 8 (of the regions encoding for Tyr-371 and His-374).

G418 and GANC were used as positive and negative selections and 11 out of 192 clones passed the positive/negative selection process. In order to confirm the presence of the

3.8kb targeted allele a Southern blot analysis was then used on these 11 clones and was digested with *SacI*.

C57BL/6 blastocysts were injected with two of the successfully targeted E14TG2a ES cell lines. As a result, male chimeric mice born and that were then mated with C57BL/6 females. These offspring mice carried the 129/C57BL/6 targeted allele. These COX-2 heterozygote mice were subsequently inbred to give rise to wild type (COX-2^{+/+}), heterozygote (COX-2^{+/-}) and homozygote (COX-2^{-/-}) mutant mice (Figure 2.3).

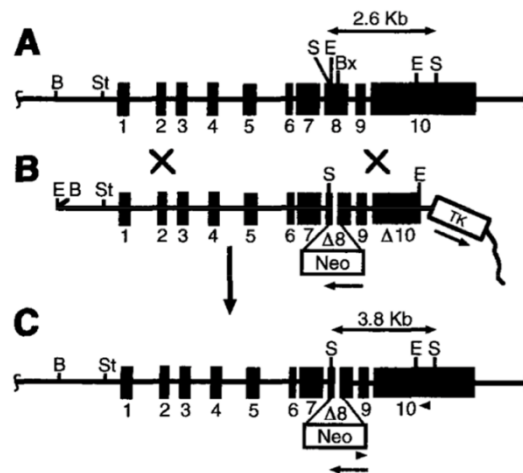


Figure 2.3: Strategic generation of COX-2^{-/-} mice. (A) COX-2 gene position. 2.6kb double arrow shows *SacI* fragment endemic to the WT gene. The restriction sites are designated *BglIII* (B), *BstXI* (Bx), *EcoRI* (E), *SacI* (S) and *StyI* (St). (B) Targeting vector construct. Wavy line represents plasmid sequence, and $\Delta 8$ indicates exon 8 (located between *EcoRI* and *BstXI*), where nucleotides essential for COX-2 activity were deleted. Neomycin resistance inserted at $\Delta 8$. Exon 10 with the TK gene was indicated as $\Delta 10$. (C) Homologous recombination of the targeting construct into the COX-2 gene, resulting in a Neo positive and Tk negative gene, which would only be present in non-homologous recombination where the plasmid DNA is incorporated into the target DNA. The 3.8 kb double arrow appears only in the targeted COX-2 gene. Black boxes indicate exons and solid line indicates introns. Figure adapted from¹³⁵.

IP receptor deletion

The IP Knockout mice were generated as described by Murata et al¹³⁷. Briefly, a 129/Sv-strain genomic DNA library was used to isolate the murine IP genomic clones, using its cDNA as a probe¹⁴². To construct the targeting vector, the Neo gene (pMC1-neo; Stratagene) was inserted instead of a 2.4-kb fragment containing parts of the putative exons II and III, which encode the sixth transmembrane domain towards the C terminus of this seven-transmembrane-domain receptor. The herpes simplex virus thymidine kinase gene (TK) was inserted downstream (Figure 2.4). The targeting vector was linearized with *Asp718* and

introduced into E14-1 ES cells by electroporation. G418 and GANC were used as positive and negative selections and the resulting clones were isolated and screened by PCR for homologous recombination, which was then confirmed by Southern blot hybridization¹³⁷.

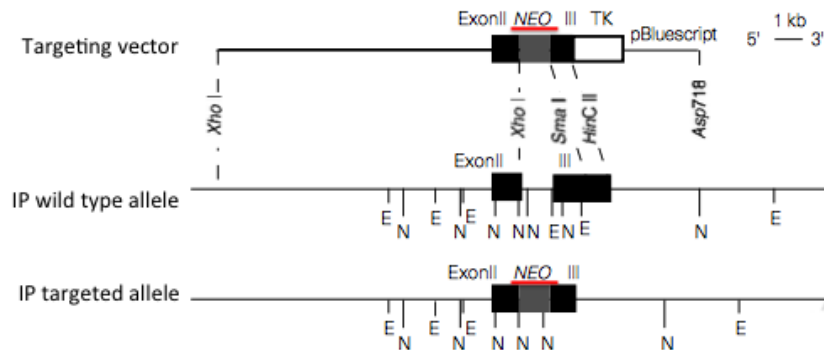


Figure 2.4: The deletion of IP gene in mice. Restriction maps for the targeting vector, the IP wild type allele and the IP targeted allele. Boxes indicate the exons: NEO, neomycin-resistant gene; TK, thymidine kinase gene; N, NcoI; E, EcoT221¹³⁷.

Mouse tissues preparation for imaging using En face confocal microscopy

Mouse preparation for staining protocol

Mice were killed using CO₂ asphyxiation and then immediately perfused under pressure using a syringe connected to a needle inserted via the left ventricle of the heart with 20ml phosphate buffered saline (PBS, Sigma, D8537x6) followed by 20ml 2% formaldehyde (5% buffered formalin, Sigma). The purpose of using formaldehyde as a fixative solution is that it will help to cross link the aldehydes and the proteins in the tissues to create a gel that will maintain the cellular components and in vivo appearance for accurate evaluation. The heart (aortic arch, the thymus that protecting the arch and the thoracic aorta) was carefully removed and placed in phosphate buffered saline (PBS). This procedure was performed by one of my co-supervisors Dr Nicholas Kirkby. The aortic arch and the thoracic aorta were then dissected from the heart and carefully cleaned off connective tissue. The arch with the thoracic part of the aorta were then placed in 96 well plate and covered with 200µl PBS and then the tissues are ready for staining.

General staining protocol for mice aortic arches

The aortic arches were blocked with 20% normal goat serum (vector labs S-1000) and permeabilised with 0.1% Triton X-100 (Sigma T8787) for 2 hours or overnight at room

temperature. Following the permeabilisation, the tissues were washed 2x with PBS and incubated with primary antibodies for 2 or 4 hours at room temperature. Secondary antibodies were added for one or two hours after washing the tissues 3x with PBS. Subsequently, primary antibody against the endothelial cell CD31 was added overnight at 4°C after the tissues were washed 3x with PBS. In order to stain the endothelial cell nuclei, 4',6'-diamidino-2-phenylindole (DAPI) was added for 5 minutes and washed off with distilled water. More details about the dilutions and reagents are listed below in Table 2.1. The aortic tissues were then cut open to reveal the luminal surface and mounted between cover slips and cover glasses (Vectashield hardset mounting medium) and left to dry for ~2 hours or until the medium set under the pressure from a box of gloves and then stored in a slide holder in the fridge until imaged using confocal microscopy (described below).

| <u>Antibodies and nuclear staining</u> | <u>Reagents</u> |
|---|--|
| Primary antibody staining 1:50 dilution in PBS | Raised in rabbit: COX-1 anti-mouse (Cayman, 160109) COX-2 rabbit anti-mouse (Cayman, 160108) |
| Secondary antibody staining 1:100 dilution in PBS | Goat anti rabbit (Invitrogen Alexa Fluor 594 conjugated, A-11012) |
| CD31 primary antibody staining 1:100 dilution in PBS | Alexa Fluor 488 conjugated anti-mouse CD31 (Biolegend, 102514) |
| DAPI nuclear stain 25µg/ml dissolved in distilled water, dH ₂ O | DAPI from Invitrogen (D1306) |

Table 2.1 Details of the antibodies and the Reagents that have been used for staining mouse aortic arches

Mounting of mouse aortic arches

Mouse tissue was mounted between cover slip (electrostatic, SC-24976) and cover glasses (electrostatic, SC-24975). One drop of Vectashield hardest mounting medium (Vector Labs, Vectashield H-1400) was used on the cover slip side and the tissue was placed on the mounting medium. Under a light dissection microscope the slide was visualised and the arches were cut open differently in some experiments depending on the purpose of the study as described below in the figure (Figure 2.5). The cut was either along the greater and

lesser curvature side, which will give the butterfly-like shape, or the arches were cut through the interface, which will split the greater and the lesser curvature each in different slid. The tissues were then flipped over carefully, the luminal side surface facing down. The cover slip was then coated with nail varnish and more mounting medium was added to the slide. 3 boxes of gloves (~7lb) were placed above the labelled slides over night at room temperature to make sure that the tissues were flattened.

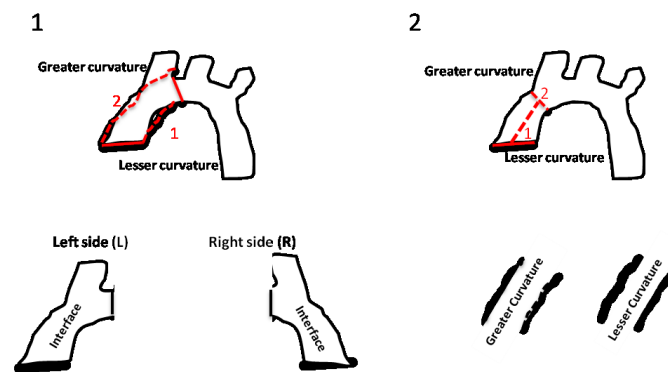


Figure 2.5: Different ways of cutting the aortic arches open. The aortic arches were either cut along the greater and lesser curvature side (1) or through the interface region (2).

En face confocal microscopy settings

A Leica SP5 inverted confocal microscope was used to image the arches and the aortic rings at the Facility for by Light Microscopy (FILM) at Imperial College. All of the images were taken using a 40X objective oil immersion lens. Laser and gain settings were set and saved at the beginning of each imaging protocol. Invitrogen spectra viewer was used to set the wavelength detection settings, and the wavelengths were: DAPI: 50% UV 405 laser detection (420-480nm), CD31: 30% Argon 488 laser detection: (500-550nm) and COX-1/COX-2 (Alexa Fluor 594): 50% Helium Neon 543 laser detection: (590-700nm).

Scanning Electron Microscope (SEM)

For SEM imaging wild type (WT, C57BL/6 mice) mice (10-12 weeks) were killed by CO₂ induced asphyxiation and then immediately perfused by a needle inserted through the left ventricle with PBS and 4% formaldehyde (10% buffered formalin) using a perfusion rig set up equating to ~100 mmHg pressure. The aortic arch and the thoracic aorta were carefully

removed and placed in a vial with 4% formaldehyde. This procedure was performed by one of my co-supervisors Dr Nicholas Kirkby.

Aortic arches were cleared of connective tissue and cut in the two different ways described above in Figure 2.5; either cut alongside the greater curvature and the lesser curvature in order to place the interface region centred in the middle of the tissue for better focus or cut along the interface region so that the focus could better be set on the greater curvature and the lesser curvature respectively. After the tissues were cut open according to their final orientation, the tissues were further fixed by immersion in 2.5% glutaraldehyde (TAAB Laboratories) for at least 12 hours at 4°C. The tissues were then handed over to the manager at the SEM unit at the Royal Brompton Hospital, Mr Andrew Rogers, for assistance with the post-fixation and gold coating procedures briefly outlined. The tissues were immersed in 0.05M sodium cacodylate buffer pH7.2 (Agar Scientific) at 4°C for at least 12 hours. Followed by post-fixation in 1% osmium tetroxide (TAAB Laboratories) for 1 hour and then dehydrated through a graded series of ethanol dilutions (70% -100%). The tissues were then dried by placing the tissues in a 1:1 mixture of 100% ethanol and hexamethyldisilazane (HMDS) for 30 minutes as described previously¹⁴³. Finally, specimens were mounted (with their 3D shape intact) onto SEM stubs, sputter coated with gold (E5350; Polaron Equipment Ltd) and examined using a S4000 SEM microscope (S4000; Hitach High-Technologies).

Quantification

COX-1 and COX-2 immunoreactivity was quantified as mean fluorescence intensity using the non-license version of the Leica Application Suite Advanced Fluorescence Lite (LAS AF) confocal program. Non-specific binding (background fluorescence) was excluded by subtracting the fluorescence of tissue in which the primary antibody was omitted from the staining protocol. For quantification of nuclear alignment, nuclear density and average nuclear size, images were quantified using image J software (NIH). The nuclei in the images were thresholded using the default criteria in order to include the nuclei and not the background and then quantified according to their area and Feret angle. Any nuclear area that was smaller than 2 μm^2 was excluded from the analysis. A more detailed description of the nuclear alignment quantification is given in the results section.

Tissue collection, processing and prostanoid release bioassay

Vascular release assays

In my thesis I have measured prostanoid release (especially PGI₂) from vascular tissue from mice. This was done using wild type (WT, C57BL/6 mice), COX-1 and COX-2 knockout mice (n=5-6 mice) (10-12 weeks old) killed by CO₂ asphyxiation. Aortas were removed and divided into 2mm rings after which, in some rings, the endothelium was removed by rubbing of the luminal surface with forceps. Aortas were allowed to equilibrate in Dulbecco's modified eagle's medium (DMEM, Sigma) for 60 minutes at 37°C, before medium was replaced and vessels incubated with A23187 (50µM, Sigma), bradykinin (100nM, Tocris Bioscience), thrombin (1U/ml, Sigma), ADP (10µM, Chronolog), acetylcholine (ACh, 10µM, Sigma), or vehicle (0.1% DMSO, VWR). After 30 minutes, medium was removed for measurement of prostanoids by immunoassay or LC/MS/MS (see below).

Plasma, serum and urine collection

Blood was collected from the inferior vena cava into heparin (10 U/mL final; Leo Laboratories, UK) or clotting-tubes (Sarstedt, UK) were centrifuged for serum/plasma. Urine was collected directly from the bladder. Serum urea was measured by a commercial veterinary diagnostics service (IDEXX Laboratories, UK)

Analysis and assays

PGI₂ measurement by immunoassay

In my study I have used a Cayman, 6-keto-PGF_{1α}, ELISA Kit (515211), a competitive immunoassay, to measure the stable PGI₂ breakdown product 6-keto PGF_{1α}. Briefly, in this assay the free 6-keto-PGF_{1α} in a test sample competes with Acetylcholinesterase (AChE) conjugated 6-keto-PGF_{1α} (tracer) for a limited number of immobilised 6-keto-PGF_{1α} specific rabbit antibody-binding sites. The concentration of Tracer is constant while the concentration of the 6-keto-PGF_{1α} varies between the samples, so the higher concentration of free 6-keto-PGF_{1α} the less Tracer will be bound by the antibody. Ellman's Reagent (which contains the substrate for the Tracer) is used to measure the extent of Tracer capture. After this enzymatic reaction the samples will be coloured with a distinct yellow colour that's absorbs strongly at 412nm. Thus, the more absorbance at 412nm there is, the less free 6-keto-PGF_{1α} was present in the sample.

The assay was performed according to the manufacturers instructions. Briefly, samples and a standard curve of pure 6-keto-PGF_{1α} were added to wells of a 96-well plate pre-coated with rabbit anti-6-keto-PGF_{1α} antibody. Tracer (6-keto-PGF_{1α} AChE-conjugate) was then added and the components allowed to equilibrate overnight at 4°C. The following day, unbound reagents were removed by washing the plate. Ellman's reagent was then added resulting in an enzymatic reaction in the wells, which causes the solution to turn yellow and absorbs at 412 nm. This colour change was read using a spectrophotometer (Infinite®F50; Tecan, Switzerland). 6-ketoPGF_{1α} concentrations in samples were calculated by interpolating from a 6-keto-PGF_{1α} standard curve such as the example given in figure 2.6.

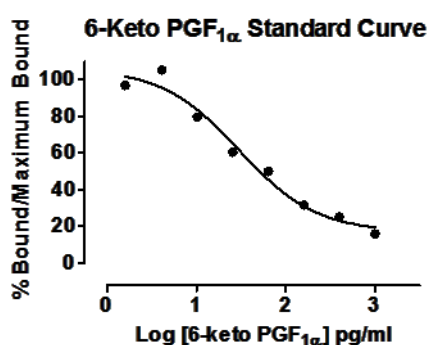


Figure 2.6 Representative 6-Keto PGF_{1α} Standard curve

Prostanoid measurement using LC/MS-MS

In my thesis release of a panel of prostanoids from mouse aortas was also measured using liquid chromatography – tandem mass spectrometry (LC/MS/MS). This protocol was carried out by collaborators at University of Bradford (Prof Anna Nicolaou and Dr Paula Urquart). This was performed according to the methodology published by their group¹⁴⁴.

Briefly, samples were mixed with 3ml ice-cold 15% methanol (v/v) and PGE₂-d₄ (40 ng) internal standard was added. The samples were then acidified to pH 3. Using solid phase extraction (Phenomenex, UK) the prostanoids were semi-purified. LC-MS/MS of the lipid extract was performed on a triple quadrupole mass spectrometer equipped with an electrospray probe and coupled to liquid chromatography (Waters, UK). Analysis of prostanoids was based on multiple reaction monitoring using the following transitions: 6-keto-PGF_{1α} *m/z* 369>163; PGE₂ *m/z* 351>271; 13, 14-dihydro 15- keto PGE₂ *m/z* 351>333;

PGD₂: *m/z* 351>271; TXB₂ *m/z* 369>169; PGF_{2α} *m/z* 353>193; PGB_{2-d4}: *m/z* 337>179. Results were expressed as pg metabolite / ml culture medium, using commercially available prostanoid standards (Cayman Chemicals, USA).

Protein and gene extractions and assays

Protein extraction

Tissue collected from mice was stored in liquid nitrogen until used. To extract the protein, tissues were homogenised using a TissueLyser II (Qiagen) in PBS with protease inhibitor (Roche, UK). Protein levels were measured using a Nanodrop SD-1000 Spectrophotometer (Thermo Scientific, MA, USA).

Western blotting

Proteins (20-30µg) were suspended in 4x Laemlli Sample Buffer (Bio-Rad, UK) and loaded into 7-12% SDS gels, depending on the proteins of interest. A pre-stained protein ladder marker (Precision Blue All-Blue Ladder, Bio-Rad, UK) was also added and the gel was run for 90 minutes at 90-150mV. Following electrophoresis, a wet transfer was performed on to a Hybond-P Immunoblot-PVDF membrane (Millipore, UK). The membrane was then blocked for 60 minutes in Tris 50mM, pH 7.4 containing 5% milk on a blocking platform. After blocking, the membrane was then incubated with the primary antibody at the necessary concentration overnight at 4°C on a rocking platform. The following day the membrane was washed for 3x5 minutes to rinse excess antibody away. The secondary antibody (Infra-red conjugate for Licor detection) was incubated with the membrane at room temperature for 60minutes. The blots were analysed using the Odyssey CLx Infrared Imaging System (Licor) at 800nm and 600nm absorbance. Relative abundance was quantified by densitometry using Image Studio Version 5 and corrected for the housekeeping protein α-tubulin content in each sample. The list of antibodies used in described in Table 2.2.

| <u>Antibody</u> | <u>Manufacturer</u> | <u>Selectivity</u> | <u>Dilution</u> | <u>kDa</u> |
|------------------------|----------------------------|---------------------------|------------------------|-------------------|
| α-tubulin | Cell Signalling | Rabbit anti-mouse | 1:500 | 50 |

| | | | | |
|-------|-----------------|--------------------|----------|-----|
| DDAH1 | Cell Signalling | Rabbit anti-mouse | 1:500 | 140 |
| 2° | Licor | Donkey anti-rabbit | 1:20,000 | N/A |
| 2° | Licor | Donkey anti-goat | 1:20,000 | N/A |

Table 2.2. Antibodies information that have been used for western blotting.

RNA extraction

RNA was extracted from murine tissue using the RNeasy plus universal mini kit (Qiagen, Venlo, Netherlands) according to the manufacturers' protocol. Tissue samples were homogenised using a TissueLyser II (Qiagen) for 5 minutes. RNA was extracted with the addition of chloroform to the trizol and centrifuged at 12,000xg at 4° C for 15 minutes. The RNA was then added to an equal volume of 70% ethanol and cleaned up using the filter columns and buffers provided in the kit. Purified RNA was eluted from the filter membrane with RNase free water (25-50ul). Concentrations of RNA were determined using a Nanodrop Spectrophotometer (Thermo Scientific, MA, USA).

RT-qPCR

iScript cDNA synthesis kit (BioRad, CA, USA) was used to convert RNA to cDNA using the following conditions; Reverse transcription for 30 minutes at 42°C and RTase inactivation for 5 minutes at 85°C. Purified cDNA (10ng) was then added to iTAQ fast SybrGreen supermix with ROX (BioRad, CA, USA) and primers run on a 7500 Fast Real-time PCR system (Applied Biosystem, USA). The program used was as follows: Initial step; 95°C at 10 minutes, Thermal cycling x40, Denaturation; 95°C for 15 seconds, Annealing; 60°C at 15 seconds. Alternatively Taqman probes and primers (0.5µl per reaction; Life Technologies, USA) were used instead of Sybr Green and its associated primers. Genes were quantified relative to housekeeping genes (Actb or Gapdh/18S) by comparative Ct methods. A full list of primers used in shown in Table 2.3 and Table 2.4.

| Primer | Forward | Reverse |
|---------------|------------------------------|---------------------------------|
| DDAH1 | 5'CACAGAAGGCCCTCAAGATC-3' | 5'-TCTCATAGACCTTTGCGCTTTC-3' |
| DDAH2 | 5-CCTGGTGCCACACCTTTCC-3' | 5'-AGGGTGACATCAGAGAGCTTCTG-3' |
| AGXT2 | 5'-GGCTTCCCCATGGCTGCAGTT-3' | 5'-CAATCACCTCAAGCACAGCAGATCC-3' |
| Beta-actin | 5'-CCAGGGTGTGATGGTGGGAATG-3' | 5'-CGCACGATTTCCCTCTCAGCTG-3' |

Table 2.3 : list of Syber Green primers used in my thesis.

| Primer | Probe |
|---------------|---------------|
| Ptgs2 | Mm00478374_m1 |
| Prmt1 | Mm00480133_m1 |
| Arg1 | Mm00475988_m1 |
| Arg2 | Mm00477592_m1 |
| 18S rRNA | Mm03928990_g1 |
| Gapdh | Mm99999915_g1 |

Table 2.4: list of Taqman primers used in my thesis.

Measurement of amino acids and methyl arginine analogues using LC-MS/MS

Methylarginine and amino acid concentrations were measured in tissues, plasma and urine samples (50µl) using Liquid chromatography-Mass Spectrometry (LC-MS/MS). Samples (50µl) were extracted by the addition of 100% methanol 1:5 (vol:vol) and incubated on ice for 5 minutes to remove proteins. An internal standard of d7 ADMA (200µM) was added to the samples to allow calculation of extraction efficiency. Samples were then vortexed and centrifuged at 13,000 RPM for 10 minutes at room temperature. The supernatant (100µl) was collected and vacuum dried for 1 hour to remove excess methanol. 50µl of the mobile phase (0.1% formic acid) was added to the remaining precipitate. The samples were then mixed carefully and transferred onto a 96 well plate for analysis on the LC-MS/MS.

The LC-MS/MS principle can be explained in four stages described below:

- 1) **Ionisation:** molecules in the sample are vaporised (by heating) and converted to ions by bombarding them with an electron beam.
- 2) **Acceleration:** the positive ions from the ionisation stage are accelerated towards a negative plate (speed of acceleration depends on the mass).
- 3) **Deflection:** the ions are deflected by a magnetic field (extent of deflection depends on the mass).
- 4) **Detection:** ions of increasing mass reach the detectors and a spectrum is provided on the computer.

In this protocol the sample components were separated by High-pressure liquid chromatography (HPLC). The separation of the sample components is based upon their binding affinity to a silica based column. 10 μ L of sample was injected on to a porous, graphite Hypercarb chromatography column (Thermo Scientific) using the HPLC system (Agilent). Samples were removed off the column using a mobile phase of 0.1% formic acid, 1% acetonitrile with a gradient increasing to 50% acetonitrile between 5 and 10 minutes of a 15 minute run per a sample. To avoid samples contamination a mobile phase consisting of 1% formic acid, 50% acetonitrile was used to wash the column clean preparing it for the next sample. The eluted samples were vaporised and ionized after passing into the Agilent 6400 series triple quadruple LC-MS/MS. The MS parameters for detection were as follows: ADMA, mass-to-charge ratio (m/z): 203.3 to 46.0, collision energy (CE; energy required to fragment the molecular ions): 12; SDMA, m/z : 203.3 to 70.2, CE: 24; monomethylarginine, m/z : 189.3 to 70.2, CE: 24; L-arginine, m/z : 175.2 to 60.1, CE: 8; d7-ADMA, m/z : 210.0 to 46.0, CE: 24.

Agilent's Masshunter Qualitative analysis programme was used to acquire and analyse the data. Chromatograms were acquired and the data extracted using the multiple reactions monitoring (MRM) method. In each sample the amount of the methylarginines were determined by the total ion count within the relevant peak and the actual concentrations were determined by running a standard curve within the sample run.

Vascular contraction and relaxation bioassays

Tissues preparation and loading for Isometric wire myography

Wild type (C57/Bl6) and COX-2 KO mice aged 10-12 weeks were killed by CO₂ asphyxiation. Aortas were collected and placed in PBS for transport and dissection. The aortas were cleaned from the connective tissues and then carefully cut in to 1.5mm rings. The rings were then transferred to Mulvany myograph chambers that contain 5 ml of warmed gasses (37°C, 95% O₂ and 5% CO₂) and physiological saline solution (PSS); consisting of NaCl 119 mM, KCL 4.7 mM, CaCl₂ 2.5 mM, MgSO₄ 1.17 mM, NaHCO₃ 25 mM, KH₂PO₄ 1.18 mM, EDTA 0.027 mM, glucose 5.5 mM. 40 μm in diameter wires were used to load the tissues in the chambers. For each tissue 2 wires were used one to fix the tissue and the second wire is connected to force transducer (attached to a PowerLab/800 recording unit; ADInstruments).

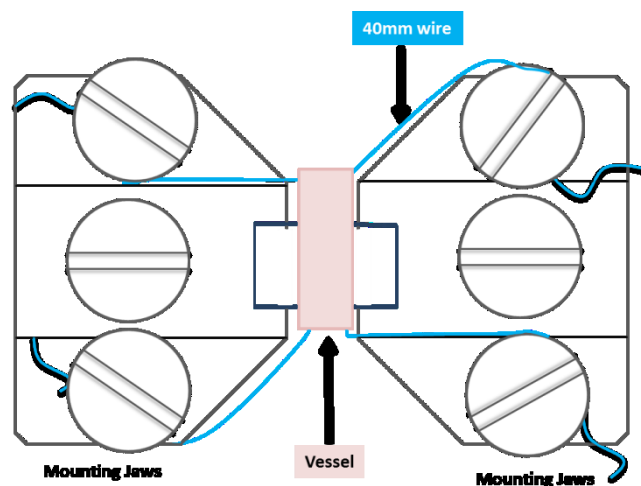


Figure 2.7: Schematic shows how the vessel was loaded on the mounting jaws.

This image shows how the vessels were loaded on the myograph chambers and the way that the wires were inserted into the tissues.

Protocol for myograph

After loading the tissues on the myograph, the tissues were then left to equilibrate for 10 minutes. In order to ensure differences in tissue size are minimized the aortas were normalised to a force of 13.3 kPa. Here, a physical tension was applied to the tissue in order to stretch the tissue and then left it to equilibrate for 3-5 minutes. When the final effective pressure of 13.3kPa is achieved, the aortas were left to equilibrate for 10 minutes.

After the normalisation step the tissues were contracted with 5 ml of high potassium physiological saline solution (KPSS; KCL 123.7 mM, CaCl₂ 2.5 mM, MgSO₄ 1.17 mM, NaHCO₃ 25 mM, KH₂PO₄ 1.18 mM, EDTA 0.027 mM, glucose 5.5 mM). Tissues were left to contract until it was stabilised and then washed 3x with PSS (5ml) until a stable baseline is achieved. In the protocol stage, vessels were contracted by serial dilutions of thromboxane mimetic (U46619; 10⁻⁹ to 10⁻⁷ M) (Cayman Chemical-UK). This contraction step was performed to establish the EC₈₀ concentration to be used for the subsequent part of the experiment. After washing tissues again with PSS an EC₈₀ concentration of U46619 was added. After a stable concentration was seen, increasing concentrations of either acetylcholine (10⁻⁹ to 10⁻⁵ M), which relaxes vessels via the release of NO from the endothelium, or sodium nitroprusside (10⁻⁹ to 10⁻⁵ M) which relaxes vessels by giving NO directly to the smooth muscle and is therefore independent of the endothelium, were added.

Blood pressure measurement using radio-telemetry

Wild-type (C57Bl/6) mice (12-14 week-old males) were treated with vehicle (water only) or parecoxib (Pfizer, US), (100 mg/kg/day) supplemented in drinking water for 4 days. The mean carotid arterial blood pressure was measured using radio-telemetry. For telemetry experiments, a 1.4F Millar MikroTip (Millar, USA) pressure catheter was inserted in the right common carotid artery of spontaneously breathing mice anaesthetised with inhaled isoflourane (Abbott, USA). Animals were allowed to recover from the anesthetic and measurements made in conscious, unrestrained animals 21 days later. Blood pressure traces were recorded continuously (every 30 minutes for a total of 24 hours) using the PowerLab and Chart 5 software (AD Instruments Ltd., UK). Blood was obtained by tail nick in conscious animals into 3.2% citrate and plasma separated by centrifugation. This work was conducted with the help of the Nitric Oxide Signalling Group (Dr James Leiper) at the MRC Clinical Sciences Centre.

Measuring methyl arginine analogues and creatinine levels in human healthy volunteer samples

In my thesis I have studied the effect of the COX-2 selective inhibitor Celebrex and the nonselective COX-1/COX-2 inhibitor naproxen in human healthy volunteers. This study was approved by the St Thomas's Hospital Research Ethics Committee (Ref. 07/Q0702/24) and

conducted according to the Declaration of Helsinki. All volunteers gave written informed consent before entering the study. The study was carried out by our collaborator Professor Timothy Warner and my supervisors Dr Nicholas Kirkby and Professor Jane Mitchell and samples provided for me to analysis for methylarginines and amino acids. A description of the basic study is below.

In this study sixteen healthy young male aged 20 to 35 who had not taken NSAID for 14 days were recruited. Eight of these healthy volunteers received the COX-2 selective inhibitor Celebrex (celecoxib; 200 mg twice a day; Pfizer USA) and the remaining eight volunteers received the nonselective COX-1/COX-2 inhibitor Naprosyn (naproxen; 500 mg twice a day; Roche Switzerland) for 7 days. These are standard anti-inflammatory doses of these drugs. Blood was collected into citrate vacutainers (BD Diagnostics, UK) and urine sampled on day 0, before the first dose, and day 7, 2 hours after the final dose. The blood was then separated by centrifugation. The plasma and the urine were then used for measurement of methyl arginine analogues and creatinine levels and analysed using LC-MS/MS.

Studies with human endothelial cells

Isolation and culture of blood outgrowth endothelial cells (BOECs)

BOEC were isolated according to published protocols¹⁴⁵⁻¹⁴⁸ with minor modifications. These cells were isolated and cultured by a number of laboratory members and shared between projects as cell lines. First the blood was collected from healthy volunteers (ethics code: 08/H0708/69) in to tubes with Ficoll (48ml; 6x8ml tubes/patient). The tubes were then inverted 8 times and then centrifuged at maximum acceleration and braking rates and a 1600 relative centrifugal force (RCF) for 30 minutes at room temperature. After centrifuging step, the tubes were then inverted again for 8 times- to mix the buffy coat and the plasma/serum fraction. The mixture of the 8 tubes containing the buffy coat and the plasma/serum fraction were then transfer in to 50ml falcon tube and 10 % Hyclone foetal bovine serum (FBS) (Biosera-UK) in Dulbecco's phosphate buffer saline (PBS; Sigma Aldrich®-UK) added to give a final volume of 50ml. the 50ml tube was then centrifuged at maximum acceleration, intermediate break, 520 RCF for 15 minutes. The supernatant was then discarded and the pellet was resuspended in 10ml of 10% FBS/PBS solution and centrifugation for 15 minutes. This step called the washing step and it was repeated two

more times. After the 3x washes, the pellet was then resuspended in 10ml Lonza-EGM2 supplemented (Lonza, Belgium; Cat no. CC-4176) with 10% FBS (ThermoFischer, UK; Hyclone), human epidermal growth factor (hEGF), hydrocortisone, GA-1000 (Gentamicin, Amphotericin-B), vascular endothelial growth factor (VEGF), human fibroblastic growth factor-B (hFGF-B), insulin-like growth factor-1 (long R3-IGF-1), ascorbic acid and heparin. The cells were then counted using the haemocytometer, a 10µl of the cells suspension was transferred to haemocytometer. The cells density was calculated for plating in pre-coated 6- well plates (Nunc, Denmark). The plates were coated with type-1 rat-tail collagen (BD biosciences-UK) (5.2 µg/cm²) and incubated for 1 hour at 37°C and 5% CO₂. The plates were then washed 3 times with PBS. The cells were then resuspended in Lonza-EGM2 with 10% FBS and seeded into the 6-well plates at a density of 3 x 10⁷ cells/well.

After 24 hours the media was removed carefully and washed with 1 ml of fresh Lonza-EGM2 10% FBS. 4 ml of fresh Lonza-EGM2 10% FBS media was added. In the first 96 hours the media was changed 3 times. After that the media change every 2 days without washing until cobblestone colonies appeared. Colonies of endothelial cells usually emerged between day 5 and day 21. Once colonies had stopped expanding (usually between 3-5 days), they were be removed by trypsin digest (Trypsin-EDTA Solution (10X); Sigma Aldrich®-UK). 2 ml 1x trypsin was then added to the Cell and then incubated for 3 minutes or until cell detachment. Trypsin was then neutralized with 4 ml of Lonza-EGM2 10% FBS. The cell/trypsin mix were then transferred to a 50 ml falcon tube and centrifuged for 5 minutes, at 37°C, 200 RCF, maximal acceleration and intermediate break. The pellet was then resuspended in 7 ml of Lonza-EGM2 with 10% FBS and seeded into collagen-coated (5.2 µg/cm²) T25 culture flasks (Nunc-Denmark) until confluent. Cells were then expended into T75 culture flasks. The media changes every 2 days prior to use in experiments.

Cells were then tested with endothelial cells marker CD31 and/or VE-cadherin expression. The list below (Table 2.5) is a summary of donor healthy volunteers that I have used in my thesis.

| <u>Donor ID</u> | <u>Sex</u> | <u>Age</u> |
|-----------------|------------|------------|
| EPCA | M | 25 |
| EPCB | F | 28 |
| EPCC | M | 41 |
| EPCM | F | - |
| EPCS | F | 26 |
| EPCAK | F | 28 |

Table 2.5: List of healthy volunteer donors with successful isolations of BOEC. – indicates a missing record on this particular isolation

Cell plating

For BOECs plating, EGM2 media was removed carefully and washed twice with PBS to completely remove any remaining EGM2 media. 1X trypsin (TrypLE; Invitrogen, UK) was then added. The cells were incubated for 1 minute in 37°C and 5% CO₂ then trypsin was neutralised with EGM2 medium with 10% FBS. The cells were centrifuged for 5 minutes at 37°C, 200 RCF, maximal acceleration and intermediate break and resuspended in 5ml of fresh EGM2 medium. For 6-well plate experiments, cells were plated at a cell density of 100,000 cells per well. All cells were plated in EGM2 media with 10% FBS.

General staining protocol for staining BOECs

In 6-well plate the media was removed and the cells were washed 3 times with PBS. 4% para-formaldehyde (PFA) was added for 10 minutes at room temperature to fix the cells, followed by 3 times washing step with PBS. 0.2% Triton X-100 was added for 10 minutes to permeabilize the cells. The cells were blocked with 4% FBS in PBS for 1 hour at room temperature.

Primary antibodies were then added in 3% bovine serum albumin (BSA) in PBS for 1 hour at room temperature. Secondary antibodies were added in 3% bovine serum albumin (BSA) in PBS for 45 minutes after washing the tissues 3 times with PBS. Subsequently, primary antibody against the endothelial cell CD31 was added overnight at 4°C after the cells were washed 3 times with PBS. In order to stain the endothelial cell nuclei, 4',6'-diamidino-2-

phenylindole (DAPI)(10µg/ml) was added for 5 minutes and washed off with dH₂O. More details about the dilutions and reagents are listed below.

| <u>Antibodies and nuclear staining</u> | <u>Reagents</u> |
|---|--|
| <p>Primary antibody staining</p> <p>VE-cadherin 1:250 dilution in 3% BSA/PBS</p> <p>CD31 1:100 dilution in 3% BSA/PBS</p> | <p>VE-cadherin species: goat anti human: From Santa Cruz Biotech,Germany;sc-6458</p> <p>CD31 species: mouse anti- human pre- conjugated488: From Biolenged,UK;303110</p> |
| <p>Secondary antibody staining</p> <p>1:400 dilution in PBS</p> | <p>Donkey anti-goat(Alexa Fluor 594) From:Invitrogen,1003216</p> |

Table 2.6: A list of the antibodies that used in staining the BOECs

Cellomics

In my thesis I have used Cellomics® VTi HCS Arrayscan (camera make/model: Arrayscan 12bit dynamic range high resolution thermo-cooled with a Zeiss Plan Neurofluour 10 x objective lens) (Thermo Fisher, Pittsburgh, USA) to image the BOEC that was plated on 6-well plates. This technique will allow us to gather information such as (1) the number of cells in each well (cell/field), (2) the number of cells in the whole well (cell/well), (3) changes in nuclear shape of the cells in the whole well (mean). After following the staining protocols for BOECs, the cells within the 6-well plates stained with DAPI (Thermo Fisher Scientific-UK) and imaged Cellomics VTi Arrayscanner. For a negative control the cells were treated with 10mM H₂O₂.

Data analysis and statistics

The data is either presented as representative images or of the mean± S.E.M. for n experiments (animals or cell isolations) details of the n-values and the statistical packages used are provided in figure legends. Unless said otherwise the analysis was performed using GraphPad Prism software.

**Chapter 3: Location of COX-1 and COX-2
immunoreactivity in blood vessels and
implications for prostacyclin release**

Rational

Endothelial cells release powerful cardioprotective hormones that play an important role in regulating vascular tone and growth, thrombosis and platelet and leukocyte interactions with the endothelium. These vasoactive hormones include nitric oxide (NO), prostacyclin, endothelin (ET)-1, interleukins, endothelial growth factors, adhesion molecules, plasminogen inhibitors and von Willebrand factor. In this chapter I will focus on endothelial cell hormone release particularly prostacyclin. prostacyclin is produced as a result of the enzymatic actions of phospholipase A₂, cyclo-oxygenase (COX) and prostacyclin synthase. It has been clearly identified that COX has two isoforms: COX-1, which is a constitutive isoform, and COX-2, which is induced at the site of inflammation.

The isoform responsible for the production of prostacyclin has been the subject of debate with some studies suggesting that constitutively expressed COX-2 is responsible for prostacyclin production throughout the vasculature. However, this is not universally accepted and experiments, including those conducted in my group suggest that COX-1 drives prostacyclin in blood vessels. Previous work from my group showed that COX-1 immunoreactivity is expressed in the endothelium of blood vessels and by using tissue from knockout mice, COX-1 but not COX-2 drives was found to be the one responsible for prostacyclin release in healthy vessels⁷⁹. However, this work did not include a detailed analysis of the expression and role of COX-1 versus COX-2 across the different layers of blood vessels or define the contribution of endothelium to COX-1 driven prostacyclin release. Also this early work analyzed prostacyclin release using antibody based ELISA technology which, as suggested by others in the field can be prone to non-specific results¹⁴⁹.

The subject of my PhD thesis was to determine how COX-1 and COX-2 function in vessels and in later chapters in the kidney and to identify mechanisms by which blocking COX-2 can cause cardiovascular side effects. Thus, here in this first results chapter I have focused on repeating and validating our earlier observations in order to make a platform for finding mechanisms, which are described, in coming chapters.

Specific Aims

The specific aims of this chapter were:

1. To investigate the localization of COX isoforms in key regions (endothelial layer, smooth muscle cells layer and adventitial side) of the freshly isolated vessel.
2. To address the role of the endothelial layer and COX-1 versus COX-2 in the production of prostacyclin by freshly isolated blood vessels.
3. To establish how ex vivo induction of COX-2 expression affects the contribution of COX-1 to prostacyclin production in blood vessels.
4. To validate prostacyclin measurements using ELISA with liquid chromatography tandem mass spectrometry (LC-MS/MS).

Methods

A detailed description of the methods used in the chapter is described in the General Methods chapter (Chapter 2). In brief, in this chapter genetically modified mice, on a C57Bl/6J background, were used where either the COX-1 or COX-2 gene was knocked out. Mice were killed by asphyxiation using CO₂ before the aortas were removed. For vessel assays, segments of the descending aorta were dissected and cut into segments of approximately 2mm width.

For staining protocols in some experiments the aortic rings were fixed immediately after dissection but for others the tissue was incubated in Dulbecco's Modified Eagle Medium (DMEM) for up to 12 hours. After fixing vessel rings cut open to allow the luminal surface to be revealed before being fixed and stained with the endothelial marker CD31, the nuclear marker DAPI or with antibodies to COX-1 and COX-2.

For bioassay experiments to measure prostacyclin release, aortas were removed and divided into 2mm rings with, for some experiments, the endothelium being removed by gentle rubbing of the luminal surface with forceps. Aortic rings were allowed to equilibrate in DMEM for 30 minutes before medium was replaced with fresh media contain A23187 (50μM), bradykinin (100nM), thrombin (1U/ml), ADP (10μM), acetylcholine (10μM), or vehicle (0.1% DMSO). As PGI₂ is unstable levels were obtained by measuring the breakdown product, 6-keto-PGF_{1α} by commercial ELISA. In some experiments 6-keto-PGF_{1α} together

with other prostanoids including prostaglandin (PG)E₂, PGD₂, thromboxane (TX)B₂ and 13,14-dihydro-15-ketoPGE₂ were measured using LC-MS/MS using published protocols (see General Methods) by our collaborator Professor Nicolaou (University of Manchester).

Analysis and statistics

Data is presented as the mean \pm S.E.M and was analysed using Prism software and statistical packages indicated in the figure legends. A p value of <0.05 was taken as significant and denoted by *.

Results

Expression of COX-1 and COX-2 in key regions of the freshly isolated vessel

Mouse aorta was prepared with an intact endothelium and imaged using Z-stacking with a confocal microscope to capture three defined regions; endothelium, vascular smooth muscle and adventitia. The endothelial layer expressed CD31 and COX-1 with low or negligible levels of COX-2. The vascular smooth muscle layer and the adventitial layer expressed detectable but significantly less COX-1 and low or undetectable levels of CD31 and COX-2 (Figure 3.1).

Role of COX-1 and COX-2 in prostacyclin release by freshly isolated blood vessels.

Freshly isolated mouse aorta from wild type mice released prostacyclin after stimulation with a number of agonists with the following order of effect; A23187> acetylcholine≥ bradykinin≥ thrombin> ADP (Figure 3.2A). In each case the release of prostacyclin was increased in vessels prepared with an intact endothelium (Figure 3.2A). Similar results for prostacyclin release were seen for all conditions in aorta from COX-2 knockout mice (Figure 3.2B). In contrast to results from tissue from wild type mice, vessels from COX-1 knockout mice released virtually undetectable levels of prostacyclin under all stimulation conditions and regardless of whether the endothelium was present or not (Figure 3.2B).

Effect of time postmortem on COX-1 and COX-2 expression and activity in mouse aorta.

The results above show that COX-1, but not COX-2, is present and is responsible for prostacyclin release in control vessels taken from healthy mice that were wild type for COX-1 and COX-2. During the time that my group had been using the knock out mice it had been proving very difficult to show that COX-2 had any effect on prostanoids released in blood vessels. This was because, as I show here in Figure 2 that COX-1 is so highly expressed and so dominant when it comes to prostacyclin release. This was becoming a concern to the group because although the genotype was looked correct we were without a confirmation of phenotype.

To see if the strong role that COX-1 was having in prostacyclin release could change in vessels in experimental conditions where COX-2 should be induced I repeated some of the

experiments above in aorta incubated in culture medium with serum for 0.5-12 hours. As in data shown in Figure 1, the endothelial layer expressed COX-1 but not COX-2 in aorta from mice fixed within 15 minutes of death. COX-1 was also expressed and did not change in the endothelium of aorta incubated in culture medium with serum for different times up to 12 hours (Figure 3.3A,B). However, COX-2, which was low in endothelium of fresh vessels was induced by culture of the aorta such that significant increases were seen in the endothelium at 4 hours, peaking at 12 hours after culture of vessels with serum (Figure 3.3A,C). In order to see if the change in immunoreactivity for COX-2 in the endothelium of vessels after culture was important for prostacyclin release, tissue prostacyclin was measured at different times after culture. Aorta from wild type and COX-2 knock out mice from the 0-2 hours incubations released prostacyclin, with little or no release from aorta from COX-1 knock out mice. However this picture changed at time points after this where now prostacyclin was released from aorta from wild type and COX-1 knock out mice but not from COX-2 knock out mice. This data shows that in fresh vessels where only COX-1 immunoreactive was seen, COX-1 drives prostacyclin but after culture to induce COX-2, even though COX-1 is still present, COX-2 takes over the job of releasing prostacyclin (Figure 3.3D).

3.5.4 Expression of COX-1 and COX-2 in key regions of the vessel after stimulation in culture.

Next we wanted to see if the COX-2 induced in the endothelium by culture with serum was accompanied by COX-2 expression in the other layers of the vessel. To do this Z-stack images were taken of aorta cultured for 12 hours using confocal microscopy (Figure 3.4). As I found in figure 3.1 the vascular smooth muscle layer and the adventitial expressed detectable but significantly less COX-1 and low or undetectable levels of and COX-2. Culturing the vessels with serum did not significantly change the expression of COX-1 and COX-2 in vascular smooth muscle layer or adventitial layer but there was a trend to increase for COX-2 immunoreactivity with culture in the adventitia layer after 4, 8 and 12 hours (Figure 3.4B,C,D and E).

The data in this chapter so far is confirmatory of the overall idea that COX-1 in blood vessels causes the release of prostacyclin and that COX-2 is expressed only in very low levels, but

can be increased in vitro by experimental conditions similar to those that would induce proliferation (eg serum). As explained in the introduction and rationale to this chapter, the experiments presented in this chapter were performed in part to address concerns raised by other groups about experiments performed by our group using ELISA technology¹⁴⁹. To be sure that the data with ELISA⁷⁹ was real 6-ketoPGF_{1α} along with other eicosanoids (PGE₂, 13,14 dihydro 15 keto PGE₂, PGD₂ and thromboxane (TX)B₂) were measured using LC-MS/MS (Figure 3.5) by our collaborator Professor Nicolaou in the samples prepared as in Figure 3.2. Just like the data with the ELISA 6-ketoPGF_{1α} measured by mass spectrometry (LC-MS/MS) was reduced in aorta from COX-1 but not from COX-2 KO mice (Figure 3.5).

Summary

It is well known that the endothelium is the main site of prostacyclin production and this is because these cells are enriched with both COX and prostacyclin synthase enzymes¹³⁹. However, prostacyclin synthase is also enriched in other layers of the vessel including the smooth muscle¹³⁹. Many of the early studies demonstrating COX expression in the endothelium with less in the smooth muscle did not take into account the idea that COX-2 might be present there. This is because those studies were performed in the 1980s¹³⁹ before COX-2 was discovered in the 1990s¹⁴.

In this chapter I have used immunoreactivity to confirm that in healthy vessels COX-1 is highly expressed and it is the dominant isoform in the endothelium. I have confirmed that a detectable but lower level of COX-1 expression is present in the vascular smooth muscle layer and the adventitial layer. Importantly I have specifically shown that COX-2 expression is also low in the endothelium, smooth muscle layer and the adventitial layers. In line with this I have shown that the release of prostacyclin by isolated blood vessels is greater when the endothelium is present. The results that I got are similar to what is expected that removing the endothelium reduced prostacyclin release by 50-80%. Work from others in my group showed that when blood vessels are stimulated with the harsh and non-physiological agonist A23187, which allows non-specific calcium entry, the prostacyclin release is COX-1 dependent. In response to reviewers and others in the field I have extended these findings by showing the same is true when blood vessels are stimulated with more physiological stimuli, which, in each case, showed that prostacyclin release is COX-1 and not COX-2, dependent. However, A23187 was the most strongest way to see a prostacyclin release in vessels with much lower effects seen with other agonists with only acetylcholine showing much difference above control or 'basal' levels of prostacyclin. This is likely to be due to the fact that the level of activation that these more physiological stimuli provide to the vessel are not much above the stimuli that the vessels have through dissection and handling as part of the necessary procedures to perform the bioassay. However, the basal level of prostacyclin release, which is actually from vessels that will be stimulated (as I mention from dissection etc) was COX-2 dependent.

It was difficult to show a role of COX-2 in prostacyclin release and so to be sure that the mice I used had a 'true' phenotype I tried an experiment where COX-2 should be induced by culturing the vessels in media with serum. Serum induces COX-2 in endothelial cells where it is involved in proliferation and angiogenesis^{150,151}. I found that COX-2 was expressed quickly (after 2 hours) and that even though COX-1 was still present, using vessels from our COX-2 knock out mice, it completely took over as the driver for prostacyclin release. This work was essential to validate all of our previous work and the data in my thesis that our COX-2 prostacyclin mice have a correct phenotype. Most of the induced COX-2 was in the endothelium but there was also evidence that it was expressed in the adventitia but not in smooth muscle. This might be because these two areas of the vessel (being on the inside and outside) has the best access to the serum. The reason that the COX-1 activity in vessels that were cultured to express COX-2 did not seem active was likely due to the known suicide inactivation that happens for COX-1 after it has been working in tissue for a while (as mentioned in my Introduction, Chapter 1). This would mean that immunoreactivity is still present but that the catalytic activity has run out.

Conclusions

It has been widely believed over the past 10 years that the production of PGI₂ is dependent on COX-2¹⁵². With papers from our group and others this view has now changed although some authors are still (in 2016) questioning the importance of COX-1 to PGI₂ synthesis¹⁵². The field of COX/ prostacyclin biology now needs further studies to explain how the differences in views within the field can be explained. Work in my coming chapters provides some insight into this.

Limitation

In this chapter, the data reiterates the overwhelming role of COX-1 in the production of prostacyclin by healthy blood vessels, regardless of the agonist used. It also suggests that the production of prostacyclin in normal vessels is dependent upon both endothelial and non-endothelial cells. One of the limitations in this chapter is that all the mice that have been studied were young, it is really important to study the localization of COX-1 and COX-2 in aged mice to investigate if same results can be obtained or in mice with mild disease such as diabetes.

Moreover, in this chapter all the experiments were performed on mice tissues and no human samples were studied. It is very important to consider studying the release of prostacyclin in human samples to address the overwhelming role of COX-1 in the production of prostacyclin in healthy and diseased volunteers.

Figure 3.1

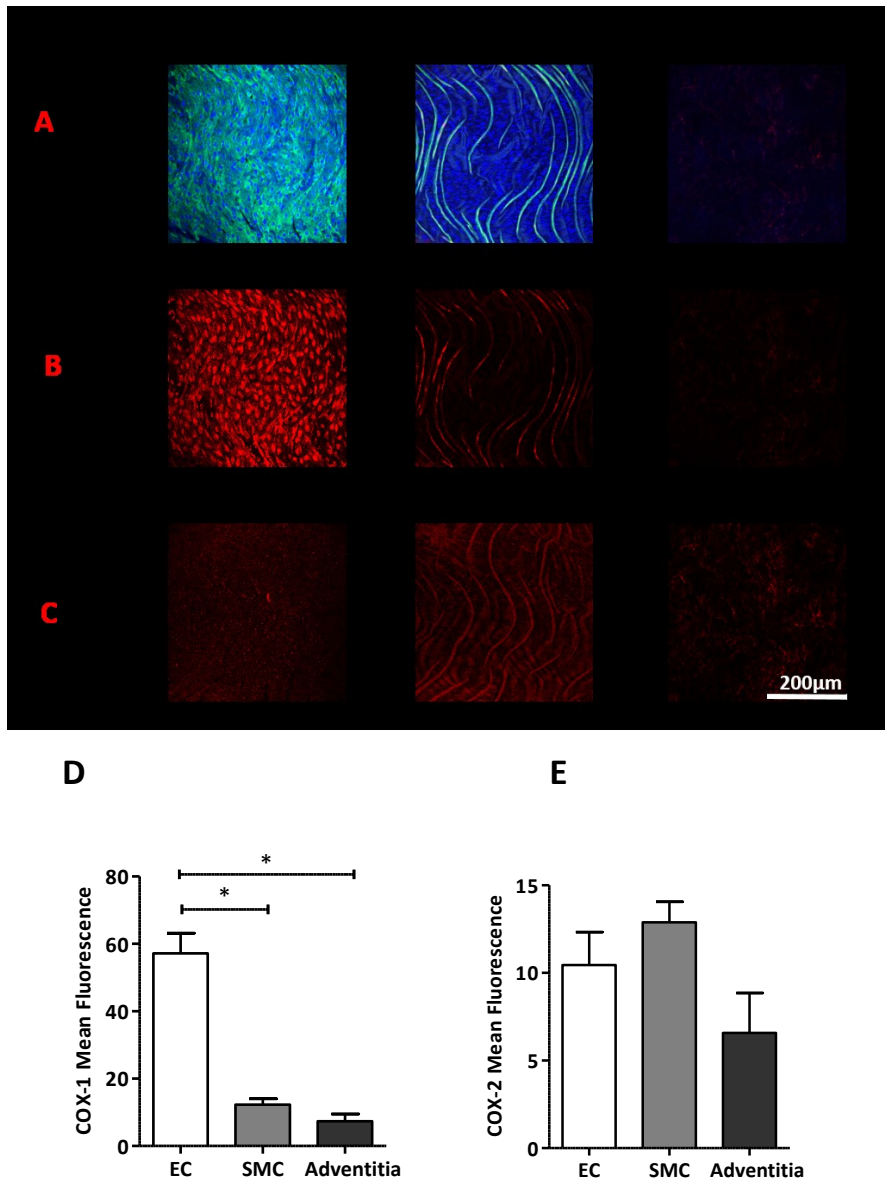


Figure 3.1: Expression of COX-1 and COX-2 in key regions of the freshly isolated vessel. Representative images taken by *en face* confocal microscopy from wild type mice thoracic aorta (n=4) showing the (A) the endothelial cells layer stained with the endothelial marker CD31 (green) and b DAPI (blue) which stain the nuclei from 10 to 12-week old wild type mice thoracic aorta (n=4), the smooth muscle cells layer where the endothelial marker CD31 is not expressed and only DAPI can be seen, and the Adventitia that does not express both the endothelial marker CD31 and the DAPI. (B) COX-1 and (C) COX-2 immunoreactivity in the endothelium, SMC and the adventitia. Pooled mean fluorescence values (D) for COX-1 and (E) COX-2 immunoreactivity. Data is the mean \pm S.E.M analysis was performed using one-way ANOVA with Dunnett's post test; *p<0.05.

Figure 3.2

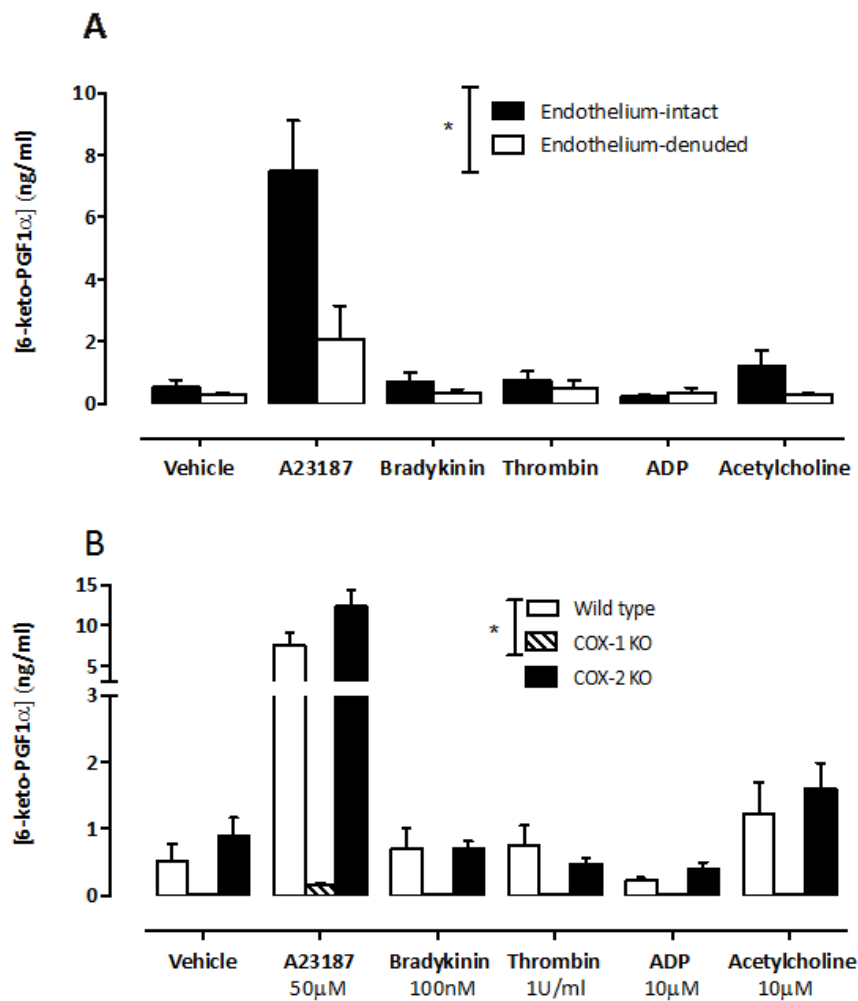


Figure 3.2: Role of the endothelium and COX-1 and COX-2 in prostacyclin release by freshly isolated blood vessels. (A) Aortas with or without endothelium from wild type mice ($n=6$, 10-12 weeks old) or **(B)** with endothelium for wild type, COX-1 or COX-2 KO mice were stimulated for 30 minutes with A23187 ($50\mu\text{M}$), bradykinin (100nM), thrombin (1U/ml), ADP ($10\mu\text{M}$), acetylcholine (ACh, $10\mu\text{M}$), or vehicle (0.1% DMSO) and prostacyclin breakdown product, 6-keto-PGF_{1α}. Data is mean \pm S.E.M; data was analysed by two-way ANOVA; $*p<0.05$.

Figure 3.3

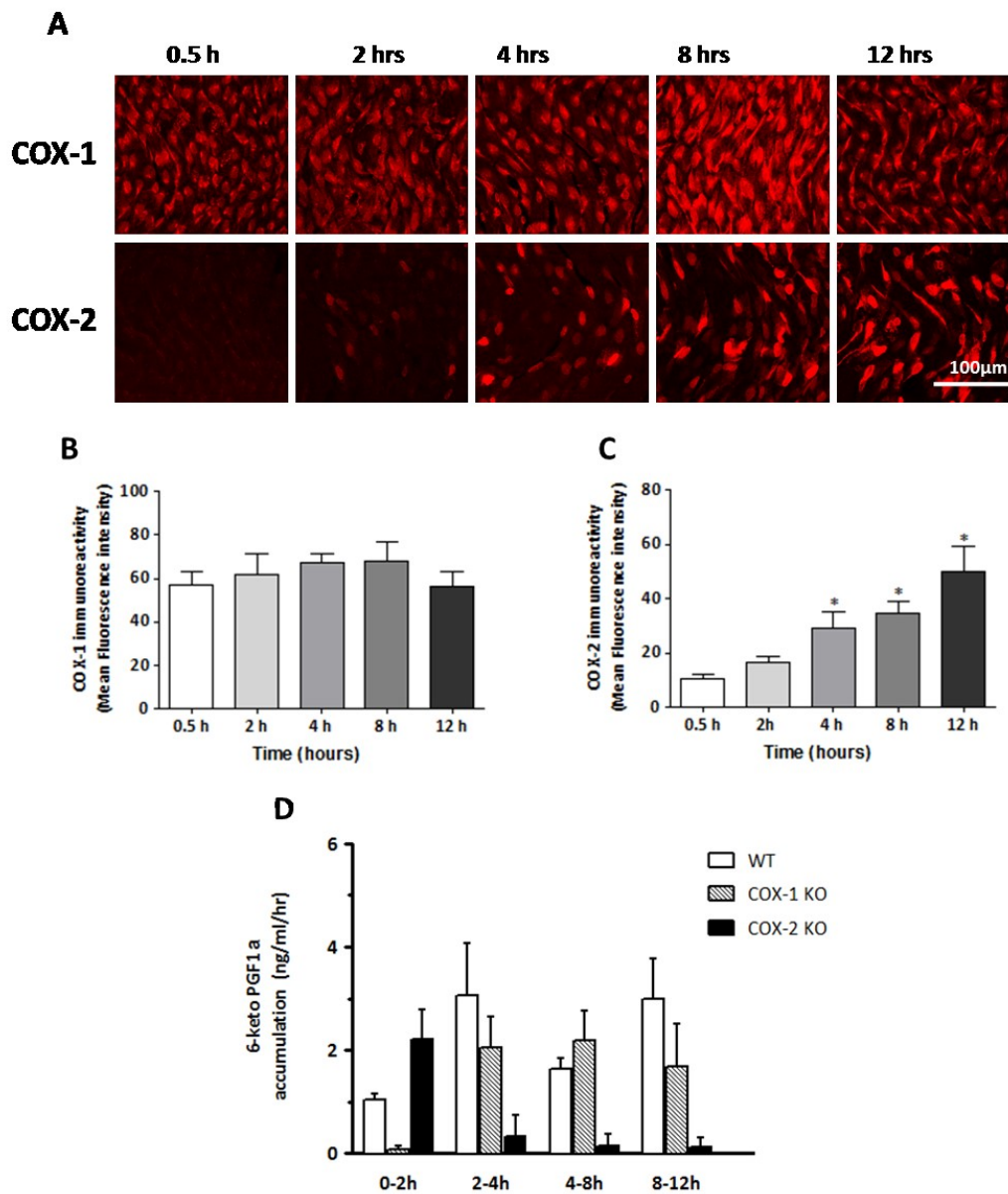


Figure 3.3: Effect of time post-mortem on COX-1 and COX-2 expression and activity in the endothelium of mouse aorta. Representative images (A) of COX-2 and COX-1 immunoreactivity in the endothelium of aorta from a wild type mouse incubated ex vivo for between 15 min and 12 h post-mortem. Scale bar 100µm. Pooled mean fluorescence values (B) for COX-1 and (C) COX-2 immunoreactivity from n=4 10 to 12-week old wild type mice. (D) COX activity (as 6-keto PGF_{1α}) measured in the same aortas over this time course from the same n = 4 mice. Data is the mean ± S.E.M analysis was performed using one-way ANOVA with Dunnett's post test; *p<0.05.

Figure 3.4

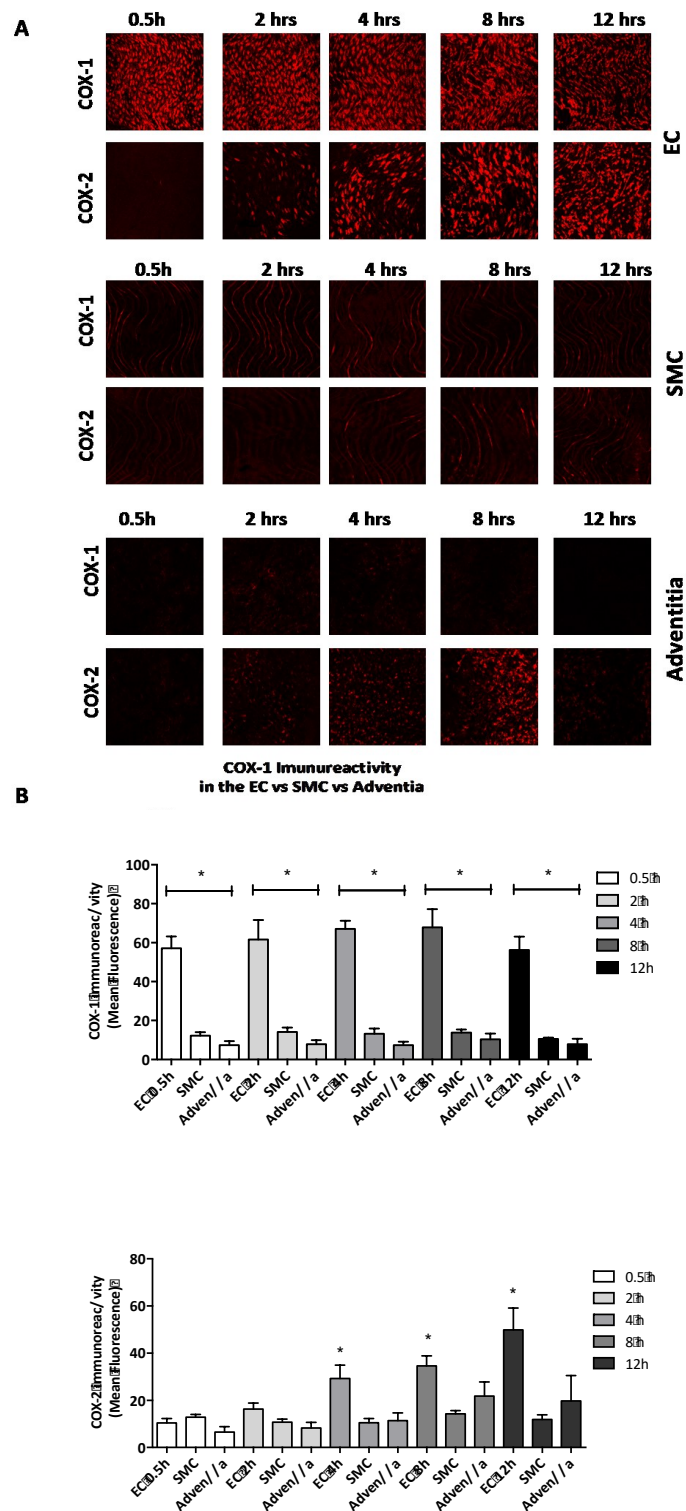


Figure 3.4: Effect of time post-mortem on COX-1 and COX-2 expression in different regions of the mouse aorta. Representative images (A) and quantified data (B) of COX-1 and COX-2 immunoreactivity in the endothelium (EC), smooth muscle (SMC) and Adventitia are shown. Data is mean \pm for $n=4$. * $P<0.05$ by one-way ANOVA followed by Dunnett's post-test; (COX-1, EC versus regions; COX-2 EC at 0.5 h vs other time points).

Figure 3.5

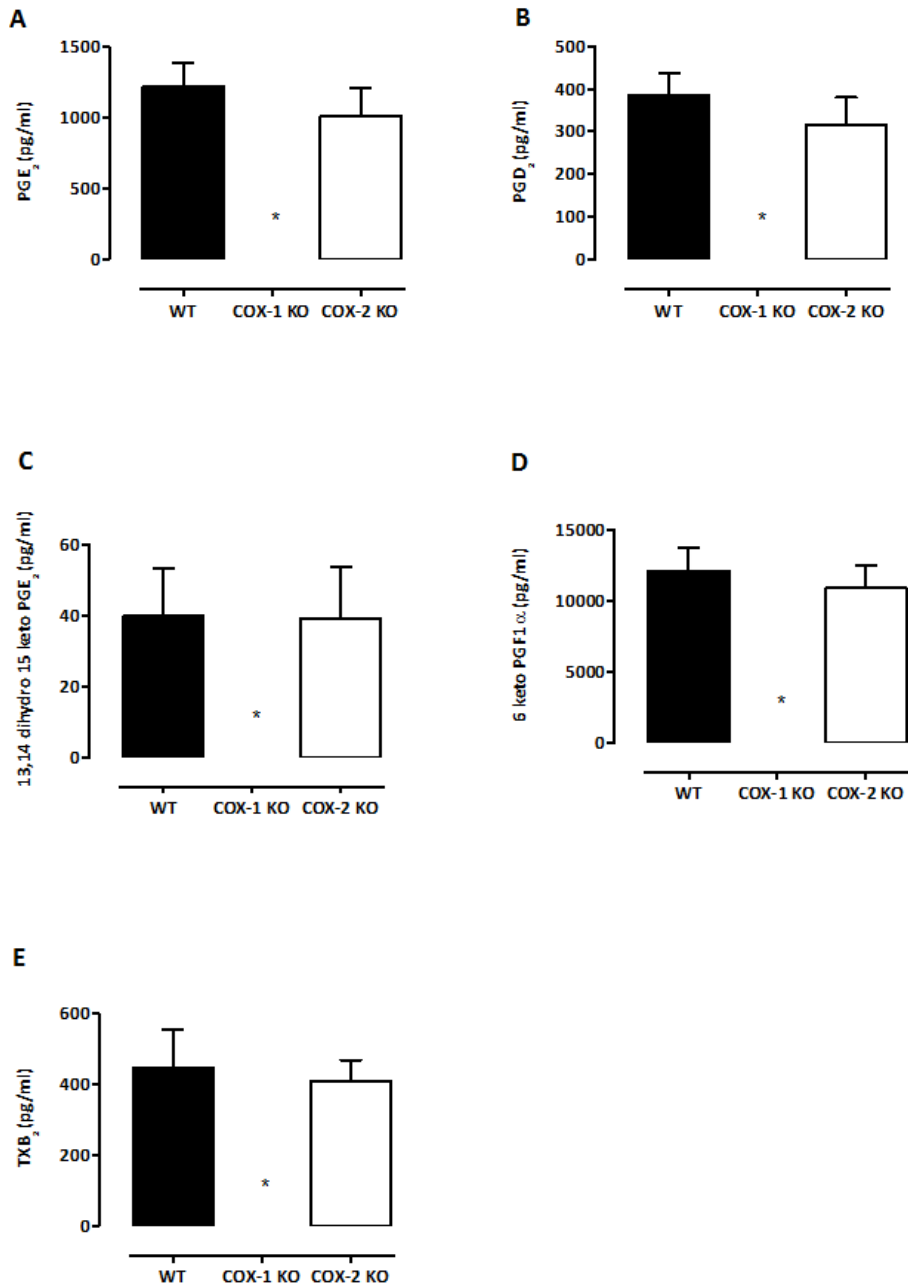


Figure 3.5: Effect of genetic knock out (KO) of COX-1 and COX-2 compared to wild type (WT) on eicosanoid formation measured using LC-MS/MS by isolated mouse aorta in vitro. Data is mean \pm for n=4. *P<0.05 by one-way ANOVA followed by Dunnett's post-test using wild type (WT) as the comparator.

Chapter 4: **The link between COX-2 and eNOS**

Rational

In the previous chapter, my data confirmed earlier studies in our group that COX-1 drives prostacyclin release from blood vessels in vitro. My work went on to show how COX-1 is expressed in different layers within blood vessels and that COX-2 was only really important for prostacyclin release if vessels were stimulated with inflammatory agents, in the case I used in Chapter 3 this was serum in culture medium. This work proves that in vessels and in the general circulation COX-2 is not important for gross prostacyclin, or other prostanoid, release. But, we know that COX-2 is expressed in some specialized locations in the body and we know that COX-2 inhibitors cause cardiovascular side effects. Work from my group using a genetically modified mouse where luciferase was knocked into the COX-2 promoter region, confirmed the kidney as a key area where COX-2 is induced¹⁵³. The kidney can be thought of as an important organ in the regulation of cardiovascular health. In this chapter I have looked in the kidney and the aorta to try to establish mechanisms that could help to explain how COX-2 inhibitors cause cardiovascular side effects. As I explain in the Introduction chapter (Chapter 1) where in animals or in human patients where the kidney function is affected then there is a knock on effect on the methylarginine pathway and so in this chapter particular attention was paid to making scientific links between the COX-2 and the methylarginine pathways. Methylarginines are endogenous inhibitors of endothelial nitric oxide synthase (eNOS) pathway; the best studied of this is asymmetric dimethylarginine (ADMA). ADMA is a biomarker and a mechanistic mediator of cardiovascular disease. Importantly for my work, ADMA metabolism involves the kidney. ADMA is increased with renal dysfunction. COX-2 inhibitors cause renal dysfunction. These facts led us to consider that there could be a mechanistic link between inhibiting COX-2 and increased ADMA. My project was involved in working on this idea based on a hypothesis made because of what is known. However, it was very helpful that also during the course of my PhD my fellow student, Ms Sarah Mazi who is also working on COX-2 but using 'omic' type experiments where there is now fixed hypothesis of what is regulating processes but performed a transcriptomic analysis on tissues from mice where COX-2 was blocked and found that genes that regulate ADMA were altered. Finally, during in the course of my PhD a paper was published showing that eNOS was reduced in vessels from COX-2 knockout mice, this work added evidence that there might be a connection between these two pathways.

Specific Aims

The specific aims of this chapter were to:

1. Confirm the relative expression of COX-1 and COX-2 in vessels (aorta) and kidney (renal medulla compared to renal cortex).
2. To establish the effect of genetic deletion of COX-1 or COX-2 in knockout mice on renal markers of injury.
3. Investigate the effect of COX-2 gene deletion in knockout mice on methylarginine and other amino acid levels.
4. To establish how COX-2 gene deletion in knockout mice affects the protein and gene expression levels of the renal methylarginine clearance enzyme DDAH1.
5. To extend these studies to look at effects of COX-2 gene deletion in knock out mice on other genes involved in methylarginine metabolism.
6. To address the role of the prostacyclin singling receptor, IP, using knockout mice in methylarginine metabolism.
7. To validate experiments above using genetically modified mice knockout mice using wild type mice and pharmacological inhibition of COX-2.
8. To extend the result in mice looking at methylarginine and other amino acid levels into a human healthy volunteer study.

Methods

A detailed description of the methods used in the chapter is described in the General Methods chapter (Chapter 2) and brief details are provided below.

Experimental animals and tissue collection

In this chapter COX-1 knockout, COX-2 knockout, IP knockout and C57Bl/6J background wild type mice were used. Mice were killed by CO₂ narcosis. Tissues (kidney, thymus, aorta and brain), blood and urine were collected details of these procedures are contained in the General Methods chapter (Chapter 2).

Western blotting

Mouse tissues (kidney, brain and thymus) were collected and homogenized using a Tissuelyser II. Protein levels were measured and the samples were loaded on to 7-12% SDS gels. The protein was then separated and transferred on to a fluorescent membrane. DDAH1 and mouse anti-alpha-tubulin were used as a primary antibody. Donkey anti-goat and donkey anti-mouse were used as a secondary antibody. The detailed protocol is given in the General Methods chapter (Chapter 2).

RT-qPCR

Tissues were collected, homogenized and total RNA was extracted. RNA was then converted to cDNA and qPCR was performed. The nomenclature for genes across species and for the related proteins can be confusing. For human and other species the nomenclature is with capital letters (similar to the protein) but for mouse genes the nomenclature is with a first letter as a capital and then lower case letters (eg DDAH1 versus Ddah1). For clarity here I have used capital letters for the gene and the protein but stuck with convention for gene levels in the figures. Levels of DDAH1, DDAH2, AGXT2, PTGS2 (COX-2), PRMT1, NOS3, ARG1, ARG2, ACTb, 18S rRNA and GAPDH were determined using the iTAQ fast SybrGreen supermix with ROX expression assays or TaqMan™ expression assays. Detailed protocol is given in the General Methods chapter (Chapter 2).

LC-MS/MS measurements

Plasma and urine samples were extracted by the addition of 100% methanol. Samples were then vortexed and centrifuged. The supernatant was collected and vacuum dried. The remaining precipitate was re-suspended in mobile phase (0.1% formic acid). Samples were analyzed using a LC-MS/MS as described previously¹³¹. The detailed protocol is described previously in the General Methods chapter (Chapter 2).

Data and statistical analysis

Data is mean \pm S.E. mean. Statistical significance (taken as $p < 0.05$) was determined using Prism software and statistical packages described in the figure legends and significance assumed where $p < 0.05$.

Results

COX-1 and COX-2 in the kidney and role on renal markers of dysfunction

In the last chapter the data showed that COX-2 was only sparsely present in vessels. In this chapter I confirm this at the gene level and compared that in aorta with the relatively high COX-2 expression seen in the renal medulla of the kidney (Figure 4.1A). Genetic deletion of COX-2 in the kidney is known to cause renal dysfunction¹⁵⁴ and here the data confirms this by showing that serum urea and creatinine, both markers of renal dysfunction, were increased in COX-2 knock mice (Figure 4.1B,C). It is important to say that whilst the renal medulla has more COX-2 than the aorta, COX-1 is still the dominant form when it comes to making prostacyclin in the whole tissue⁷⁹. But, even though this is the case, the markers of renal dysfunction, serum urea and creatinine, were not increased in blood from COX-1 knockout mice (Figure 4.1B,C). This suggests that COX-2 in the renal medulla is very important and operates in specific cells to regulate function.

Effects of COX-2 gene deletion of methylarginine and amino acid levels

In other types of renal dysfunction methylarginine metabolism can be disrupted. As I mentioned in the introduction, the methylarginines ADMA and LNMMA are important regulators of vascular homeostasis and inhibit the enzyme eNOS. In kidney homogenates ADMA but not LNMMA were increased in tissue from COX-2 but not COX-1 knockout mice compared to wild type control animals (Figure 4.2A,B). Also, like others have shown with different models of renal dysfunction, ADMA and now also LNMMA were increased in the plasma of COX-2 knockout, but not COX-1 knockout mice (Figure 4.3A,B). Levels of ADMA and LNMMA were not different in urine between any of the genotypes used (Table 4.1). It is important to consider methylarginine levels together with L-arginine levels because L-arginine can compete with methylarginines at the active site of eNOS. Because of this the field of methylarginine biology often uses a ratio value calculated from levels of ADMA and L-arginine in the same sample to predict what this might mean for eNOS activity or cardiovascular risks. In plasma of COX-2 knockout mice there was no significant change in L-arginine levels (Figure 4.4A) and the resulting ADMA:L-arginine ratio and LNMMA:L-arginine ratio were increased in line with the expectation that eNOS might be affected in these circumstances (Figure 4.4B,C). The consequences of changes in methylarginines on vessel function are discussed in detail in the next chapter (see Chapter 5). The third

methylarginine, SDMA, is excreted in the kidney but not metabolized by DDAH enzymes. SDMA is not biologically active and in my experiments levels did not change in kidney, plasma or urine between any of the genotypes of mice studied (Table 4.1).

The metabolism and nutritional pathways in the body involving L-arginine are in balance with other amino acids. In the case of eNOS activity the amino acids L-citrulline and L-glutamine have been shown to directly affect eNOS activity¹⁵⁵, by an action on cycling of L-arginine. The technique used to measure L-arginine and methylarginines that I used in my thesis is designed to provide a full range of other amino acid readouts, which was used to see if COX-2 gene deletion had effects outside of the L-arginine-methylarginine pathway. I found that among all the amino acids that we measured (ornithine, citrulline and arginine) the only amino acid that increases was the citrulline in COX-2 KO mice kidney (Table 4.1).

Effect of COX-2 gene deletion on Ddah1 and related methylarginine pathways

In the kidney the main enzymatic pathway that metabolises ADMA and LNMMA is DDAH1. In order to see if a decrease in DDAH1 might explain the increased methylarginine levels in plasma of the COX-2 knockout mice DDAH1 was measured at the protein and gene level by western blotting (Figure 4.5) and PCR (Figure 4.6) respectively. In addition to the kidney COX-2 is highly expressed in the brain and in the thymus⁸³. DDAH1 was detected in the kidney (Figure 4.5A,B) and in the brain (Figure 4.5A,C) but was not found in the thymus of wild type mice (Figure 4.5A,D). DDAH1 protein was increased in the kidney of COX-1 knockout mice and reduced in tissue from COX-2 knockout mice (Figure 4.5A,B).

In line with the protein expression data, DDAH1 gene expression was also reduced in the kidney of COX-2 KO mice (Figure 4.6A). The most studied form of DDAH in the kidney is DDAH1, but there is another form which is less well studied, DDAH2, which is found various cells including macrophages¹³⁰. In contrast to DDAH1, DDAH2 showed a trend to be increased in renal medulla of COX-2 KO mice compared to levels in tissue from wild type animals but this did not reach statistical significance (Figure 4.6B). Other genes that affect methylarginine and arginine metabolism are (i) AGXT2, which like DDAH, removes methylarginines, and (ii) arginase (which has two forms ARG1 and ARG2), which removes L-arginine. AGXT2 expression was reduced in renal medulla of COX-2 knockout mice (Figure

4.7). In my studies ARG2 but not ARG1 was detected mouse renal medulla. ARG2 was not significantly changed in tissue from COX-2 KO mice (Figure 4.7).

Next it was important to consider the enzyme that is involved in the formation of methylarginines. Methylarginines are formed when arginine in protein residues are methylated and released when the protein is broken down. Methylation of arginine at protein sites that leads to methylarginine production is mainly catalyzed by the enzyme PRMT1. In my experiments, PRMT1 was found to be increased in renal medulla tissue from COX-2 knockout mice (Figure 4.8).

To test further the mechanism that be behind the effect of COX-2 knockout on methylarginine levels in the plasma of mice I study the effect of loss of the prostacyclin receptor IP in IP knockout mice. As was found in plasma of COX-2 knockout mice, ADMA was increased in the plasma of IP knockout mice (Figure 4.9A) but L-NMMA was not increased (Figure 4.9B). L-arginine levels tended to decrease (Figure 4.9C) meaning that the relative increase in ADMA (as a ratio of L-arginine) was still increased. However, the increase in ADMA that was found in plasma from IP knockout mice was relative (to what was seen in plasma from COX-2 knockout mice) lower (Figure 4.9D). Unlike data from COX-2 knockout mice there were no associated change in any of the genes associated with methylarginine and arginine metabolism in tissue from IP knockout mice (Figure 10, 11 and 12). These data suggest that prostacyclin might have some role in the effects of COX-2 on methylarginine biology but that it is not the whole story and that other prostanoids or that other receptors could be important too. It was not possible to test this idea during the time I had in my PhD, as discussed in the limitations section at the end of this chapter.

Effects of inhibiting COX-2 pharmacologically in wild type mice and in healthy human volunteers on methylarginine and other amino acid levels

To understand if my data from genetically modified mice could be also seen when COX-2 activity was inhibited as opposed to being knocked out in a mouse through the whole stages of development (ie like was the case for my COX-2 knockout mice), wild type mice were treated with the COX-2 inhibitor paracoxib (100mg/kg/day) for 4 days and blood pressure was measured using radio-telemetry. As we would expect inhibition of COX-2 with paracoxib

caused increases in blood pressure (Figure 4.13A). As mentioned in my Introduction chapter (Chapter 1) this is a known effect of inhibiting COX-2 in the kidney. As was seen in plasma of COX-2 knockout mice, methylarginine levels for ADMA and LNMMA were increased in mice administered paracoxib (Figure 4.13B,C). There was no significant change in L-arginine levels in mice administered paracoxib (Figure 4.14A) and the resulting ADMA:L-arginine ratio and L-NMMA:L-arginine ratio were increased in line with the expectation that eNOS might be affected in these circumstances(Figure 4.14B,C). Finally, I had the opportunity to obtain plasma samples from a clinical study conducted by our collaborator Professor Timothy Warner and my supervisors Dr Nicholas Kirkby and Professor Jane Mitchell where healthy volunteers were administered standard anti-inflammatory doses of the mixed COX-1/COX-2 inhibitor naproxen or the selective COX-2 inhibitor Celebrex (celecoxib). From these samples I was able to obtain the measurements for methylarginines in the same way that I had done for the mouse samples. In healthy human volunteers both naproxen and Celebrex caused a small but statistically significant increase in ADMA levels (Table 4.2) suggesting that the effects seen in mice are relevant to human subjects.

Summery

In this chapter I have shown:

- 1) Kidney renal medulla expressed COX-2 more than renal cortex. This finding is in line with what is known about COX-2 expression in the kidney, which under normal or high salt conditions is predominantly expressed in the medulla region, particularly in the interstitial fibroblasts.
- 2) COX-2 gene deletion with COX-2 knockout mice causes increases the markers of renal dysfunction, serum urea and creatinine in blood. However, the levels of these makers did not increase in blood for COX-1 knockout mice. This finding was very important because it serves the purpose of highlighting the role of COX-2 in renal medulla in regulating cells and function.
- 3) COX-1 and COX-2 gene deletion in knockout mice had no effect on the levels of ADMA and LNMMA in kidney tissues but the plasma levels of ADMA and LNMMA were actually increased in mice that are lacking COX-2 but not COX-1 because of gene knockout.
- 4) DDHA1, which is the enzyme that is responsible for renal methylarginine metabolism, protein and gene expressions increased in kidney from COX-1 knockout mice and decreased in COX-2 knockout mouse kidneys.
- 5) Adding another line of explanation for increased ADMA, AGXT2, which is a gene that is also involved with removing methylarginine in the kidney, at the gene expression level was decreased in tissues from COX-2 knockout mice. However, COX-2 gene deletion had no effect on the levels of arginase, the gene that is responsible for removing L-arginine, at the gene expression level.
- 6) IP gene deletion in knockout mice caused increased ADMA levels in plasma but when comparing these changes with the changes found in ADMA levels in plasma from COX-2 knockout mice I found that this increase was lower than I found in plasma from COX-2 knockout mice. This suggested that prostacyclin may have a more minor effect than COX-2 on and methylarginine biology.
- 7) Inhibiting COX-2 pharmacologically in wild type mice and healthy human volunteers produced an increase in ADMA and LNMMA in plasma.

Conclusions

COX-2, partly through prostacyclin signaling, acts in a way in the kidney to keep in check the levels of the methylarginines ADMA and L-NMMA. These findings are very important because these methylarginines have effects of eNOS and that this might be able to explain the side effects caused by NSAIDs that work by blocking COX-2.

Limitation

In this chapter I have confirmed what was previously known that COX-2 is expressed constitutively in the kidney. More interestingly, I have shown a link between COX-2/eNOS pathway in the kidney and this link could be the explanation of the cardiovascular risk in patients taking traditional NSAIDs as well as COX-2 selective inhibitors. One limitation of this chapter is that we were not able to perform a similar study in mice or people with cardiovascular disease and/or that were of an older age bracket such as is associated with the type of people that take NSAIDs (ie over 65 years). Also it would have been good to have seen if L-arginine could reverse the blood pressure effect in mice given paracoxib. It would also have been good to have worked out the other pathways (other than IP) that are mediating the effects of COX-2 on the methylarginine levels and genes.

The key limitation in this chapter is to show an association (cause and effect) between the increased methylarginines and vascular eNOS function. I have addressed this to some extent in the next results chapter (Chapter 5).

Figure 4.1

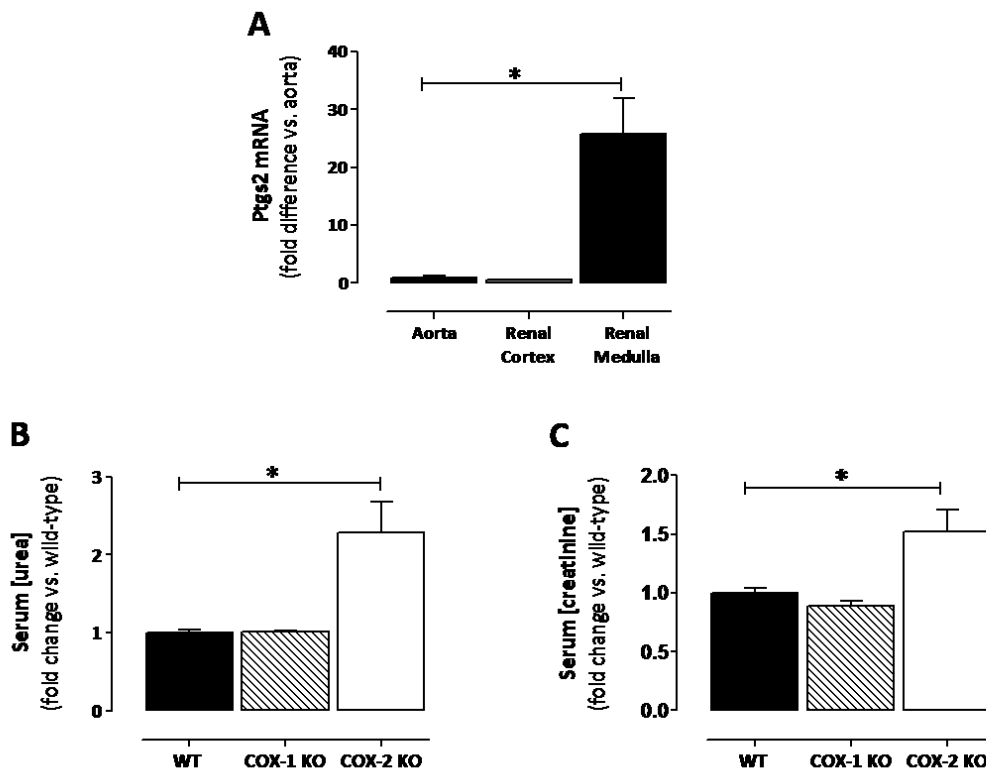


Figure 4.1: Role of COX-1 and COX-2 on renal markers of dysfunction. (A) COX-2 expression in mice aorta, renal cortex and renal medulla. (B) Serum urea and (C) serum creatinine levels in wild type, COX-1 and COX-2 KO mice. Data is mean \pm S.E.M from n=8-14 mice in each group. Data was analysed using Kruskal-Wallis with Dunn's post-hoc test, * $P < 0.05$ vs wild type.

Figure 4.2

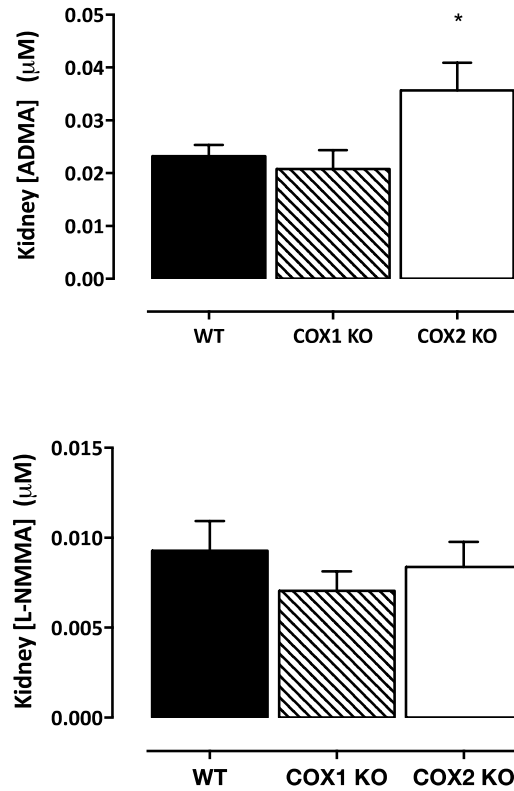


Figure 4.2: Effects of COX-2 gene deletion on methylarginine levels in kidney. (A) ADMA and (B) L-NMMA levels in kidney from WT, COX-1 and COX-2 KO mice. Data is mean \pm S.E.M from $n = 4$ mice. Data was analysed using a one-way ANOVA with Dunnet's post-hoc test, * $P < 0.05$ vs wild type.

Figure 4.3

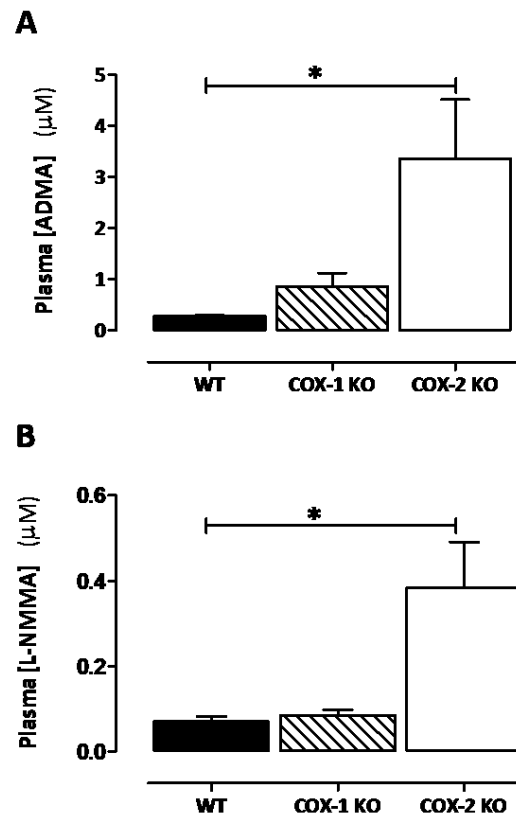


Figure 4.3: Effects of COX-2 gene deletion on methylarginine levels in plasma. (A) ADMA and (B) L-NMMA levels in plasma from WT, COX-1 and COX-2 KO mice. Data is mean \pm S.E.M from $n = 4$ mice. . Data was analysed using Kruskal-Wallis with Dunn's post-hoc test, $*P < 0.05$.

Figure 4.4

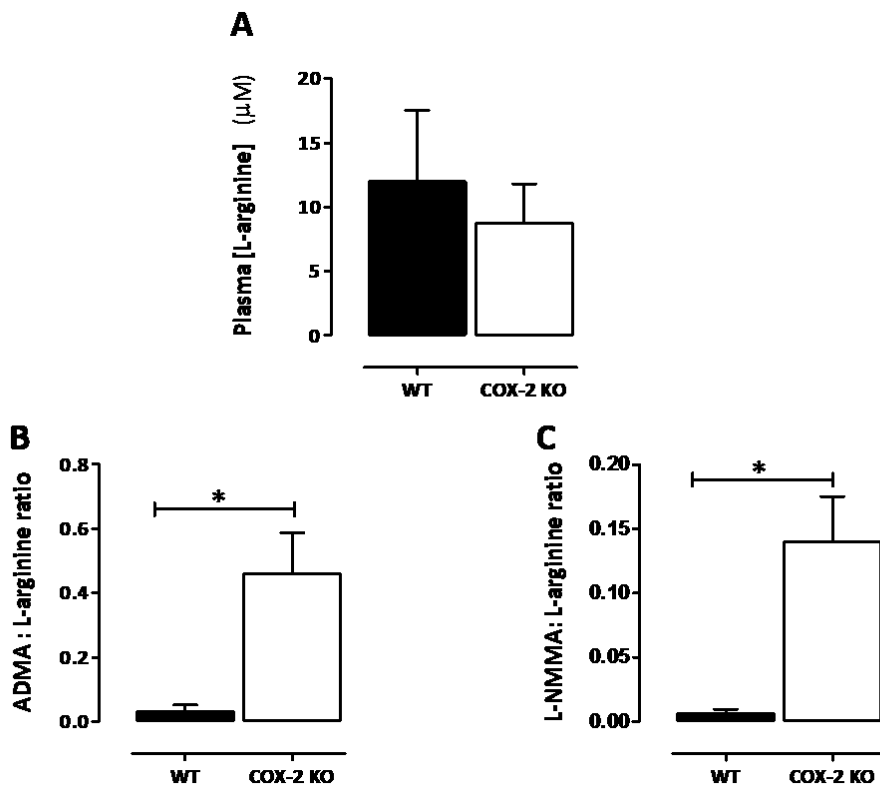


Figure 4.4: Effects of COX-2 gene deletion on plasma L-arginine levels. Plasma levels of (A) L-arginine, (B) ratio of ADMA: L-arginine and (C) L-NMMA: L-arginine in wild type and COX-2 KO. The data is the mean \pm S.E.M for $n=4$. Data was analysed Mann-Whitney U-test.

Table 4.1

| | | Ornithine | Citrulline | Arginine | ADMA | L-NMMA | SDMA |
|---------------|-----------------|-----------------|-------------------|-----------------|-----------------|-----------------|-----------------|
| Kidney | WT | 1.00 ± 0.12 | 1.00 ± 0.07 | 1.00 ± 0.12 | 1.00 ± 0.09 | 1.00 ± 0.18 | 1.00 ± 0.16 |
| | COX-1 KO | 1.10 ± 0.06 | 1.07 ± 0.14 | 1.30 ± 0.18 | 0.89 ± 0.15 | 0.76 ± 0.12 | 1.18 ± 0.17 |
| | COX-2 KO | 0.91 ± 0.16 | 2.32 ± 0.25* | 0.91 ± 0.12 | 1.54 ± 0.22* | 0.90 ± 0.15 | 0.14 ± 0.33 |
| | <i>p value</i> | <i>(p=0.57)</i> | <i>(p=0.0002)</i> | <i>(p=0.18)</i> | <i>(p=0.04)</i> | <i>(p=0.54)</i> | <i>(p=0.42)</i> |
| Plasma | WT | 1.00 ± 0.43 | 1.00 ± 0.72 | 1.00 ± 0.39 | 1.00 ± 0.06 | 1.00 ± 0.18 | 1.00 ± 0.06 |
| | COX-1 KO | 1.28 ± 0.12 | 1.44 ± 0.63 | 0.65 ± 0.16 | 3.11 ± 0.92 | 1.22 ± 0.17 | 2.61 ± 0.58 |
| | COX-2 KO | 0.92 ± 0.19 | 2.02 ± 1.44 | 0.48 ± 0.19 | 12.07 ± 4.18* | 5.52 ± 1.53* | 5.21 ± 2.75 |
| | <i>p value</i> | <i>(p=0.58)</i> | <i>(p=0.80)</i> | <i>(p=0.38)</i> | <i>(p=0.03)</i> | <i>(p=0.01)</i> | <i>(p=0.31)</i> |
| Urine | WT | 1.00 ± 0.17 | 1.00 ± 0.16 | 1.00 ± 0.17 | 1.00 ± 0.16 | 1.00 ± 0.39 | 1.00 ± 0.18 |
| | COX-1 KO | 0.75 ± 0.27 | 1.08 ± 0.40 | 0.76 ± 0.27 | 0.95 ± 0.06 | 0.82 ± 0.03 | 0.64 ± 0.15 |
| | COX-2 KO | 0.56 ± 0.01 | 2.16 ± 1.38 | 0.56 ± 0.01 | 0.56 ± 0.04 | 0.58 ± 0.31 | 0.63 ± 0.15 |
| | <i>p value</i> | <i>(p=0.32)</i> | <i>(p=0.41)</i> | <i>(p=0.32)</i> | <i>(p=0.22)</i> | <i>(p=0.76)</i> | <i>(p=0.34)</i> |

Table 4.1: Effects of COX deletion on kidney, plasma and urine methylarginine metabolites. Ornithine, citrulline and arginine levels in kidney (n=5), plasma (n=5) and urine (n=2-4) from wildtype, COX-1 and COX-2 KO mice. Data is represented as fold change compared to wild type and shown as mean ± SEM. P-values were determined by a one-way ANOVA and Dunnett's post-hoc test compared to WT values.

Figure 4.5

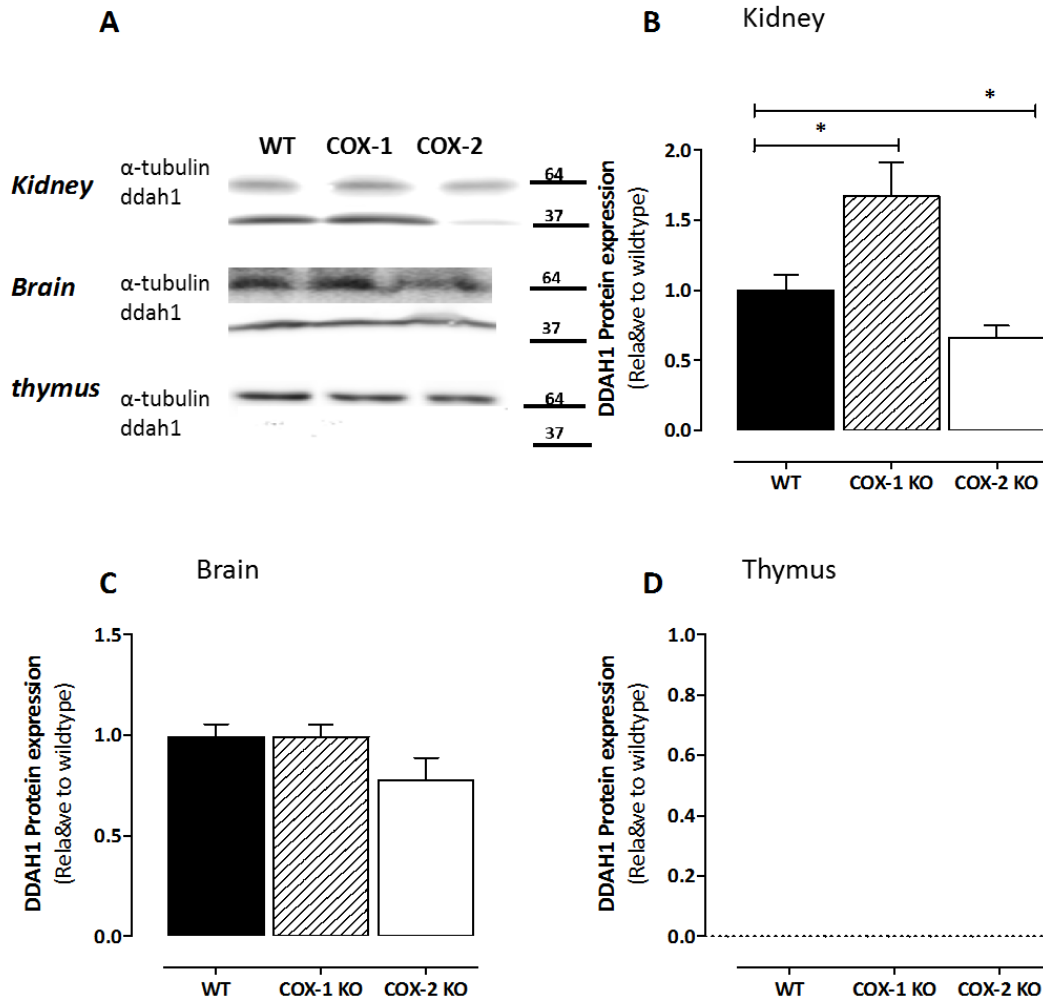


Figure 4.5: Effect of COX-2 gene deletion on DDAH1 in different tissues. (A) Relative expression of DDAH1 in kidney, brain and thymus in wild type, COX-1 and COX-2 KO mice. DDAH1 protein expression in WT, COX-1 and COX-2 KO mice from different tissues: (B) kidney, (C) brain and (D) thymus. Data is mean \pm S.E.M from $n=4-8$ mice. Data was analysed by one-way ANOVA and Dunnet's post-hoc t -test.

Figure 4.6

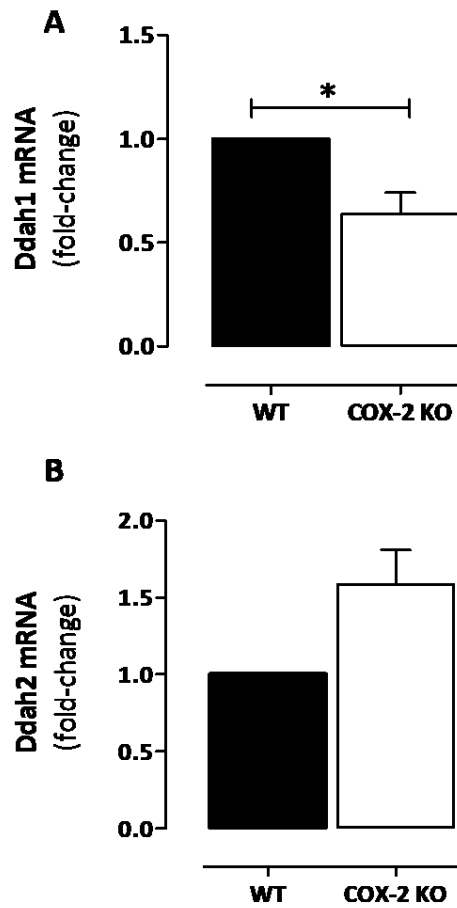


Figure 4.6: Effect of COX-2 gene deletion on mRNA expression of DDAH1 and DDAH2 in renal medulla. mRNA expression of (A) DDAH1 and (B) DDAH2 in wild type and COX-2 KO renal medulla. Data is mean \pm S.E.M from $n = 7-8$ mice. Data was analysed using Mann-Whitney U-test, * $P < 0.05$.

Figure 4.7

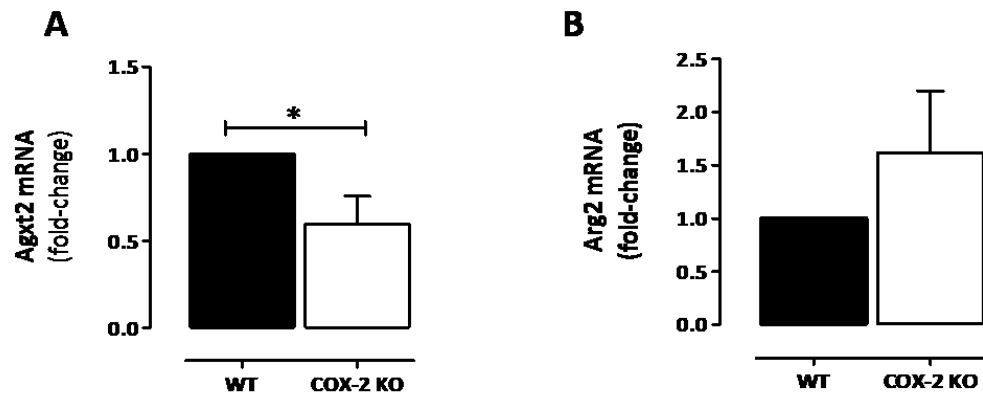


Figure 4.7: Effect of COX-2 gene deletion on related methylarginine pathways (Agxt2 and Arg2). mRNA expression of (A) Agxt2 and (B) Arg2 in wild type and COX-2 KO renal medulla. Data is mean \pm S.E.M from $n = 7-8$ mice. Data was analysed using Mann-Whitney U-test, * $P < 0.05$.

Figure 4.8

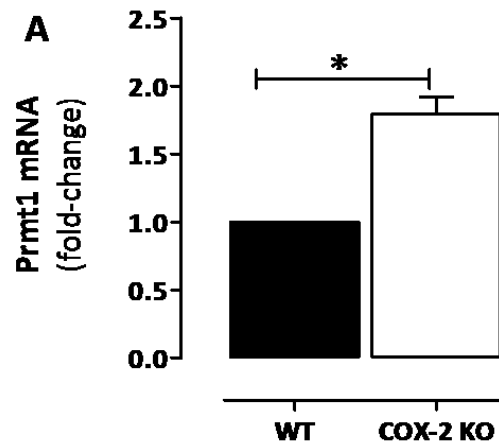


Figure 4.8: Effect of COX-2 gene deletion on related methylarginine pathways (Prmt1). mRNA expression of (A) Prmt1 in wild type and COX-2 KO renal medulla. Data is mean \pm S.E.M from $n = 7-8$ mice. Data was analysed using Mann-Whitney U-test, * $P < 0.05$.

Figure 4.9

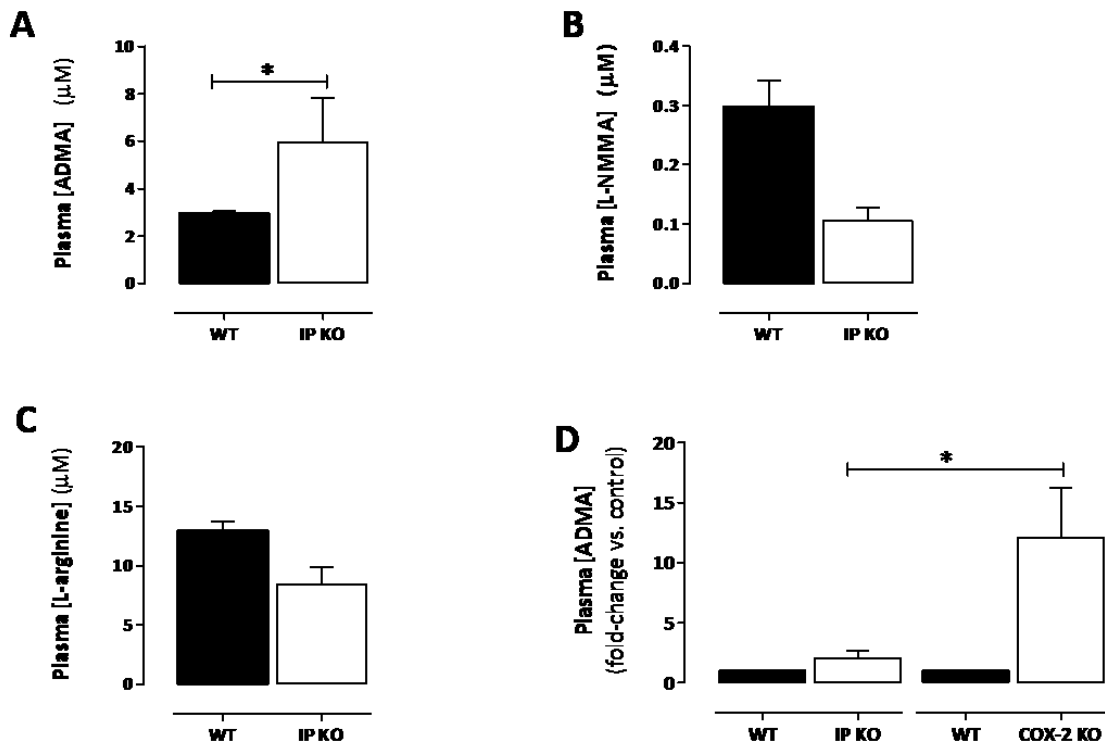


Figure 4.9: Effect of IP gene deletion on methylarginine levels in plasma. (A) Plasma ADMA, (B) L-NMMA and (C) L-arginine levels in wild type and IP KO mice. (D) A comparison between the levels of plasma ADMA in IP KO and COX-2 KO mice. Data is mean \pm S.E.M from $n = 8$ mice. Data was analysed using Mann-Whitney U-test, * $P < 0.05$.

Figure 4.10

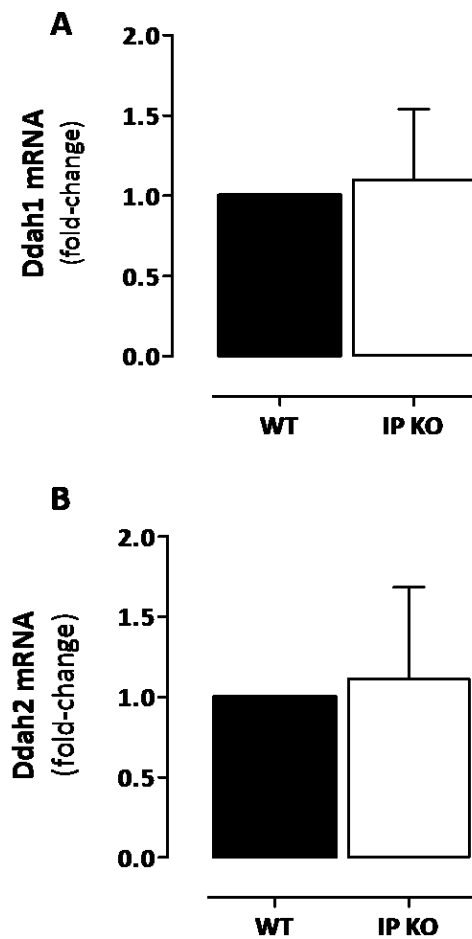


Figure 4.10: Effect of IP gene deletion on mRNA expression of DDAH1 and DDAH2 in renal medulla. mRNA expression of (A) *Ddah1* and (B) *Ddah2* in wild type and IP KO renal medulla. Data is mean \pm S.E.M from $n = 8$ mice. Data was analysed using Mann-Whitney U-test, * $P < 0.05$.

Figure 4.11

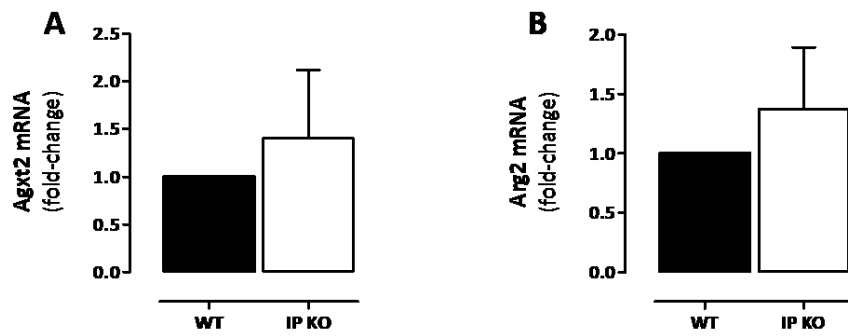


Figure 4.11: Effect of IP gene deletion on related methylarginine pathways (Agxt2 and Arg2).

mRNA expression of (A) Agxt2 and (B) Arg2 in wild type and IP KO renal medulla. Data is mean \pm S.E.M from $n=8$ mice. Data was analysed using Mann-Whitney U-test, * $P<0.05$.

Figure 4.12

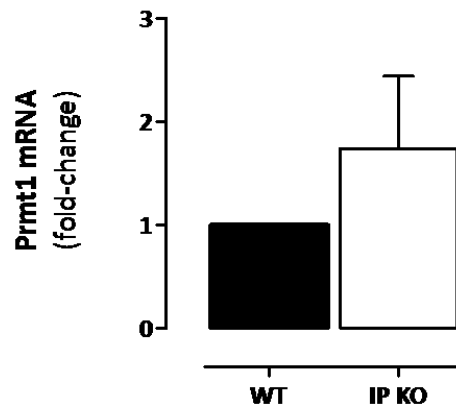


Figure 4.12: Effect of IP gene deletion on related methylarginine pathways (Prmt1). mRNA expression of Prmt1 in wild type and IP KO mice renal medulla. Data is mean \pm S.E.M from $n = 8$ mice. Data was analysed using Mann-Whitney U-test, * $P < 0.05$.

Figure 4.13

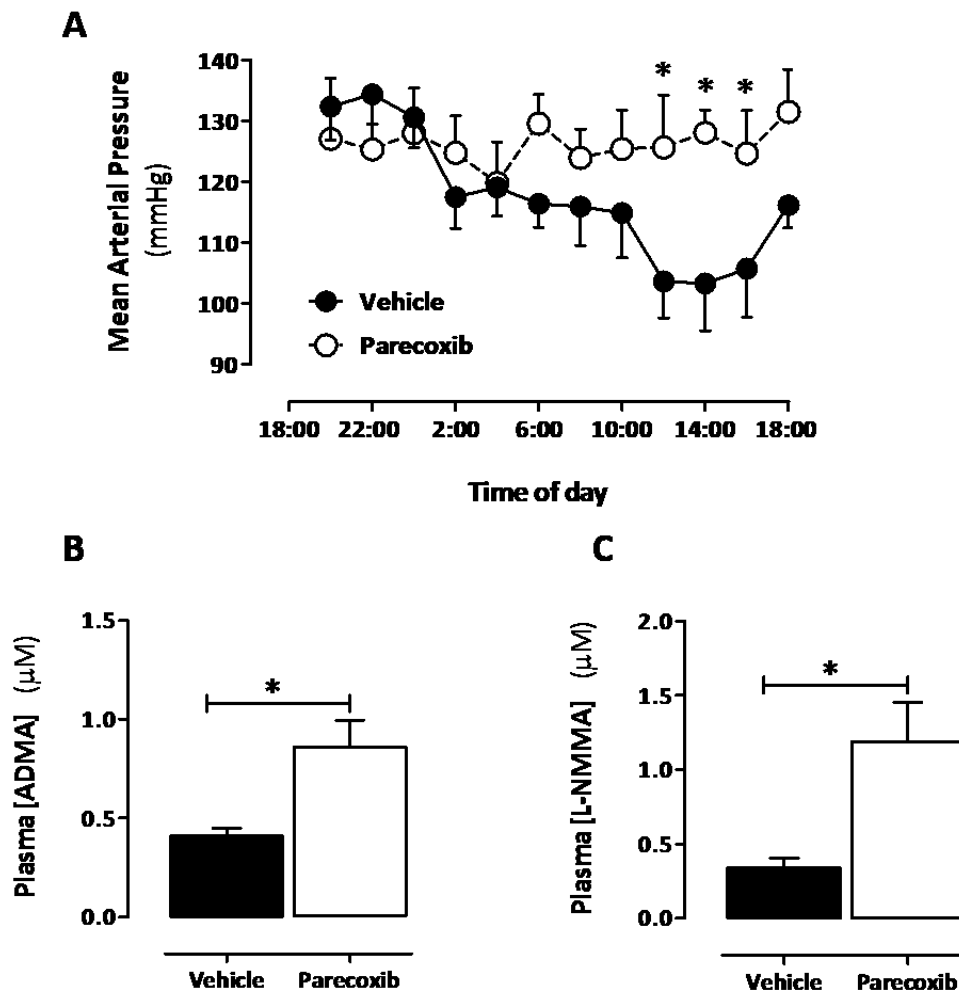


Figure 4.13: Effects of inhibiting COX-2 pharmacologically on arterial pressure in mice. (A) The effect of Paercoxib (COX-2 pharmacological inhibitor) on mice arterial pressure. (B) Levels of ADMA and (C) L-NMMA is mice plasma with or without Parecoxib. Data is mean \pm S.E.M from $n = 3-7$ mice and was analysed by two-way ANOVA in (A) and by Mann-Whitney U-test in (B) and (C).

Figure 4.14

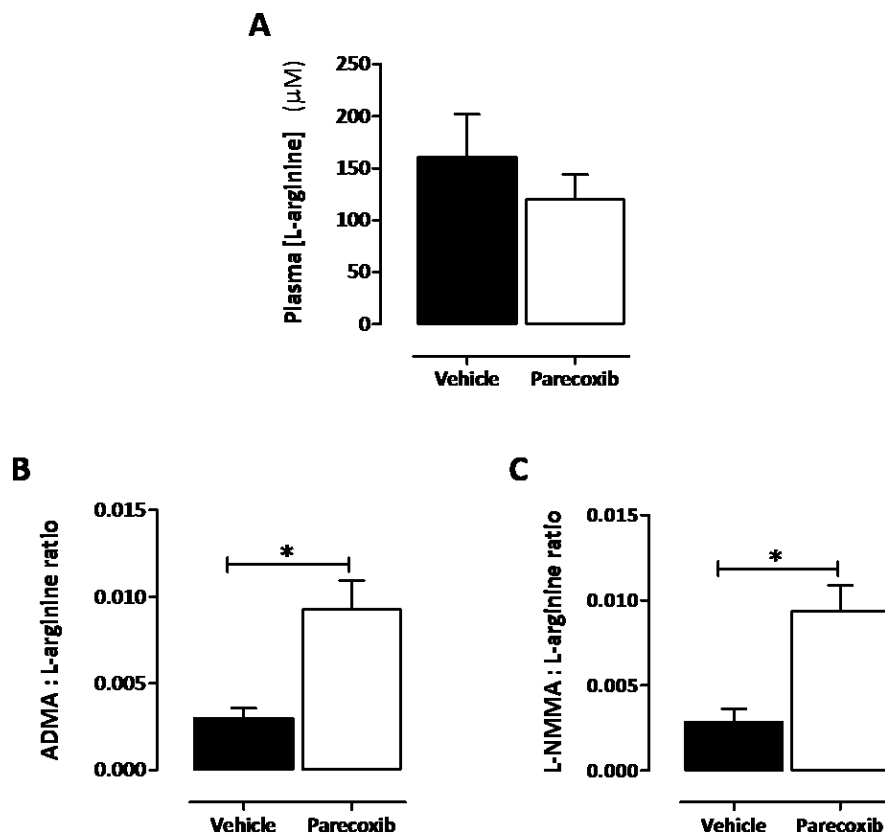


Figure 4.14: The effect of Paercoxib (COX-2 pharmacological inhibitor) on the levels of plasma L-arginine in mice treated with or without Paercoxib. (A) Levels of L-arginine (B) ADMA: L-arginine ratio and (C) L-NAME: L-arginine ratio in mice plasma with and without Paercoxib. Data is mean \pm S.E.M from $n = 3-7$ mice and were analysed by two-way ANOVA in (A) and by Mann-Whitney U-test in (B) and (C).

Table 4.2

| | | ADMA (μM) | L-NMMA (μM) | SDMA (μM) | Creatinine (fold change vs control) |
|---------------|------------------|--|--|--|--|
| Plasma | Control | 0.81 \pm 0.044 | 0.30 \pm 0.024 | 0.44 \pm 0.063 | 1.00 \pm 0.11 |
| | Naproxen | 1.01 \pm 0.049* | 0.31 \pm 0.020 | 0.58 \pm 0.049 | 1.51 \pm 0.05* |
| | | (<i>p</i> <0.01) | (<i>p</i> =0.84) | (<i>p</i> =0.19) | (<i>p</i> <0.01) |
| | Control | 0.75 \pm 0.067 | 0.29 \pm 0.013 | 0.44 \pm 0.049 | 1.00 \pm 0.08 |
| | Celecoxib | 0.90 \pm 0.050* | 0.33 \pm 0.025 | 0.51 \pm 0.045 | 1.55 \pm 0.08* |
| | | (<i>p</i> =0.05) | (<i>p</i> =0.31) | (<i>p</i> =0.81) | (<i>p</i> <0.01) |
| Urine | Control | 71.2 \pm 38.14 | 0.29 \pm 0.03 | 25.80 \pm 11.74 | 1.00 \pm 0.32 |
| | Naproxen | 18.76 \pm 5.65 | 0.28 \pm 0.015 | 21.22 \pm 14.56 | 1.12 \pm 0.37 |
| | | (<i>p</i> =0.27) | (<i>p</i> =0.78) | (<i>p</i> =0.69) | (<i>p</i> =0.78) |
| | Control | 36.02 \pm 11.10 | 0.30 \pm 0.014 | 9.16 \pm 3.12 | 1.00 \pm 0.34 |
| | Celecoxib | 35.61 \pm 19.50 | 0.27 \pm 0.015 | 7.90 \pm 2.48 | 0.42 \pm 0.07 |
| | | (<i>p</i> =0.90) | (<i>p</i> =0.54) | (<i>p</i> =0.73) | (<i>p</i> =0.13) |

Table 4.2: Plasma and urine methylarginines in healthy volunteers taking naproxen or celecoxib. Methylarginine (ADMA, L-NMMA and SDMA) and creatinine levels in plasma and urine of patients before (control) and after 7 days standard anti-inflammatory dosing with naproxen or celecoxib (n=8). Data is represented as mean \pm SEM. P-values by a Wilcoxon signed rank test compared to baseline values for each individual.

Chapter 5: Effects of Global COX-2 gene deletion on eNOS response in isolated aorta

Rational

In the previous chapter my data showed that global gene deletion of cyclooxygenase (COX)-2, but not COX-1, caused increases in the methylarginines asymmetric dimethylarginine (ADMA) and monomethylarginine (L-NMMA) that are methylated forms of L-arginine and that when a ratio of these methylarginines and normal L-arginine was calculated the in the plasma, methylarginines were high relative to arginine in COX-2 knockout mice. The same results were seen when COX-2 was inhibited by the selective drug paracoxib. The data also showed that the effect of COX-2 on methylarginine was to a small extent dependent on the prostacyclin receptors (IP) but mainly independent of these receptors. In the previous chapter my data showed how inhibition of COX-2 with paracoxib increased blood pressure, this is an observation also made by other groups and has been suggested to be linked to changes in the kidney. My thesis takes into account the hypothesis that blood pressure effects of nonsteroidal anti-inflammatory drugs (NSAIDs) and maybe the cardiovascular side effects in people could be in part mediated by methylarginines.

In order to obtain relevant evidence to support this hypothesis, in this chapter I have used myography to bioassay relaxant and contractile (both endothelial dependent and endothelial independent) responses in mouse aorta studied in vitro from wild type and COX-2 knockout mice. I have gone on then to see if the effect of COX-2 knockout on these responses can be reversed in the presence of L-arginine and on the potency of exogenous methylarginines studied in a way where the basal release of NO from the endothelium can be seen.

Specific Aims

The specific aims of this chapter were:

- 1) Determine the effects of COX-2 gene deletion in COX-2 knockout mice on standard vasomotor (contraction and relaxation) responses of isolated aorta
- 2) To investigate the effect of COX-2 gene knockout on endothelial dependent and endothelial independent relaxant responses, using acetylcholine and sodium nitroprusside, in isolated aorta.
- 3) To investigate the effect of L-arginine supplementation on responses of acetylcholine and sodium nitroprusside on in aorta from wild type and COX-2 knockout mice

- 4) To compare the potency and efficacy of methylarginines (ADMA and LNMMA) along with another eNOS inhibitor, L-NAME on enhanced contractile effects in isolated aorta from wild type and COX-2 knockout mice.
- 5) To establish the effect of COX-2 gene deletion in COX-2 knockout mice on eNOS expression in aorta

Methods

Experimental animals and tissue collection

In this chapter COX-2 knockout and C57Bl/6J background mice were used. Mice were killed by CO₂ narcosis. Tissues aorta were dissected and prepared for mounting in wire myographs as detailed in the General Methods chapter (Chapter 1).

Protocols for myograph studies

Figure 1-3

Aorta was cut in to rings of about 5mm width and were mounted in wire myographs containing warmed (37°C) Krebs buffer (PSS; composition in mM: NaCl 119, KCl 4.69, CaCl₂ 2.5, MgSO₄ 1.17, NaHCO₃ 25, KH₂PO₄ 1.18, EDTA 0.027 and glucose 5.5) and gassed (5% CO₂, 95% O₂) at resting tension of 13.3 kPa. Aorta was allowed equilibrate for 30 minutes. Tissues were then 'washed' by replacing the Krebs buffer and contracted with a single 'hyperpolarising' concentration of potassium chloride (125 mM) in Krebs buffer (KPSS; composition in mM: KCl 123.7, CaCl₂ 2.5, MgSO₄ 1.17, NaHCO₃ 25, KH₂PO₄ 1.18, EDTA 0.027 and glucose 5.5). After maximum contraction was achieved, tissues were washed again with Krebs buffer and cumulative responses curves to the contractile agent (U46619; 10⁻⁹ to 10⁻⁷ M) which is a thromboxane mimetic and acts on TP receptors. An approximate EC₈₀ concentration was obtained from these curves and used for the subsequent part of the experiment. After washing tissues again with Krebs buffer an EC₈₀ concentration of U46619 was added and after a stable concentration was seen increasing concentrations of either acetylcholine (10⁻⁹ to 10⁻⁵ M), which relaxes vessels via the release of NO from the endothelium, or sodium nitroprusside (10⁻⁹ to 10⁻⁵ M) which relaxes vessels by giving NO directly to the smooth muscle and independent of the endothelium. After the potassium stage of the protocol, in some rings the substrate for eNOS, L-arginine (100 mM), was added to the Krebs buffer and kept there for all washings and drug additions.

Figures 4-6

Aorta was treated as above until after the addition of the EC₈₀ concentration of U46619, then, increasing concentrations of the methylarginines (ADMA or LNMMA; 0.1-300 μM) or L-NMAE (0.1-300 μM) were added in a cumulative manner.

Data and statistical analysis:

Data is mean ± S.E. mean. Statistical significance (taken as $p < 0.05$) was determined using statistical packages described in the figure legends and significance assumed where $p < 0.05$.

Results

Effects of COX-2 gene deletion on vasomotor responses of mouse aorta

Mouse aorta from wild type and COX-2 knockout mice contracted similarly to KPSS (Figure 5.1A) and contracted similarly to cumulative concentrations of U46619 (Figure 5.1B). The potency and efficacy of U46619 was not significantly different in aorta from wild type and COX-2 knockout mice (Table 5.1). L-arginine had no effect on the cumulating response curve to U46619 in either wild type or COX-2 knockout mice (Table 5.1).

Effect of COX-2 gene deletion on endothelial dependent and independent relaxation responses of aorta

Acetylcholine caused relaxation of U46619 contracted aorta from both genotypes of mice with responses being significantly less and reduced in tissue from COX-2 knockout mice (Figure 5.2A, B). This effect was abolished by the addition of L-arginine (100 μ M) into the organ bath (Figure 5.2C). Sodium nitroprusside induced relaxation was not different in U46619 contracted aorta between the genotypes (Figure 5.3A, B) and, in this case, L-arginine had no effect on the responses (Figure 5.3C).

Effect of COX-2 gene deletion on the potency and efficacy of the methylarginine eNOS inhibitors and, for comparison, with L-NAME

The experiments above show that aorta from COX-2 knockout mice have reduced eNOS responses and that this can be prevented and rescued by giving the substrate, L-arginine, into the Krebs buffer. This work, together with the data in the previous chapter showing methylarginines are increased in the plasma of COX-2 knockout mice, suggests that the eNOS effects might be due to accumulated ADMA/L-NMMA in the vessels that remain active *ex vivo*. In order to test this idea separate experiments were done with a new set of mice where the potency of the methylarginine eNOS inhibitors along with another NOS inhibitor, LNAME, was studied in aorta. For these experiments the easiest way to study potency is to look at the contractile effects of NOS inhibitors that occur as additional to pre contractile vessels. In these protocols the contraction caused by the NOS inhibitors are endothelial dependent and driven by a blocking effect and therefore a loss of NO from the aorta that is stimulated by the force of contraction caused by the U46619.

In these experiments ADMA (Figure 5.4), L-NMMA (Figure 5.5) and L-NAME (Figure 5.6) each caused concentration dependent contractions on top of U46619 contracted aorta. The efficacy of each of the eNOS inhibitors was increased in aorta from COX-2 knockout mice when compared to tissue from wild type mice (Figure 5.4-6).

Effect of COX-2 gene deletion in COX-2 knockout mice on eNOS expression

The experiments above go along with the hypothesis that when COX-2 is lost, methylarginines are increased and that they remain in the blood vessels causing reduced eNOS responses. However, another group also found that eNOS responses were reduced in COX-2 knockout aorta⁸⁰ found that this was accompanied by reduced eNOS expression⁸⁰. In their work they did not consider methylarginines. In order to see if COX-2 gene deletion reduces eNOS expression and that this might contribute to the effects seen with acetylcholine, eNOS gene and protein was measured in aorta from wild type and COX-2 knockout. Aorta from wild type and COX-2 knockout mice had similar levels of eNOS gene and protein expression (Figure 5.7). In fact I found the opposite because eNOS expression was higher in aorta from COX-2 knockout mice (Figure 5.7).

Summary

In this chapter I have shown:

- 1) Vessels that lacking COX-2 contracted similarly to wild type vessels when contracting the vessels with KPSS and U46619.
- 2) COX-2 gene deletion has reduced the relaxation response after relaxing the vessels with Ach, however, SNP did not show the same effect in COX-2 knockout mice.
- 3) The addition of L-arginine prevented the reduction in relaxation responses that we saw after treating COX-2 knockout mice vessels with Ach, but has no effect on vessels that relaxed with SNP.
- 4) COX-2 gene deletion has increased the contractile responses in vessel treated with eNOS inhibitor ADMA, LNMMA (methylarginine eNOS inhibitor) or with L-NAME

Limitation

One key limitation of the results in this chapter is that I did not actually measure the methylarginine levels in the aorta of mice. This really would be the way to be sure that the response that I saw was actually due to accumulated methylarginines. This experiment is something that should be repeated and performed in the future.

Figure 5.1



Figure 5.1: Effects of COX-2 gene deletion on vasomotor responses of mouse aorta. (A) Contractile responses of KPSS on aortas from Wild type and COX-2 knockout mouse. (B) U46619 and (C) PE contractile responses in wild type and COX-2 knockout mouse aortas. Data is mean \pm S.E.M from for n=6-10. Data was analysed using a two-way ANOVA. *p<0.05.

Table 5.1

| U46619 (Log M) | WT | WT + L-arginine (100µM) | COX-2 KO | COX-KO + L-arginine (100µM) |
|--|--------------|--|-----------------|--|
| 1x10⁻⁹ | 0.50 ± 0.26 | 0.23 ± 0.11 | 0.18 ± 0.06 | 0.18 ± 0.05 |
| 3x10⁻⁹ | 1.24 ± 0.58 | 0.84 ± 0.38 | 0.50 ± 0.27 | 0.59 ± 0.22 |
| 1x10⁻⁸ | 5.01 ± 1.45 | 4.06 ± 1.20 | 5.25 ± 1.20 | 4.80 ± 1.31 |
| 3x10⁻⁸ (EC₈₀) | 9.19 ± 1.31 | 7.42 ± 1.07 | 9.46 ± 1.36 | 9.37 ± 1.04 |
| 1x10⁻⁷ | 12.47 ± 1.31 | 10.4 ± 1.10 | 12.0 ± 1.50 | 11.6 ± 1.05 |
| 3x10⁻⁷ | 13.4 ± 1.31 | 11.2 ± 1.08 | 13.0 ± 1.56 | 12.5 ± 1.13 |

Table 5.1: The effect of the admission of L-arginine on contractile responses of U46619 on mice aorta. Contractile response to U46619 (10⁻⁹ to 10⁻⁷ M) in vessels from wild type and COX-2 knockout mouse aortas with and without the present of L-arginine. Data is mean ± S.E.M from for n=6-10.

Figure 5.2

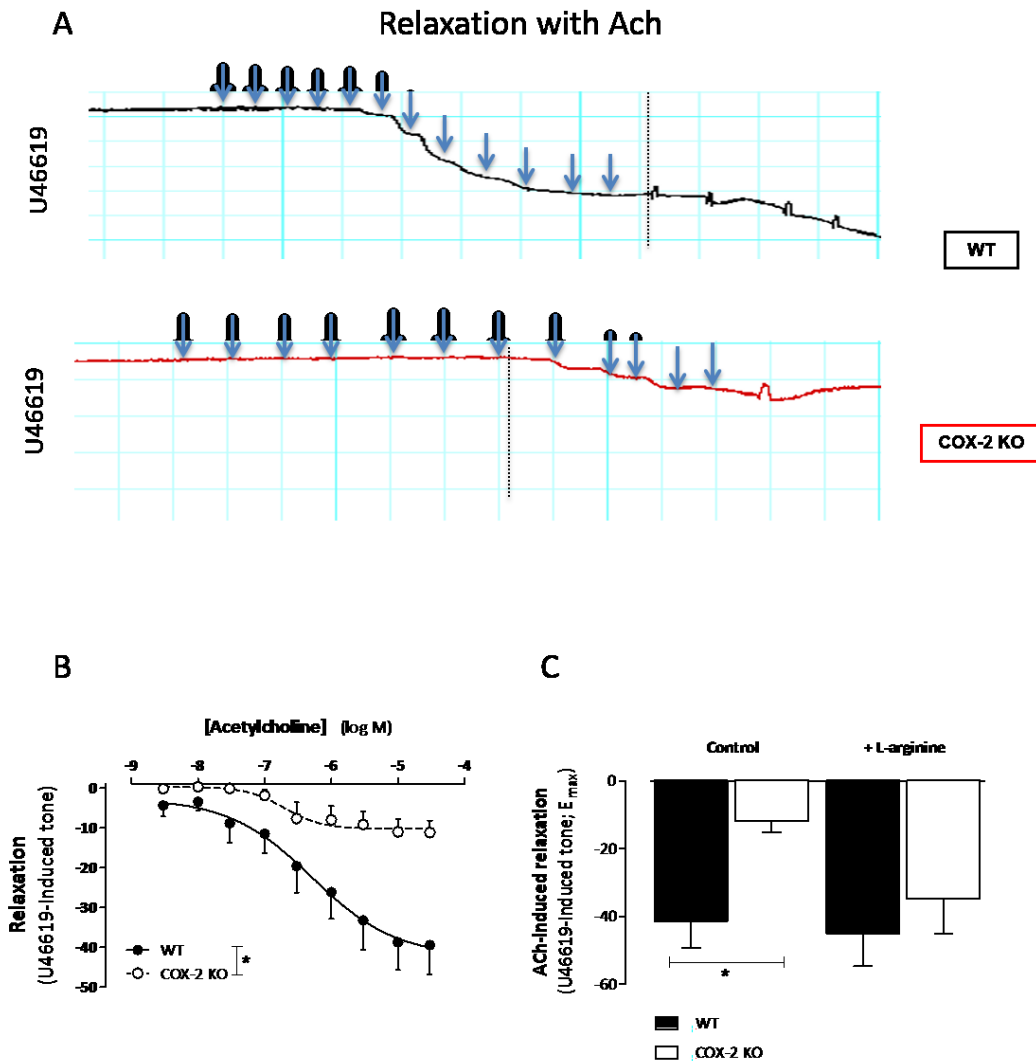


Figure 5.2: Effects of COX-2 gene deletion on relaxation responses with Ach of mouse aorta with and without L-arginine. (A) Representative traces showing the relaxation responses curves with Ach in wild type and COX-2 knockout mice aorta. (B) Relaxation response to Ach in vessels from wild type and COX-2 knockout mouse. (C) Comparison between vessels treated and untreated with L-arginine in wild type and COX-2 knockout mice aorta. . Data is mean \pm S.E.M from for n=6-10. Data was analysed two-way ANOVA. *p<0.05.

Figure 5.3

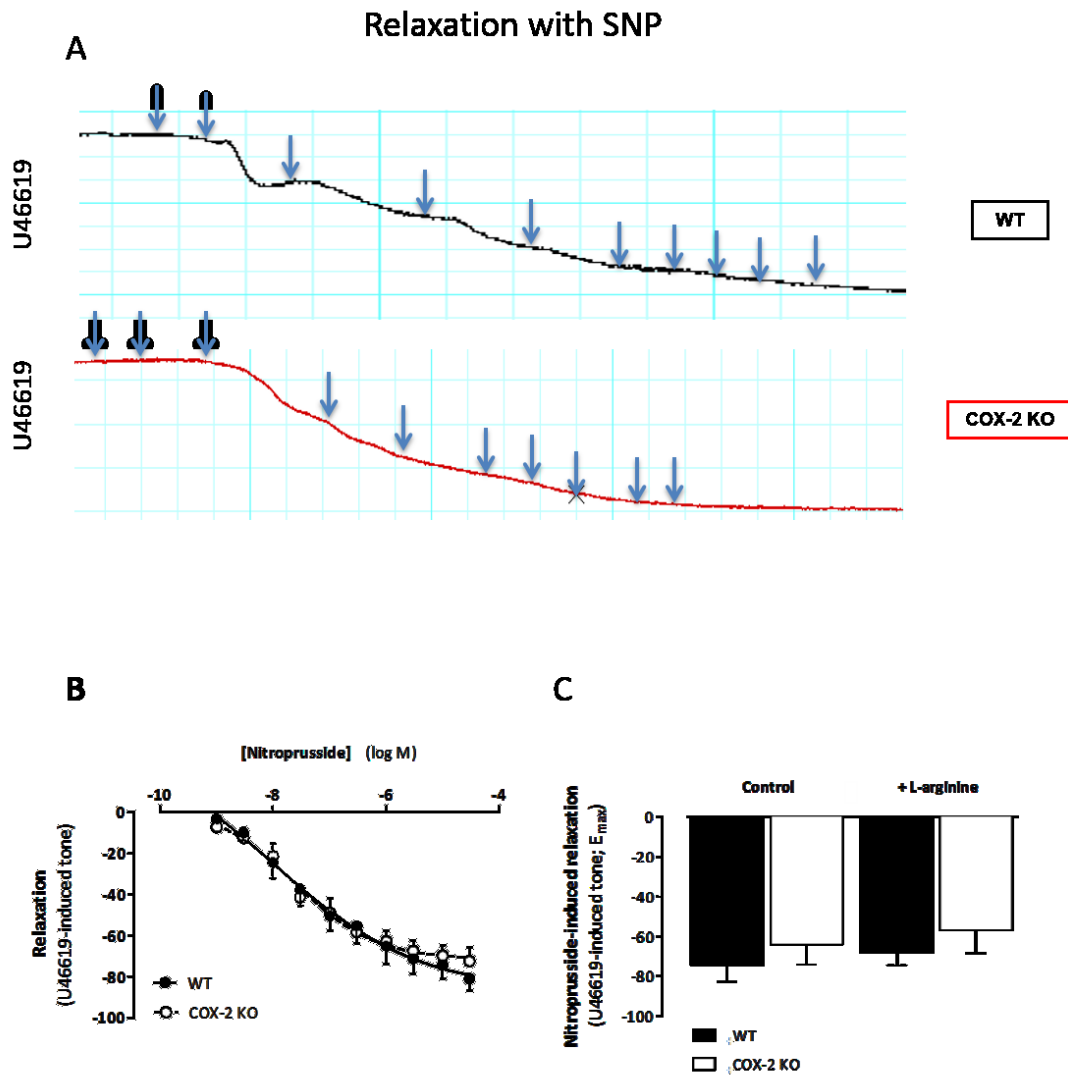


Figure 5.3: Effects of COX-2 gene deletion on relaxation responses with SNP of mouse aorta with and without L-arginine. (A) Representative traces showing the relaxation responses curves with SNP in wild type and COX-2 knockout mice aorta. (B) Relaxation response to SNP in vessels from wild type and COX-2 knockout mouse. (C) Comparison between vessels treated and untreated with L-arginine in wild type and COX-2 knockout mice aorta. . Data is mean \pm S.E.M from for n=6-10. Data was analysed two-way ANOVA.

Figure 5.4

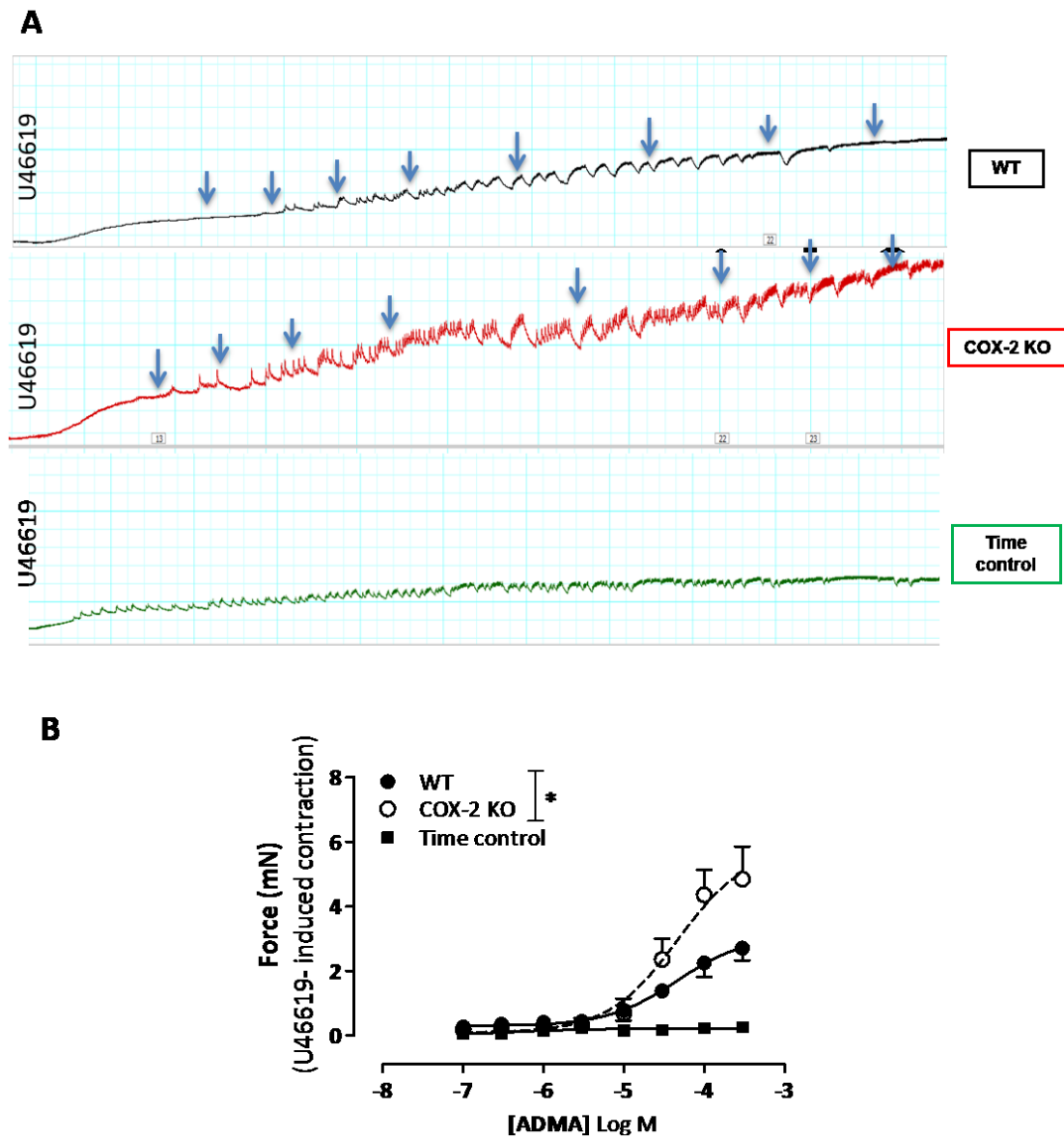


Figure 5.4: Effect of COX-2 gene deletion on the potency and efficacy of the methylarginine eNOS inhibitor (ADMA). (A) Representative traces showing the contractile response for U46619 in aorta from wild type, COX-2 knockout mice. (B) ADMA induced contraction of aorta from wild-type and COX-2 knockout mice. Data is the mean \pm S.E.M for $n=6-10$. Data was analysed by repeated measures two-way ANOVA.

Figure 5.5

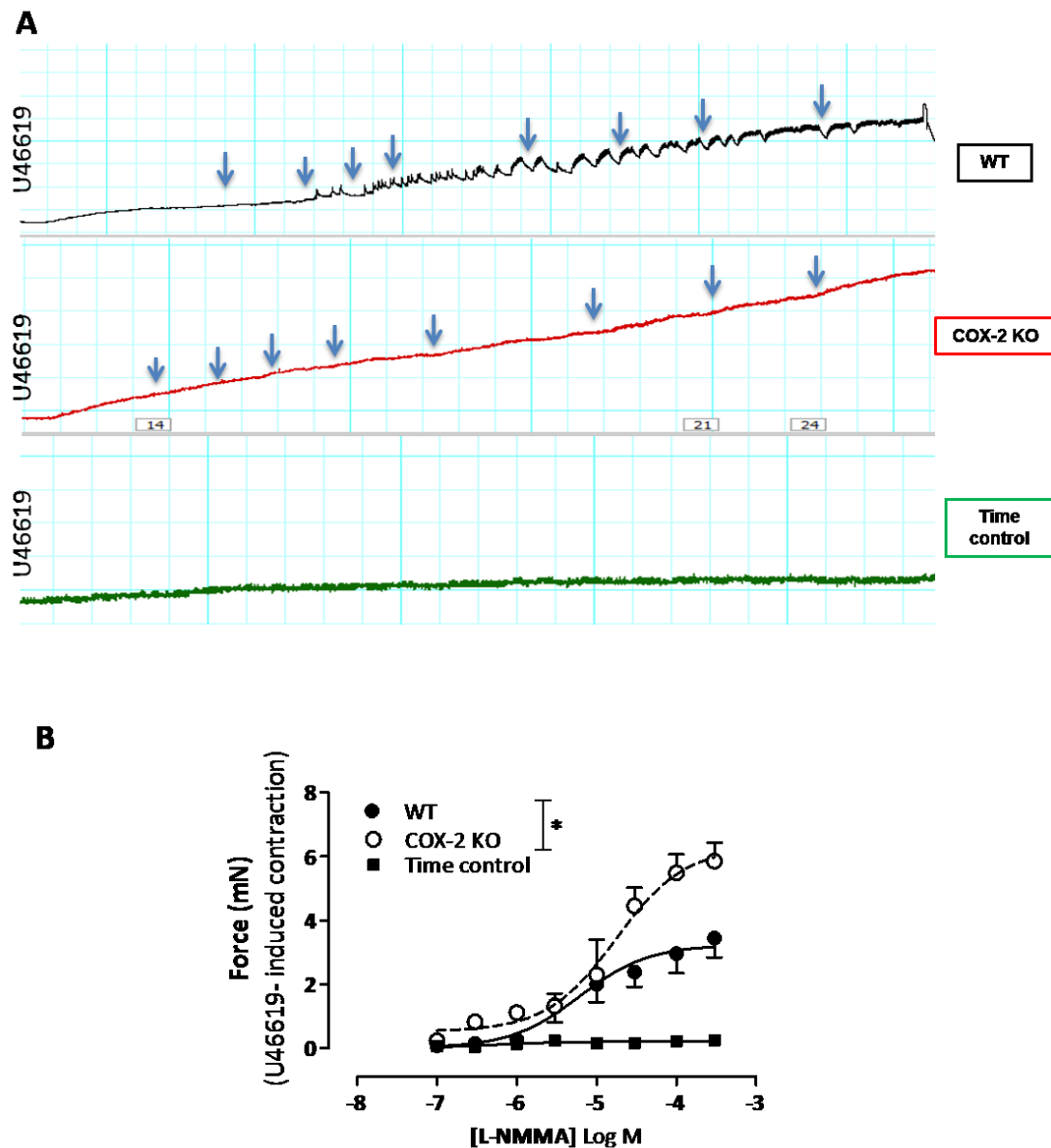


Figure 5.5: Effect of COX-2 gene deletion on the potency and efficacy of the methylarginine eNOS inhibitor (L-NMMA). (A) Representative traces showing the contractile response for U46619 in aorta from wild type, COX-2 knockout mice. (B) L-NMMA induced contraction of aorta from wild-type and COX-2 knockout mice. Data is the mean \pm S.E.M for $n=6-10$. Data was analysed by repeated measures two-way ANOVA.

Figure 5.6

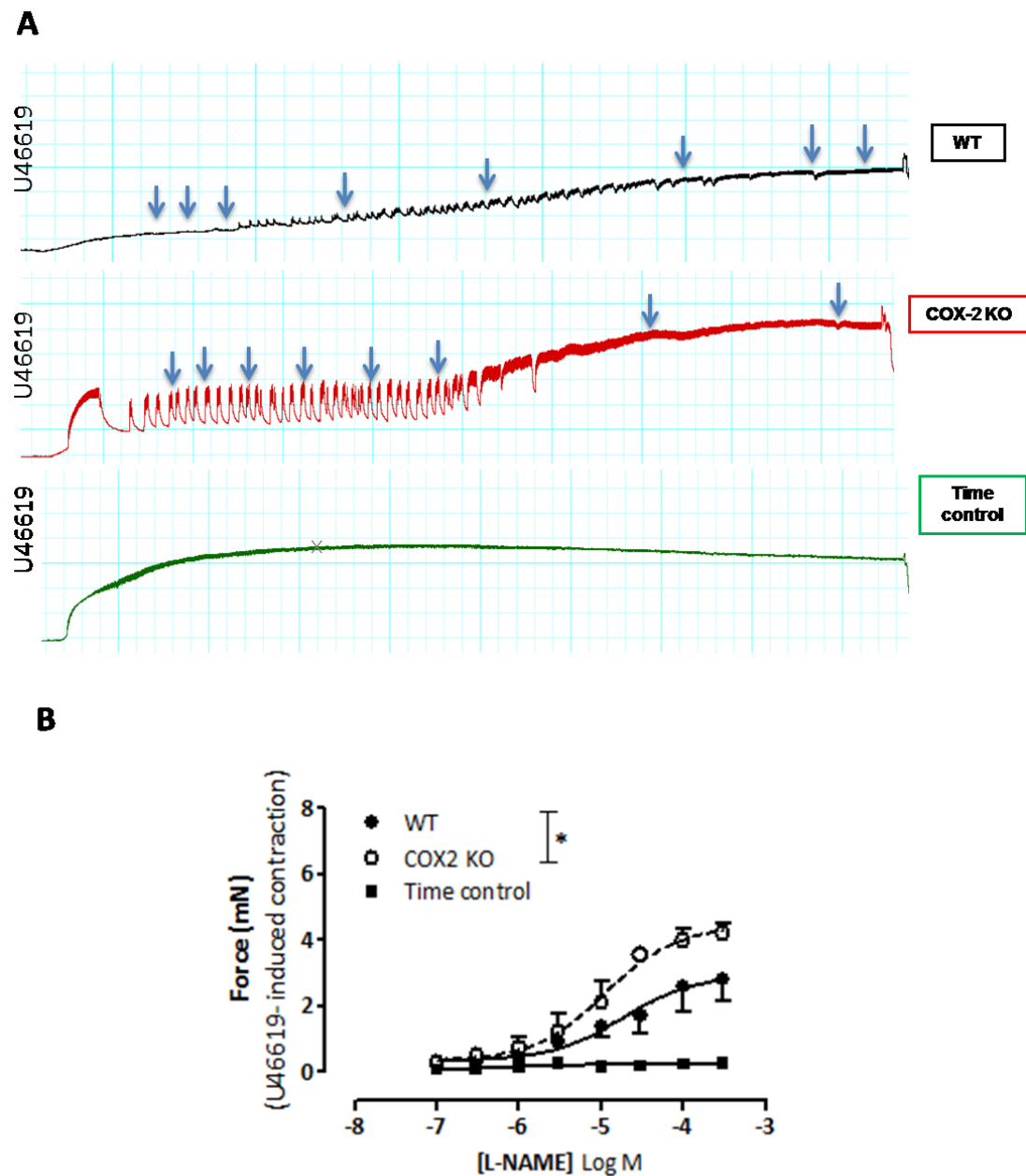


Figure 5.6: Effect of COX-2 gene deletion on the potency and efficacy of eNOS inhibitor (L-NAME). (A) Representative traces showing the contractile response for U46619 in aorta from wild type, COX-2 knockout mice. (B) L-NAME induced contraction of aorta from wild-type and COX-2 knockout mice. Data is the mean \pm S.E.M for $n=6-10$. Data was analysed by repeated measures two-way ANOVA.

Table 5.2

| | WT | COX-2 KO |
|------------------------------------|-----------------------|-----------------------|
| EC₅₀ (Log M) | | |
| ADMA | 4.66x10 ⁻⁵ | 4.69x10 ⁻⁵ |
| L-NMMA | 6.16x10 ⁻⁶ | 1.75x10 ⁻⁵ |
| L-NAME | 1.73x10 ⁻⁵ | 1.08x10 ⁻⁵ |
| E_{max} (Force; mN) | | |
| ADMA | 2.71 ± 0.38 | 4.85 ± 1.01 |
| L-NMMA | 3.45 ± 0.60 | 5.85 ± 0.58 |
| L-NAME | 2.82 ± 0.70 | 4.20 ± 0.31 |

Table 5.2: Effect of COX-2 gene deletion on the potency and efficacy of the methylarginine eNOS inhibitors and, for comparison, with L-NAME. (A) The EC₅₀ concentration for wild type and COX-2 knockout mouse vessels treated with ADMA, L-NMMA and L-NAME. (B) The E_{max} (maximum contraction) in for wild type and COX-2 knockout mouse vessels treated with ADMA, L-NMMA and L-NAME. Data is the mean ± S.E.M for n=6-10. Data was analysed by unpaired Student t-test

Figure 5.7

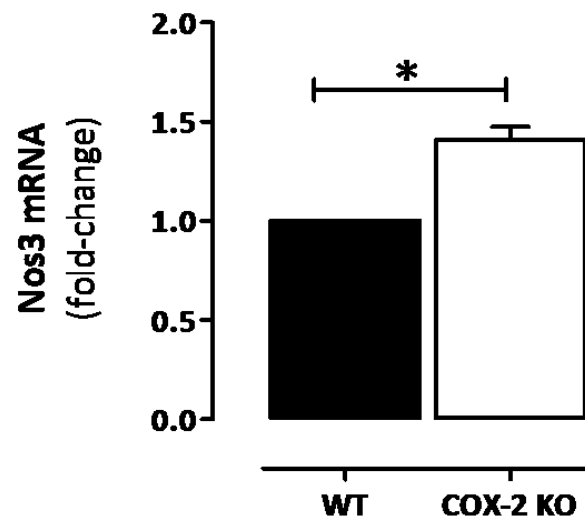


Figure 5.7: Effect of COX-2 gene deletion on Nos3 expression. mRNA expression of Nos3 in wild type and COX-2 knockout mice aorta. Data is the mean \pm S.E.M for n=5-7 mice and was analysed using a Mann-Whitney U-test.

**Chapter 6: Endothelial cell morphology and shear
stress: design of an algorithm to quantify
alignment**

Introduction

The idea that blood vessels have an important internal lining, what we now call the endothelium started in the 1800s when von Recklinghausen established that vessels were more than merely '*tunnels bored through tissues*', and that they were lined by particular types of cell¹⁵⁶. In 1865 the anatomist Wilhelm His first used the term endothelium^{157,158}. Shortly after that Heidenhahn described the endothelium as an active secretory cell system¹⁵⁹. A few years later, Starling proposed that the endothelium was a selective physical barrier that allowed for capillary exchange^{160,161}. Then after numerous studies in the 1950s and 1960s of the vessel wall by Palade using electron microscopy and after other studies by Gowan of the physiological aspects of the endothelium, the view of the endothelium was extended to include a more as a dynamic, heterogeneous organ involved in many aspects of vascular biology^{158,162-164}.

The first successful isolation of endothelial cells in vitro was made in the 1970s by Jaffe and his colleagues. Previous attempts by other groups to culture endothelial cells had had limited success since it was difficult to definitely identify the endothelial cells and in fact most of the cells that had been cultured turned out to be fibroblasts. Aware of these challenges, Jaffe decided to culture the endothelial cells with some changes to the cell culture conditions. For instance, instead of using trypsin to digest the cells, he used collagenase and he also increased the percentage of the calf serum used in the culture media from 5% to 20%¹⁶⁵. Moreover, it was known at that time that von Willebrand factor antigen is present in endothelial cells but not in smooth muscle cells (SMCs) or fibroblasts. Hence, Jaffe used von Willebrand factor antigen to identify the endothelial cells and was therefore able to isolate and grow a pure culture in vitro. After his successful isolation of endothelial cells he proposed that in vitro studies can lead to a better understanding of the role of endothelial cells in important biological events, such as blood vessel permeability, haemostasis and the response of the blood vessel to other physiological and pathological stimuli^{162,166 167}. Now it is well known that endothelial cells line the interior surface of blood vessels throughout the entire circulatory system and that they play an important role in the control of vascular contraction and dilatation by releasing vasodilator substances^{168,169} (see General Introduction, Chapter 1). Moreover, they are involved in many aspects of vascular biology, including blood pressure control, blood clotting, atherosclerosis, angiogenesis and

inflammation. Thus, dysfunction of endothelial cell homeostasis is associated with several human diseases, including ischemic heart diseases, hypertension, atherosclerosis, tumours, diabetes and arthritis^{170,171}.

Endothelial cell morphology

Morphology of endothelial cells have been investigated and reported in many publications. In a study of rat blood vessels Kibria reported that pulmonary artery endothelial cells were shorter (30×14µm) than aortic endothelial cells (55×10µm) and that they had a more rectangular shape¹⁷². In another study of rabbit endothelial cells from two different regions of the arterial tree, the ventral mid thoracic and ventral abdominal aorta, they reported that the endothelial cells in the abdominal aorta were longer and narrower than the cells in the thoracic aorta. They used eight calculated parameters to describe the morphology of the endothelial cells: area, perimeter, length, width, angle of orientation, width to length ratio, axis intersection ratio and shape index with different equations to calculate the size of the cells¹⁷³. In a more recent study from our group, the endothelial cells were studied using scanning ion conductance microscopy (SICM), endothelial cells were isolated from porcine aortas and then cultured and exposed to different patterns of shear stress (randomly orientated non-directional shear stress and uniformly oriented directional shear stress). The endothelial cells were found to be more elongated and less compliant when they were exposed to uniform shear stress than the endothelial cells that were exposed to shear stress with no preferred orientation or the cells that were grown under static conditions¹⁷⁴.

The table below illustrates some of the imaging techniques that have been used to study the morphology of endothelial cells over time and in different species.

| Technique | Observation | Reference |
|---|--|-----------|
| Electron microscopy | To study the fine structure of the endothelium of large arteries (rats, rabbits, puppies, cat, and ferrets) | 175 |
| Electron microscopy | To Study the Normal Rat Aorta | 176 |
| Electron microscopy | To determine the changes from the normal pathway in vascular transport of colloidal particles (rabbit) | 177 |
| Scanning electron microscopy (SEM) and transmission electron microscopy | In vitro culture of ECs derived from human umbilical veins | 162 |
| <i>En face</i> (Hautchen) technique | The effect of dietary-induced hypercholesterolemia on the endothelium of rabbit aorta | 178 |
| SEM | To investigate EC morphology in situ in the aortic arch of the rabbit during atherogenesis. | 179 |
| Photomicrography | To study the quantitative and qualitative interaction of normal washed platelets with normal and abnormal sub endothelium | 180 |
| <i>En face</i> Confocal microscopy | To compare inducible adhesion molecule expression in normal and hypercholesterolemic mice and rabbits. | 181 |
| <i>En face</i> Confocal microscopy | To study the level of nuclear NFκ-B and cell adhesion molecules in the endothelium of the lesser curvature of the mouse aortic arch. | 182 |
| Confocal microscopy | To investigate whether endothelial cells convey signals to glia in the mature brain (rats) | 183 |

Table 6.1: Development of endothelial cell imaging.

Shear stress and the endothelium

In 1982 Fishman stated:

“it seems reasonable that the endothelium, because of its location as the living lining of blood vessels, is continuously adapting to the composition of the blood that traverses its surface, to the volume flow across its face, and to the pulsatile hydrostatic pressures that operate incessantly and rhythmically over a lifetime to deform it”¹⁸⁴.

It is now known that the endothelium is comprised of heterogeneous phenotypes that are subject to different biochemical forces including hydrostatic pressure (blood pressure) shear stress (the frictional force of blood flow) and cyclic strain (pulsatile pressure) and that this can have consequences for their morphology and susceptibility for disease¹⁸⁵. For instance, endothelial cells that experience non-directional shear stress (such as in the lesser curvature of the aortic arch) have been reported to be associated with inflammation and an increased susceptibility to the formation of atherosclerotic plaques, typically display a cobblestone morphology^{181,186,187}. On the contrary, endothelial cells that experience unidirectional shear stress (such as seen in the greater curvature of the aortic arch) are associated with protection from inflammation and typically display an elongated morphology^{188,189}. The aortic arch, because of its architecture and with its spectrum types of shear stress of protected and susceptible endothelial cell phenotypes in the greater and lesser curvature respectively is therefore a useful model for the study of different kinds of endothelial cells and their relevance to disease¹⁸¹.

Rational

Blood vessels are exposed to a range of physical forces. These forces include (i) fluid shear stress caused by the passage of blood over the luminal surface of the vessel. This can be unidirectional or multidirectional. (ii) Cyclic strain which is caused by blood pressure and (iii) hydrostatic pressure caused by gravity¹⁹⁰. Endothelial cells line the luminal surface of all blood vessels and their morphology is regulated by, and associated with, these different types of physical forces¹⁹⁰. In areas of unidirectional laminar shear stress endothelial cells appear aligned whereas in areas of multidirectional flow they typically have a cobblestone appearance¹⁹¹⁻¹⁹⁵. Endothelial cells are very sensitive to their biomechanical environment and shear stress is known to affect gene expression and the development of atherosclerosis^{190,196}. Most data suggests that unidirectional shear stress confers protection of the endothelium whilst multidirectional shear links with inflammation and atherosclerosis¹⁹⁷⁻¹⁹⁹. This situation is well illustrated in the aortic arch where, because of the architecture of the vessel, complex shear stress patterns are present. In the mouse ascending aortic arch, for example, the endothelium of the greater curvature is exposed to unidirectional and high wall shear stress with an estimated magnitude of 600 dynes/cm²,

whereas the lesser curvature is associated with wall shear stress of a relatively lower magnitude (averaging approximately 150 dynes/cm²), which is more multidirectional in character¹⁹¹. Importantly, endothelial cells lining the lesser curvature of the mouse aortic arch are non-aligned, have a cobblestone morphology and are particularly susceptible to inflammation whilst the endothelial cells lining the greater curvature have an aligned morphology and a protected phenotype^{192,193,200-204}.

However, most studies report endothelial cell morphology in a qualitative manner with no validated way of quantifying morphology in terms of 'alignment' with shear stress. It is important to find a way to quantify endothelial cell morphology since, amongst other reasons; associations have been made between morphology, inflammation and atherosclerosis. Also while there are studies looking at endothelial cell morphology there is less work looking at the direction or shape of the smooth muscle cells that are underneath the endothelium. Finally because there is no current application of quantifying how endothelial cells align in vessels we have no way of using this important part of endothelial cell biology as an experimental endpoint in experimental models of disease.

Specific Aims

In this chapter I have used imaging of whole vessels, including those from genetically modified animals; specifically those ones relevant to my thesis that is cyclooxygenase (COX)-1, COX-2 and endothelial nitric oxide synthase (eNOS) as well as human endothelial cells in culture exposed to different types of shear stress to devise a system where morphology can be quantified. The specific aims of this chapter were:

- Using confocal imaging, study in detail the morphology of endothelial cells in the aortic arch at areas thought to experience; (1) unidirectional (laminar) shear stress, (2) mixed shear stress and (3) non-directional (turbulent) shear stress. This type of study has been done before, although the endothelial morphology at the interface region of the aortic arch where endothelium experiences a mixed pattern of laminar and turbulent shear has not been studied. Images from the thoracic aorta (from a straight segment of the aorta that experience laminar shear stress) was also analysed for comparison. This study was also extended to the underlying smooth muscle cells (SMC) at different depths. The main challenge for my thesis in this aim

has been to devise a strategy of quantifying nuclear 'alignment' of endothelial and smooth muscle cells.

- Confocal microscopy has limitations as the tissue is fixed and squashed against a glass cover slip. This could hypothetically result in distortion of cell morphology. My second aim was therefore to corroborate the endothelial cell morphology types I have seen in these predefined regions of the aortic arch by using scanning electron microscopy (SEM), which allows for imaging of opened vessels with their 3D shape intact.
- Establish a technique to quantify morphology of endothelial cells in different regions of the aortic arch.
- Use this technology to address an important experimental question that is relevant to my thesis and to the whole field of vascular hormones and cell morphology. To do this I have applied the approach that I worked out to quantify the alignment of cells to endothelial cells in the aortic arch COX-1, COX-2 and eNOS knock out mice.
- Translate the findings and the quantification methodology from endothelium in mouse aortic arch to human endothelial cells grown in culture and subjected to direction versus non-directional shear stress

Methods

Mouse tissue and associated staining

In this chapter aortic arch tissue from mice was removed, cleaned and fixed for imaging; details of these procedures are contained in the General Methods Chapter.

Human endothelial cells

In this chapter I have used human endothelial cells cultured from blood cells (blood outgrowth endothelial cells; BOECs). Details of donors, culture procedures and fixing/staining protocols are given in the General Methods Chapter.

Imagining

In this chapter I have used en face confocal imagining together with SEM to capture morphology of endothelial cells on blood vessels (aortic arch) and isolated human endothelial cells (BOECs). The detailed protocols for these imaging procedures are given in the General Methods Chapter.

Data and statistical analysis

The data is shown as representative images with details of the number of experiments performed contained in the figure legends. Where pooled data is shown this is the mean +/- S.E.M for n experiments, where each n-value represents data from a separate animal (in the case of aortic tissue) or from separate isolations of cells (for BOECs studies). Analysis is performed using statistical packages described in the figure legends and significance assumed where $p < 0.05$.

Results

Morphology of endothelium in the aortic arch

As others have reported previously¹⁸¹, the endothelium of the mouse aortic arch displayed two defined morphologies, a more cobblestoned endothelial cell phenotype in the lesser curvature and a more elongated/aligned endothelial phenotype in the greater curvature (Figure 6.1). In my thesis I have also examined the morphology of the endothelium in the interface region (Figure 6.1). The endothelium in the interface region appeared to be of mixed morphology (the alignment of cells of these regions are quantified below) and as far as I could find this is the first time the endothelial morphology in the interface region has been studied and described. It is important to know that *en face* confocal imaging can result in a distortion of the tissue because of the mounting procedure (including flattening against a coverslip glass surface). In my thesis I have solved this problem by imaging the endothelium in these regions using SEM and the 3D morphology of the endothelium in the greater curvature, interface region, the lesser curvature of the aortic arch and in the and the thoracic aorta (Figure 6.2). In each of these the 3D images appeared to similar to the observations made from the images with the confocal microscopy.

Quantification of nuclear alignment

Once I had obtained the imaging data using confocal imaging and SEM imaging, it was clear that we needed a way to quantify the degree of alignment of the endothelial cells that were present in the various regions of the aortic arch and in other regions of the vessel. It was important to ensure that the quantification was blinded, objective and allowed for cells to be quantified regardless of their direction of alignment. Others have tried to quantify endothelial cell alignment manually by outlining the endothelial cells, however, it is difficult to recognize where one endothelial cell outline ends and another begin. In my thesis I therefore instead opted to focus on alignment of the endothelial cell nucleus which can be captured using ImageJ software. Firstly, the original image composite of green endothelial cell outline (by CD31) and blue nuclei (visualised by the nuclear stain DAPI) were split into separate grey scale images and then by using the automated default criteria in Image J, thresholded to include the nuclei in the analysis and not the background (Figure 6.3). Automated analysis by ImageJ then provided a Feret angle for each thresholded nucleus. In imageJ, the Feret angle (or angle of orientation) is calculated using the primary axis, which is

maximum diameter or the length, the secondary axis, which is the minimum diameter or the width, and the image x-axis (straight vertical line across the image which is the point of reference for the analysis). In summary, the Feret angle (angle of orientation) is the angle between the primary axis and the x-axis (Figure 6.4).

However, this way of quantifying the nuclear angle of orientation depends on the shape of the nuclei and if all of the nuclei were perfectly round the angle between the primary axis and the x-axis would always be 90 degrees, therefore it would be difficult to distinguish the direction of alignment (Figure 6.5). To solve this it was important to ensure that the nuclei were of a comparable shape between the different regions and therefore in order to verify our nuclear alignment results we also quantified the circularity index for these cells according to this formula $4\pi (\text{area}/\text{perimeter}^2)$ where a circularity value of 1.0 indicates a perfect circle and where the value approaches 0.0, it shows an increasingly elongated polygon (Figure 6.4). Importantly the majority of nuclei in all areas of the arch were not rounded but elongated and there were no apparent difference in circularity distribution between the regions (Figure 6.4).

Once I had assured myself about the majority of the nuclei being elongated and therefore suitable for the Feret angle analysis, nuclear alignment was quantified based on the highest number of thresholded DAPI positive nuclei within 20° of separation of each other (according to their Feret angle), normalised to the total number of nuclei in the image (Figure 6.5). This analysis yields the % of nuclei orientated in the same direction (nuclear alignment).

In this way, when I had quantified the DAPI positive nuclei in both regions in the arch (greater and lesser curvature) I found that the endothelial cell nuclei in the greater curvature were significantly more aligned in one direction compared to the EC nuclei in the lesser curvature, which were more randomly orientated (Figure 6.6). The same was the case for the endothelial cell nuclei in the thoracic aorta that were aligned to a comparative level as the endothelial nuclei in the greater curvature, whereas the endothelial nuclei in the interface region tended to be more randomly orientated (Figure 6.6).

Another key observation was that the lesser curvature region and the interface region appear to be more 'dense' with the presence of nuclei than the greater curvature region or the thoracic aorta (Figure 6.6). Similarly, when quantifying the average nuclear size it was found that in the lesser curvature region the nuclei are larger in size compared to the nuclei size in the greater curvature (Figure 6.6). Interestingly, the average nuclear size was also significantly larger in the thoracic aorta compared to the greater curvature (Figure 6.6).

Moreover, I also studied SMC morphology using the z-stack function in the confocal microscope (images were taken at increasing depths: 5 μ m, 10 μ m and 15 μ m depth) and I got very interesting results from this. I used the same process with measuring alignment that I did for the endothelial layer I found that SMCs directly underneath the endothelial cells layer (at 5 μ m depth) were more aligned in the greater curvature than in the lesser curvature (Figure 6.7). However, the following layers (10 μ m and 15 μ m) showed a comparable degree of alignment in all regions of the aortic arch. This means that the degree of alignment in the endothelial layer seems to be followed by the superficial SMC layer. As well as this it was found that the nuclear density in the lesser curvature in both the endothelial layer and SMC layers was significantly higher than in the greater curvature (Figure 6.7). The average SMC nuclear size was however similar between regions (Figure 6.8). In addition, the nuclear density and average nuclear size was higher in the superficial SMC layer at 5 μ m depth compared to deeper layers in the greater curvature and the thoracic aorta (Figure 6.7), whereas the nuclear density was higher overall in all layers in the lesser curvature (Figure 6.7).

Effect of COX-1, COX-2 or eNOS knock out on endothelial cell morphology

After designing a way to quantify endothelial cell morphology within a vessel I was able to use the technology to determine if loss of the key endothelial hormone pathways of prostacyclin or NO affects endothelial cell morphology in the different regions of the aortic arch.

First I analysed the effect of loss of the prostacyclin-generating pathway of COX-1 or COX-2. Loss of COX-1, which we know from my first results chapter (Chapter 3) results in almost complete loss of prostacyclin, had no effect on endothelial cell morphology (as found by

looking at the nuclear measures described above). As I saw in chapter 3 COX-2 is only very sparsely expressed in the aorta, but where it is present it is found in the lesser curvature of the aortic arch⁷⁹, where endothelial cells are exposed to nondirectional shear stress and where low grade inflammation is happening all the time. The endothelium, more correctly the nuclear morphology of the endothelium in the arch of COX-2 appeared different next to results from wild type aortic arch. Just like in endothelial cells of wild type mice the nuclei measurements in the lesser curvature region were different to those in the greater curvature region (Figure 6.8) but when comparing measurements alignment (Figure 6.8 or area (Figure 6.8) there was what looked like a trend for the endothelium to be more aligned and lower in density in the lesser curvature of arches from COX-2 knock out mice than from wild type mice. When it came to nuclear size this difference was statistically significant (Figure 6.8). To gather all the nuclear measures and increase the power of my analysis I then constructed a 'composite' set of data that took into account all of the measurements. To do this the composite score was calculated as the mean of nuclear size, 1/nuclear density and 1/alignment each normalised to their respective values for the wild type greater curvature region (Figure 6.8). Calculated like this then the lower the score means a closer characteristic of the endothelial cells in the greater curvature and so means (theoretically) more protected and so being a good thing in terms of vascular health. Doing this I found that the composite score showed higher values for all genotypes in the lesser curvature, as we would expect, but in the same way as I saw for the significant data with area of nuclei in Figure 6.8 the composite score showed statistically significant differences in the data from endothelial cells in the lesser curvature of the arch from COX-2 knock out mice. This was not significantly true for data from arches from COX-1 knock out mice (Figure 6.8).

We should remember that these morphological changes in the endothelium of the lesser curvature happen just where the COX-2 is expressed. This could be because the COX-2 at this specific location is important for maintaining morphological unity – or that this is a response of a 'susceptible' region to increased ADMA present in the plasma of COX-2 knock out mice (see Chapter 4). In Chapter 5 I show how the aorta from COX-2 knock out mice have reduced eNOS responses and that this is corrected with additional L-arginine, suggesting that the loss of eNOS response is because of increased ADMA/LNMMA caused by the effect of loss of COX-2 in the kidney.

This means that the effect I see here in the morphology of endothelial cells from the aortic arch of COX-2 knockout mice could be due to reduced eNOS activity. This is something that I could test because I could get the tissue from eNOS knock out mice and look in exactly the same way at the morphology of endothelial cells in the aortic arch where any effect of COX-2/ADMA pathways would not feature as all eNOS activity is absent in these vessels.

First I showed that the phenotype of the aorta from the eNOS knock out mice was correct because the aorta did not relax to the endothelial stimulant acetylcholine. As I say in my introduction this is because the endothelium makes NO from the eNOS enzyme (Figure 6.9).

Endothelial cells in the aortic arch of eNOS knock out mice showed data just like wild type and COX knock out mice in terms of the differences in the lesser curvature and greater curvature regions. It was important to see though that there was no differences, even when the composite score was made, between endothelial cell morphology in arches of either region in tissue from eNOS knock out mice compared to wild type ones (Figure 6.10).

This work was very important and makes use of my technology to quantify endothelial cell morphology and says something very interesting about how COX-2 knock out has a real effect on the endothelium. To take another step with this part of my PhD work I wanted to see how this type of analysis could be used in human endothelial cells.

Morphology of human endothelial cells in culture versus mouse aortic arch

Work in my group has found before that endothelial cells grown from porcine aorta respond to the application directional (laminar) shear stress in vitro to form an aligned phenotype²⁰⁵ by using a very simple method of growing cells in 6-well plates and then just putting them on an orbital shaker. Here, I have used endothelial cells grown from blood progenitors (blood outgrowth endothelial cells; BOECs) to investigate how this type of laboratory method with what is the same type of complex shear stress that we can see in the aortic arch affects their morphology and if it can be quantified in the same way that I have done above for endothelium on the aortic arch from mice.

BOEC and modelling of shear stress in vitro

BOEC were isolated as described previously^{148,206,207} and provide a model of endothelial cells in vitro (Figure 6.11). Endothelial cell alignment under shear stress was determined using a model previously defined by our group^{205,208} where cells are placed on an orbital shaker and the movement generates a wave of media that oscillates around the well resulting in a complex pattern of shear applied with directional (laminar) shear towards the edge of the well, and non-directional (turbulent) shear at the centre. In this model therefore, cells at the centre and edge of the well are analogous to those in the lesser and greater curvature of the aortic arch respectively. After application of shear stress for 4 days, cells were washed and fixed in 4% paraformaldehyde for staining. Alignment of cells was visualised by light microscopy and by fluorescence imaging of cells stained with endothelial cell markers.

Human BOECs cultured under static conditions had the typical cobble stone morphology (Figure 6.13). After 4 days of BOECs being exposed to shear stress on the orbital shaker cells at the edge of the well, exposed to directional shear, were elongated and aligned, whilst those in the centre of the well, being exposed to non-directional shear, appeared cobble stone in appearance and resembled cells grown under static.

Images of BOECs cultured under the difference conditions were then processed in ImageJ as described above and the following morphological determinants nuclear alignment, (ii) nuclear density and (iii) nuclear size (Figure 6.13). In quantifying these images it was seen that statistically significant effects of shear stress on morphology could be detected (Figure 6.10). In general, it was found that the morphology of BOECs or mouse endothelium exposed to directional or non-directional shear stress (ie edge/ center of well and greater curvature/ lesser curvature of the aortic arch respectively) were similar in terms of alignment. However, the difference that I found between the nuclear density and average size in mouse greater curvature and lesser curvature could not be detected in sheared BOECs (Figure 6.13).

Summary

In this chapter I have shown:

- 1) Like others have shown that there is clear difference in morphology of endothelial cells that are in the mouse aortic arch that maps to regions of directional and non-directional shear stress. Specifically that endothelial cells under directional shear are aligned and those under non-directional shear are cobblestoned in morphology. I have confirmed these observations and gone further to show that (i) these two types of endothelial cell morphology represent the opposite ends of a continuum with degrees of alignment and elongation being apparent in interface regions of the arch and (ii) I compliment with data using confocal en face microscopy with more accurate structural imaging using SEM.
- 2) In order to quantify the qualitative information obtained in imaging data regarding cell morphology I have used ImageJ and devised a mathematical strategy where by (i) nuclear alignment, (ii) nuclear density and (iii) average nuclear size can be data can be captured and collated.
- 3) Quantification of morphology showed statistically significant differences between endothelial cells across the regions of the arch. It was particularly interesting to see that differences were detected in some characteristics between cells in the interface region versus lesser and greater curvature.
- 4) Taking a similar approach I have imaged and quantified morphology of the underlying smooth muscle cells in the aortic arch. As far as I am aware no one else has done this. Morphological differences in the smooth muscle cells were sensitive to distance from the endothelium.
- 5) I used my own technology to look to see if there are differences in endothelial cell morphology by applying the measurements of nuclear shape etc to tissue from animals where COX-1, COX-2 or eNOS was knocked out.
- 6) I found that for COX-2 knock out, but not for COX-1 or eNOS, there were in fact statistical differences in how the morphology of the endothelium looked compared to cells in aorta from wild type mice.
- 7) Using human endothelial cells (BOECs) I translated some of these observations in to a purely cell based model.

- 8) BOECs subjected to directional shear were aligned whilst those subjected to non-direction shear were cobblestone in nature.
- 9) Using images of the sheared BOECs analyzed in ImageJ and applying the same mathematical processing I was able to show that these morphological characteristics were quantifiable and statistically significant.

Limitations

I am very happy with the work in this chapter because I have been able to come up with a way of quantifying endothelial cell morphology quite simple steps. In the end the numbers that I get from my calculations fit with what we see with our eye. But very important I think is that I could use this to statistically show something that was not easy to see with the eye – this is that there are differences in the morphology of endothelial cells in the lesser curvature of aorta from COX-2 knockout mice. This meant that I could use my technology for a genuine research question. This also fits with the rest of my thesis because the other parts are about how COX enzymes affect cardiovascular health and disease. Here I showed that knocking COX-2 out did affect the endothelium and because the morphology is linked to a disease phenotype this might be very important. What it means is that the endothelium in the lesser curvature (ie where there is a susceptibility to inflammation and atherosclerosis) the endothelium in aorta of COX-2 knock out mice looked more like it did in areas of the greater curvature and so we would predict that this is a protected phenotype. This means that I might hypothesize that ‘COX-2 in the lesser curvature of the aortic arch is acting in a pro-inflammatory way and that blocking it would be protective’. But, of course, we know that blocking COX-2 or knocking COX-2 out actually increases atherosclerosis and thrombosis when we consider the whole intact animal. The idea that COX-2 in areas of atherosclerosis is actually protective locally is backed up by some other studies that suggest that COX-2 is pro-inflammatory in those types of areas.

This chapter shows some interesting and novel data but is essentially confirmatory of what we know in terms of endothelial cell morphology. The novelty of this work relates to the application of imaging and modeling to quantification of endothelial cell morphology. One limitation of this chapter is that we were not able to show any functional correlates with the

distinct morphology that was quantified. Others show that morphology of endothelial cells that experience non-directional shear stress (such as in the lesser curvature of the aortic arch) have been reported to be associated with inflammation and an increased susceptibility to the formation of atherosclerotic plaques, typically display a cobblestone morphology.

When I studied the morphology of the aortic arch my focus was on the endothelial layer, for this reason I have used only CD31 as a marker for the endothelial cells and I did not include a marker for smooth muscle cells, however, this did not affect my results since I have used the z stacking technique in taking these images.

Figure 6.1

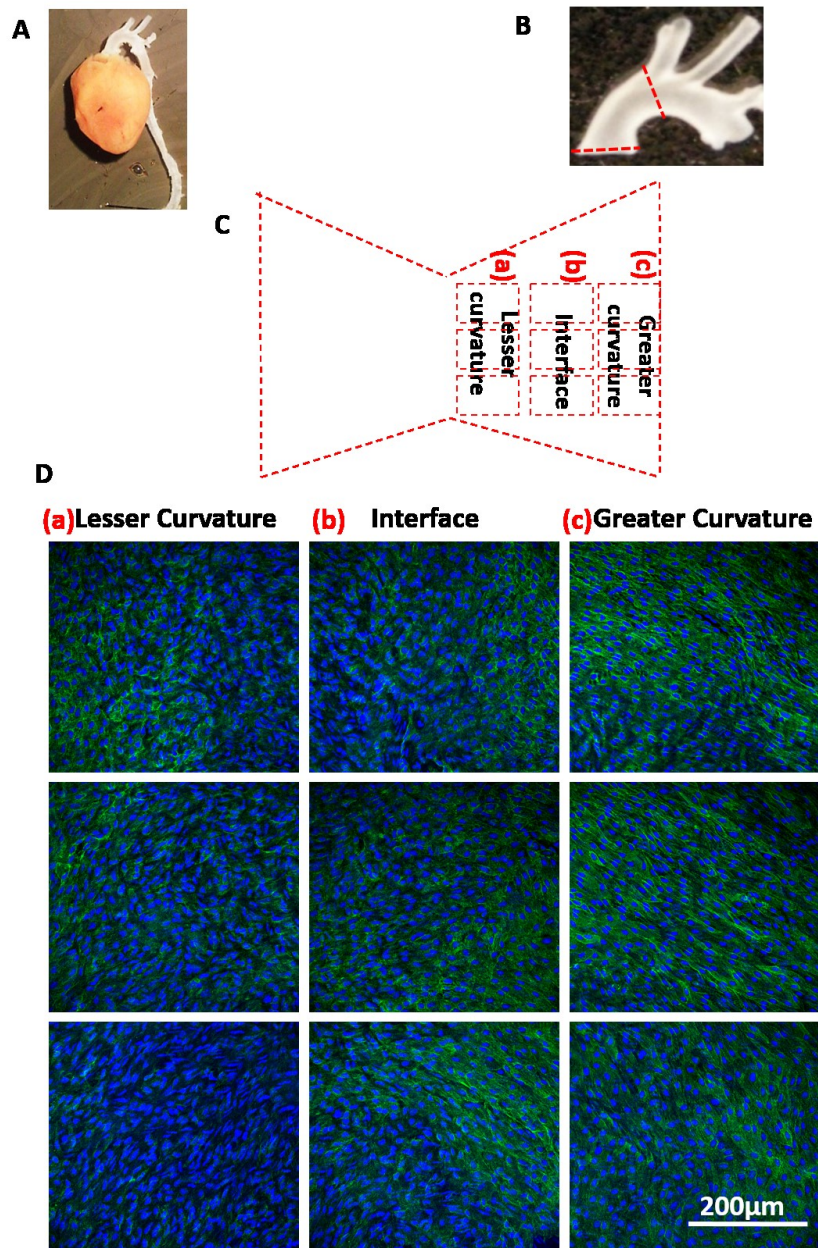


Figure 6.1: the three different regions within the mouse aortic arch. (A) Picture of a mouse heart cleared of connective tissue, showing the location of the aortic arch. (B) Picture of the proximal ascending aortic arch from a wild type (C57BL/6J) mouse. Red dotted line indicates cutting points along the greater curvature. (C) A schematic showing the aortic arch after it has been cut open and flattened into a butterfly shape. (D) A manual tile of representative full size images ($387.5\mu\text{m} \times 387.5\mu\text{m}$) taken by *en face* confocal microscopy from wild type mice ($n=5$) showing the morphological differences between the three regions in the luminal side of the mouse aortic arch: (a) the greater curvature, (b) the interface and (c) the lesser curvature. Green is the endothelial marker CD31 and blue is the DAPI staining for nuclei. Scale bar $200\mu\text{m}$.

Figure 6.2

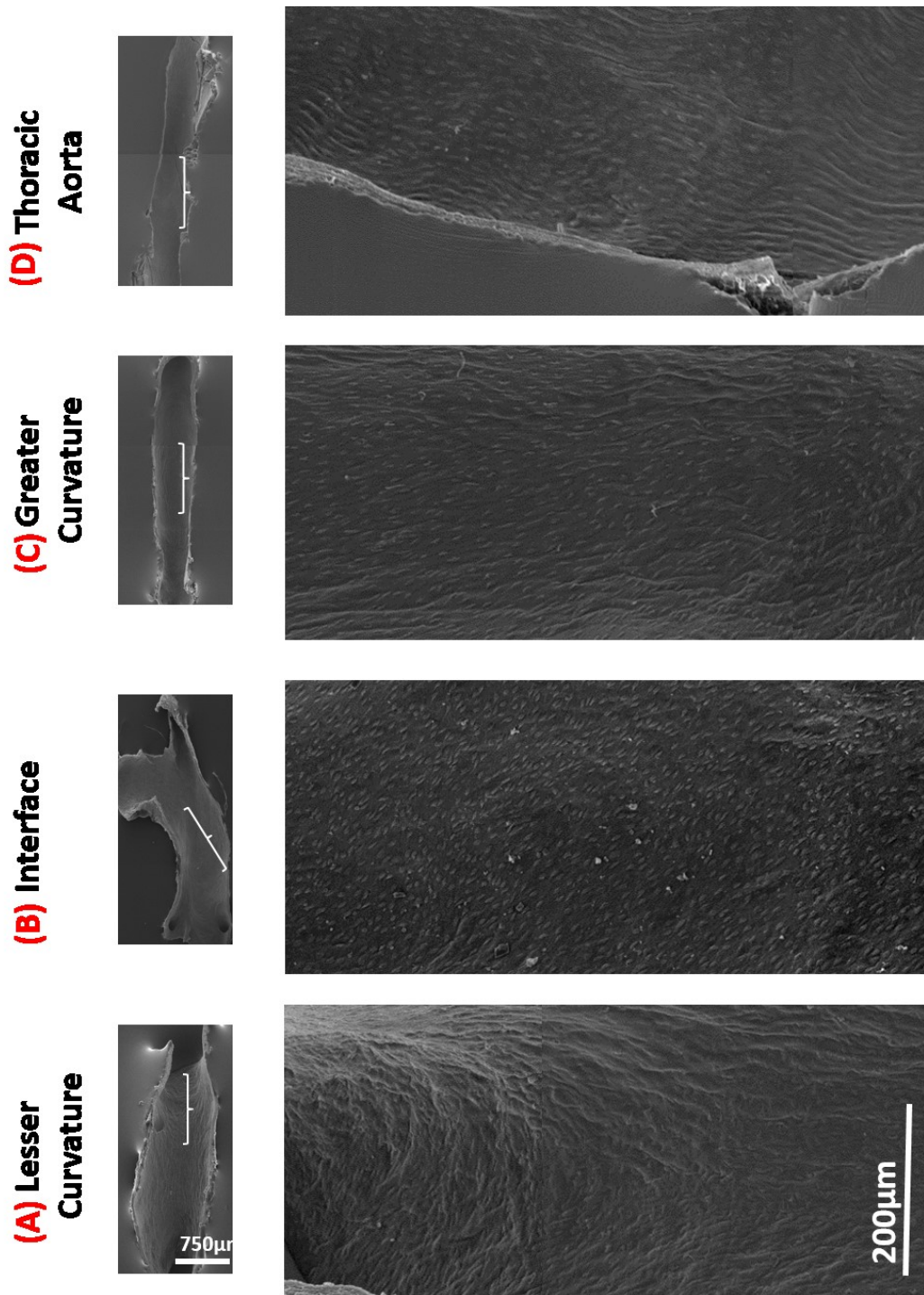


Figure 6.2: Scanning electron microscopy images of the mouse aortic arch and thoracic aorta. Representative images from $n=5$ mice showing the (A) lesser curvature, (B) interface, (C) greater curvature and D) thoracic aorta of mouse aortic arches. White bar indicates the location of the zoomed in images from each region. Scale bar 750-200µm.

Figure 6.3

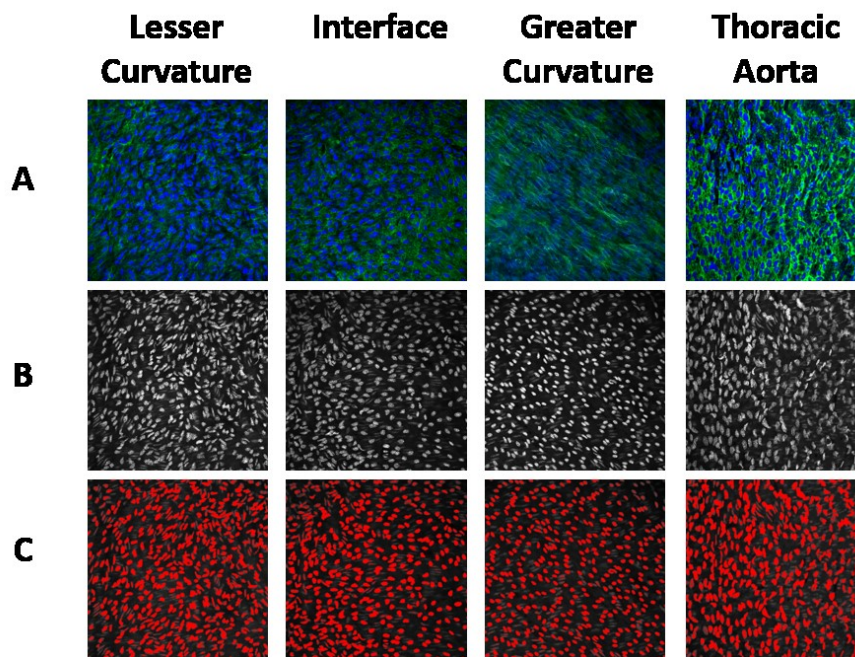
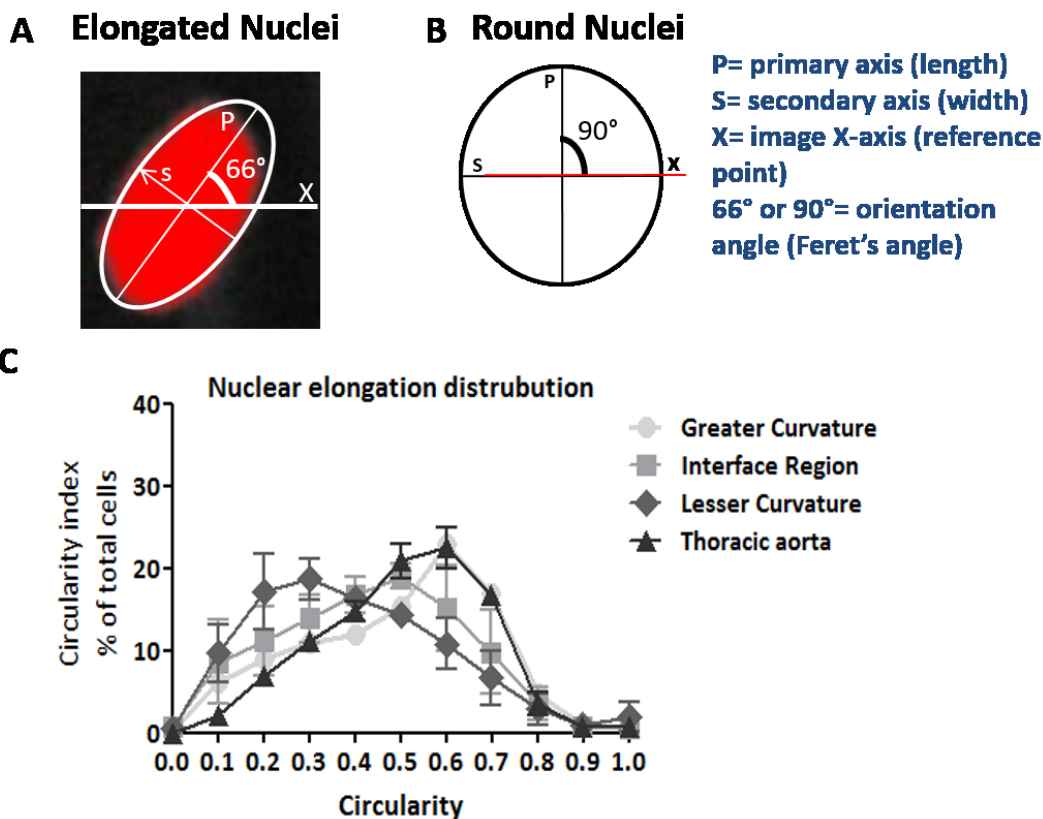


Figure 6.3: The steps that have been used to measure the nuclear alignment, density and size. (A) Shows the original full size images (387.5x387.5 μ m) that have been captured using the en face confocal microscope (green is the endothelial marker CD31 and blue is the DAPI staining for nuclei). (B) Shows the result of splitting the image into different gray scale channels (using Image J software) and the gray scale image from the blue nuclei that was used for analysis. (C) Shows the thresholded gray scale image (red is the thresholded nuclei that was used for quantification).

Figure 6.4

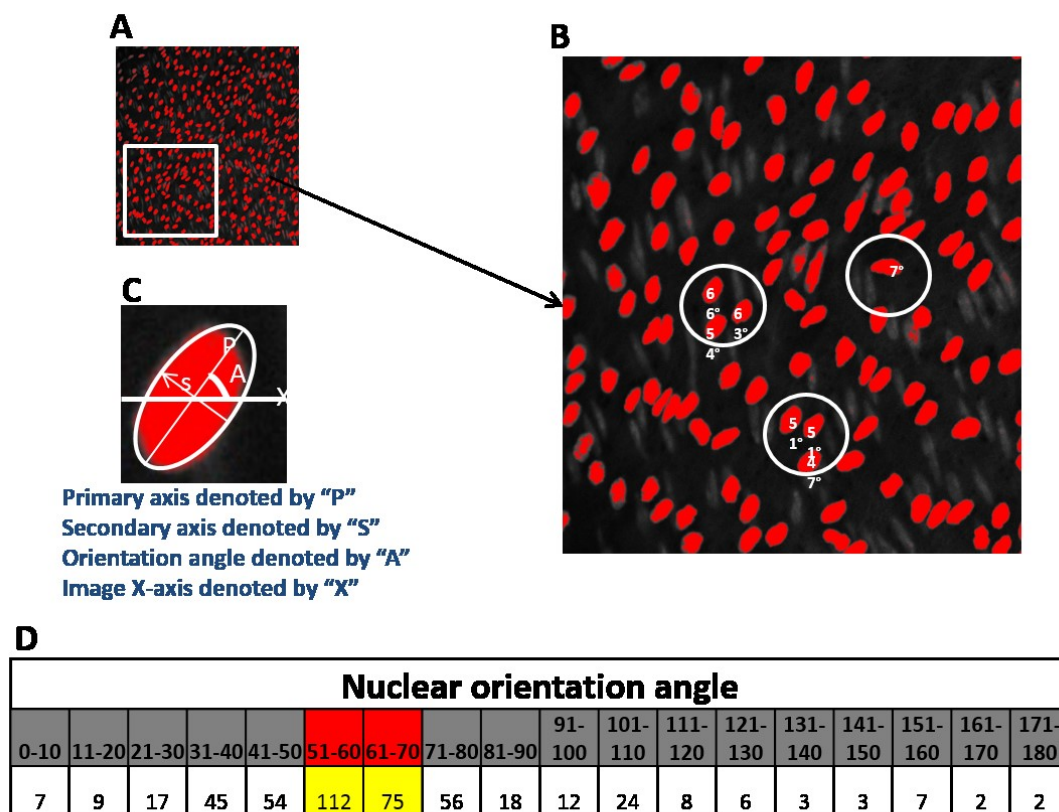


Circularity = $4\pi(\text{area}/\text{perimeter}^2)$

A circularity value of 1.0 indicates a perfect circle. As the value approaches 0.0, it indicates an increasingly elongated polygon.

Figure 6.4: Calculation of nuclear angle of orientation in Image J software. This figure illustrates the primary axis which is a line drawn through the longest point to point of the nuclei (length) and the secondary axis is the diameter across (width) of the nuclei. Image J has the image x-axis (straight line drawn across the image) as a reference point from where an angle of orientation is estimated (between the image x-axis and the primary axis). As long as the nucleus has an elongated shape (A), an angle of orientation can be estimated (i.e. 66°), whereas if all of the nuclei were round (B) the angle between the x-axis and the primary axis would always be 90°. (C) The nuclear elongation distribution (circularity index) for the greater curvature (GC), interface region (IF) and lesser curvature (LC) (n=4) calculated as $\text{circularity} = 4\pi(\text{area}/\text{perimeter}^2)$ and normalised to the total number of nuclei in the image. A circularity value of 1.0 indicates a perfect circle and as the value approaches 0.0 it indicates an increasingly elongated polygon.

Figure 6.5



1. Identify the highest number of nuclei that are orientated within a 20 degree angle span (112 nuclei orientated between 51-60 and 75 nuclei orientated between 61-70 degrees)
2. Take the sum of the number of cells the are aligned within this 20 degree angle span (112+75= 187)
3. 'nuclear alignment measure' obtained by dividing number of nuclei in one direction by the total number of nuclei in the image (187/469)x100=40%

Figure 6.5: An outline for how the nuclear alignment density and average size were quantified. (A) A full size (387.5x387.5µm) image that has been thresholded and the white box indicate the location of the cropped image (200x200µm) in (B). (1 and 2) is two clusters of nuclei that are orientated in similar degree of angels cluster 1: 66, 63, 54°and cluster 2: 51, 51, 47° and aligned in the same direction. Nr 3 shows an example of a nucleus which is orientated in a different direction with an orientation angle of 7°. (C) Indicate how the angle of orientation is calculated (between the image x-axis and the primary axis of the nuclei). (D) Shows the number of endothelial cell nuclei nuclear orientation angles in 10° angle spans distributed between 0-180°. The highest number of nuclei within a 20° angle span was identified and added together and normalised to the total number of nuclei in that image.

Figure 6.6

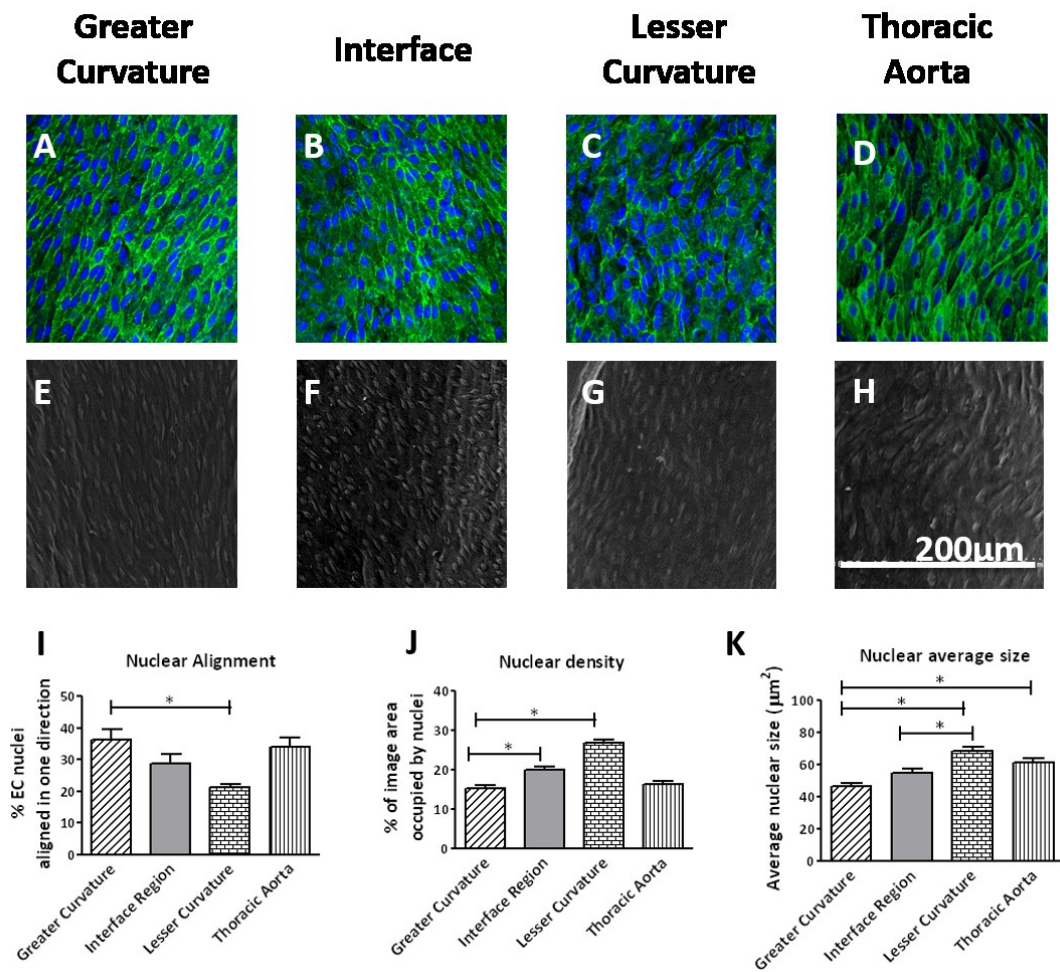


Figure 6.6: Quantification of endothelial cells in mouse aortic arch. (A-C) Confocal images from different regions of the endothelium in mouse aortic arch: the greater curvature, interface and lesser curvature (representative images from $n=11$ mice.) (D) Confocal image from the thoracic aorta (representative from $n=4$ mice). (E-G) SEM images from mouse aortic arch regions: greater curvature, interface and lesser curvature (H) and thoracic aorta (representative from $n=4-5$ mice). (I-L) Nuclear morphology profile (nuclear alignment, nuclear density and average nuclear size) quantified from the confocal images ($n=4-11$ mice). Green is the endothelial marker CD31 and blue is the DAPI staining for nuclei. Cropped images ($200 \times 200 \mu\text{m}$), scale bar $200 \mu\text{m}$. Data is the mean \pm S.E.M and was analysed using one-way ANOVA with Bonferroni's multi comparison post-test and $*p < 0.05$ was taken as significant and denoted by*.

Figure 6.7

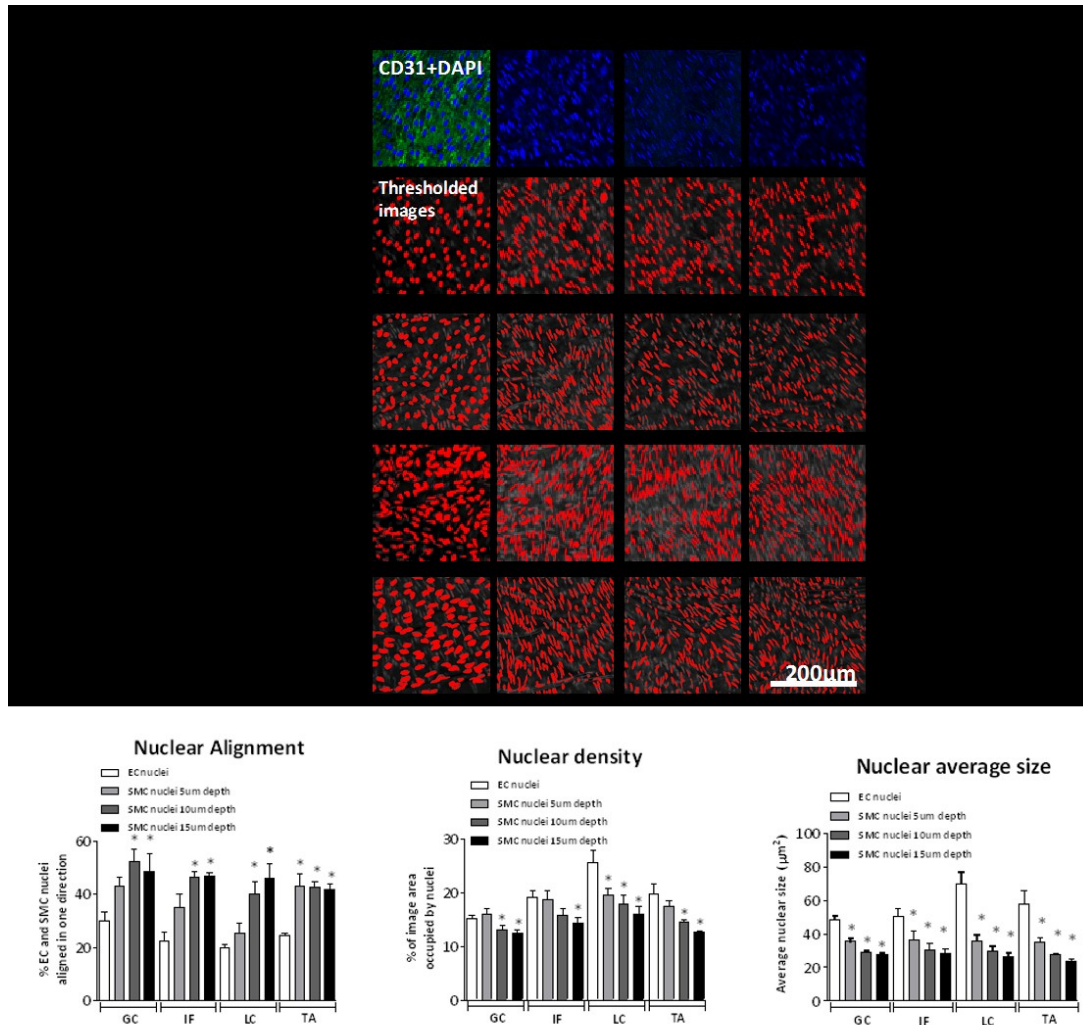


Figure 6.7: Quantification of EC and SMC layers at 5μm, 10μm and 15μm depth. (A) En face confocal images taken from the greater curvature, interface, lesser curvature and thoracic aorta regions at the surface CD31 positive endothelial cell (EC) layer and then at the directly underlying CD31 negative smooth muscle cell (SMC) layers at 5μm, 10μm and 15μm depth. Green is the endothelial marker CD31 and blue is the DAPI staining for nuclei. Red is thresholded nuclei included in analysis. Cropped images (200x200μm), scale bar 200μm. Nuclear morphology profile of the (B) nuclear alignment, (C) nuclear density and (D) average nuclear size of the EC nuclei and underlying SMC nuclei in confocal images taken from aortic arches from (n=5) wild type mice. Data is the mean ± S.E.M. Within region analysis was performed using one-way ANOVA with Dunnett's post test compared to EC layer, *p<0.05.

Figure 6.8

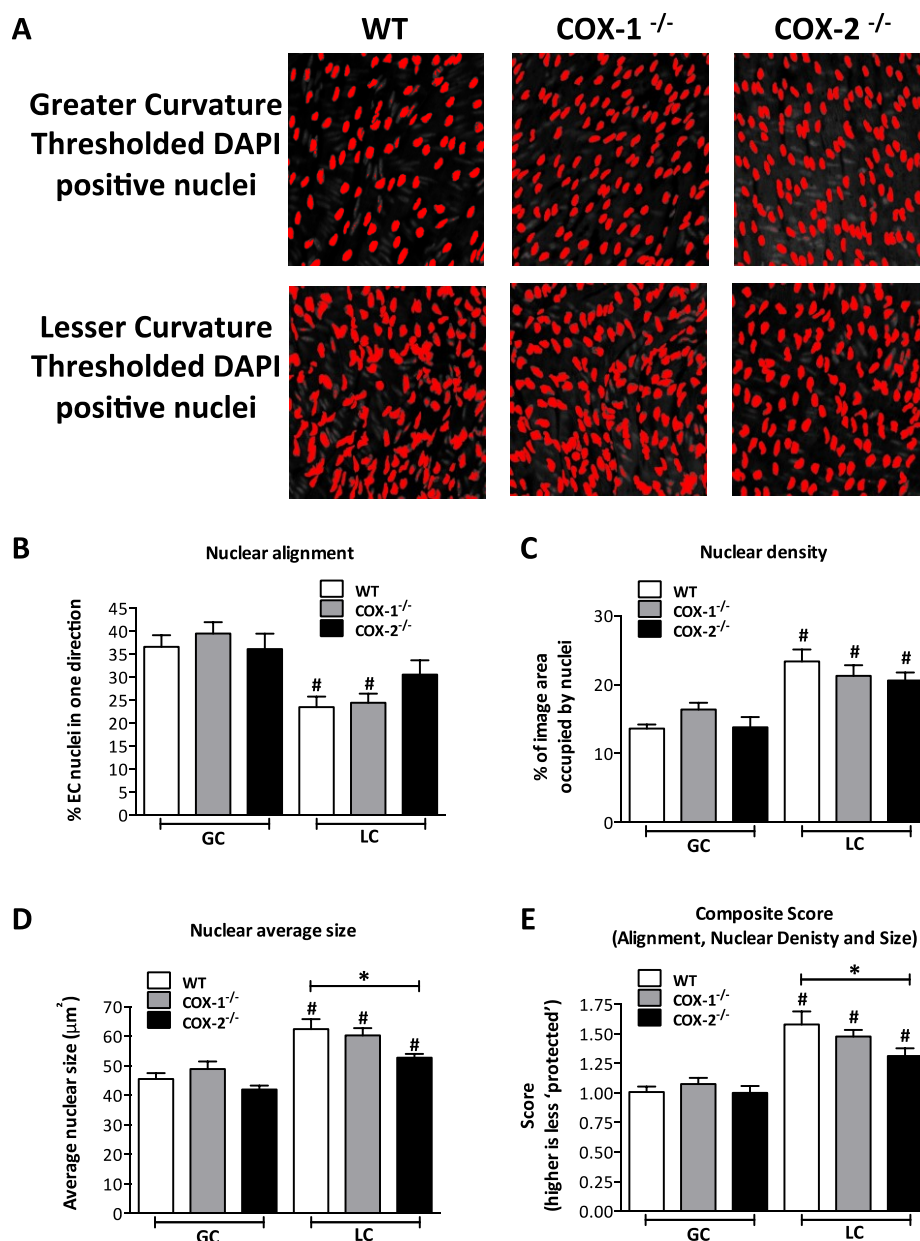


Figure 6.8: Quantification of EC in WT, COX-1 and COX-2 KO mouse aortic arches. (A) Representative images of thresholded nuclei from the endothelial layer of the lesser and greater curvature of the mouse aortic arch. Nuclear morphology profile; (B) nuclear alignment, (C) nuclear density, (D) the average nuclear size of EC in the greater curvature and lesser curvature of aortic arches and (E) the composite score calculated as the mean of nuclear size, 1/nuclear density and 1/alignment each normalised to their respective values for the WT GC region. Data are mean \pm S.E.M from (n=6) wild type (WT), COX-1 knock out (KO) and COX-2 KO mice. Between genotype analysis was performed using two-way ANOVA with Holm-Sidak post test compared to wild type, * $p < 0.05$. Within genotype analysis of GC versus LC data was performed using paired t-test, # $p < 0.05$.

Figure 6.9

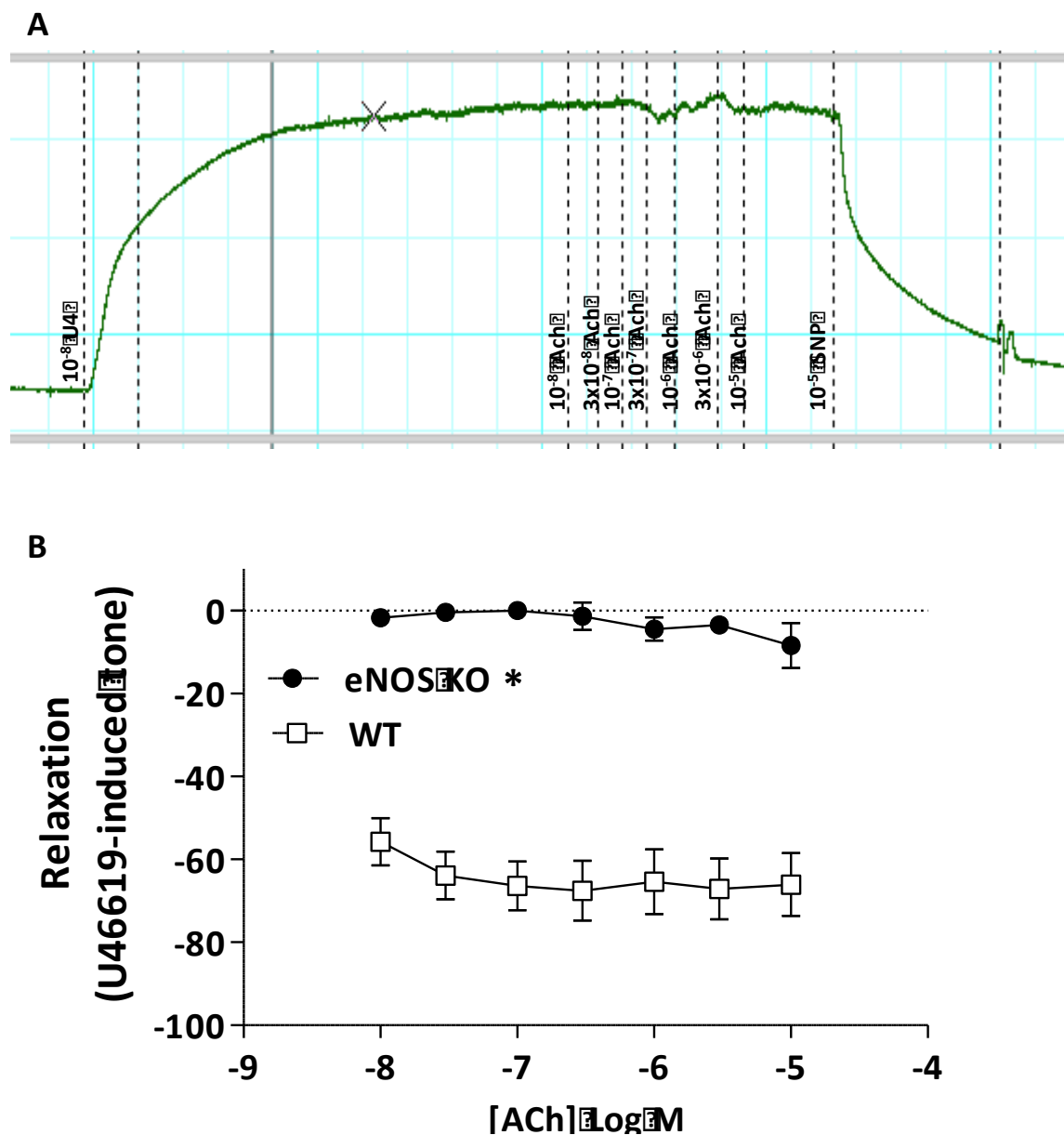


Figure 6.9: The effect of eNOS gene deletion on the relaxation responses of mice aorta. (A) Representative myograph traces showing wild type mouse aorta contracting with U46619 and then relaxed with different concentrations of ACh and then SNP. (B) relaxation responses of mice aorta from wild type (WT) and eNOS KO mice, aortas were contracted with U46619 and relaxation was induced with different concentrations of ACh. The data the mean \pm S.E.M for $n=4$. Data was analysed using two-way ANOVA and a p value of <0.05 was assumed statistically significant and denoted by*.

Figure 6.10

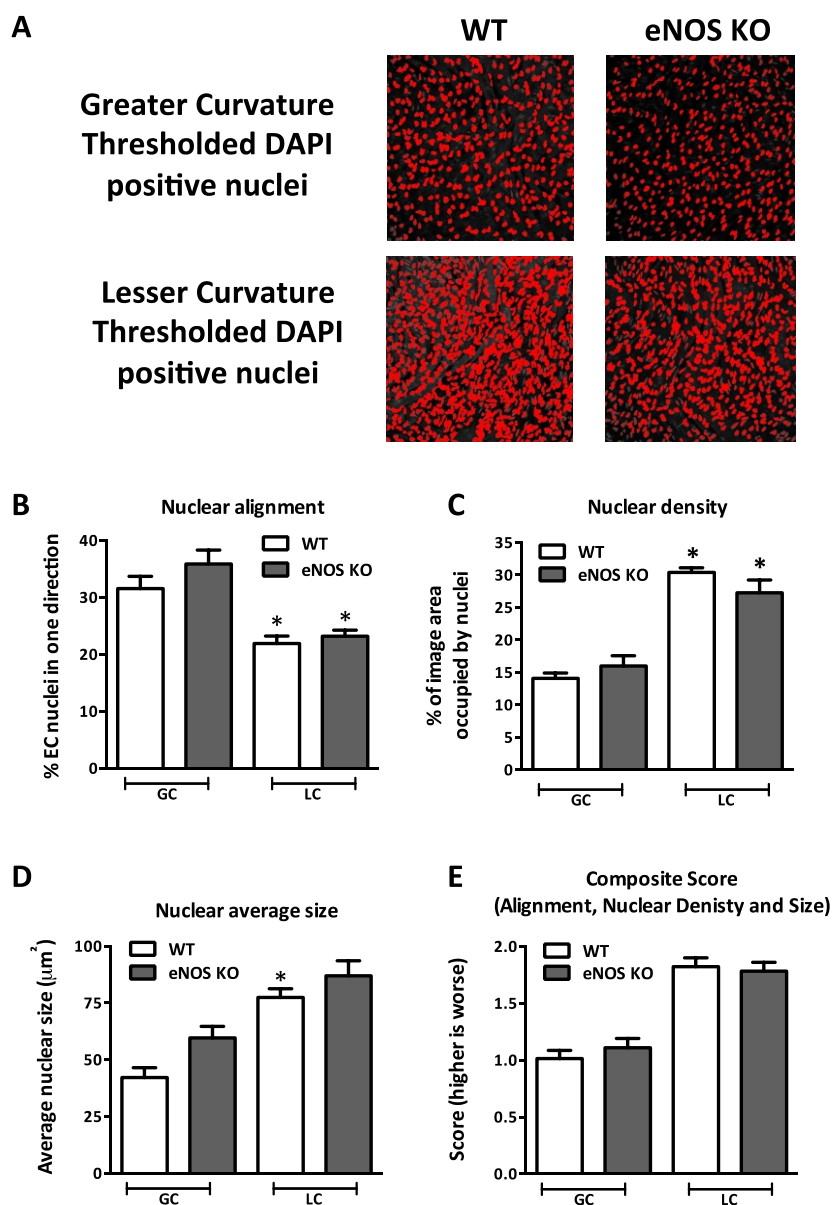


Figure 6.10: Quantification of EC in WT and eNOS KO mouse aortic arch. (A) Representative images of thresholded nuclei from the endothelial layer of the lesser and greater curvature of the mouse aortic arch. Nuclear morphology profile; (B) nuclear alignment, (C) nuclear density, (D) the average nuclear size of EC in the greater curvature and lesser curvature of aortic arches and (E) the composite score calculated as the mean of nuclear size, 1/nuclear density and 1/alignment each normalised to their respective values for the WT GC region. Data are mean \pm S.E.M from (n=3-8) wild type (WT) and eNOS knock out (KO) mice. Between genotype analysis was performed using two-way ANOVA with Holm-Sidak post test compared to wild type, * $p < 0.05$. Within genotype analysis of GC versus LC data was performed using paired t-test, # $p < 0.05$.

Figure 6.11

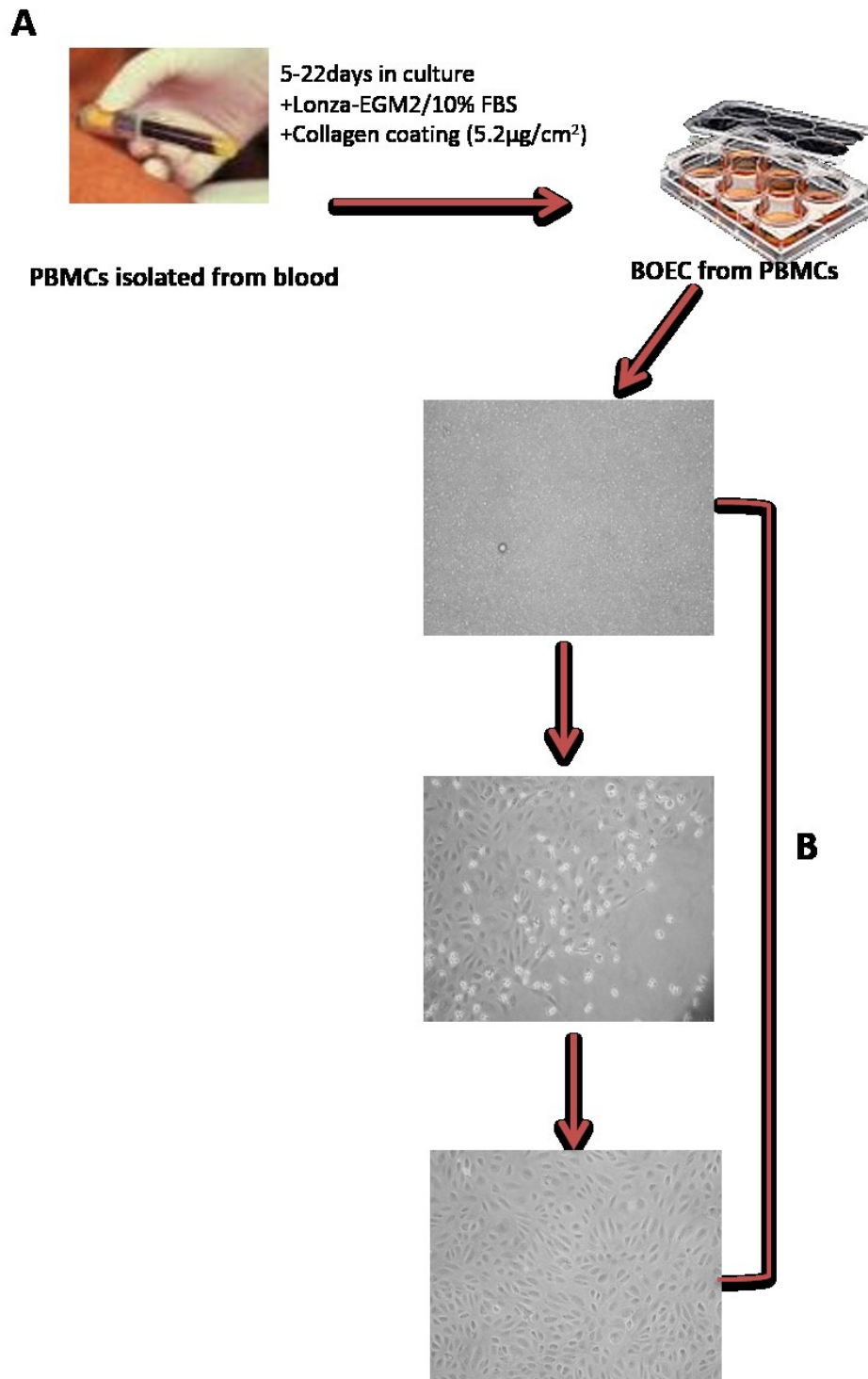


Figure 6.11: Isolating blood outgrowth endothelial Cells (BOECs). (A) Isolation of blood outgrowth endothelial cells from blood. (B) A representative image showing BOEC colonies emerging.

Figure 6.12

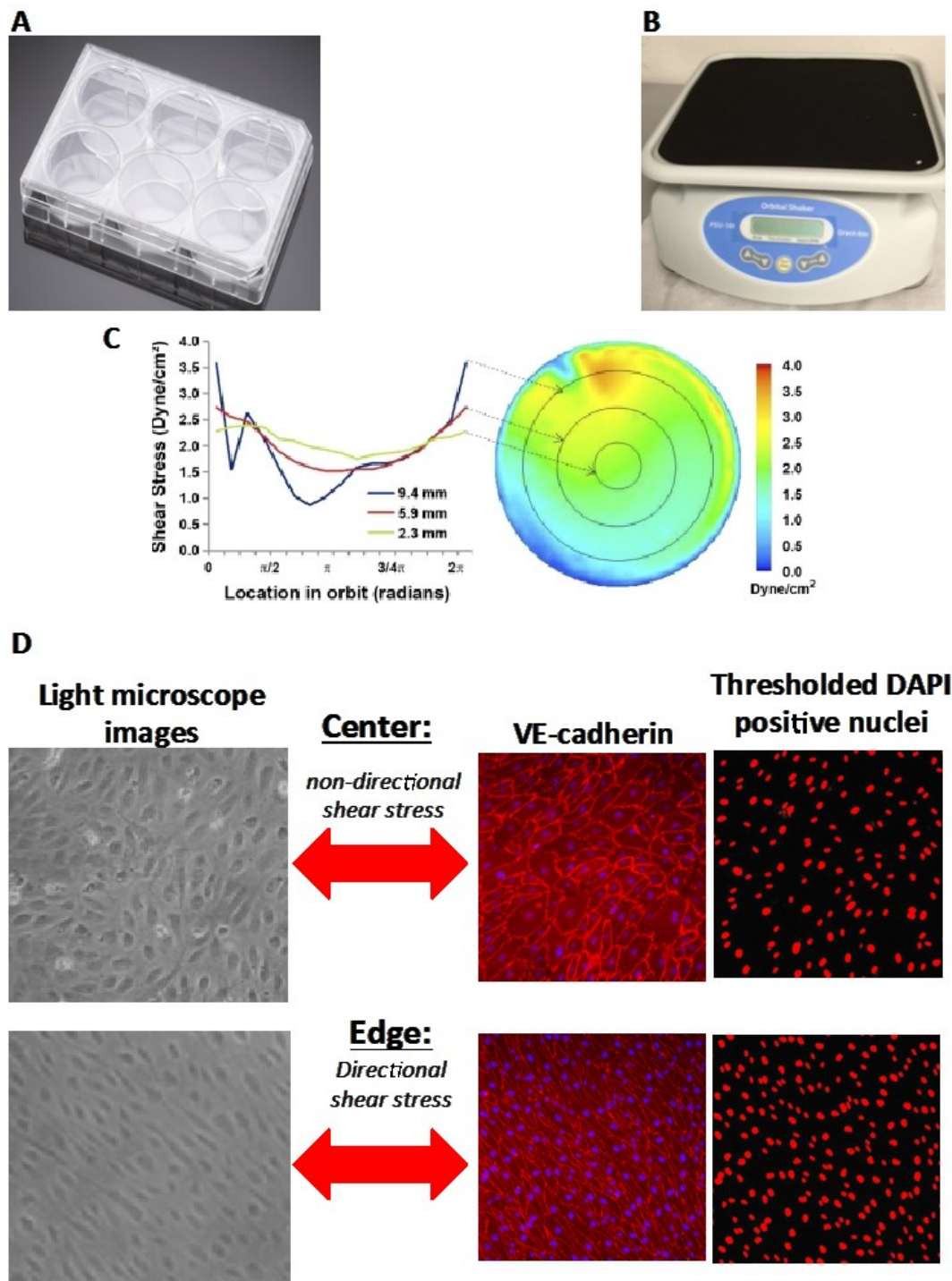


Figure 6.12: Modeling shear stress on the orbital shaker using Blood out growth endothelial cells from human. (A) An image for the 6- well plate that has been used for growing BOECs for shear/static experiment. (B) The POS-300 orbital shaker that has been used to apply shear stress on BOECs. (C) The computational fluid dynamics solution over the area of a single well of a 6 well plate.(D) light microscope images and Cellomics VTi HCS images for BOEC showing the different areas(center and edge of the plate) present after shearing the plate for 4 days.

Figure 6.13

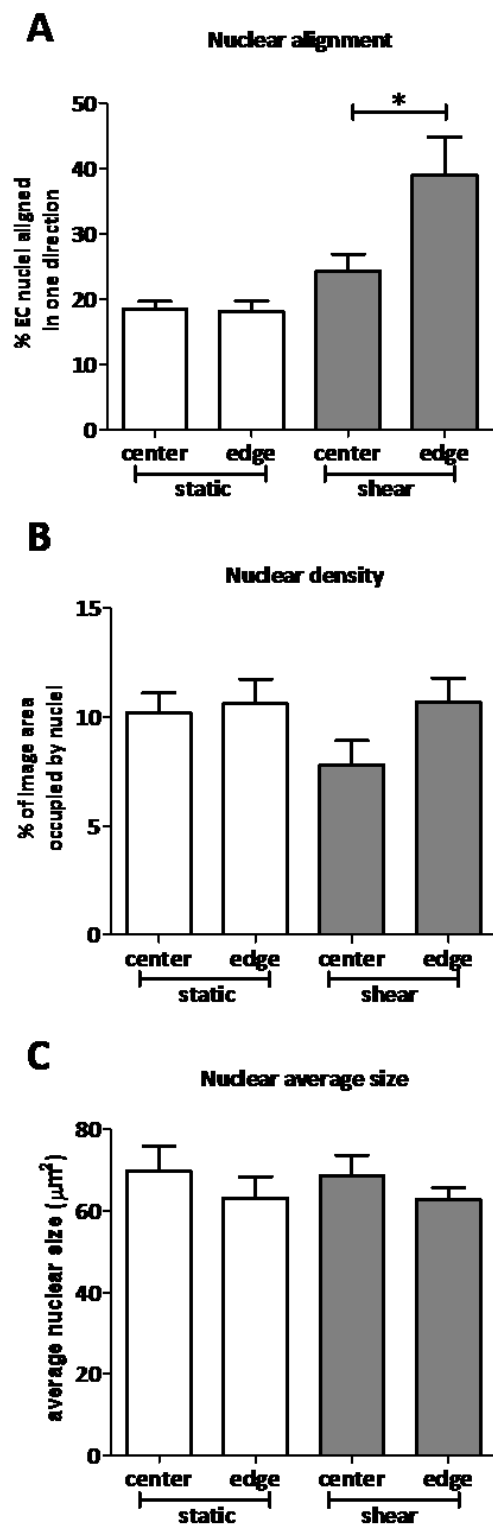



Figure 6.13: Nuclear morphology profile for human cultured cells (Blood out growth endothelial cells). (A) Nuclear alignment, (B) nuclear density and (C) average nuclear size of the EC nuclei growing in culture from human blood (BOEC) (n=6). Data are the mean \pm S.E.M and was performed using one-way ANOVA with Dunnett's post test, * $p < 0.05$.


Chapter 7: General Discussion

My thesis has worked to find how the anti-inflammatory pain medications know as a group of drugs as nonsteroidal anti-inflammatory drugs (NSAIDs) cause their highly feared side effects in the cardiovascular system. These are heart attacks and strokes. I think that cardiovascular side effect area of NSAIDs has had some very unusual and dangerous events that mean that people taking these drugs now have a kind of fear that affects their daily lives. If you take a look on the Internet you can find evidence how this fear affects ordinary people. Here are just two representative comments on just one patient forum that were posted last year after the FDA added a new degree of caution about heart attacks and NSAIDs²⁰⁹.

http://forums.compuserve.com/discussions/Chronic_Pain_Forum/Make_It_Stop/ws-chronicpain/4?tsn=1&tid=196&redirCnt=1&nav=messages²¹⁰


TO: Jan | POSTED: 9/9/15 10:32 AM | MSG: 196.2 (2 of 13) | REPLY TO: 196.1




Daryl (Sysop) 
POSTS: 685
Report

That's really bad news for people like me who rely on NSAIDs on a daily basis to be able to get up and move. I'm hoping that what was found earlier this year is true, that Naproxen might be somewhat safer. There's more on that in [this thread](#).

☆☆☆☆☆ 0 [Please login to Rate](#) [Options](#) [Quote](#) [Reply](#)

TO: **Daryl (Sysop)**  | POSTED: Jun-26 1:54 PM | MSG: 196.3 (3 of 13) | REPLY TO: 196.2



rad.red.fox
POSTS: 3
Report

I know I am replying to a really old message, but I feel like I need to express my feelings on this. I am a longtime NSAID user, maybe ten years or more. I cried when FDA took Vioxx off the market for the same STUPID reason: some small group had strokes and/or heart attacks, so the rest of us who could not walk without Vioxx, were punished. I would gladly have signed a non adversarial release, just give me my Vioxx back. But no. I've taken most of the NSAIDs, Meloxicam being the last one I was on. Took it for a few years, one in the morning and one at night. Then I was hospitalized for something non-related, and because of other drugs they gave me, I came off the Meloxicam. I have been doing fine without it, go figure, or maybe because my surgery lessened the problem the Meloxicam was 'fixing'.

It just seems to me that the people who need these drugs the most are the people who end up suffering even more, because FDA has once again pulled a very helpful drug from the market.

Figure 7.1: example of comments online.

The effect of Merck Co withdrawing Vioxx after the results of the APPROVE study were published were very great for Merck and now mean that there are no new COX-2 inhibitors

being developed. This is what happened to Merck's share prices after they took Vioxx off the market.



Figure 7.2: Share prices for Merck Co after withdrawing Vioxx⁷²

This image is published on a web page that describes the *The 7 Most Famous Product Recalls: How Did Stock Prices React⁷²?* Vioxx is the 2nd product. This is what they say about it and stock prices ‘

‘Vioxx was a drug that treated arthritis that was manufactured by Merck (MRK) and approved by the FDA in 1999. In 2004, after receiving results from a clinical trial that the drug increased the risk of heart attacks, MRK recalled Vioxx. Merck has spent approximately \$4.85 billion to settle 27,000 lawsuits related to heart attacks and stroke incidents. MRK’s share price collapsed on the news, taking over a year to recover⁷².’

Later another COX-2 inhibitor Valdecoxib was withdrawn over fears of heart attacks. Valdecoxib is number 3 on the list of 7 most famous product recalls. Valdecoxib was withdrawn on the advice of the FDA and the FDA cited

‘potential increased risk for serious cardiovascular (CV) adverse events,” an “increased risk of serious skin reactions” and the “fact that Bextra has not been shown to offer any unique advantages over the other available NSAID^{211s}’

This is what they say about it on the web site

‘Pfizer’s (PFE) arthritis treatment Valdecoxib was removed from shelves due to heart attack and stroke concerns related to Merck’s massive Vioxx recall. The recall resulted in \$1.8 billion in legal charges for PFE. In addition to its general legal fees, PFE was also subject to one of

the largest criminal fines in U.S. history. Despite the recall, PFE's share price did not see any long term decline⁷²



Figure 7.3: Share prices for Pfizer after withdrawing Valdecoxib⁷²

My PhD thesis contains very important work that could, if my results using basic science ways prove to be true in regular people that need to take their drugs, change the situation for COX-2 inhibitors. I am very proud to have been able to do this work and sincerely hope that one day it will be used to improve the lives of those with serious pain such as happens in arthritis, those with cancer and those who are at a risk of cardiovascular disease in a general setting.

When COX-2 was first discovered in the late 1980s/early 1990s it was strictly thought to be a form of the enzyme that is only present at the sites of inflammation. This is because it was found in cells that were stimulated with inflammatory agents. Interestingly the most early studies were using inflammatory agents like TPA that are cancer causing substances. This relevant now because COX-2 inhibitors can prevent cancer. Anyway, in the first reports of COX-2 it was not thought that this form was present in healthy tissues. For this reason it was assumed that, for example, endothelial cells and blood vessels, would only have the constitutive form of COX-1. In fact Professor Vane and my supervisor Professor Mitchell used endothelial cells as their experimental system for COX-1 when they were testing how NSAIDs that were around at the time (early 1990s) had potencies for COX-1 compared to COX-2. For their COX-2 system they used macrophages activated with LPS. At the time they knew that endothelial cells are full of 'COX' and that the main product is prostacyclin, as

covered in my introduction section. It was only after a paper showed that the COX-2 inhibitor Vioxx could reduce prostacyclin markers in the urine without reducing thromboxane (TX)₂ in the urine that the idea started to take shape that COX-2 could be the form making prostacyclin. Then when the VIGOR trial was published showing that Vioxx increased heart attacks and strokes people were putting two and two together to make the idea that prostacyclin is made in blood vessels by COX-2 (and not by COX-1 as everyone had thought in the beginning). This idea was so attractive that it was generally accepted. This was shown when the American Heart Association published advice for doctors prescribing COX-2 inhibitors in 2007. Their advice published in the journal *Circulation* said that a step-wise approach should be used where after paracetamol (called acetaminophen in the US), aspirin and ‘narcotic analgesics’ (opiate type drugs) then the order of prescribing should be non COX-2 selective NSAIDs>NSAIDs with some COX-2 activity>COX-2 selective drugs’ (Figure 7.4). Examples would be naproxen>ibuprofen/diclofenac>Celebrex.

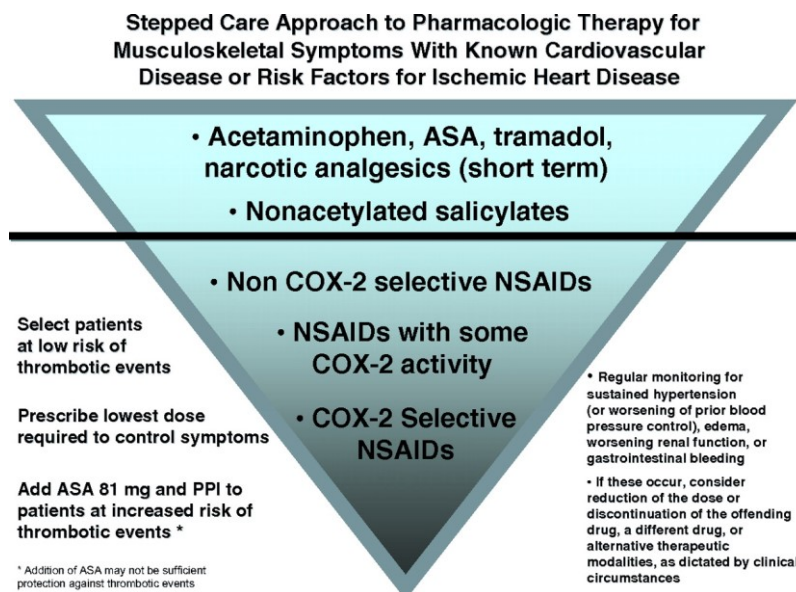


Figure 7.4: Stepped care approach to management of musculoskeletal symptoms. In patients with known cardiovascular disease or who are at risk for ischemic heart disease, clinicians should use a stepped care approach to pharmacological therapy that focuses on agents with the lowest reported risk of cardiovascular events and then progress toward other agents with consideration of the risk/benefit balance at each step¹⁰³.

This step wise approach suggested in 2007 is now of course seen as not completely logical because those drugs with ‘some COX-2 selectivity’ like diclofenac and ibuprofen do in fact

cause as much increased risk of having a cardiovascular response as do the COX-2 selective drugs like Vioxx and Celebrex (sometimes known as 'coxibs')¹⁰⁴.

So now we have a situation where all kinds of NSAIDs have cardiovascular side effects. We are still not sure about aspirin and naproxen. These drugs inhibit the platelet and so can also protect the cardiovascular system. These means that for aspirin, which is in fact taken by people to prevent heart attacks and strokes might have the effect of blocking COX-2 in the cardiovascular system canceled out by blocking the platelet. Naproxen could be similar as it also can inhibit the platelet when taken by patients. This is because unlike the other NSAIDs that also block COX-2 (this includes diclofenac and ibuprofen) because of naproxen's duration in the blood it can affect platelets. But still, we are not truly sure that naproxen is safe on the cardiovascular system and a recent paper stated that

*'our analyses suggest that **naproxen** might **not be associated with an increased risk of major vascular events**, but this result should be interpreted with caution. **First**, we do not know whether this would be true in patients treated with aspirin, in whom naproxen will not result in any additional inhibition of COX-1 and might actually interfere with the antiplatelet effect of low-dose aspirin. **Secondly**, the effects of lower naproxen doses, such as those typically used in over-the-counter preparations (eg, 220 mg twice a day), are uncertain since they would be less likely to mimic the aspirin-like effect of 500 mg twice a day. **Thirdly**, the apparent advantage of naproxen regimens might not be preserved after longer term use. **Finally**, naproxen substantially increases the risk of upper gastrointestinal complications'¹⁰⁴.*

So for the small sample of evidence above it seems that we really need to understand how COX-2 inhibitors are causing cardiovascular side effects.

COX-2 prostacyclin hypothesis versus my work

In my thesis I have carried on the work of the group looking in more detail about the isoform in blood vessels that makes prostacyclin. As I said in my introduction prostacyclin is a very important protective hormone that works against TXA₂. I found what others in my group had found that prostacyclin in blood vessels from mice are completely made by COX-1. This work is shown in my first results chapter (Chapter 3) that used blood vessels from knock out mice. Prostacyclin was more or less completely absent in vessels from COX-1 knock out mice but not changed in vessels from COX-2 knock out mice. I also showed that this is true however you activate the vessel and that the endothelium is the main site for

prostacyclin release. I also make an important experiment to show that COX-2 could be the main enzyme to drive prostacyclin in the vessel if the vessel was just left in culture for a few hours. This was very important because we did not have any positive control data showing that COX-2 was in anyway important locally in the blood vessel. Carrying on from my interest in imaging I showed how COX-1 and COX-2 were localized within the vessel using confocal microscopy. One other important thing that I was able to be involved with was to show that the release of prostacyclin that we had previously measured using ELISAs was the same when our collaborator had used an analytical approach with LC-MS/MS. I was not able to perform these measurements directly myself, they were done by Professor Nicolaou.

In this way the results shown in Chapter 3 completely confirm that COX-1 and not COX-2 is the form in blood vessels responsible for prostacyclin release. This data set the stage for my next chapter where I was able to make what I think was a very important finding.

As I explain in my introduction chapter (Chapter 1) there are two very important facts that were considered together firstly that It was always known that NSAIDs affect renal function and secondly that when renal function is reduced then it can happen that the natural inhibitor of eNOS, called ADMA can be increased. This is because the kidney is the main site that ADMA is removed from the body. So taking these two separate things together it could be that inhibiting COX-2 in the kidney when taking an NSAID would reduce the renal function and that this would result in increased ADMA. If this happened then the increased ADMA would act in the body to inhibit eNOS in the endothelial cells and that this would then be a detriment to cardiovascular health.

The link between the kidney, COX-2 and ADMA

In my second result chapter I did find this to be the case. What was important I think is that I found that ADMA was increased in COX-2 knock out mice but not in COX-1 knock out mice. This was surprising to me in a way because the majority of the prostacyclin in the kidney as a gross organ was coming from COX-1. This means that the COX-2 which is present in the kidney, as I describe in Chapter 1, that is present in the renal intestinal fibroblasts, must be extremely important.

Also it was important that I found that the increase in ADMA in COX-2 knock out mice was not only because of any reduced function in normal renal function but that it was mediated to some degree by actual changes in the expression of the enzyme pathways that lead to ADMA synthesis (PRMTs) and removal (DDAH and AGXT2). I also found that ADMA could be increased in mice where COX-2 was blocked with the COX-2 inhibitor parecoxib and in actual healthy volunteers that were taking naproxen or Celebrex.

Seeing the increase in ADMA healthy human volunteers with Celebrex fits with the idea that blocking COX-2 could cause cardiovascular side effects by increasing ADMA. As I say in my General Introduction (Chapter 1), ADMA is after all a well-known marker cardiovascular risk and that it has the mechanism that we understand is at the level of blocking the protective release of NO from the blood vessels. But at first it might seem an unexpected finding that naproxen also increased ADMA since naproxen is thought to have fewer cardiovascular side effects than Celebrex¹⁰⁴. However, we need to consider that naproxen will still provide the same block of COX-2 in the kidney that Celebrex causes because this is the therapeutic dose and the therapeutic dose must block COX-2 or it won't be effective at treating inflammation and pain. So in this way it was expected that where there is a COX-2 affect both naproxen and Celebrex would look the same. Also, naproxen, just like Celebrex can affect kidney function, again this is because it is regulated by COX-2. As I mention above, the fact that naproxen is different in terms of cardiovascular side effects is because of its effects on platelets. This was in fact the reason that was first used to explain the findings in the VIGOR study where Vioxx had more cardiovascular events than the comparator arm which was people taking naproxen¹⁰⁸.

In all other aspects of the cardiovascular side effects caused by NSAIDs that work by blocking COX-2 prostacyclin is always considered to be the prostanoid that is protecting the system. In my thesis this seemed to be the case also because when we measured ADMA the plasma from the prostacyclin IP receptor knock out mouse ADMA was increased, although it didn't seem to be to the same extent as seen for the full COX-2 knock out. In this case the ADMA measurements were made by our collaborator Dr James Tomlinson. But the fact that the levels of ADMA did not completely match the increases that I found in samples from COX-2 knock out mice could mean that the IP receptor pathway is not the only way that this

is happening. As I cover in my introduction, prostacyclin is working on other receptors, particularly the PPAR β receptor. Currently work in my group is continuing in this area and they will soon look to see if samples from PPAR β knock out mice have increased ADMA, this will be interesting to see.

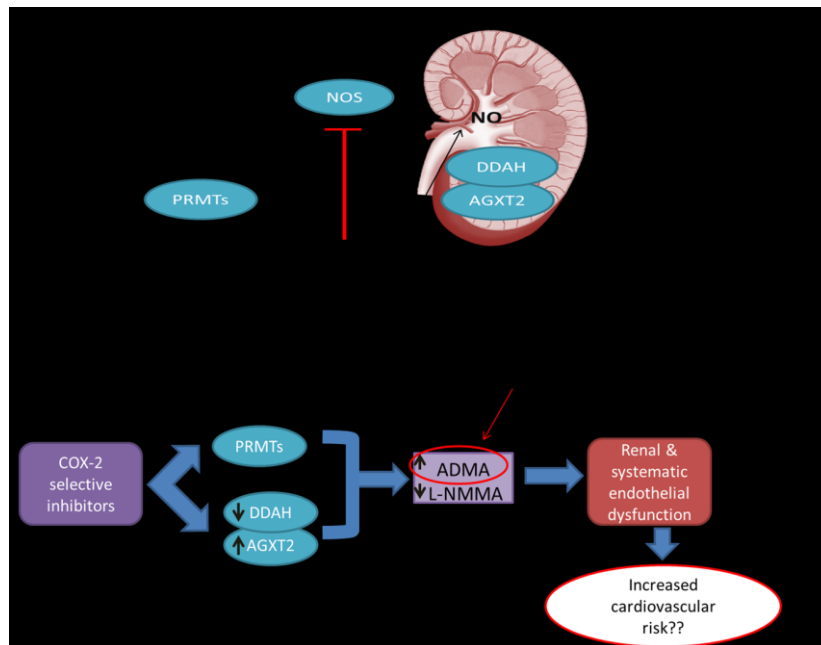


Figure 7.5: COX-2/NO pathway in the Kidney. (A) The NO pathway in normal kidney. (B) The effect of COX-2 selective inhibitors on the NO pathway in the kidney.

In addition to ADMA on the Liquid-Chromatography Tandem Mass-Spec (LCMS) that was used to measure ADMA other amino acids were also measured. From the methylarginines this was LNMMA and SDMA. In addition to ADMA I found that LNMMA was increased in some cases so was SDMA. The fact that LNMMA was increased would increase the likelihood that effects would be seen on eNOS as LNMMA is active but SDMA is not. I also was able to get the measurement of L-arginine using the LCMS and this is important because the effect of methylarginines on eNOS activity is a balance between levels of methylarginines and levels of arginine. This is because arginine and methylarginines compete with each other for eNOS. In fact in the ADMA literature it is most often that the ratio of ADMA to L-arginine is reported. When I made these type of calculations the increase in ADMA was still valid because the ratio, even when taking arginine into consideration, was increased. All of this work was pointing towards the fact that in COX-2 knock out mice then there could be effects on eNOS responses and that this could be because the ADMA was increased.

Responses to eNOS in vessels from COX-2 knock out mice.

The best way to know if the increase in ADMA and L-NMMA that was occurring in plasma from the COX-2 knock out mice was having an effect on eNOS was to look at responses in isolated blood vessels ex vivo. In my third results chapter (Chapter 5), which was a short chapter, but a very important one, I used isolated aorta in the myograph. Here you can see what has happened on eNOS without the complicating factors seen using an in vivo technique. Also the aorta is a very good blood vessel to consider for this experiment because it does not relax to prostacyclin and so relaxation responses in this vessel are really all mediated by NO from the endothelium.

I found that in the aorta from COX-2 knock out mice eNOS responses activated when the stimulate acetylcholine was added were reduced. This could have been because the endothelium was damaged or that the smooth muscle underneath was not working. However, this was not the case because the NO-donor sodium nitroprusside (SNP) that works directly on the smooth muscle and does not rely on NO from the endothelium caused the same relaxation in vessels from control and COX-2 knock out mice. Second from my work shown in Chapter 3, I knew that the endothelium was clearly present and not damaged in aorta from COX-2 knockout mice as shown by my images on confocal microscopy where the endothelial maker CD31 and COX-1 were clearly present in these vessels. But the real test to see if the reduced responses to acetylcholine were due to increased accumulation of methylarginines would be if they were reversed when we added arginine because arginine would compete away the methylarginine effect.

This is what I found. When the relaxation responses to acetylcholine were performed with arginine added to the organ bath the responses in COX-2 knock out aorta were restored. I also found, as you might expect, that the potency of methylarginines and the synthetic arginine analogue, L-NAME were increased as 'basal eNOS blockers' in aorta from COX-2 knock out mice.

This work together strongly suggests that there is in fact a real effect of the increased methylarginines that are due to blocked COX-2 in the kidney.

Taken all together the key findings in the main part of my thesis can be that COX-1 is the enzyme in blood vessels but that blocking COX-2 in the kidney is the site for the cardiovascular side effects and that increased levels of ADMA and L-NMMA could be the mechanism by which the endothelium in the whole circulation is compromised. In this way ADMA could be a future biomarker for finding those people out that might be a greatest risk of getting a side effect and even that taking arginine might protect people from side effects. This would definitely need more work but considering that arginine can be easily bought in any health food shop it is something that in future studies should be considered.

Morphology of endothelial cells, correlation with regions of directional shear and influence by loss of COX-2 and eNOS

Finally, although it did not start off as a central research question for me I completed some very interesting and nice work looking at the morphology of endothelial cells in vessels. This work shown in the final results chapter of my thesis (Chapter 6) is work that I am very proud. The main work of my thesis discussed above is very important and I am proud of that too but it fitted into a very active and competitive area where there was lots of papers and information to go on. However the work in my last chapter was relaxed because there is less known in the field and although the work was really observational it was I think interesting and important.

Endothelial cells have the function to align with the direction of blood passing over their surface. This means that in area of blood vessel where blood is directional, sometimes referred to as 'laminar' endothelial cells all line up. They are elongated and form in a common direction. In areas where blood flow is non-directional, sometimes referred to as 'turbulent' there the endothelial cells are not elongated they are more cobble stone in shape. In fact this is also how endothelial cells look when they are cultured without any shear stress under static conditions in vitro. This is how most of the experiments are performed using cultured cells because it is not so easy to culture cells for the whole duration of an experiment, ie from getting the cells off the vessel in the first place to adding the test reagents.

But the effect of blood flow and shear stress on endothelial cells is very important because not only does their shape change also their sensitivity to inflammation changes. So endothelial cells that are lined up under directional flow are protected from inflammation and atherosclerosis while those looking like cobblestones in turbulent areas are prone to inflammation and atherosclerosis. For these reasons it is important to understand endothelial cell morphology. However, it has proved difficult to really know what these endothelial phenotype shapes mean. In fact the work showing how the cells are lined up or not lined up in vessels has generally relied on using confocal microscopy where vessels are mounted and fixed endothelial side exposed. This technically could result in physical changes on the endothelial cells such as squashing. In my final results chapter (Chapter 6) I addressed this by comparing what endothelial cells look like in regions of directional and non-directional shear stress using confocal microscopy versus using scanning electron microscopy (SEM) because using SEM would provide a true structural image of the endothelium. I found in doing this that the endothelial surface at areas of directional shear were indeed elongated and aligned in the direction of shear and that those in non-directional regions were indeed cobblestone in appearance. As far as I am aware this was the first study to demonstrate this. Next I used confocal microscopy with Z-stacking to see how the underlying smooth muscle cells align with the above endothelium. It was already well known that the underlying smooth muscle runs perpendicular to the endothelium at areas with directional shear.

To quantify alignment of vascular cells was not as straight forward as you might imagine since this would need to be done using images from the microscope and some way to collate data from experimental repeats and from one region to another. An easy way that I did this was by simply blind scoring images because the direction of cells lining blood vessels is very obvious to the human eye – but how to quantify this? To do this I used images in ImageJ and adopted the use of the Feret angle (or angle of orientation) to make a useful algorithm. The quantified data that I obtained from my algorithm fitted very well with the blind scoring data that I obtained just from looking at images of the cells.

I went on to show that this approach could be used in human endothelial cells cultured under directional and non directional shear stress.

Finally I was able to link this work into the main research question of my thesis because I was able to use my algorithm to calculate the effect of knocking out COX-2 on the morphology of endothelial cells in the aortic arch. This was very exciting to me because of the link that I mention above between endothelial cell morphology and alignment and vascular inflammation and atherosclerosis. It was surprising but rewarding when I found that there was in fact a significant difference in endothelial morphology in the aorta from COX-2 knock out mice. In fact what I found was that loss of COX-2 was associated with detectable morphological changes in the endothelium of the lesser curvature. As I have written above and in the introduction COX-1 is the main enzyme in the endothelium, but there is a small detectable level in the lesser curvature of the arch, and although this is detectable with antibodies⁷⁹ and in luciferase mice¹⁵³, it does not contribute on a gross level to prostacyclin released as a whole by the aortic arch. But my work looking at morphology shows that in COX-2 knockout mice exactly where that small amount of COX-2 is expressed there were detectable changes in endothelial morphology.

As my results in Chapter 4 and 5 show knocking out COX-2 leads to increases in ADMA and this results in reduced eNOS activity. To see if the morphological changes that I was able to calculate in the endothelium of the lesser curvature of the aortic arch we because of loss of eNOS activity I checked the endothelium in aortic arches from eNOS knock out mice. What I found was that the changes were not due to loss of eNOS.

The importance of this work needs to be seen after further experiments but it serves to show how my work on imaging, morphology and generating an algorithm can be useful as a new type of a tool in endothelial cell pharmacology and importantly show that there are some important effects on the vessel itself of loss of COX-2 that is in fact completely independent of any effect of the ADMA/eNOS axis.

Implications of my work, limitations and future experiments

I am proud of my work and I think that it will have important implications. For example the next step would be to see if measuring ADMA in patients taking NSAIDs is linked with any change in blood pressure. Also my group is collaborating with people that ran the SCOT study who have plasma samples from the ≈7000 patients taking NSAIDs of which around

140 had cardiovascular events. The full details of the trial design for SCOT are published in the BMJ²¹². The future work will be to measure levels of ADMA in the people that had heart attacks and strokes and see if they are higher than in matched people from SCOT that did not.

Another approach for future experiments will be to see if supplementing with L-arginine can reverse the cardiovascular phenotype seen in laboratory animals where COX-2 is knocked out or inhibited with drugs. Here in mice then loss of COX-2 is associated with increased thrombosis²¹³ and atherosclerosis⁸². If these experiments work then the next step would be to try this in people taking drugs.

Finally, I think that the implications of my work in the final chapter could be that the endothelial morphology is easily measured in cardiovascular experiments. This has so far only really been done in a qualitative manner.

The limitations of experiments in my thesis are mainly related to the fact that I have used generally laboratory animals, although my work has where possible tried to use human systems.

References

- 1 Smith, W. L., Marnett, L. J. & DeWitt, D. L. Prostaglandin and thromboxane biosynthesis. *Pharmacol Ther* **49**, 153-179 (1991).
- 2 Hemler, M. E. & Lands, W. E. Biosynthesis of prostaglandins. *Lipids* **12**, 591-595 (1977).
- 3 DeWitt, D. L. & Smith, W. L. Primary structure of prostaglandin G/H synthase from sheep vesicular gland determined from the complementary DNA sequence. *Proc Natl Acad Sci U S A* **85**, 1412-1416 (1988).
- 4 Rosen, G. D., Birkenmeier, T. M., Raz, A. & Holtzman, M. J. Identification of a cyclooxygenase-related gene and its potential role in prostaglandin formation. *Biochem Biophys Res Commun* **164**, 1358-1365 (1989).
- 5 Kujubu, D. A., Fletcher, B. S., Varnum, B. C., Lim, R. W. & Herschman, H. R. TIS10, a phorbol ester tumor promoter-inducible mRNA from Swiss 3T3 cells, encodes a novel prostaglandin synthase/cyclooxygenase homologue. *J Biol Chem* **266**, 12866-12872 (1991).
- 6 Tippetts, M. T., Varnum, B. C., Lim, R. W. & Herschman, H. R. Tumor promoter-inducible genes are differentially expressed in the developing mouse. *Mol Cell Biol* **8**, 4570-4572 (1988).
- 7 Xie, W. L., Chipman, J. G., Robertson, D. L., Erikson, R. L. & Simmons, D. L. Expression of a mitogen-responsive gene encoding prostaglandin synthase is regulated by mRNA splicing. *Proc Natl Acad Sci U S A* **88**, 2692-2696 (1991).
- 8 Hla, T. & Neilson, K. Human cyclooxygenase-2 cDNA. *Proc Natl Acad Sci U S A* **89**, 7384-7388 (1992).
- 9 Marnett, C. A. R. a. L. J. Vol. doi: 10.1194/jlr.R800042-JLR200 S29-34 (Journal of Lipid Research, 2009).
- 10 Botting, Y. S. B. a. R. M. Vol. 5 305-323 (Mediators of Inflammation, 1996).
- 11 Murakami, M. *et al.* Recent progress in phospholipase A(2) research: from cells to animals to humans. *Progress in lipid research* **50**, 152-192, doi:10.1016/j.plipres.2010.12.001 (2011).

- 12 de Beer, F. C., and Webb, N. R. Inflammation and atherosclerosis Group Ila and Group V sPLA(2) are not redundant. *Arterioscl Throm Vas* **26**, 1421-1422 (2006).
- 13 Burke, J. E. & Dennis, E. A. Phospholipase A2 structure/function, mechanism, and signaling. *J Lipid Res* **50 Suppl**, S237-242, doi:10.1194/jlr.R800033-JLR200 (2009).
- 14 Mitchell, J. A., Larkin, S. & Williams, T. J. Cyclooxygenase-2: regulation and relevance in inflammation. *Biochem Pharmacol* **50**, 1535-1542 (1995).
- 15 Moncada, S., Gryglewski, R., Bunting, S. & Vane, J. R. An enzyme isolated from arteries transforms prostaglandin endoperoxides to an unstable substance that inhibits platelet aggregation. *Nature* **263**, 663-665 (1976).
- 16 Moncada, S. Prostacyclin and arterial wall biology. *Arteriosclerosis* **2**, 193-207 (1982).
- 17 Douglas W. Kawkaa, M. O., Pierre-Olivier Hétab, Irwin I. Singera, Denis Riendeau. Double-label expression studies of prostacyclin synthase, thromboxane synthase and COX isoforms in normal aortic endothelium. *Biochimica et Biophysica Acta* **1771**, 45-54 (2007).
- 18 Bos, C. L. Vol. 36 (ed Tita Ritsema Dick J. Richel , Maikel P. Peppelenbosch , Henri H. Versteeg) 1187–1205 (The International Journal of Biochemistry & Cell Biology, 2004).
- 19 Moncada, S., Herman, A. G., Higgs, E. A. & Vane, J. R. Differential formation of prostacyclin (PGX or PGI₂) by layers of the arterial wall. An explanation for the anti-thrombotic properties of vascular endothelium. *Thromb Res* **11**, 323-344 (1977).
- 20 DeWitt, D. L. & Smith, W. L. Purification of prostacyclin synthase from bovine aorta by immunoaffinity chromatography. Evidence that the enzyme is a hemoprotein. *J Biol Chem* **258**, 3285-3293 (1983).
- 21 Wade, M. L., Voelkel, N. F. & Fitzpatrick, F. A. "Suicide" inactivation of prostaglandin I₂ synthase: characterization of mechanism-based inactivation with isolated enzyme and endothelial cells. *Arch Biochem Biophys* **321**, 453-458, doi:10.1006/abbi.1995.1417 (1995).
- 22 Mitchell, J. A., de Nucci, G., Warner, T. D. & Vane, J. R. Different patterns of release of endothelium-derived relaxing factor and prostacyclin. *Br J Pharmacol* **105**, 485-489 (1992).
- 23 Nakayama, T. Genetic polymorphisms of prostacyclin synthase gene and cardiovascular disease. *Int Angiol* **29**, 33-42 (2010).

- 24 Hamberg, M., Svensson, J. & Samuelsson, B. Thromboxanes: a new group of biologically active compounds derived from prostaglandin endoperoxides. *Proc Natl Acad Sci U S A* **72**, 2994-2998 (1975).
- 25 Smyth, E. M. Thromboxane and the thromboxane receptor in cardiovascular disease. *Clin Lipidol* **5**, 209-219, doi:10.2217/clp.10.11 (2010).
- 26 Piper, P. J. & Vane, J. R. Release of additional factors in anaphylaxis and its antagonism by anti-inflammatory drugs. *Nature* **223**, 29-35 (1969).
- 27 Chen, C. Y., Poole, E. M., Ulrich, C. M., Kulmacz, R. J. & Wang, L. H. Functional analysis of human thromboxane synthase polymorphic variants. *Pharmacogenet Genomics* **22**, 653-658, doi:10.1097/FPC.0b013e3283562d82 (2012).
- 28 Kimouli, M. *et al.* The effect of an exon 12 polymorphism of the human thromboxane synthase (CYP5A1) gene in stroke patients. *Med Sci Monit* **15**, BR30-35 (2009).
- 29 Park, J. Y., Pillinger, M. H. & Abramson, S. B. Prostaglandin E2 synthesis and secretion: the role of PGE2 synthases. *Clin Immunol* **119**, 229-240, doi:10.1016/j.clim.2006.01.016 (2006).
- 30 Jakobsson, P. J., Thoren, S., Morgenstern, R. & Samuelsson, B. Identification of human prostaglandin E synthase: a microsomal, glutathione-dependent, inducible enzyme, constituting a potential novel drug target. *Proc Natl Acad Sci U S A* **96**, 7220-7225 (1999).
- 31 Larsson, K. & Jakobsson, P. J. Inhibition of microsomal prostaglandin E synthase-1 as targeted therapy in cancer treatment. *Prostaglandins Other Lipid Mediat* **120**, 161-165, doi:10.1016/j.prostaglandins.2015.06.002 (2015).
- 32 Bahia, M. S., Katare, Y. K., Silakari, O., Vyas, B. & Silakari, P. Inhibitors of microsomal prostaglandin E2 synthase-1 enzyme as emerging anti-inflammatory candidates. *Med Res Rev* **34**, 825-855 (2014).
- 33 Korotkova, M. *et al.* Variants of gene for microsomal prostaglandin E2 synthase show association with disease and severe inflammation in rheumatoid arthritis. *Eur J Hum Genet* **19**, 908-914, doi:10.1038/ejhg.2011.50 (2011).
- 34 Watanabe, K., Kurihara, K. & Suzuki, T. Purification and characterization of membrane-bound prostaglandin E synthase from bovine heart. *Biochim Biophys Acta* **1439**, 406-414 (1999).

- 35 Tanikawa, N. *et al.* Identification and characterization of a novel type of membrane-associated prostaglandin E synthase. *Biochem Biophys Res Commun* **291**, 884-889, doi:10.1006/bbrc.2002.6531 (2002).
- 36 Jania, L. A. *et al.* Microsomal prostaglandin E synthase-2 is not essential for in vivo prostaglandin E2 biosynthesis. *Prostaglandins Other Lipid Mediat* **88**, 73-81, doi:10.1016/j.prostaglandins.2008.10.003 (2009).
- 37 Joo, M. & Sadikot, R. T. PGD synthase and PGD2 in immune response. *Mediators Inflamm* **2012**, 503128, doi:10.1155/2012/503128 (2012).
- 38 Narumiya, S. Physiology and pathophysiology of prostanoid receptors. *Proc Jpn Acad Ser B Phys Biol Sci* **83**, 296-319, doi:10.2183/pjab/83.296 (2007).
- 39 Dubois, R. N. *et al.* Cyclooxygenase in biology and disease. *FASEB J* **12**, 1063-1073 (1998).
- 40 Breyer, R. M. Prostaglandin EP(1) receptor subtype selectivity takes shape. *Mol Pharmacol* **59**, 1357-1359 (2001).
- 41 Mitchell, J. A. *et al.* Role of prostacyclin in pulmonary hypertension. *Glob Cardiol Sci Pract* **2014**, 382-393, doi:10.5339/gcsp.2014.53 (2014).
- 42 Lezoualc'h, F., Fazal, L., Laudette, M. & Conte, C. Cyclic AMP Sensor EPAC Proteins and Their Role in Cardiovascular Function and Disease. *Circ Res* **118**, 881-897, doi:10.1161/CIRCRESAHA.115.306529 (2016).
- 43 Lim, H. & Dey, S. K. A novel pathway of prostacyclin signaling-hanging out with nuclear receptors. *Endocrinology* **143**, 3207-3210, doi:10.1210/en.2002-220159 (2002).
- 44 Ali, F. Y., Hall, M. G., Desvergne, B., Warner, T. D. & Mitchell, J. A. PPARbeta/delta agonists modulate platelet function via a mechanism involving PPAR receptors and specific association/repression of PKCalpha--brief report. *Arterioscler Thromb Vasc Biol* **29**, 1871-1873, doi:10.1161/ATVBAHA.109.193367 (2009).
- 45 Ali, F. Y. *et al.* Role of nuclear receptor signaling in platelets: antithrombotic effects of PPARbeta. *FASEB J* **20**, 326-328, doi:10.1096/fj.05-4395fje (2006).
- 46 Hao, C. M., Redha, R., Morrow, J. & Breyer, M. D. Peroxisome proliferator-activated receptor delta activation promotes cell survival following hypertonic stress. *J Biol Chem* **277**, 21341-21345, doi:10.1074/jbc.M200695200 (2002).

- 47 Harrington, L. S. *et al.* The PPARbeta/delta agonist GW0742 relaxes pulmonary vessels and limits right heart hypertrophy in rats with hypoxia-induced pulmonary hypertension. *PLoS One* **5**, e9526, doi:10.1371/journal.pone.0009526 (2010).
- 48 Kojonazarov, B. *et al.* The peroxisome proliferator-activated receptor beta/delta agonist GW0742 has direct protective effects on right heart hypertrophy. *Pulm Circ* **3**, 926-935, doi:10.1086/674755 (2013).
- 49 Gupta, R. A. *et al.* Prostacyclin-mediated activation of peroxisome proliferator-activated receptor delta in colorectal cancer. *Proc Natl Acad Sci U S A* **97**, 13275-13280, doi:10.1073/pnas.97.24.13275 (2000).
- 50 Stitham, J., Stojanovic, A. & Hwa, J. Impaired receptor binding and activation associated with a human prostacyclin receptor polymorphism. *J Biol Chem* **277**, 15439-15444, doi:10.1074/jbc.M201187200 (2002).
- 51 Patrignani, P. *et al.* Differential association between human prostacyclin receptor polymorphisms and the development of venous thrombosis and intimal hyperplasia: a clinical biomarker study. *Pharmacogenet Genomics* **18**, 611-620, doi:10.1097/FPC.0b013e328301a774 (2008).
- 52 Hirata, M. *et al.* Cloning and expression of cDNA for a human thromboxane A2 receptor. *Nature* **349**, 617-620, doi:10.1038/349617a0 (1991).
- 53 Huang, J. S., Ramamurthy, S. K., Lin, X. & Le Breton, G. C. Cell signalling through thromboxane A2 receptors. *Cell Signal* **16**, 521-533 (2004).
- 54 Zhang, L., DiLizio, C., Kim, D., Smyth, E. M. & Manning, D. R. The G12 family of G proteins as a reporter of thromboxane A2 receptor activity. *Mol Pharmacol* **69**, 1433-1440, doi:10.1124/mol.105.019703 (2006).
- 55 Fontana, P. *et al.* Identification of functional polymorphisms of the thromboxane A2 receptor gene in healthy volunteers. *Thromb Haemost* **96**, 356-360, doi:10.1160/TH06-05-0288 (2006).
- 56 Pan, Y., Li, S., Xie, X. & Li, M. Association between thromboxane A2 receptor polymorphisms and asthma risk: a meta-analysis. *J Asthma*, 1-7, doi:10.3109/02770903.2015.1126849 (2016).
- 57 Shao, J. *et al.* Thromboxane A2 receptor polymorphism in association with cerebral infarction and its regulation on platelet function. *Curr Neurovasc Res* **12**, 15-24 (2015).

- 58 Reader, J., Holt, D. & Fulton, A. Prostaglandin E2 EP receptors as therapeutic targets in breast cancer. *Cancer Metastasis Rev* **30**, 449-463, doi:10.1007/s10555-011-9303-2 (2011).
- 59 McCullough, L. *et al.* Neuroprotective function of the PGE2 EP2 receptor in cerebral ischemia. *J Neurosci* **24**, 257-268, doi:10.1523/JNEUROSCI.4485-03.2004 (2004).
- 60 Xiao, C. Y. *et al.* Prostaglandin E2 protects the heart from ischemia-reperfusion injury via its receptor subtype EP4. *Circulation* **109**, 2462-2468, doi:10.1161/01.CIR.0000128046.54681.97 (2004).
- 61 Nakanishi, M. & Rosenberg, D. W. Multifaceted roles of PGE2 in inflammation and cancer. *Semin Immunopathol* **35**, 123-137, doi:10.1007/s00281-012-0342-8 (2013).
- 62 Zhang, J., Gong, Y. & Yu, Y. PG F(2alpha) Receptor: A Promising Therapeutic Target for Cardiovascular Disease. *Front Pharmacol* **1**, 116, doi:10.3389/fphar.2010.00116 (2010).
- 63 Hall, I. P. *et al.* Efficacy of BI 671800, an oral CRTH2 antagonist, in poorly controlled asthma as sole controller and in the presence of inhaled corticosteroid treatment. *Pulm Pharmacol Ther* **32**, 37-44, doi:10.1016/j.pupt.2015.03.003 (2015).
- 64 Vane, J. R. Inhibition of prostaglandin synthesis as a mechanism of action for aspirin-like drugs. *Nat New Biol* **231**, 232-235 (1971).
- 65 Jeremiah Stitham, C. M., Kathleen A. Martin and John Hwa. Vol. 2 1-8 (Frontiers in Pharmacology, 2011).
- 66 FitzGerald, E. R. a. G. A. Vol. 31 986-1000 (Arterioscler Thromb Vasc Biol., 2011).
- 67 Williams, T. J. & Morley, J. Prostaglandins as potentiators of increased vascular permeability in inflammation. *Nature* **246**, 215-217 (1973).
- 68 Chen, L., Yang, G. & Grosser, T. Prostanoids and inflammatory pain. *Prostaglandins Other Lipid Mediat* **104-105**, 58-66, doi:10.1016/j.prostaglandins.2012.08.006 (2013).
- 69 Kirkby, N. S. *et al.* Differential COX-2 induction by viral and bacterial PAMPs: Consequences for cytokine and interferon responses and implications for anti-viral COX-2 directed therapies. *Biochem Biophys Res Commun* **438**, 249-256, doi:10.1016/j.bbrc.2013.07.006 (2013).
- 70 Gilroy, D. W., Lawrence, T., Perretti, M. & Rossi, A. G. Inflammatory resolution: new opportunities for drug discovery. *Nat Rev Drug Discov* **3**, 401-416, doi:10.1038/nrd1383 (2004).

- 71 Dorris, S. L. & Peebles, R. S., Jr. PGI₂ as a regulator of inflammatory diseases. *Mediators Inflamm* **2012**, 926968, doi:10.1155/2012/926968 (2012).
- 72 Wallace, J. L., McKnight, W., Reuter, B. K. & Vergnolle, N. NSAID-induced gastric damage in rats: requirement for inhibition of both cyclooxygenase 1 and 2. *Gastroenterology* **119**, 706-714 (2000).
- 73 Drew, D. A., Cao, Y. & Chan, A. T. Aspirin and colorectal cancer: the promise of precision chemoprevention. *Nat Rev Cancer* **16**, 173-186, doi:10.1038/nrc.2016.4 (2016).
- 74 Wang, D. & Dubois, R. N. The role of COX-2 in intestinal inflammation and colorectal cancer. *Oncogene* **29**, 781-788, doi:10.1038/onc.2009.421 (2010).
- 75 Hao, C. M. & Breyer, M. D. Physiological regulation of prostaglandins in the kidney. *Annu Rev Physiol* **70**, 357-377, doi:10.1146/annurev.physiol.70.113006.100614 (2008).
- 76 Kirkby, N. S. *et al.* Systematic study of constitutive cyclooxygenase-2 expression: Role of NF-kappaB and NFAT transcriptional pathways. *Proc Natl Acad Sci U S A* **113**, 434-439, doi:10.1073/pnas.1517642113 (2016).
- 77 Harris, R. C. *et al.* Cyclooxygenase-2 is associated with the macula densa of rat kidney and increases with salt restriction. *J Clin Invest* **94**, 2504-2510, doi:10.1172/JCI117620 (1994).
- 78 Cheng, H. F. *et al.* Genetic deletion of COX-2 prevents increased renin expression in response to ACE inhibition. *Am J Physiol Renal Physiol* **280**, F449-456 (2001).
- 79 Kirkby, N. S. *et al.* Cyclooxygenase-1, not cyclooxygenase-2, is responsible for physiological production of prostacyclin in the cardiovascular system. *Proc Natl Acad Sci U S A* **109**, 17597-17602, doi:10.1073/pnas.1209192109 (2012).
- 80 Yu, Y. *et al.* Vascular COX-2 modulates blood pressure and thrombosis in mice. *Sci Transl Med* **4**, 132ra154, doi:10.1126/scitranslmed.3003787 (2012).
- 81 Mitchell, J. A. & Warner, T. D. COX isoforms in the cardiovascular system: understanding the activities of non-steroidal anti-inflammatory drugs. *Nat Rev Drug Discov* **5**, 75-86, doi:10.1038/nrd1929 (2006).
- 82 Kirkby, N. S. *et al.* COX-2 protects against atherosclerosis independently of local vascular prostacyclin: identification of COX-2 associated pathways implicate Rgl1 and

- lymphocyte networks. *PLoS One* **9**, e98165, doi:10.1371/journal.pone.0098165 (2014).
- 83 Kirkby, N. S. *et al.* Aspirin-triggered 15-epi-lipoxin A4 predicts cyclooxygenase-2 in the lungs of LPS-treated mice but not in the circulation: implications for a clinical test. *FASEB J* **27**, 3938-3946, doi:10.1096/fj.12-215533 (2013).
- 84 Turker, R. K. Evidence for a prostacyclin-mediated chronotropic effect of angiotensin II in the isolated cat right atria. *Eur J Pharmacol* **83**, 271-275 (1982).
- 85 Harding, P. & Murray, D. B. The contribution of prostaglandins versus prostacyclin in ventricular remodeling during heart failure. *Life Sci* **89**, 671-676, doi:10.1016/j.lfs.2011.07.025 (2011).
- 86 Hohlfeld, T., Zucker, T. P., Meyer, J. & Schror, K. Expression, function, and regulation of E-type prostaglandin receptors (EP3) in the nonischemic and ischemic pig heart. *Circ Res* **81**, 765-773 (1997).
- 87 Harding, P. *et al.* Gene expression profiling of dilated cardiomyopathy in older male EP4 knockout mice. *Am J Physiol Heart Circ Physiol* **298**, H623-632, doi:10.1152/ajpheart.00746.2009 (2010).
- 88 Hishikari, K. *et al.* Pharmacological activation of the prostaglandin E2 receptor EP4 improves cardiac function after myocardial ischaemia/reperfusion injury. *Cardiovasc Res* **81**, 123-132, doi:10.1093/cvr/cvn254 (2009).
- 89 Mitchell, J. A., Akarasereenont, P., Thiemermann, C., Flower, R. J. & Vane, J. R. Selectivity of nonsteroidal antiinflammatory drugs as inhibitors of constitutive and inducible cyclooxygenase. *Proc Natl Acad Sci U S A* **90**, 11693-11697 (1993).
- 90 Peura, D. A. & Goldkind, L. Balancing the gastrointestinal benefits and risks of nonselective NSAIDs. *Arthritis Res Ther* **7 Suppl 4**, S7-13, doi:10.1186/ar1793 (2005).
- 91 Giovannucci, E. *et al.* Aspirin and the risk of colorectal cancer in women. *N Engl J Med* **333**, 609-614, doi:10.1056/NEJM199509073331001 (1995).
- 92 Cook, N. R. *et al.* Low-dose aspirin in the primary prevention of cancer: the Women's Health Study: a randomized controlled trial. *JAMA* **294**, 47-55, doi:10.1001/jama.294.1.47 (2005).
- 93 Sturmer, T. *et al.* Aspirin use and colorectal cancer: post-trial follow-up data from the Physicians' Health Study. *Ann Intern Med* **128**, 713-720 (1998).

- 94 Langley, R. E. Clinical evidence for the use of aspirin in the treatment of cancer. *Ecancermedicalscience* **7**, 297, doi:10.3332/ecancer.2013.297 (2013).
- 95 Rothwell, P. M. *et al.* Short-term effects of daily aspirin on cancer incidence, mortality, and non-vascular death: analysis of the time course of risks and benefits in 51 randomised controlled trials. *Lancet* **379**, 1602-1612, doi:10.1016/S0140-6736(11)61720-0 (2012).
- 96 Cao, Y. *et al.* Population-wide Impact of Long-term Use of Aspirin and the Risk for Cancer. *JAMA Oncol* **2**, 762-769, doi:10.1001/jamaoncol.2015.6396 (2016).
- 97 Thun, M. J., Jacobs, E. J. & Patrono, C. The role of aspirin in cancer prevention. *Nat Rev Clin Oncol* **9**, 259-267, doi:10.1038/nrclinonc.2011.199 (2012).
- 98 Eberhart, C. E. *et al.* Up-regulation of cyclooxygenase 2 gene expression in human colorectal adenomas and adenocarcinomas. *Gastroenterology* **107**, 1183-1188 (1994).
- 99 Tsujii, M. *et al.* Cyclooxygenase regulates angiogenesis induced by colon cancer cells. *Cell* **93**, 705-716 (1998).
- 100 Dona, I. *et al.* Trends in hypersensitivity drug reactions: more drugs, more response patterns, more heterogeneity. *J Investig Allergol Clin Immunol* **24**, 143-153; quiz 141 p following 153 (2014).
- 101 Martin-Garcia, C. *et al.* Celecoxib, a highly selective COX-2 inhibitor, is safe in aspirin-induced asthma patients. *J Investig Allergol Clin Immunol* **13**, 20-25 (2003).
- 102 Scheiman, J. M. NSAID-induced Gastrointestinal Injury: A Focused Update for Clinicians. *J Clin Gastroenterol* **50**, 5-10, doi:10.1097/MCG.0000000000000432 (2016).
- 103 Antman, E. M. *et al.* Use of nonsteroidal antiinflammatory drugs: an update for clinicians: a scientific statement from the American Heart Association. *Circulation* **115**, 1634-1642, doi:10.1161/CIRCULATIONAHA.106.181424 (2007).
- 104 Coxib *et al.* Vascular and upper gastrointestinal effects of non-steroidal anti-inflammatory drugs: meta-analyses of individual participant data from randomised trials. *Lancet* **382**, 769-779, doi:10.1016/S0140-6736(13)60900-9 (2013).
- 105 Lanza, F. L., Chan, F. K., Quigley, E. M. & Practice Parameters Committee of the American College of, G. Guidelines for prevention of NSAID-related ulcer complications. *Am J Gastroenterol* **104**, 728-738, doi:10.1038/ajg.2009.115 (2009).

- 106 Shah, N. H. *et al.* Proton Pump Inhibitor Usage and the Risk of Myocardial Infarction in the General Population. *PLoS One* **10**, e0124653, doi:10.1371/journal.pone.0124653 (2015).
- 107 Washio, E. *et al.* Proton Pump Inhibitors Increase Incidence of Nonsteroidal Anti-Inflammatory Drug-Induced Small Bowel Injury: A Randomized, Placebo-Controlled Trial. *Clin Gastroenterol Hepatol* **14**, 809-815 e801, doi:10.1016/j.cgh.2015.10.022 (2016).
- 108 Bombardier, C. *et al.* Comparison of upper gastrointestinal toxicity of rofecoxib and naproxen in patients with rheumatoid arthritis. VIGOR Study Group. *N Engl J Med* **343**, 1520-1528, 1522 p following 1528, doi:10.1056/NEJM200011233432103 (2000).
- 109 Silverstein, F. E. *et al.* Gastrointestinal toxicity with celecoxib vs nonsteroidal anti-inflammatory drugs for osteoarthritis and rheumatoid arthritis: the CLASS study: A randomized controlled trial. Celecoxib Long-term Arthritis Safety Study. *JAMA* **284**, 1247-1255 (2000).
- 110 McAdam, B. F. *et al.* Systemic biosynthesis of prostacyclin by cyclooxygenase (COX)-2: the human pharmacology of a selective inhibitor of COX-2. *Proc Natl Acad Sci U S A* **96**, 272-277 (1999).
- 111 Bresalier, R. S. *et al.* Cardiovascular events associated with rofecoxib in a colorectal adenoma chemoprevention trial. *N Engl J Med* **352**, 1092-1102, doi:10.1056/NEJMoa050493 (2005).
- 112 Sibbald, B. Rofecoxib (Vioxx) voluntarily withdrawn from market. *CMAJ* **171**, 1027-1028, doi:10.1503/cmaj.1041606 (2004).
- 113 Grosser, T., Fries, S. & FitzGerald, G. A. Biological basis for the cardiovascular consequences of COX-2 inhibition: therapeutic challenges and opportunities. *J Clin Invest* **116**, 4-15, doi:10.1172/JCI27291 (2006).
- 114 Johnson, A. G. NSAIDs and increased blood pressure. What is the clinical significance? *Drug Saf* **17**, 277-289 (1997).
- 115 Aneja, A. & Farkouh, M. E. Adverse cardiovascular effects of NSAIDs: driven by blood pressure, or edema? *Ther Adv Cardiovasc Dis* **2**, 53-66, doi:10.1177/1753944707088184 (2008).
- 116 Furchgott, R. F. & Zawadzki, J. V. The obligatory role of endothelial cells in the relaxation of arterial smooth muscle by acetylcholine. *Nature* **288**, 373-376 (1980).

- 117 Palmer, R. M., Ferrige, A. G. & Moncada, S. Nitric oxide release accounts for the biological activity of endothelium-derived relaxing factor. *Nature* **327**, 524-526, doi:10.1038/327524a0 (1987).
- 118 Koshland, D. E., Jr. The molecule of the year. *Science* **258**, 1861 (1992).
- 119 Palmer, R. M., Ashton, D. S. & Moncada, S. Vascular endothelial cells synthesize nitric oxide from L-arginine. *Nature* **333**, 664-666, doi:10.1038/333664a0 (1988).
- 120 Pollock, J. S. *et al.* Purification and characterization of particulate endothelium-derived relaxing factor synthase from cultured and native bovine aortic endothelial cells. *Proc Natl Acad Sci U S A* **88**, 10480-10484 (1991).
- 121 Gross, S. S. & Wolin, M. S. Nitric oxide: pathophysiological mechanisms. *Annu Rev Physiol* **57**, 737-769, doi:10.1146/annurev.ph.57.030195.003513 (1995).
- 122 Bredt, D. S. & Snyder, S. H. Isolation of nitric oxide synthetase, a calmodulin-requiring enzyme. *Proc Natl Acad Sci U S A* **87**, 682-685 (1990).
- 123 Stuehr, D. J., Cho, H. J., Kwon, N. S., Weise, M. F. & Nathan, C. F. Purification and characterization of the cytokine-induced macrophage nitric oxide synthase: an FAD- and FMN-containing flavoprotein. *Proc Natl Acad Sci U S A* **88**, 7773-7777 (1991).
- 124 Vallance, P., Leone, A., Calver, A., Collier, J. & Moncada, S. Accumulation of an endogenous inhibitor of nitric oxide synthesis in chronic renal failure. *Lancet* **339**, 572-575 (1992).
- 125 Boger, R. H., Maas, R., Schulze, F. & Schwedhelm, E. Asymmetric dimethylarginine (ADMA) as a prospective marker of cardiovascular disease and mortality--an update on patient populations with a wide range of cardiovascular risk. *Pharmacol Res* **60**, 481-487, doi:10.1016/j.phrs.2009.07.001 (2009).
- 126 Boger, R. H. *et al.* Plasma asymmetric dimethylarginine and incidence of cardiovascular disease and death in the community. *Circulation* **119**, 1592-1600, doi:10.1161/CIRCULATIONAHA.108.838268 (2009).
- 127 McDermott, J. R. Studies on the catabolism of Ng-methylarginine, Ng, Ng-dimethylarginine and Ng, Ng-dimethylarginine in the rabbit. *Biochem J* **154**, 179-184 (1976).
- 128 Ogawa, T., Kimoto, M. & Sasaoka, K. Purification and properties of a new enzyme, NG,NG-dimethylarginine dimethylaminohydrolase, from rat kidney. *J Biol Chem* **264**, 10205-10209 (1989).

- 129 Leiper, J. & Nandi, M. The therapeutic potential of targeting endogenous inhibitors of nitric oxide synthesis. *Nat Rev Drug Discov* **10**, 277-291, doi:10.1038/nrd3358 (2011).
- 130 Lambden, S. *et al.* Dimethylarginine dimethylaminohydrolase 2 regulates nitric oxide synthesis and hemodynamics and determines outcome in polymicrobial sepsis. *Arterioscler Thromb Vasc Biol* **35**, 1382-1392, doi:10.1161/ATVBAHA.115.305278 (2015).
- 131 Leiper, J. *et al.* Disruption of methylarginine metabolism impairs vascular homeostasis. *Nat Med* **13**, 198-203, doi:10.1038/nm1543 (2007).
- 132 Rodionov, R. N., Jarzebska, N., Weiss, N. & Lentz, S. R. AGXT2: a promiscuous aminotransferase. *Trends Pharmacol Sci* **35**, 575-582, doi:10.1016/j.tips.2014.09.005 (2014).
- 133 Takada, Y. & Noguchi, T. Subcellular distribution, and physical and immunological properties of hepatic alanine: glyoxylate aminotransferase isoenzymes in different mammalian species. *Comp Biochem Physiol B* **72**, 597-604 (1982).
- 134 Langenbach, R. *et al.* Prostaglandin synthase 1 gene disruption in mice reduces arachidonic acid-induced inflammation and indomethacin-induced gastric ulceration. *Cell* **83**, 483-492 (1995).
- 135 Morham, S. G. *et al.* Prostaglandin synthase 2 gene disruption causes severe renal pathology in the mouse. *Cell* **83**, 473-482 (1995).
- 136 Nusing, R. M. *et al.* Dominant role of prostaglandin E2 EP4 receptor in furosemide-induced salt-losing tubulopathy: a model for hyperprostaglandin E syndrome/antenatal Bartter syndrome. *J Am Soc Nephrol* **16**, 2354-2362, doi:10.1681/ASN.2004070556 (2005).
- 137 Murata, T. *et al.* Altered pain perception and inflammatory response in mice lacking prostacyclin receptor. *Nature* **388**, 678-682, doi:10.1038/41780 (1997).
- 138 Reddy, S. T., Tiano, H. F., Langenbach, R., Morham, S. G. & Herschman, H. R. Genetic evidence for distinct roles of COX-1 and COX-2 in the immediate and delayed phases of prostaglandin synthesis in mast cells. *Biochem Biophys Res Commun* **265**, 205-210, doi:S0006-291X(99)91658-3 10.1006/bbrc.1999.1658 (1999).
- 139 DeWitt, D. L., Day, J. S., Sonnenburg, W. K. & Smith, W. L. Concentrations of prostaglandin endoperoxide synthase and prostaglandin I2 synthase in the

- endothelium and smooth muscle of bovine aorta. *J Clin Invest* **72**, 1882-1888, doi:10.1172/JCI111151 (1983).
- 140 Morham, S. G. *et al.* Prostaglandin synthase 2 gene disruption causes severe renal pathology in the mouse. *Cell* **83**, 473-482, doi:0092-8674(95)90125-6 [pii] (1995).
- 141 O'Banion, M. K., Winn, V. D. & Young, D. A. cDNA cloning and functional activity of a glucocorticoid-regulated inflammatory cyclooxygenase. *Proc Natl Acad Sci U S A* **89**, 4888-4892 (1992).
- 142 Namba, T. *et al.* cDNA cloning of a mouse prostacyclin receptor. Multiple signaling pathways and expression in thymic medulla. *J Biol Chem* **269**, 9986-9992 (1994).
- 143 Robards AW, W. A. Procedures in Electron Microscopy. *John Wiley and Sons.Ltd.* **11**, 2-4 (1992).
- 144 Masoodi, M. & Nicolaou, A. Lipidomic analysis of twenty-seven prostanoids and isoprostanes by liquid chromatography/electrospray tandem mass spectrometry. *Rapid Commun Mass Spectrom* **20**, 3023-3029, doi:10.1002/rcm.2697 (2006).
- 145 Reed, D. M. *et al.* in *The Twelfth International Conference on Endothelin* (pA2 online, Cambridge, UK, 2011).
- 146 Starke, R. D. *et al.* Endothelial von Willebrand factor regulates angiogenesis. *Blood*, doi:doi: 10.1182/blood-2010-01-264507 (2010).
- 147 Ingram, D. A. *et al.* Identification of a novel hierarchy of endothelial progenitor cells using human peripheral and umbilical cord blood. *Blood* **104**, 2752-2760, doi:10.1182/blood-2004-04-1396 (2004).
- 148 Martin-Ramirez, J., Hofman, M., van den Biggelaar, M., Hebbel, R. P. & Voorberg, J. Establishment of outgrowth endothelial cells from peripheral blood. *Nat Protoc* **7**, 1709-1715, doi:10.1038/nprot.2012.093 (2012).
- 149 Ricciotti, E., Yu, Y., Grosser, T. & Fitzgerald, G. A. COX-2, the dominant source of prostacyclin. *Proc Natl Acad Sci U S A* **110**, E183, doi:10.1073/pnas.1219073110 (2013).
- 150 Masferrer, J. L., Koki, A. & Seibert, K. COX-2 inhibitors. A new class of antiangiogenic agents. *Ann N Y Acad Sci* **889**, 84-86 (1999).
- 151 Leahy, K. M. *et al.* Cyclooxygenase-2 inhibition by celecoxib reduces proliferation and induces apoptosis in angiogenic endothelial cells in vivo. *Cancer Res* **62**, 625-631 (2002).

- 152 Patrono, C. Cardiovascular Effects of Cyclooxygenase-2 Inhibitors: A Mechanistic and Clinical Perspective. *British journal of clinical pharmacology*, doi:10.1111/bcp.13048 (2016).
- 153 Kirkby, N. S. *et al.* LC-MS/MS confirms that COX-1 drives vascular prostacyclin whilst gene expression pattern reveals non-vascular sites of COX-2 expression. *PLoS One* **8**, e69524, doi:10.1371/journal.pone.0069524 (2013).
- 154 Khan, K. N., Paulson, S. K., Verburg, K. M., Lefkowitz, J. B. & Maziasz, T. J. Pharmacology of cyclooxygenase-2 inhibition in the kidney. *Kidney Int* **61**, 1210-1219, doi:10.1046/j.1523-1755.2002.00263.x (2002).
- 155 Swierkosz, T. A., Mitchell, J. A., Sessa, W. C., Hecker, M. & Vane, J. R. L-glutamine inhibits the release of endothelium-derived relaxing factor from the rabbit aorta. *Biochem Biophys Res Commun* **172**, 143-148 (1990).
- 156 Recklinghausen., V. D. v. Eine Methode, mikroskopische hohle und solide Gebilde von einander zu unterscheiden. (1860).
- 157 His, W. *Die Häute und Höhlen des Körpers: Akademisches Programm.* (Basel, 1865).
- 158 Aird, W. C. Phenotypic Heterogeneity of the Endothelium: I. Structure, Function, and Mechanisms. *Circ Res* **100**, 158-173 (2007).
- 159 Heidenhain, V. R. Versuche und Fragen zur Lehre von der Lymphbildung. *Pflügers Archiv European Journal of Physiology* **49**, 209-301 (1891).
- 160 Douglas B. Cines, E. S. P., Clayton A. Buck, Joseph Loscalzo, Guy A. Zimmerman,, Rodger P. McEver, J. S. P., Timothy M. Wick, Barbara A. Konkle, Bradford S. Schwartz, & Elliot S. Barnathan, K. R. M., Bruce A. Hug, Ann-Marie Schmidt, and David M. Stern. Endothelial Cells in Physiology and in the Pathophysiology of Vascular Disorders. *The Journal of The American Society of Hematology* **91**, 3527-3561 (1998).
- 161 Starling, E. H. On the Absorption of Fluids from the Connective Tissue Spaces. *J Physiol* **19**, 312-326 (1896).
- 162 Jaffe EA, N. R., Becker CG, Minick CR. Culture of human endothelial cells derived from umbilical veins: Identification by morphologic criteria. *J Clin Invest* **52**, 12 (1973).
- 163 G., P. Fine structure of blood capillaries. *J Appl Physiol* **24**, 1424-1428 (1953).
- 164 Gowans, J. L. The recirculation of lymphocytes from blood to lymph in the rat. *J Physiol* **146**, 54-69 (1959).

- 165 Jaffe, E. A., Nachman, R. L., Becker, C. G. & Minick, C. R. Culture of human endothelial cells derived from umbilical veins. Identification by morphologic and immunologic criteria. *J Clin Invest* **52**, 2745-2756, doi:10.1172/JCI107470 (1973).
- 166 Lewis LJ, H. J., Maca RD, Fry GL. Replication of human endothelial cells in culture. *Science* **181**, 453 (1973).
- 167 Jaffe, R. L. N. a. E. A. Endothelial cell culture: beginnings of modern vascular biology. *The Journal of Clinical Investigation* **114**, 1037–1040 (2004).
- 168 P. M. Vanhoutte, H. S., E. H. C. Tang and M. Feletou. Endothelial dysfunction and vascular disease. *Acta Physiol* **196**, 193–222 (2009).
- 169 Alexander, K. K. G. A. R. W. Endothelial control of the cardiovascular system: recent advances. *The FASEB Journal* **10**, 283-292 (1996).
- 170 Harrison, H. C. a. D. G. Endothelial Dysfunction in Cardiovascular Diseases: The Role of Oxidant Stress. *Circ Res* **87**, 840-844 (2000).
- 171 M Hanson, P. G. Endothelial dysfunction and cardiovascular disease: the role of predictive adaptive responses. *Heart* **91**, 864-866 (2005).
- 172 Kibria G, H. D., Smith P, Biggar R. Pulmonary endothelial pavement patterns. *Thorax*. **35**, 186 –191 (1980).
- 173 J. Fredrick Cornhill, M. J. L., Edward E. Herderick, Robert M Nerem, James W. Kilman and John S. Vasko. Quantitative Study Of The Rabbit Aortic Endothelium Using Vascular Casts. *Atherosclerosis* **35**, 321-337 (1980).
- 174 Potter CMF, S. S., Lundberg MH, Weinberg PD, Mitchell JA, et al. Shape and Compliance of Endothelial Cells after Shear Stress In Vitro or from Different Aortic Regions: Scanning Ion Conductance Microscopy Study. *PLoS ONE* **7**, e31228 (2012).
- 175 R. C. BUCK, M. D. The Fine Structure of Endothelium of Large Arteries. *THE JOURNAL OF BIOPHYSICAL AND BIOCHEMICAL CYTOLOGY* **4** (1957).
- 176 M. K. KEECH. Electron Microscope Study of the Normal Rat Aorta. *J. BIOPHYSIC. AND BIOCHEM, CYTOL* **7**, 533-538 (1959).
- 177 Pappas, G. D. & Tennyson, V. M. An electron microscopic study of the passage of colloidal particles from the blood vessels of the ciliary processes and choroid plexus of the rabbit. *J Cell Biol* **15**, 227-239 (1962).
- 178 Silkworth, J. B., McLean, B. & Stehbens, W. E. The effect of hypercholesterolemia on aortic endothelium studied en face. *Atherosclerosis* **22**, 335-348 (1975).

- 179 Goode, T. B., Davies, P. F., Reidy, M. A. & Bowyer, D. E. Aortic endothelial cell morphology observed in situ by scanning electron microscopy during atherogenesis in the rabbit. *Atherosclerosis* **27**, 235-251 (1977).
- 180 Booyse, F. M., Feder, S. & Quarfoot, A. J. Culture-produced subendothelium. II. Effect of plasma, F.VIII:WF and fibronectin on interaction of normal platelets with normal and von Willebrand porcine aortic subendothelium. *Thromb Res* **28**, 299-311 (1982).
- 181 Iiyama K, H. L., Iiyama M, Li H, DiChiara M, Medoff BD, Cybulsky MI. Patterns of vascular cell adhesion molecule-1 and intercellular adhesion molecule-1 expression in rabbit and mouse atherosclerotic lesions and at sites predisposed to lesion formation. *Circulation Research*, 199-207 (1999).
- 182 Leena Hajra, A. I. E., Mian Chen, Sharon J. Hyduk, Tucker Collins, and Myron I. Cybulsky. The NF- κ B signal transduction pathway in aortic endothelial cells is primed for activation in regions predisposed to atherosclerotic lesion formation. *PNAS* **97**, 9052-9057 (2000).
- 183 Sandrine De Seranno, C. E., Anne Loyens, Anda Cornea, Sergio R. Ojeda, Jean-Claude Beauvillain, and V. Prevot. Vascular Endothelial Cells Promote Acute Plasticity in Ependymogial Cells of the Neuroendocrine Brain. *The Journal of Neuroscience*, **24**, 10353–10363 (2004).
- 184 AP, F. Endothelium: A distributed organ of diverse capabilities. *Ann NY Acad Sci* **401**, 8 (1982).
- 185 Bunday, R. A. Endothelial cell mechanosensitivity. Focus on “Cyclic strain and motion control produce opposite oxidative responses in two human endothelial cell types”. *Am J Physiol Cell Physiol* **293**, C33-C34 (2007).
- 186 Paul A. VanderLaan, C. A. R., Godfrey S. Getz. Site Specificity of Atherosclerosis: Site-Selective Responses to Atherosclerotic Modulators. *Arterioscler Thromb Vasc Biol* **24**, 12-22 (2004).
- 187 Claire M.F. Potter, M. H. L., Louise S. Harrington, Christina M. Warboys, Timothy D. Warner, R. Eric Berson, Alexey V. Moshkov, Julia Gorelik, Peter D. Weinberg and Jane A. Mitchell. Role of Shear Stress in Endothelial Cell Morphology and Expression of Cyclooxygenase Isoforms. *Arterioscler Thromb Vasc Biol* **31**, 384-391 (2011).

- 188 CHIEN, J.-J. C. A. S. Effects of Disturbed Flow on Vascular Endothelium: Pathophysiological Basis and Clinical Perspectives. *Physiol Rev* **91**, 327–387 (2011).
- 189 Jenny Jongstra-Bilen, M. H., Su-Ning Zhu, Mian Chen, Daipayan Guha, and Myron I. Cybulsky. Low-grade chronic inflammation in regions of the normal mouse arterial intima predisposed to atherosclerosis. *J Exp Med* **203**, 2073–2083 (2006).
- 190 Hahn, C. & Schwartz, M. A. Mechanotransduction in vascular physiology and atherogenesis. *Nat Rev Mol Cell Biol* **10**, 53–62, doi:10.1038/nrm2596 (2009).
- 191 Suo, J. *et al.* Hemodynamic shear stresses in mouse aortas: implications for atherogenesis. *Arteriosclerosis, thrombosis, and vascular biology* **27**, 346–351, doi:10.1161/01.ATV.0000253492.45717.46 (2007).
- 192 Iiyama, K. *et al.* Patterns of vascular cell adhesion molecule-1 and intercellular adhesion molecule-1 expression in rabbit and mouse atherosclerotic lesions and at sites predisposed to lesion formation. *Circulation research* **85**, 199–207 (1999).
- 193 Hajra, L. *et al.* The NF-kappa B signal transduction pathway in aortic endothelial cells is primed for activation in regions predisposed to atherosclerotic lesion formation. *Proc Natl Acad Sci U S A* **97**, 9052–9057, doi:10.1073/pnas.97.16.9052 (2000).
- 194 Potter, C. M. *et al.* Role of shear stress in endothelial cell morphology and expression of cyclooxygenase isoforms. *Arteriosclerosis, thrombosis, and vascular biology* **31**, 384–391, doi:10.1161/ATVBAHA.110.214031 (2011).
- 195 Potter, C. M. *et al.* Shape and compliance of endothelial cells after shear stress in vitro or from different aortic regions: scanning ion conductance microscopy study. *PLoS one* **7**, e31228, doi:10.1371/journal.pone.0031228 (2012).
- 196 Weinberg, P. D. & Ross Ethier, C. Twenty-fold difference in hemodynamic wall shear stress between murine and human aortas. *J Biomech* **40**, 1594–1598, doi:10.1016/j.jbiomech.2006.07.020 (2007).
- 197 Glagov, S., Zarins, C., Giddens, D. P. & Ku, D. N. Hemodynamics and atherosclerosis. Insights and perspectives gained from studies of human arteries. *Arch Pathol Lab Med* **112**, 1018–1031 (1988).
- 198 Davies, P. F. Hemodynamic shear stress and the endothelium in cardiovascular pathophysiology. *Nat Clin Pract Cardiovasc Med* **6**, 16–26, doi:10.1038/ncpcardio1397 (2009).

- 199 Caro, C. G. Discovery of the role of wall shear in atherosclerosis. *Arteriosclerosis, thrombosis, and vascular biology* **29**, 158-161, doi:10.1161/ATVBAHA.108.166736 (2009).
- 200 Ali, F. *et al.* Induction of the cytoprotective enzyme heme oxygenase-1 by statins is enhanced in vascular endothelium exposed to laminar shear stress and impaired by disturbed flow. *J Biol Chem* **284**, 18882-18892, doi:10.1074/jbc.M109.009886 (2009).
- 201 Zakkar, M. *et al.* Increased endothelial mitogen-activated protein kinase phosphatase-1 expression suppresses proinflammatory activation at sites that are resistant to atherosclerosis. *Circulation research* **103**, 726-732 (2008).
- 202 Jongstra-Bilen, J. *et al.* Low-grade chronic inflammation in regions of the normal mouse arterial intima predisposed to atherosclerosis. *J Exp Med* **203**, 2073-2083, doi:10.1084/jem.20060245 (2006).
- 203 Won, D. *et al.* Relative reduction of endothelial nitric-oxide synthase expression and transcription in atherosclerosis-prone regions of the mouse aorta and in an in vitro model of disturbed flow. *Am J Pathol* **171**, 1691-1704, doi:10.2353/ajpath.2007.060860 (2007).
- 204 Haidari, M. *et al.* Increased oxidative stress in atherosclerosis-predisposed regions of the mouse aorta. *Life sciences* **87**, 100-110, doi:10.1016/j.lfs.2010.05.016 (2010).
- 205 Potter, C. M. *et al.* Role of shear stress in endothelial cell morphology and expression of cyclooxygenase isoforms. *Arterioscler Thromb Vasc Biol* **31**, 384-391, doi:10.1161/ATVBAHA.110.214031 (2011).
- 206 Paschalaki, K. E. *et al.* A3907 (*American Journal of Respiratory and Critical Care Medicine*).
- 207 Starke, R. D. *et al.* Cellular and molecular basis of von Willebrand disease: studies on blood outgrowth endothelial cells. *Blood* **121**, 2773-2784, doi:10.1182/blood-2012-06-435727 (2013).
- 208 Warboys, C. M., Eric Berson, R., Mann, G. E., Pearson, J. D. & Weinberg, P. D. Acute and chronic exposure to shear stress have opposite effects on endothelial permeability to macromolecules. *Am J Physiol Heart Circ Physiol* **298**, H1850-1856, doi:10.1152/ajpheart.00114.2010 (2010).
- 209 Perini, R., Fiorucci, S. & Wallace, J. L. Mechanisms of nonsteroidal anti-inflammatory drug-induced gastrointestinal injury and repair: a window of opportunity for

- cyclooxygenase-inhibiting nitric oxide donors. *Can J Gastroenterol* **18**, 229-236 (2004).
- 210 Singh, G. *et al.* Consequences of increased systolic blood pressure in patients with osteoarthritis and rheumatoid arthritis. *J Rheumatol* **30**, 714-719, doi:0315162X-30-714 (2003).
- 211 Wallace, J. L., Keenan, C. M. & Granger, D. N. Gastric ulceration induced by nonsteroidal anti-inflammatory drugs is a neutrophil-dependent process. *Am J Physiol* **259**, G462-467 (1990).
- 212 Macdonald, T. M. *et al.* Methodology of a large prospective, randomised, open, blinded endpoint streamlined safety study of celecoxib versus traditional non-steroidal anti-inflammatory drugs in patients with osteoarthritis or rheumatoid arthritis: protocol of the standard care versus celecoxib outcome trial (SCOT). *BMJ Open* **3**, doi:10.1136/bmjopen-2012-002295 (2013).
- 213 Cheng, Y. *et al.* Cyclooxygenases, microsomal prostaglandin E synthase-1, and cardiovascular function. *J Clin Invest* **116**, 1391-1399, doi:10.1172/JCI27540 (2006).